Journal of Immunology Research

Fate and Function of CD4+Th Cell Subsets in Autoimmune Diseases

Lead Guest Editor: Dawei Cui
Guest Editors: Jie Tian and Xinyi Tang

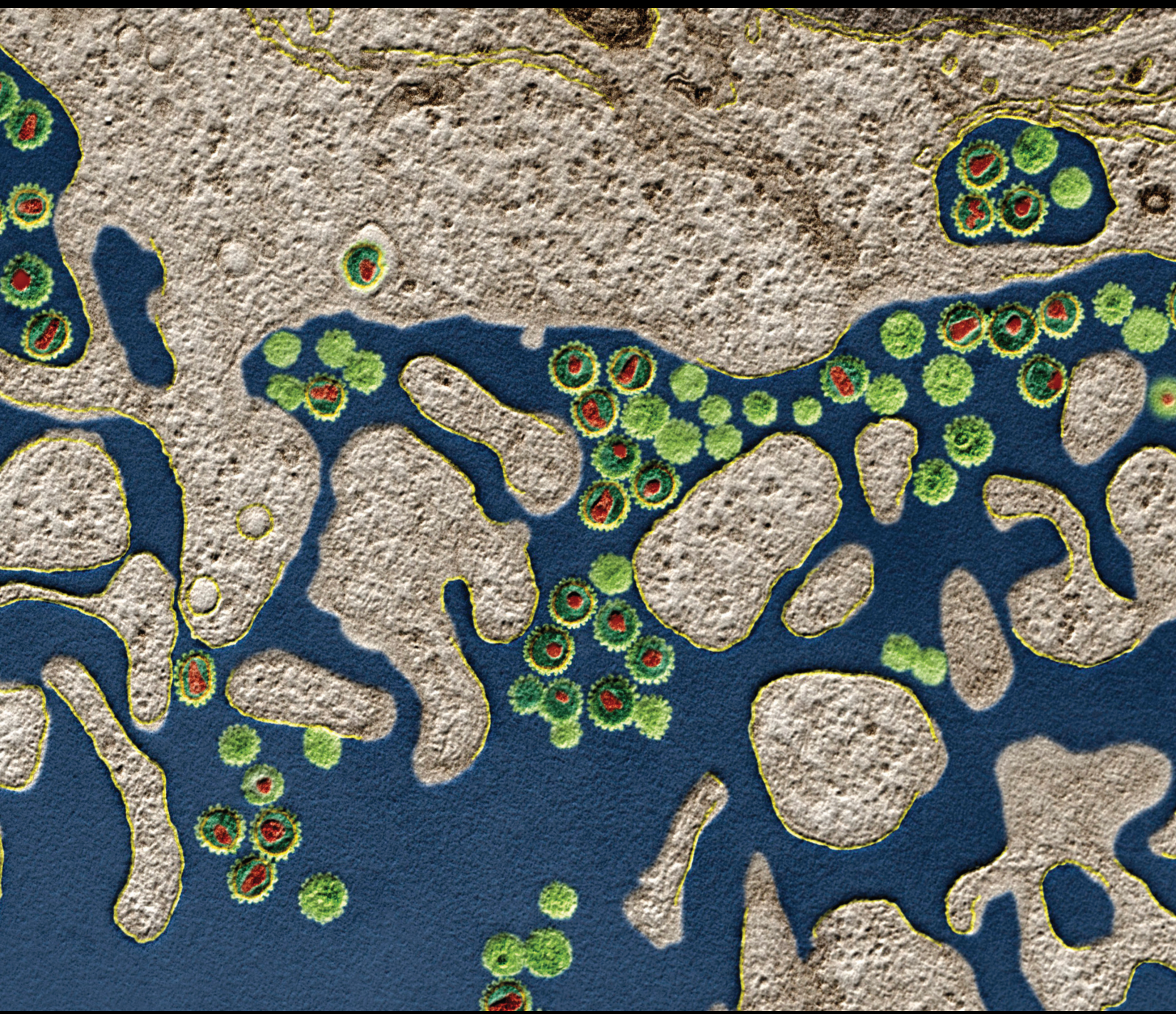

Fate and Function of CD4+Th Cell Subsets in Autoimmune Diseases

Journal of Immunology Research

Fate and Function of CD4+Th Cell Subsets in Autoimmune Diseases

Lead Guest Editor: Dawei Cui
Guest Editors: Jie Tian and Xinyi Tang

Copyright © 2021 Hindawi Limited. All rights reserved.

This is a special issue published in "Journal of Immunology Research." All articles are open access articles distributed under the Creative Commons Attribution License, which permits unrestricted use, distribution, and reproduction in any medium, provided the original work is properly cited.

Associate Editors

Douglas C. Hooper, USA
Senthamil R. Selvan, USA
Jacek Tabarkiewicz, Poland
Baohui Xu, USA

Academic Editors

Nitin Amdare, USA
Lalit Batra, USA
Kurt Blaser, Switzerland
Dimitrios P. Bogdanos, Greece
Srinivasa Reddy Bonam, USA
Carlo Cavaliere, Italy
Cinzia Ciccacci, Italy
Robert B. Clark, USA
Marco De Vincentiis, Italy
M. Victoria Delpino, Argentina
Roberta Antonia Diotti, Italy
Lihua Duan, China
Nejat K. Egilmez, USA
Theodoros Eleftheriadis, Greece
Eyad Elkord, United Kingdom
Weirong Fang, China
Elizabeth Soares Fernandes, Brazil
Steven E. Finkelstein, USA
JING GUO, USA
Luca Gattinoni, USA
Alvaro González, Spain
Manish Goyal, USA
Qingdong Guan, Canada
Theresa Hautz, Austria
Weicheng Hu, China
Giannicola Iannella, Italy
Juraj Ivanyi, United Kingdom
Ravirajsinh Jadeja, USA
Peirong Jiao, China
Youmin Kang, China
Sung Hwan Ki, Republic of Korea
Bogdan Kolarz, Poland
Vijay Kumar, USA
Esther Maria Lafuente, Spain
Natalie Lister, Australia
Daniele Maria-Ferreira, Saint Vincent and the Grenadines
Eiji Matsuura, Japan
Juliana Melgaço, Brazil
Cinzia Milito, Italy
Prasenjit Mitra, India
Chikao Morimoto, Japan
Paulina Niedźwiedzka-Rystwej, Poland
Enrique Ortega, Mexico
Felipe Passero, Brazil
Anup Singh Pathania, USA
Keshav Raj Paudel, Australia
Patrice Xavier Petit, France
Luis Alberto Ponce-Soto, Peru
Massimo Ralli, Italy
Pedro A. Reche, Spain
Eirini Rigopoulou, Greece
Ilaria Roato, Italy
Suyasha Roy, India
Francesca Santilli, Italy
Takami Sato, USA
Rahul Shivahare, USA
Arif Siddiqui, Saudi Arabia
Amar Singh, USA
Benoit Stijlemans, Belgium
Hiroshi Tanaka, Japan
Bufu Tang, China
Samanta Taurone, Italy
Mizue Terai, USA
Ban-Hock Toh, Australia
Shariq M. Usmani, USA
Ran Wang, China
Shengjun Wang, China
Paulina Wlasiuk, Poland
Zhipeng Xu, China
Xiao-Feng Yang, USA
Dunfang Zhang, China
Qiang Zhang, USA
Qianxia Zhang, USA
Bin Zhao, China
Jixin Zhong, USA
Lele Zhu, China

Contents

sB7H3 in Children with Acute Appendicitis: Its Diagnostic Value and Association with Histological Findings

Xiaochen Du, Yan Chen, Jie Zhu, Zhenjiang Bai, Jun Hua, Ying Li, Haitao Lv, and Guangbo Zhang

Research Article (11 pages), Article ID 2670527, Volume 2020 (2020)

Hindawi
Journal of Immunology Research
Volume 2021, Article ID 8880585, 24 pages
https://doi.org/10.1155/2021/8880585

Research Article

Gene Regulatory Network of Human GM-CSF-Secreting T Helper Cells

Szabolcs Éliás,[1] **Angelika Schmidt**,[1] **David Gomez-Cabrero**,[1,2,3,4] **and Jesper Tegnér**[1,5]

[1]*Unit of Computational Medicine, Center for Molecular Medicine, Department of Medicine Solna, Karolinska Institutetki.seKarolinska University Hospital & Science for Life Laboratory, 17176 Solna, Stockholm, Sweden*
[2]*Mucosal & Salivary Biology Division, King's College London Dental Institute, London SE1 9RT, UK*
[3]*Navarrabiomed, Complejo Hospitalario de Navarra (CHN), Universidad Pública de Navarra (UPNA), IdiSNA, 31008 Pamplona, Spain*
[4]*Biological and Environmental Sciences and Engineering Division, King Abdullah University of Science and Technology (KAUST), Thuwal 23955–6900, Saudi Arabia*
[5]*Biological and Environmental Sciences and Engineering Division, Computer, Electrical and Mathematical Sciences and Engineering Division, King Abdullah University of Science and Technology (KAUST), Thuwal 23955–6900, Saudi Arabia*

Correspondence should be addressed to Szabolcs Éliás; sz.e@outlook.com and Jesper Tegnér; jesper.tegner@ki.se

Received 12 August 2020; Revised 14 March 2021; Accepted 20 March 2021; Published 5 July 2021

Academic Editor: Dawei Cui

Copyright © 2021 Szabolcs Éliás et al. This is an open access article distributed under the Creative Commons Attribution License, which permits unrestricted use, distribution, and reproduction in any medium, provided the original work is properly cited.

GM-CSF produced by autoreactive CD4-positive T helper cells is involved in the pathogenesis of autoimmune diseases, such as multiple sclerosis. However, the molecular regulators that establish and maintain the features of GM-CSF-positive CD4 T cells are unknown. In order to identify these regulators, we isolated human GM-CSF-producing CD4 T cells from human peripheral blood by using a cytokine capture assay. We compared these cells to the corresponding GM-CSF-negative fraction, and furthermore, we studied naïve CD4 T cells, memory CD4 T cells, and bulk CD4 T cells from the same individuals as additional control cell populations. As a result, we provide a rich resource of integrated chromatin accessibility (ATAC-seq) and transcriptome (RNA-seq) data from these primary human CD4 T cell subsets and we show that the identified signatures are associated with human autoimmune diseases, especially multiple sclerosis. By combining information about mRNA expression, DNA accessibility, and predicted transcription factor binding, we reconstructed directed gene regulatory networks connecting transcription factors to their targets, which comprise putative key regulators of human GM-CSF-positive CD4 T cells as well as memory CD4 T cells. Our results suggest potential therapeutic targets to be investigated in the future in human autoimmune disease.

1. Introduction

CD4-positive T helper cells (Th) are crucial players in the immune system which exert their effects mainly by producing cytokines. CD4 T cell subsets are usually classified based on expression of "lineage-defining" transcription factors (TFs) as well as the signature cytokines they secrete [1]. However, the distinction is not clear-cut, since different signature cytokines can be expressed simultaneously and plasticity between subsets occurs [2, 3]. In view of the "classical" distinction of CD4 T cell subsets, particularly, Th1 and Th17 subsets are involved in the establishment of autoimmune diseases such as multiple sclerosis (MS) and the corresponding rodent model experimental autoimmune encephalomyelitis (EAE), which are thought to be driven by the T cell-released cytokines interleukin-17 (IL-17), interferon-γ (IFN-γ), IL-22, and granulocyte-macrophage colony-stimulating factor (GM-CSF). Of these, GM-CSF was determined as the key cytokine in EAE pathogenesis, since only knocking out GM-CSF (but neither IFN-γ, IL-17A, nor IL-17F) could completely protect the animals from induced EAE [4–6]. Furthermore, it has been demonstrated that specifically, the GM-CSF produced by autoreactive T cells was necessary for EAE induction, while T cell-produced IFN-γ

and IL-17 were dispensable [7–9]. In line with these results, GM-CSF expression by Th cells was required for neuroinflammation in EAE, and even in the presence of IFN-γ- and IL-17A-producing Th cells, pathogenicity vanished upon loss of GM-CSF [10]. Importantly, in humans, the fraction of GM-CSF-positive (and IFN-γ-positive) cells within CD4 T cells was elevated in MS patients' cerebrospinal fluid compared to controls, while IL-17A-positive cell fractions were not strikingly different in these reports [11, 12]. The fractions of GM-CSF-positive and IFN-γ-positive cells were also increased in peripheral blood of MS patients in one report [13], but not in another [11]. A third study found a trend of increased IFN-γ-producing peripheral blood cells in MS patients, but among 12 different cytokines tested, only GM-CSF-positive cells were significantly increased in MS patients compared to controls [14]. Interestingly, the expanded Th subset-producing GM-CSF that was found in blood and CNS of MS patients could be diminished by disease-modifying therapy [14], suggesting GM-CSF-producing Th cells to be an attractive therapeutic target. Similarly, enhanced fractions of GM-CSF-producing CD4 T cells have been observed in synovial fluid of patients with juvenile arthritis along with the well-known enhanced GM-CSF levels in synovial fluid [15, 16]. Of note, targeting GM-CSF in MS or arthritis is subject to several ongoing clinical studies, highlighting the importance of this cytokine in these diseases [16]. Based on this cumulative evidence of the significance of GM-CSF-producing CD4 T cells in human autoimmune disease, understanding the factors driving and defining GM-CSF-positive T cells would be of utmost importance for targeting them therapeutically.

Beyond their established pathogenic role in autoimmune diseases, GM-CSF-producing Th cells have also been implicated in other inflammatory diseases. In sepsis, enhanced fractions of GM-CSF-producing T cells were associated with a poor outcome [17]. Notably, GM-CSF-producing Th cells have also been implicated in SARS-CoV-2 infection, especially in patients with a severe course of coronavirus disease 2019 (COVID-19) [18–20]. Due to the pleiotropic roles of GM-CSF in immune disease and lung inflammation, GM-CSF-targeting therapeutic approaches are currently explored in clinical trials to treat COVID-19 [21].

Murine CD4 T cell populations expressing IL-17A and GM-CSF have been observed and termed "pathogenic Th17" cells because they have the potential to induce EAE [22–24]. However, only one of these studies showed coexpression of both cytokines on the single-cell level [24]. Although a T cell can express GM-CSF simultaneously with other cytokines such as IFN-γ, a "GM-CSF-only-producing" murine T cell subset was also proposed and associated with enhanced encephalitogenic activity over IL-17 and IFN-γ-producing T cells in EAE [9]. The existence of a corresponding separate "GM-CSF-only" human T cell subset has also been proposed [25], because a substantial subset of *ex vivo*-restimulated human GM-CSF-positive CD4 T cells produces GM-CSF in the absence of any other classical Th1, Th2, and Th17 lineage-defining cytokines (such as IFN-γ, IL-4, and IL-17), transcription factors, or surface markers [11, 26]. Furthermore, GM-CSF-producing CD4 T cells are induced by different sets of cytokines compared to other Th cell subsets [11, 25, 27]. In fact, GM-CSF and IL-17A expression by human CD4 T cells has been found to be mutually exclusive on the single-cell level [11] or at least substantially less frequent than coexpression of IFN-γ and GM-CSF [11, 26, 27]; also, IL-4 coproduction with GM-CSF was negligible [11]. A more recent study [14] has extended the analysis of cytokine coexpression in human PBMCs upon Phorbol 12-myristate 13-acetate (PMA) and ionomycin restimulation to a range of 13 different cytokines by the use of mass cytometry and also included MS patients along with controls. Of these cytokines tested, cytokines typical for Th2, Th17, Th22, or Tfh cells were not coproduced by GM-CSF-positive Th cells, while a substantial fraction coproduced the Th1-cytokine IFN-γ, as well as TNFα and IL-2 [14].

Despite the importance of GM-CSF-producing T cells, there is no specific marker to distinguish such cells from others to date. Although combinations of the presence and absence of nonexclusive surface markers have been useful to delineate "GM-CSF-only" cells [11], the fraction of GM-CSF-producing cells that also produces other cytokines such as IFN-γ is excluded by this approach. Furthermore, the driving factors for GM-CSF production remain unclear. Together, these observations suggest that the characterization of human GM-CSF-positive CD4 T cells isolated based on their functional profile (GM-CSF production) rather than using the "classical" Th1 and Th17-like phenotypic markers may enable the identification of factors regulating GM-CSF production in CD4 T cells. Hence, in order to understand the regulators and molecular patterns defining human GM-CSF-positive CD4 T cells, we isolated those cells actively secreting GM-CSF from human peripheral blood *ex vivo* by cytokine "capture" assay, starting with bulk CD4 T cells. We then studied their transcriptome by RNA-sequencing (RNA-seq). Studying a single data type like mRNA expression separately may not be sufficient for identification of all regulatory factors, since TFs themselves are often regulated by posttranscriptional modifications, intracellular translocation, or cobinding with other TFs, rather than by changes in their gene expression. Thus, we assessed in parallel the DNA accessibility of the same samples in order to gain a global picture of putative TF binding patterns and enabling integration with the expression of regulated target genes on the RNA level. Due to the limited number of primary, *ex vivo*-isolated GM-CSF-positive human T cells, we employed a recently described highly sensitive method assay for transposase-accessible chromatin using sequencing (ATAC-seq) [28] to study DNA accessibility from 50,000 cells per replicate. As a control, we used the respective GM-CSF-depleted (GM-CSF-negative) fraction derived from the capture assay procedure. Since GM-CSF-positive cells (which may also coproduce additional cytokines and hence may represent "activated" T cells) may differ from GM-CSF-negative CD4 T cells merely by containing largely reduced fractions of naïve cells, we furthermore undertook RNA-seq and ATAC-seq profiling of several control cell populations from the same donors, namely, naïve CD4 T cells and memory CD4 T cells. As an additional control, we studied bulk CD4 T cells without a capture assay procedure.

This study hence reveals molecular patterns of GM-CSF-positive CD4 T cells as well as those shared with memory, naïve, or bulk CD4 cells. To our knowledge, this is the first study of global molecular signatures of GM-CSF-positive CD4 T cells derived *ex vivo* without restimulation. Although this population does not only contain "GM-CSF-only" cells, but may include cells producing other cytokines, the *ex vivo* isolation based on active GM-CSF secretion results in a pure population of cells producing GM-CSF versus cells not producing GM-CSF. Besides serving as a control, we furthermore provide a novel resource of ATAC-seq and RNA-seq data of human primary naïve, memory, and bulk CD4 T cells from several human healthy donors. A large body of knowledge exists on molecular signatures and regulation of human naïve and memory T cells [29]. This encompasses large consortium efforts to map human memory and naïve CD4 T cell subsets' transcriptomes and epigenomes including chromatin accessibility [30], albeit these authors did not use the ATAC-seq method. Recently, few reports using ATAC-seq for T cells have been published and the impactful results support the power of the methodology. Many of these studies focus on murine CD8 T cell differentiation and exhaustion [31–35], and several recent studies also comprise ATAC-seq on CD4 T cells [10, 28, 36–40]. However, none of these works studied all the types of CD4 T cell subsets that we analyzed here.

Through interpreted, integrative analysis of mRNA expression and DNA accessibility data from primary human CD4 T cell subsets, we provide novel gene regulatory networks underlying GM-CSF production as well as the memory phenotype in human CD4 T cells and we propose novel key TFs regulating these cells. The enrichment of the identified genes for human immune system diseases and especially MS for GM-CSF-positive cells underlines the clinical relevance of our data, which may be exploited in a multitude of basic and applied immunology studies in the future.

2. Materials and Methods

2.1. Ethics Statement. Peripheral blood mononuclear cells were freshly isolated from anonymized healthy donor buffy coats purchased from the Karolinska University Hospital (Karolinska Universitetssjukhuset, Huddinge), Sweden. Research was performed according to the national Swedish ethical regulations (ethical review act, SFS number 2003:460).

2.2. Experimental Methods

2.2.1. PBMC and T Cell Isolation. Human peripheral blood mononuclear cells (PBMCs) were isolated using Ficoll-Paque gradient centrifugation from buffy coats according to standard procedures. In brief, buffy coats were diluted in PBS, layered on Ficoll-Paque (GE Healthcare), and centrifuged ($1200 \times g$, 20 min, without break). Subsequently, the PBMC ring was collected. PBMCs were washed with PBS ($450 \times g$, 10 min) and monocytes were depleted by plastic adherence in RPMI 1640 medium containing GlutaMAX (Life Technologies, Thermo Fisher Scientific) and 10% (v/v) heat-inactivated fetal bovine serum (FBS) (Gibco Performance Plus certified; Thermo Fisher Scientific) for 60–80 minutes at 37°C, 5% CO_2. Platelets were removed by centrifugation ($200 \times g$, 5–10 min, 20°C, 4 times). Subsequently, human naïve, memory, and total CD4 T cells were isolated negatively ("untouched") in parallel by magnetic-activated cell sorting (MACS) from each donor. The following MACS kits were used according to the instructions from the manufacturer (Miltenyi Biotec): human naïve $CD4^+$ T cell isolation kit II, human memory $CD4^+$ T cell isolation kit II, and human $CD4^+$ T cell isolation kit II. The purity of naïve, memory, and total CD4 T cells was controlled by flow cytometry (see below). Cells were counted with the Countess Automated Cell Counter (Invitrogen), and viability (determined by Trypan blue stain) was $96.5 \pm 1.5\%$ (mean ± SD). T cells were cultured at 37°C and 5% CO_2 in serum-free X-Vivo 15 medium (Lonza) supplemented with GlutaMAX (Gibco), unless otherwise stated. T cells were rested overnight before sample preparation for RNA-seq, ATAC-seq, and GM-CSF secretion assay (see below). 6 healthy male anonymized donors (aged 35.7 ± 8.5 years, mean ± SD; range 22–44 years) were used for molecular profiling.

2.2.2. GM-CSF Secretion Assay (Capture Assay). Total CD4 T cells were isolated and rested as above, before capturing GM-CSF-producing cells using the "GM-CSF Secretion Assay-Cell Enrichment and Detection Kit (PE), human" (Miltenyi Biotec) according to the manufacturer's instructions with the following modifications and details. $65–150 \times 10^6$ ($98.3 \times 10^6 \pm 33.7 \times 10^6$, mean ± SD) unstimulated purified CD4 T cells were centrifuged ($300 \times g$, 10 min), X-Vivo 15 medium was removed completely, and cells were washed with 15 ml MACS buffer (0.5% human serum albumin (HSA) and 2 mM EDTA in PBS, 4°C). Cells were resuspended in ice-cold RPMI 1640 medium including GlutaMAX (Life Technologies, Thermo Fisher Scientific) and 10% (v/v) FBS (Gibco Performance Plus certified, heat inactivated; Thermo Fisher Scientific). GM-CSF catch reagent was added, mixed, and incubated for 5 minutes on ice. The GM-CSF secretion period was performed by adding prewarmed (37°C) RPMI 1640 medium (containing GlutaMAX and 10% FBS) to a cell density of 1×10^6 cells/ml, under continuous rotation (10 rpm orbital mixing) of the cells for 45 minutes at 37°C, 5% CO_2. Labeling cells with GM-CSF Detection Antibody (Biotin) and Anti-Biotin-PE and magnetic labeling with Anti-PE MicroBeads UltraPure were performed as per manufacturer's instructions, and cells were washed in 50 ml MACS buffer. Cells were resuspended in 3 ml MACS buffer, cell suspensions were filtered with 30 μm Filcon strainer (BD Biosciences), and magnetic separation was performed on LS columns (Miltenyi Biotec) according to standard protocols. For donor A, the GM-CSF+ eluate was passed over a second MS column following the LS column procedure, but since a second column did not increase purity but led to loss of cells (data not shown), for all other donors, the GM-CSF+ eluate from the first LS column was used for subsequent analyses. The GM-CSF− fraction from the flow-through was passed over a second column (except for donor A) to increase purity of the negative fraction. The yield of GM-CSF+ cells was

$1.2 \pm 0.6\%$ of CD4 T cells (mean ± SD) and purity was controlled by flow cytometry (see below).

2.2.3. Flow Cytometry. Purity of MACS-isolated naïve CD4 T cells, memory CD4 T cells, and total CD4 T cells was verified by surface staining using the following antibodies (all against the human proteins): CD4-PerCP (clone SK3, BD Biosciences), CD45RA-FITC (clone T6D11, Miltenyi Biotec), CD45RO-PE (clone UCHL1, BD Biosciences), CD19-APC (clone HIB19, BD Biosciences), and CD8-eFlour450 (clone OKT8, eBioscience). Staining was performed in the dark with antibody dilutions in FACS buffer (PBS with 0.5% HSA) for 15 minutes at 20°C. Single-stained PBMC or T cell samples were used as compensation controls. Cells were washed once with PBS, resuspended in FACS buffer, and acquired on a CyAn ADP 9-Color Analyzer (Beckman Coulter). Compensation was performed with the CyAn software (Summit) tool. Purity of GM-CSF+ and GM-CSF− samples after GM-CSF secretion assay from bulk CD4 T cells was assessed by measuring the fraction of PE-labeled (GM-CSF-positive) cells. Cell purities and gating strategy are shown in Figure 1 and Supplementary Figure S1. We also confirmed in independent experiments (including PMA and ionomycin restimulation) that the PE label in GM-CSF-captured cells correlated well with the GM-CSF signal based on intracellular staining with an anti-GM-CSF antibody (clone BVD2-21C11, APC conjugated, Miltenyi Biotec; data not shown). Flow cytometry data analysis and visualization were performed using the FlowJo software v7.6.5 (Tree Star), and exported percentage values were plotted using GraphPad Prism v7.02 (GraphPad Software Inc.).

2.2.4. ATAC-Seq Sample Preparation. Nuclear isolation, tagmentation, and PCR amplification was carried out according to Buenrostro et al. [28]. In brief, 50,000 cells per replicate were transferred to 0.2 ml tubes and centrifuged ($500 \times g$, 6 min, 4°C) and the supernatant was removed. Cells were washed with PBS ($500 \times g$, 6 min, 4°C) and lysed in lysis buffer (10 mM Tris-HCl, pH 7.4; 10 mM NaCl; 3 mM $MgCl_2$; and 0.1% IGEPAL CA-630) to isolate nuclei. 3 technical replicates (50,000 cells each) were processed in parallel for each sample (except donor A, 2 technical replicates). Nuclei were washed in PBS ($500 \times g$, 6 min, 4°C) and resuspended in Transposase Reaction mix. Transposition was carried out at 37°C for 30 minutes, followed by clean up using the QIAGEN MinElute Reaction Clean Up Kit according to the manufacturer's instructions (QIAGEN). PCR amplification using reagents from the Nextera DNA Sample Preparation Kit (Illumina) and barcoding of replicates were performed with reaction conditions and index primers as described in [28]. 20 different index primers were used and distributed across replicate samples and donors in a balanced way to control for potential batch effects. The PCR product was cleaned up using the QIAGEN MinElute Reaction Clean Up Kit. Subsequently, gel size selection was performed by gel electrophoresis (1.8% (*w*/*v*) certified low-melt agarose (Bio-Rad) in 1x UltraPure Tris-Acetate-EDTA (TAE) buffer including SYBR Safe DNA Gel Stain (Invitrogen, Thermo Fisher Scientific), with a free well between each of the samples) and DNA in the size range of 150–230 bp was excised using surgical blades. Replicate samples were allocated to the gels in a balanced way regarding donor and experimental condition to control for potential batch effects. Resulting DNA libraries were purified using QIAGEN MinElute Gel Extraction Kit according to the manufacturer's instructions (QIAGEN).

Size distribution of ATAC-seq sequencing libraries was determined on a 2100 Bioanalyzer Instrument (Agilent Technologies) using the Agilent DNA High Sensitivity Kit according to the manufacturer's instructions. Libraries were quantified by real-time PCR on a StepOnePlus detector system (Applied Biosystems) using the KAPA Library Quantification Kit (KAPA Biosystems). Sequencing was performed on an Illumina HiSeq 2500 instrument (Illumina) with a single-read setting and read length of 42 bp.

2.2.5. RNA-Seq Sample Preparation. Cells were centrifuged ($1000 \times g$, 5 min, 20°C), washed with PBS, and lysed in QIAzol Lysis Reagent (QIAGEN) by vortexing and incubating for 5 minutes at 20°C. Lysates were stored at −80°C until RNA extraction. RNA was extracted with the miRNeasy Micro Kit (QIAGEN) according to the manufacturer's instructions. RNA concentration was determined on a NanoDrop 2000 spectrophotometer (Thermo Fisher Scientific), and RNA quality was controlled on a 2100 Bioanalyzer Instrument (Agilent Technologies) using an Agilent RNA 6000 Pico Kit. RNA integrity numbers (RIN) were 8.5 ± 0.3 (mean ± SD). Libraries were prepared in one batch with the TruSeq Stranded mRNA HT Kit (Illumina) with Dual Index Adapters and Ambion ERCC Spike-In Control (Thermo Fisher Scientific). Samples were allocated to sequencing indexes and lanes in a balanced fashion to control for potential batch effects (7–8 samples/lane). Library concentration was determined on a Qubit 2.0 Fluorometer (Thermo Fisher Scientific). The library size and quality were measured on a 2100 Bioanalyzer Instrument (Agilent Technologies) using an Agilent High Sensitivity DNA Kit. Libraries were quantified with the KAPA Library Quantification Kit (KAPA Biosystems). Sequencing was performed on a HiSeq 2500 Sequencing Platform (Illumina; High Output Run) with 76 nt paired-end reads.

2.3. Computational Methods

2.3.1. Preprocessing of Sequencing Data. BCL base call files were demultiplexed and converted to FASTQ files using bcl2fastq version 2.17.1.14. For quality control, FastQC version 0.11.5 was used.

FASTQ files from the ATAC-seq experiments were trimmed from adapters, and low-quality bases using scythe version 0.991. and sickle version 1.33. FASTQ files from the ATAC-seq experiments were aligned to the human genome version hg38 using bowtie version 2.3.0 with the '–very-sensitive' option. After alignment, BAM files of ATAC-seq experiments were filtered to eliminate: duplicates (samtools rmdup), alignments with a mapping score below 10, and alignments that are not mapped to chromosome 1-22, chromosome X, or chromosome Y. ATAC-seq peaks were called using the 'findPeaks' script from the HOMER suite (version

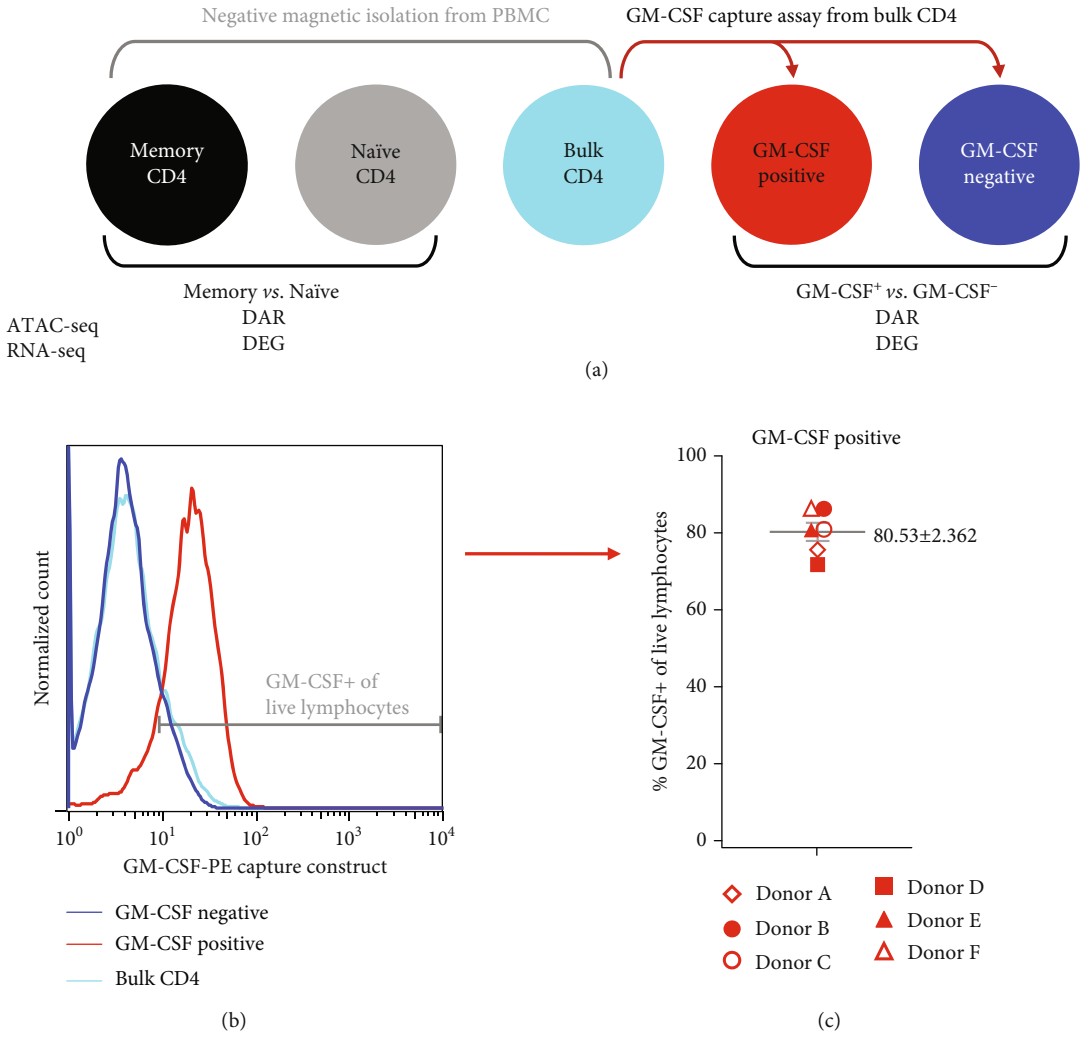

Figure 1: Experimental setup and quality control for human CD4 T cell transcriptome and chromatin accessibility analysis. (a) Human PBMCs for each donor were split in three fractions, and memory CD4 T cells, naïve CD4 T cells, and bulk (total) CD4 T cells were isolated in parallel by negative (untouched) magnetic isolation (cell purities; see Supplementary Figure S1). From bulk CD4 T cells, GM-CSF-secreting cells (GM-CSF positive) were captured and the negative fraction was used as the corresponding GM-CSF-negative population. The five indicated cell populations were used for molecular profiling by ATAC-seq and RNA-seq. Differentially accessible DNA regions (DAR) and differentially expressed genes (DEG) were determined for the comparison of memory versus naïve CD4 T cells and for GM-CSF-positive versus GM-CSF-negative CD4 T cells, respectively. (b, c) High purity of isolated (captured) GM-CSF+ CD4 T cells was confirmed by flow cytometry. The histograms show the signal of the GM-CSF capture construct for the indicated cell populations, pregated on live singlet lymphocytes based on forward scatter, side scatter, and pulse width. Here, bulk CD4 T cells represent an aliquot taken after labeling with the GM-CSF-PE capture construct, but without further capture assay procedure. (b) shows a representative donor and (c) shows summarized data for $n = 6$ donors from 4 independent experiments (mean and SEM are indicated in grey). Each donor is represented by a symbol; same symbol shape (but filled or unfilled) indicates donors processed within the same experiment.

4.9.1) with the '-style factor' option [41]. ATAC-seq peaks were assigned to a gene using the 'annotatePeaks' script from the HOMER suite.

FASTQ files from the RNA-seq experiments were aligned using STAR version 2.5.2b. Indexes for RNA-seq alignment were created using the gencode version 25 annotation file. RNA-seq alignment was run with STAR's built-in adapter trimming option ('–clip3pAdapterSeq AGATCGGAAGAGCACACGTCTGAACTCCAGTCAC AGATCGGAAGAGCGTCGTGTAGGGAAAGAGTGTA') and its built-in counting option ('–quantMode'). Only genes with more than 1 count per million in at least 3 samples were included in the downstream RNA-seq analysis.

2.3.2. Generation of Consensus Peak Set. In order to generate a set of comparable features (genomic regions) for read counting and quantifying differential accessibility from the ATAC-seq data, a set of consensus peaks was generated in two subsequent steps: (1) generation of consensus peaks on the technical replicate level: first, the peaks that appeared in at least two technical replicates (out of a total of three, except one donor with a total of two technical replicates) with at

least 75% reciprocal overlap were selected. Then, these selected regions were partitioned into disjoint nonempty subsets so that each element is contained in precisely one subset. Only the partitions appearing in at least two replicates were retained, and afterwards, adjacent regions were merged. A bed file resulting from these steps is herein referred to as a sample and (2) next, all bed files containing each set of technical replicate level consensus regions were concatenated and the presence of each region was counted within each experimental sample; one occurrence corresponds to one donor (biological replicate) and one cell type (experimental condition). Only the regions appearing in at least four samples were kept ($n = 5$ is the number of biological replicates in the smallest group regarding experimental condition). Regions having a distance of 42 bases or less between them were subsequently merged (the number 42 corresponds to the sequencing read length in bases). Afterwards, reads were counted using the featureCounts tool [42] with the criterion that at least half of the read had to overlap with a feature to be assigned to that feature.

2.3.3. Calculation of Differential Expression and Differential Accessibility. Differential expression and accessibility was calculated using the edgeR [43] library version 3.18.1 from Bioconductor. Donors (biological replicates) and cell types (experimental conditions) were used as explanatory variables in the generalized linear models. ATAC-seq data were normalized to length and GC content by conditional quantile normalization (CQN) [44]. Comparisons were made between GM-CSF-positive CD4 T cells and GM-CSF-negative CD4 T cells or between memory and naïve CD4 T cells (see Figure 1(a)). The cutoff to call differentially expressed genes (DEGs) or differentially accessible regions (DARs) was FDR < 0.05 and >25% fold change (in the direction of either up- or downregulation, that is either 1.25 or 0.75 fold change).

2.3.4. Footprinting. Footprinting was carried out using the Wellington algorithm [45], i.e., the wellington_footprints.py script from the pyDNase library version 0.2.5 with the following settings: -fp 6,41,1 -sh 7,36,1 -fdr 0.01 -fdriter 100 -fdrlimit -30 -A. The footprint occupancy score (FOS) for each footprint was calculated using the pyDNase library as described in [46]. For subsequent network reconstruction, we considered only footprints with a FOS smaller than the following threshold: median (FOS) + [median (FOS) − minimum (FOS)].

2.3.5. Network Reconstruction. A directed network was reconstructed by combining information from the ATAC-seq and RNA-seq data in two subsequent steps: (1) identifying source nodes: peaks were ranked based on their combined measure of significance and direction of differential accessibility $[-\log_{10}(\text{FDR}) \times \text{sign}(\log_2(\text{fold change}))]$. Peaks containing footprints were scanned for TF binding motifs using the TRANSFAC database [47]. An enrichment score was calculated to identify TFs with binding sites enriched in differentially accessible peaks, using tools similar to gene set enrichment analysis (GSEA) [48]. In detail, random permutation was performed on the ranked list of peaks to assess how probable it is to observe at least the same enrichment by chance (P value) [49]. After multiple testing correction, TFs with FDR < 0.05 were selected and the normalized enrichment score (NES) was obtained. Only those source nodes (TFs) that were detectably expressed on the RNA level (according to a minimal RNA-seq filtering rule) were considered. Of these, most fell into the class of highly expressed genes (HEGs) according to [50]. (2) identifying target nodes: target nodes are defined as peaks with an assigned gene. The selection criteria were that (i) the peak contains a footprint with a binding motif of the source node (TF) and (ii) the peak or the assigned gene has to be differentially accessible or differentially expressed, respectively.

To assign an importance measure to the source nodes in networks generated as above, the PageRank [51] of the network nodes was calculated after inverting the directionality of all edges in the network (only for the purpose of this computation). After this computation, the nodes with high PageRank values (higher than the 99th percentile of all node values within a given network) were selected from both the GM-CSF and memory network, and afterwards, their values were investigated in each of the two networks.

3. Results and Discussion

GM-CSF-positive CD4 T cells are enriched in MS patients and play a crucial role in EAE; nevertheless, the factors driving and markers defining those cells are largely unknown. To better understand the features and regulatory networks of GM-CSF-positive CD4 T cells, we therefore studied the transcriptional profiles and chromatin accessibility of these cells. *In vitro*-differentiated GM-CSF-producing cells comprise several subsets [27] and are likely to differ from those generated *in vivo*. Further, *ex vivo* restimulation with strong artificial stimuli such as PMA and ionomycin—which is usually necessary to reach sufficient signal strength for detection by intracellular cytokine staining—drastically alters the transcriptome of T cells [52–54]. Hence, we aimed to isolate GM-CSF-producing cells *ex vivo* in an as much as possible unmanipulated state by GM-CSF secretion assay, "capturing" and isolating those cells that actively secrete GM-CSF (experimental setup; see Figure 1(a)), here defined as GM-CSF-positive cells. The capture assay was performed starting from highly purified CD4 T cells derived from human peripheral blood (purity 97.3 ± 0.6%, mean ± SEM, Supplementary Figure S1A). As controls, we used the respective GM-CSF-negative fraction from the isolation procedure, as well as the bulk CD4 T cells before any capture assay procedure. The latter should, given the low fraction of GM-CSF-positive cells, be very similar to the GM-CSF-negative fraction and hence allows for estimation of the effects arising from the capture assay procedure. The purity of GM-CSF-positive and GM-CSF-negative fractions was assessed by flow cytometry (Figures 1(b) and 1(c)) and the yield of isolated GM-CSF-positive cells was 1.2 ± 0.6% (mean ± SD) of CD4 T cells. To measure the transcriptome and DNA accessibility from limited cell numbers, we employed highly sensitive next-generation sequencing

(NGS) methods (RNA-seq and ATAC-seq, respectively). Since cytokine-secreting cells may differ from naïve cells due to a memory-like phenotype and a large fraction of CD4 T cells are naïve (mean ± SEM, 42.3 ± 5.8% in the donors used here; see Supplementary Figure S1A), we further profiled highly purified naïve and memory CD4 T cells from the same donors (Figure 1(a) and Supplementary Figure S1B-D).

Altogether, we obtained DNA accessibility and transcriptome data from highly purified *ex vivo*-derived human naïve CD4 T cells, memory CD4 T cells, bulk CD4 T cells, and GM-CSF-positive and the corresponding GM-CSF-negative CD4 T cells. To enable paired analysis within a donor, these cell populations were isolated in parallel within a donor, for 6 donors in total. DNA accessibility and mRNA data were obtained in parallel from the same samples allowing for matched integration of the data.

3.1. Unique and Shared DNA Accessibility and Gene Expression Signatures of GM-CSF-Positive and Memory CD4 T Cells. We studied the above-described five different CD4 T cell populations by RNA-seq and ATAC-seq. To minimize potential batch effects due to technical factors, the library preparations and sequencing runs were designed in such a way that donors, cell populations, and (for ATAC-seq) technical replicates were distributed in a balanced fashion. It is also worth noting that only donors of the same gender were studied here (male, aged 35.7 ± 8.5 years, mean ± SD), which may be important since it was recently shown that gender was the largest source of variation explaining chromatin accessibility in primary human CD4 T cells measured by ATAC-seq [36]. That study further discovered novel elements escaping X chromosome inactivation and affecting immune genes [36]. To assess which factors explained most of the variability between the samples under study here, we performed principle component analysis (PCA). Indeed, for both data types, there was a grouping of the samples based on the cell subset, outweighing donor or experimental variation (Figures 2(a) and 2(b)) and confirming the quality of our samples and data. Notably, for RNA data, the cell populations were generally more distinct from each other than for DNA accessibility data. However, the GM-CSF-positive and corresponding GM-CSF-negative fractions appeared relatively similar to each other in the PCA performed on RNA data, while PCA results from ATAC-seq data were closer to the expected pattern, that is, bulk CD4 T cells appearing "between" GM-CSF-positive and GM-CSF-negative populations (Figures 2(a) and 2(b)). The difference between RNA-seq and ATAC-seq data with respect to separation of GM-CSF-positive and negative cells may indicate that the capture assay procedure imposes distinct changes on the transcriptome, highlighting the importance of using correspondingly treated controls to determine differential expression. In contrast, changes in DNA accessibility appeared more robust towards changes due to the experimental procedure at least within the experimental time frame under study, although the distinction of the other groups was generally less apparent with ATAC-seq data. The advantage of PCA is that the displayed distances between samples along the axes can directly be interpreted but it is not suited to reduce all the data variability to only two dimensions. Indeed in our analysis, the first two PCs in the two-dimensional space only explained about 50% of the variation in the data. Therefore, we also used another dimensionality reduction method to explore the sample-to-sample relationships, namely, t-distributed stochastic neighbor embedding (t-SNE) [55]. t-SNE allows for visualization of sample-to-sample similarity in two dimensions, and furthermore, in contrast to PCA, it is a nonlinear dimensionality reduction algorithm and it is especially suited for capturing local relationships. The t-SNE results (Figures 2(c) and 2(d)) generally confirmed the results of the PCA analysis (Figures 2(a) and 2(b)), that is, the groups (cell types) being more distinct in RNA data than ATAC-seq data, with the exception of GM-CSF-positive and GM-CSF-negative cells.

We defined significantly differentially accessible DNA regions (DARs) and significantly differentially expressed genes (DEGs) in GM-CSF-positive CD4 T cells or in memory CD4 T cells. To do so, we specifically analyzed the signatures of GM-CSF-positive versus GM-CSF-negative CD4 T cells, as well as the profiles of memory versus naïve CD4 T cells (Figures 1(a), 3(a), 3(b), 3(c), and 3(d)). We used generalized linear models based on the negative binomial distribution (edgeR) [43] to determine differential expression and accessibility, and we called DEGs and DARs, respectively, based on combined FDR and fold change cutoffs. We called 16571 DARs in GM-CSF-positive CD4 T cells (compared to corresponding GM-CSF-negative cells; Figure 3(b)) and 13705 DARs in memory CD4 T cells (compared to naïve CD4 T cells; Figure 3(a)). On the transcriptome level, we called 124 DEGs in GM-CSF-positive and 5383 DEGs in memory CD4 T cells (Figures 3(c) and 3(d)). The relatively low number of DEGs in GM-CSF-positive cells is in agreement with the PCA and t-SNE data (Figures 2(b) and 2(d)) and may suggest that combination with ATAC-seq data drastically improves the possibility to define molecular signatures specific to GM-CSF-positive *ex vivo*-captured cells.

Next, we studied the DARs and DEGs in more detail. We first focused on the signatures of memory CD4 T cells, which are well studied in the literature [29] and hence enabled to assess the biological quality of our data, besides providing a new NGS dataset of human primary memory and naïve CD4 T cells. DARs and DEGs defined in memory cells are shown in Supplementary Figure S2, along with their molecular patterns in the other cell types under study. Accessible regions (consensus peaks) were annotated to the major categories promoter-TSS (46.6% of all peaks), intron (26.8%), and intergenic (18.7%), followed by exon (4.1%) and TTS (3.8%). Regions differentially accessible (DARs) in memory cells showed a similar distribution across annotated categories (44.7% in promoter-TSS, 26.9% intron, 20.4% intergenic, 3.9% exon, and 4.1% TTS). We next extracted those memory-specific DARs that were assigned to a gene from a list of genes known to be involved in T cell memory as compiled by Durek and colleagues [30]. Several of the DARs in memory cells were assigned to such known memory-associated genes, about

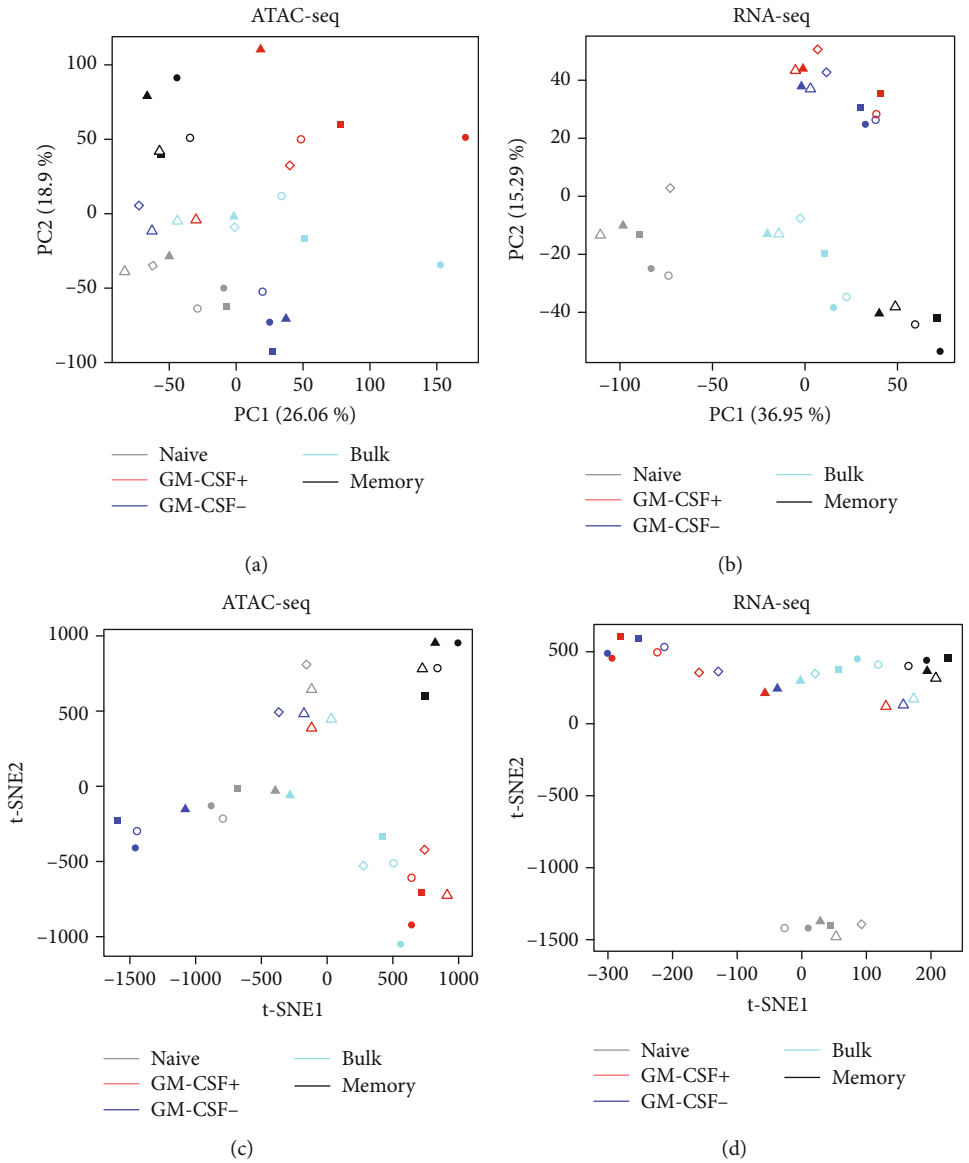

Figure 2: Explorative analysis of ATAC-seq and RNA-seq samples. (a) Principal component analysis (PCA) was carried out on CQN-normalized ATAC-seq data given as $\log_2(\text{RPKM} + 1)$ centered by mean subtraction for each feature (genomic region). PC1 and PC2 are shown, along with the % variation explained. Symbol colors indicate the given cell populations and symbol shapes and fillings represent individual donors ($n = 5$–6 donors) as in Figure 1(c). Data from technical replicates were pooled before analysis. (b) PCA for RNA-seq data given as $\log_2(\text{FPKM} + 1)$ centered by mean subtraction for each feature (gene). Labels as in (a). (c, d) t-SNE dimensionality reduction visualization of (c) ATAC-seq and (d) RNA-seq data, processed and labeled as in (a) and (b), respectively.

half (12 of 23) of those selected regions were falling in the promoter-TSS region and about a quarter (6 of 23) were assigned to intronic regions (Figure 3(e)). Furthermore, we assessed a selected subset of memory-related genes that were shown to be up- or downregulated on the RNA level in memory T cells [30]. The majority of these genes were DEGs in memory cells in our data, notably up- or downregulated almost exclusively (36 of 37 studied genes; 97%) in the expected direction (Figure 3(f)), validating our data. In addition, we confirmed the quality of the memory T cell data by performing gene set enrichment analysis (GSEA) using several published transcriptome datasets comprising naïve and memory T cell subsets. Indeed, genes described to be up- or downregulated in memory (versus naïve) CD4 T cells in these published datasets were significantly enriched on the expected ends of the ranked gene list from our novel memory versus naïve T cell dataset (Figure 3(g) and Supplementary Figure S3).

3.2. The Molecular Signature of GM-CSF-Positive CD4 T Cells. Next, we focused on the signatures of GM-CSF-positive cells by studying the respective DARs and DEGs in more detail. All the DARs in GM-CSF-positive cells are displayed in Figure 4(a) with the color scale representing accessibility. A substantial fraction of DARs in GM-CSF-positive cells displayed a similar pattern in memory cells, while naïve

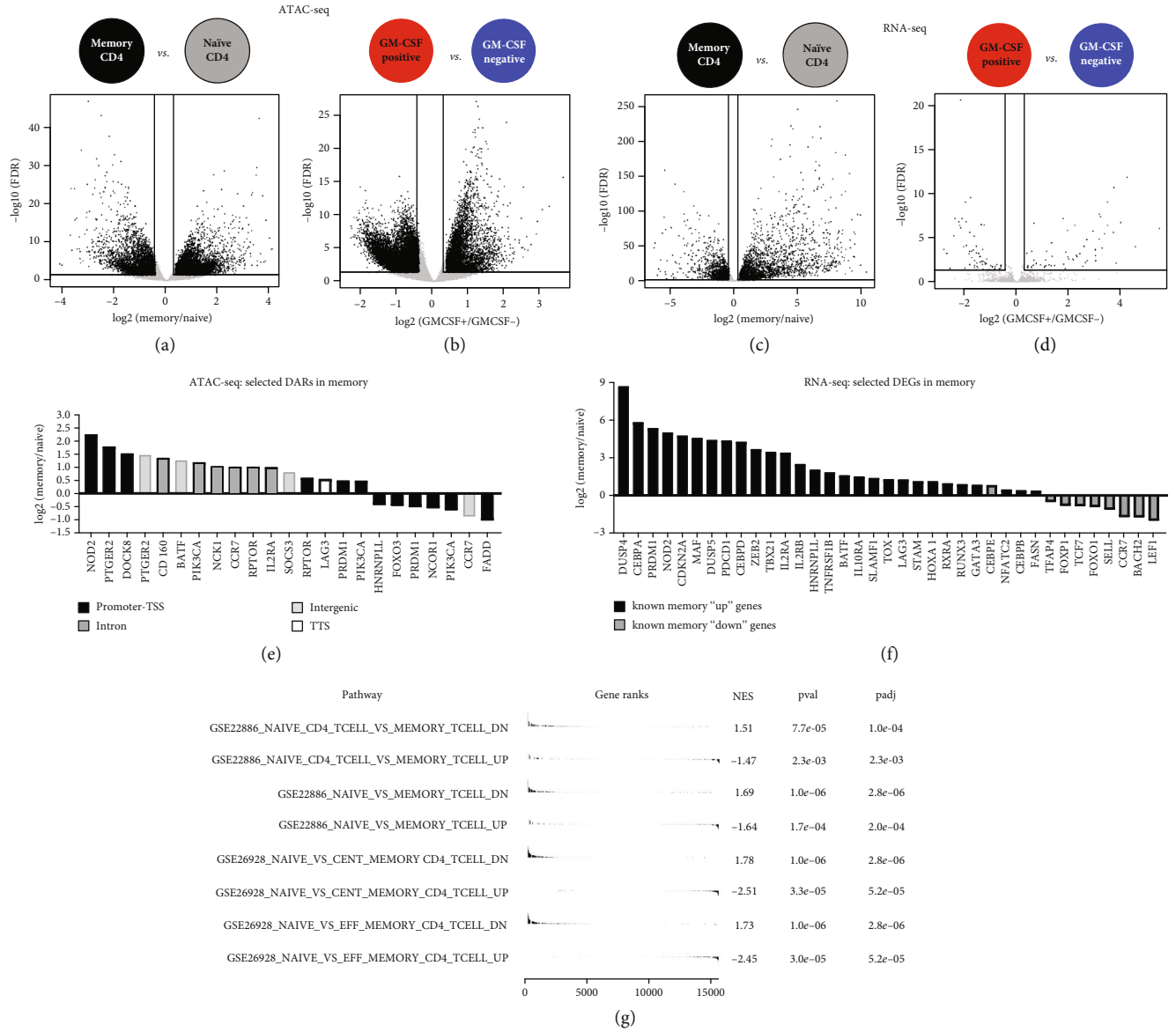

Figure 3: Differential chromatin accessibility and gene expression in memory versus naïve CD4 T cells as well as in GM-CSF-positive versus negative cells. (a, b) ATAC-seq data were CQN normalized and differential accessibility between the indicated cell population comparisons was calculated ((a) memory *vs.* naïve CD4 T cells; (b) GM-CSF-positive *vs.* negative CD4 T cells). Volcano plots show each consensus peak as a single dot, and lines indicate the threshold for calling a DAR (FDR < 0.05 and >25% fold change); DARs are depicted in black. (c, d) Differential gene expression was calculated from RNA-seq data for cell population comparisons as in (a, b). Lines indicate the threshold for calling a DEG (FDR < 0.05 and >25% fold change); DEGs are depicted in black. (e) A selection of DARs in memory *vs.* naïve was studied for being assigned to genes known to play a role in T cell memory. $\log_2$(fold change (memory/naïve)) for selected DARs are plotted, and colors indicate the category that the respective region is assigned to (TSS: transcription start site; TTS: transcription termination site). (f) Known T cell memory "up" (black) or T cell memory "down" (grey) genes based on previous literature were selected if differentially expressed (DEG in memory *vs.* naïve) in the present data. $\log_2$(fold change (memory/naïve)) for these selected DEGs is plotted; values > 0 represent upregulation and values < 0 represent downregulation in memory T cells. Colors indicate whether the gene was previously described to be "up" or "down" in memory T cells. (g) Gene set enrichment analysis (GSEA) using gene sets from published transcriptome data featuring naïve and memory T cell subsets (GSE accession numbers as displayed) and a ranked gene list of our memory versus naïve T cell data. Ranking was based on $-\log_{10}(P\,\text{value}) \times \text{sign}\,(\log_2(\text{fold change (memory/naïve)}))$. Gene sets containing both human naïve and memory T cell data were retrieved from the MSigDB database [48]. NES: normalized enrichment score; pval: *P* value; padj: FDR.

cells and GM-CSF-negative cells were most distinct from GM-CSF-positive cells (Figure 4(a)). In bulk CD4 T cells, DARs defined in GM-CSF-positive cells showed heterogeneity between donors (Figure 4(a)), which may reflect the variability in the fraction of memory and naïve cells within bulk CD4 T cells depending on the donor (Supplementary Figure S1A). Importantly, several DARs displayed a unique accessibility pattern in GM-CSF-positive cells distinct from

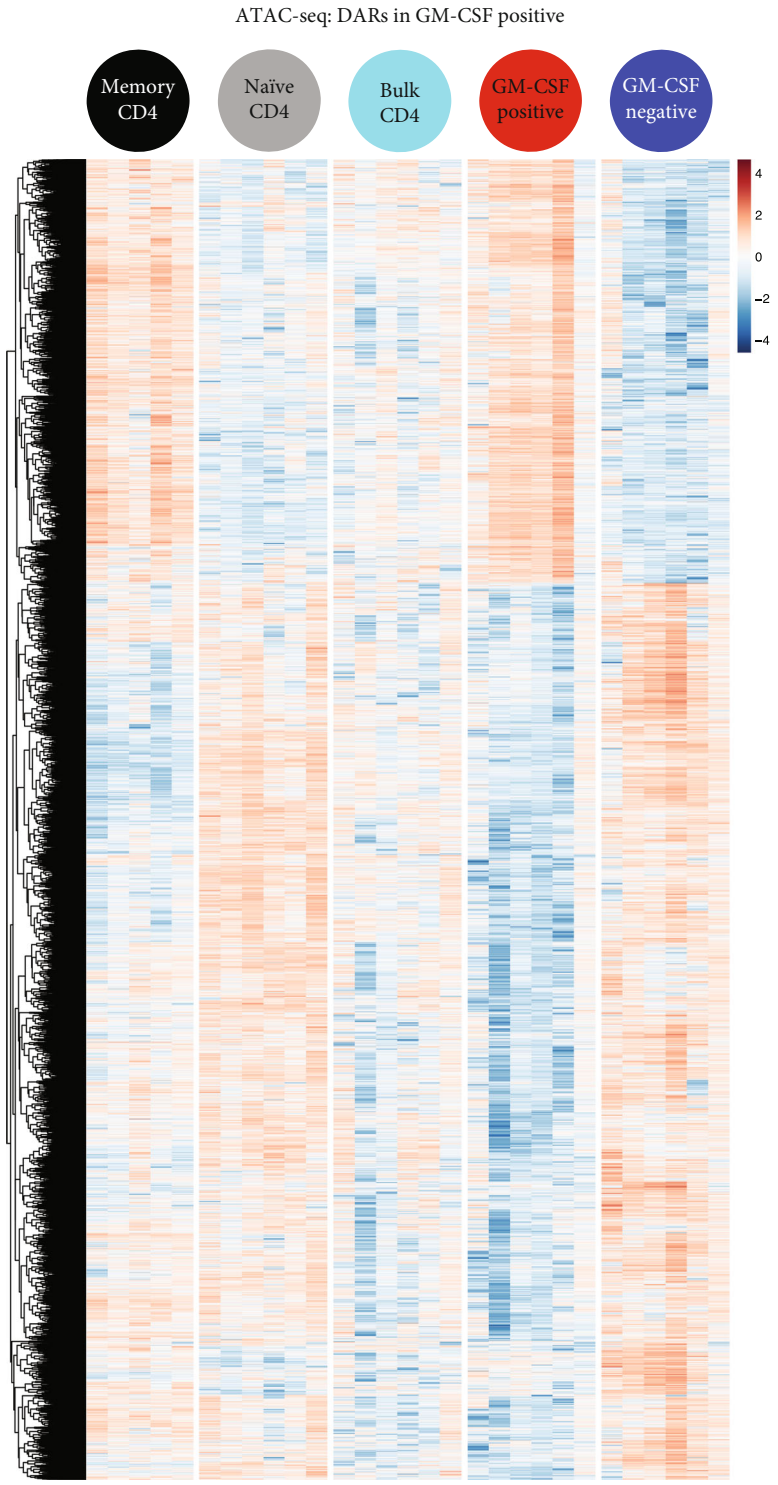

(a)

Figure 4: Continued.

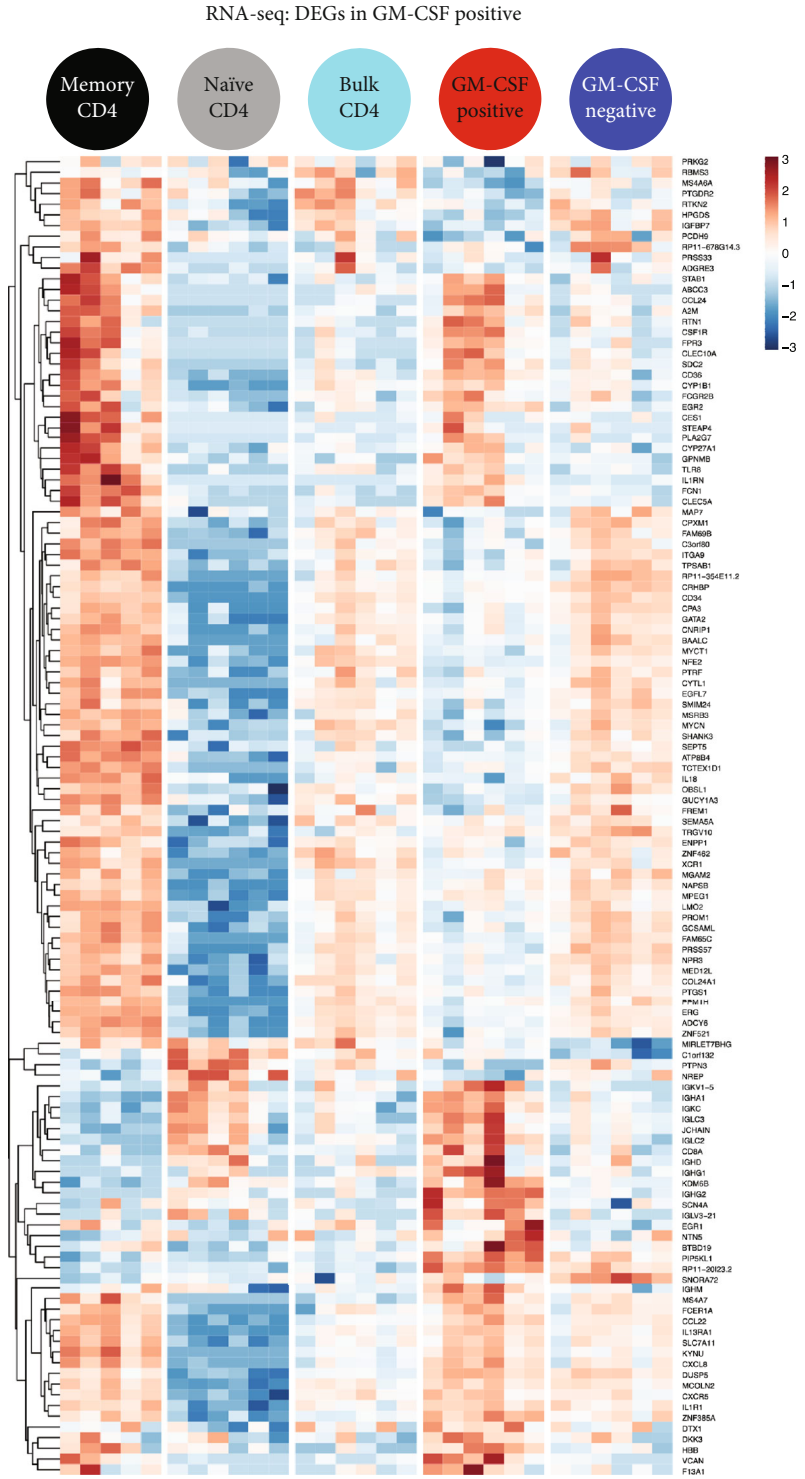

(b)

Figure 4: Continued.

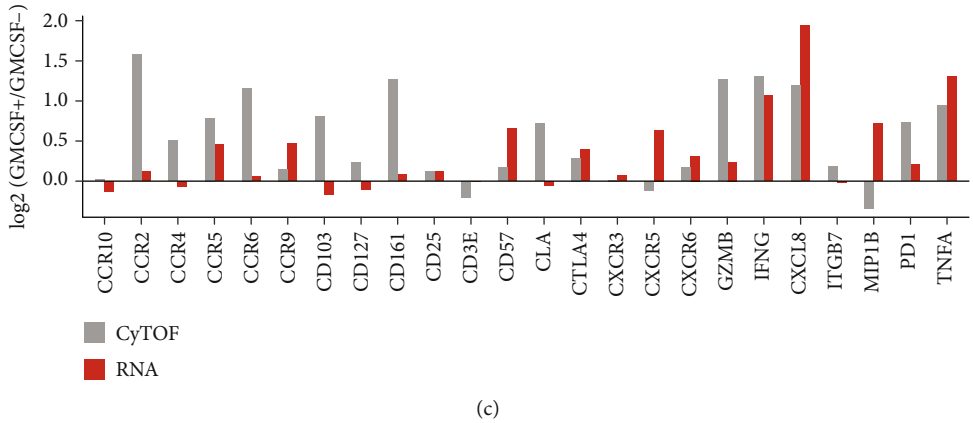

(c)

Figure 4: Expression profile and DNA accessibility signatures of human GM-CSF-positive CD4 T cells. (a) Differentially accessible DNA regions (DARs) in GM-CSF-positive versus GM-CSF-negative CD4 T cells are plotted as a heat map showing their accessibility in all the five cell populations studied. CQN normalized $\log_2(\text{RPKM}+1)$ is represented by the color scale, indicating accessibility (blue: low, red: high). Data were row scaled and clustered (Euclidean distance, complete linkage clustering). (b) Differentially expressed genes (DEGs) in GM-CSF-positive versus GM-CSF-negative CD4 T cells are plotted as a heat map showing their expression in all the five cell populations studied. Gene expression is displayed as $\log_2(\text{FPKM}+1)$ with blue indicating low and red indicating high expression according to the color scale. Data were row scaled and clustered (Euclidean distance, complete linkage clustering). (c) The mean of $\log_2(\text{fold change})$ of GM-CSF+/GM-CSF− cell populations using the median intensity values from CyTOF measurements are shown, using CD4 T cell-gated PBMC data from Wong et al. [64] and designated as "CyTOF" (grey bars). For the genes corresponding to the proteins measured in CyTOF, the $\log_2(\text{fold change})$ of GM-CSF+/GM-CSF− cell populations from the RNA-seq data of this study is plotted and labeled as "RNA" (red).

other cell populations under study (Figure 4(a)). These data show that GM-CSF-positive cells can be assigned a specific pattern of accessible DNA regions that distinguish them from other CD4 T cell subsets, and that may contribute important information about regulation of GM-CSF-positive cells. Different DNA accessibility can functionally affect the status of a cell by, for example, modifying expression of genes regulated through these regions.

Next, we studied the DEGs defined in GM-CSF-positive cells by analyzing their expression in GM-CSF-positive cells along with the other CD4 T cell subsets under study. Like it was observed for the DARs, DEGs in GM-CSF-positive cells shared a large part of the RNA signature with memory cells but also displayed distinct patterns and differed largely from naïve cells and GM-CSF-negative and bulk CD4 T cells (Figure 4(b)). Despite the general similarity of cells treated with the capture assay regarding the global transcriptome (Figures 2(b) and 2(d)), subsetting on the DEGs defined between GM-CSF-positive and negative cells with stringent statistical cutoffs visualized clearly the differences in these "signature genes" for those cell types (Figure 4(b)). Importantly, subsetting on these genes that were defined as DEGs in GM-CSF-positive versus corresponding negative cells (that is, without considering the bulk CD4 T cell samples) also clearly showed the expected similarity of bulk CD4 T cells and GM-CSF-negative CD4 T cells (Figure 4(b)) that was not apparent in the RNA-seq PCA or t-SNE using all genes (see above; Figures 2(b) and 2(d)), confirming that the selected GM-CSF-positive cell "signature" DEGs are likely not affected by the capture assay and column procedure.

DEGs in GM-CSF-positive cells comprised several genes with a well-known role in T cells such as *EGR2*, *CXCL8*, and *CXCR5* along with multiple genes with an unknown role in T cells and potentially regulating GM-CSF-positive cells (Figure 4(b)). *CSF2RB* (encoding for the high-affinity receptor subunit for IL-3, IL-5, and GM-CSF) was not among the DEGs in GM-CSF-positive cells, and *CSF2RB* expression being lower (albeit not passing the significance threshold) in GM-CSF-positive than negative cells makes a technical artifact of isolation of cells binding GM-CSF through this receptor unlikely (Figure 4(b)).

It should be mentioned that while captured GM-CSF-positive cells displayed high purity regarding captured secreted GM-CSF and CD4 T cell marker positivity (Figures 1(b) and 1(c) and Supplementary Figure S1), this represents an enrichment of GM-CSF-producing cells versus cells not producing GM-CSF but it does not mean that the cells do not coexpress other cytokines typical for other Th subsets. Albeit not passing the significance threshold for being called a DEG in GM-CSF+ cells, relatively higher expression of *IFNG* mRNA in GM-CSF-positive cells versus GM-CSF-negative cells (Supplementary Figure S4A) is in accordance with our and others' previous findings from flow or mass cytometry of T cells from healthy donors as well as MS patients demonstrating coexpression of IFN-γ and GM-CSF on the single-cell level in some, but not all, GM-CSF-producing human CD4 T cells or clonal populations thereof [11, 14, 15, 26, 27, 56]. Also in line with the majority of these studies on human T cells regarding a lack of coexpression of GM-CSF and IL-17, *IL17A* and *IL17F* expression was below the detection limit in GM-CSF-positive cells (but also in any other cell population under study; Supplementary Figure S4A). Besides IFN-γ, TNFα and IL-2 proteins have also been found to be frequently coexpressed in GM-CSF-positive Th

cells upon PMA + ionomycin restimulation [14], and as for *IFNG*, also *TNF* was slightly higher expressed in GM-CSF-positive versus negative cells, although not statistically significant (Supplementary Figure S4A). Importantly, it has to be noted that in human T cells restimulated *ex vivo* with PMA and ionomycin to detect cytokines by intracellular staining and cytometry as in the above studies, the fractions of TNFα-, IL-2-, and IFN-γ-producing Th cells are generally high (for example, up to 90% of all Th cells producing TNFα, up to 75% of Th cells producing IL-2, and up to 40% of Th cells producing IFN-γ) while cytokines typical for Th2, Th17, Th22, or Tfh cells are generally low (<5% of Th cells being positive for the respective cytokines) [14]. Consequently, coproduction of IL-2, TNFα, or IFN-γ protein is generally likely for any T cell subset restimulated with PMA and ionomycin. Nevertheless, due to the importance of IFN-γ and GM-CSF in the context of MS, we studied intracellular protein expression of GM-CSF and IFN-γ (requiring PMA and ionomycin restimulation) in bulk CD4 T cells of the donors used in this study. 49.98 ± 4.61% (mean ± SEM) of the GM-CSF-positive CD4 T cells coexpressed IFN-γ (Supplementary Figure S4B), although it remains unknown how this is influenced by the PMA and ionomycin restimulation needed for this analysis procedure *per se*. In this context, it is notable that strong restimulation by PMA and ionomycin, as needed in single-cell cytokine protein studies, may cause expression of abundant T cell cytokines such as IL-2 protein even in purified naïve Th cells after only 3 to 5 hours of stimulation (unpublished observation and [57]) that may not be truly present *in vivo* without artificial restimulation, as naïve Th cells are not expected to actively produce cytokines. Also on the global transcriptome level, PMA and ionomycin stimulation for only 30 minutes to 3 hours was shown to drastically alter the T cell gene expression signature [52–54]. Hence, to identify the *ex vivo* gene expression signature of GM-CSF-positive cells, we isolated GM-CSF-producing CD4 T cells without PMA and ionomycin restimulation in all our NGS profiling studies, which results in a low yield of cells yet represents cells in a state without artificial restimulation and hence preserving their gene signature as much as possible in the *ex vivo* state. While the low cell yield did not allow for parallel capture of other cytokines or protein analysis in the captured cells in these donors, the above-described cytokine mRNA analyses as well as parallel intracellular cytokine staining in bulk CD4 T cells from the same donors suggest that *IFNG* may be expressed in GM-CSF-positive, but also GM-CSF-negative, Th cells. However, it is noteworthy that expression of many cytokines on the mRNA level is rather low if the cells are not artificially restimulated *ex vivo*. Along these lines, many cytokine mRNAs were below or close to the detection limit and, hence, excluded from further differential expression analysis (Supplementary Figure S4A). Although many cytokine mRNAs were lowly expressed and did not pass the detection threshold, we nevertheless analyzed mRNA counts of relevant T cell cytokines in the cell populations under study even when expressed very lowly (Supplementary Figure S4A). Of the cytokines passing the detection threshold (*IFNG*, *TNF*, *IL13*, *IL17C*, *CXCL8*, and *GZMB*), only *CXCL8* (encoding for IL-8) was differentially expressed in GM-CSF-positive versus negative cells, while all except *IL13* were differentially expressed in memory versus naïve T cells. It should be noted that *CSF2* mRNA, which encodes for GM-CSF, was lowly expressed in all samples (RNA-seq counts close to the detection limit), which may be explained by rapid mRNA decay conferred by the adenine- and uridine-rich elements (ARE) in the GM-CSF promoter—AREs in fact have been discovered in the *CSF2* gene which codes for a particularly unstable transcript [58–60]. Importantly, considering the instability of *CSF2* mRNA and relatively low expression levels, our approach of isolating GM-CSF protein–secreting cells is likely to be more suitable to define signatures of *ex vivo*-derived GM-CSF-positive cells, as opposed to, for example, single–cell RNA-seq of mixed T cell populations. Strikingly, a recent study [61] performing single-cell RNA-seq of immune cells from MS patients confirmed that, despite the known importance of GM-CSF-producing Th cells in MS pathogenesis [11, 13, 14], *CSF2* mRNA was not detectable in that study, neither in the blood nor in cerebrospinal fluid samples [61]. Hence, signatures derived from our study designating GM-CSF-positive human T cells may be useful to identify such cells based on their signature in RNA studies where *CSF2* cannot be used as a suitable marker.

To our knowledge, there is no other comparable dataset available that studied the signatures of purified GM-CSF-secreting cells without PMA/ionomycin restimulation. Thus, the RNA expression signatures defined in the GM-CSF-positive cells in this study could not be directly validated externally in an independently published transcriptome dataset. Nevertheless, we strived to confirm the expression signature from GM-CSF-positive captured cells by comparing with a completely independent dataset and experimental setup. A recent report [62] provides RNA-seq data of GM-CSF-, IFN-γ-, and IL-17-producing captured cells from healthy donors; however, PMA and ionomycin restimulation renders it difficult to directly compare these data to ours. Interestingly, the authors [62] observed a large overlap of the gene expression signature between the cells producing either cytokine and, importantly, also to (PMA + ionomycin-stimulated) naïve CD4 T cells. This suggests that the strong stimulatory effect of PMA and ionomycin may largely dominate the gene expression signatures, which is supported by several studies that showed a large influence of even short (30 minutes to 3 hours) PMA plus ionomycin stimulation on the global transcriptome of human Th cells [52–54]. In addition, capture assay and flow cytometry-based cell sorting as used by Al-Mossawi et al. [62] may cause rapid changes to the transcriptome. Indeed, studies of the transcriptome after diverse cell isolation procedures have revealed that different isolation procedures have an impact on the global transcriptome [54, 63]. Nevertheless, we compared the published data with our transcriptome data to determine whether GM-CSF-positive cells may be closely related to cells producing GM-CSF or other cytokines in that study. However, PMA and ionomycin restimulation (or other differences in experimental setup) seemed to largely determine the sample-to-sample similarity, as all

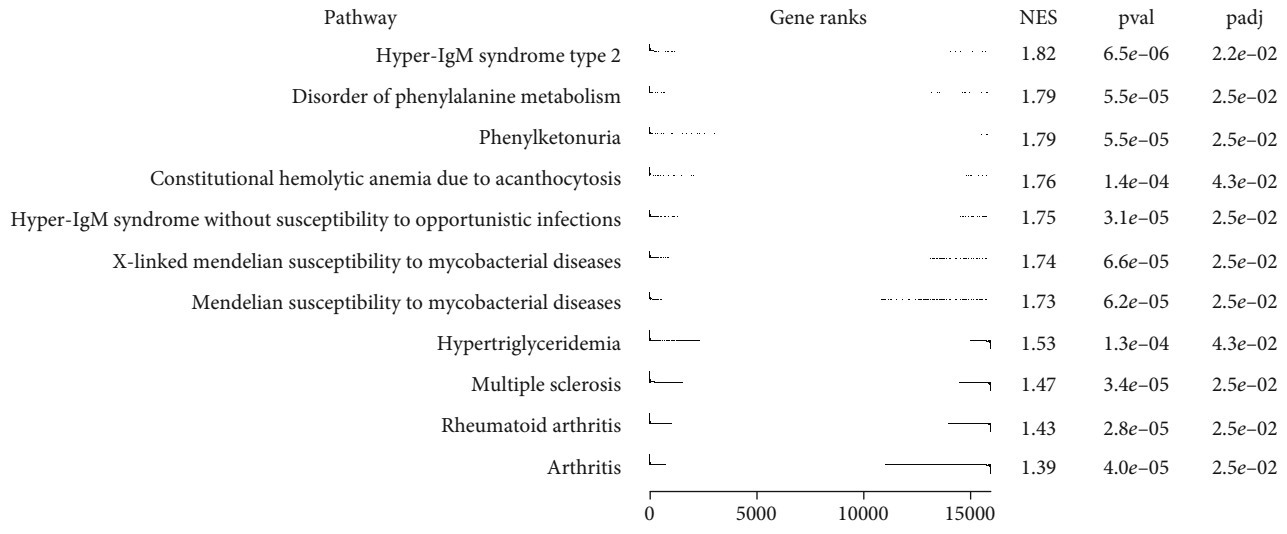

(a)

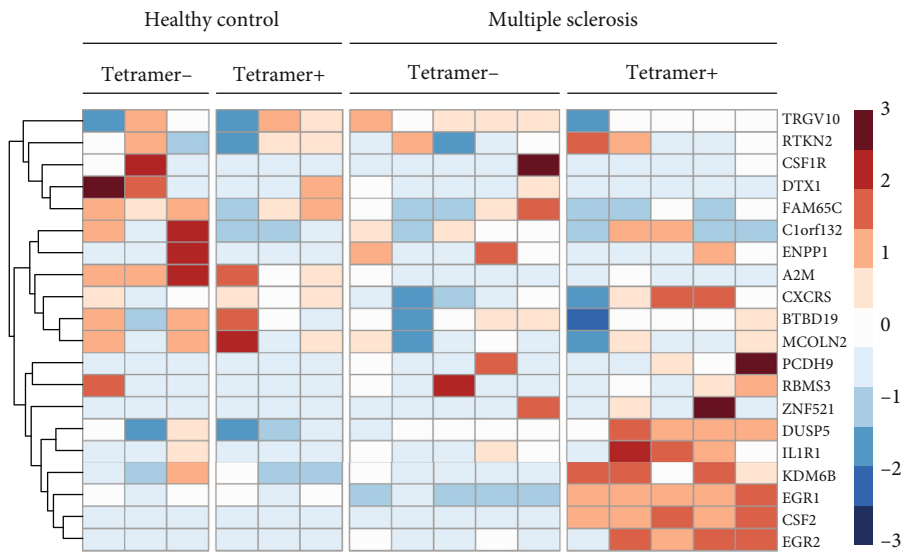

(b)

SNP	Gene Name	Annotation	Distance to TSS	log2(GMCSF+/GMCSF−)	FDR
rs1323292	*RGS1*	Intergenic	−3818	−0.972	0.005
rs60600003	*ELMO1*	promoter-TSS	−129	−0.258	0.047

(c)

Figure 5: GM-CSF-positive CD4 T cell signatures are associated with autoimmune diseases, especially MS. (a) Gene set enrichment analysis is shown using genes ranked by the $-\log_{10}(\text{FDR}) \times \text{sign}\,(\log_2(\text{GM} - \text{CSF+}/\text{GM} - \text{CSF} -))$ function, and the Open Targets database [68] was used to provide gene sets associated with diseases. NES: normalized enrichment score; pval: *P* value; padj: FDR. (b) The heat map represents the row-scaled $\log_2(\text{RPKM} + 1)$ expression values from RNA-seq data of CD4 T cells from MS patients or healthy controls (data from [26]). Groups are separated based on disease status (MS or healthy) and myelin antigen reactivity (reactive: tetramer+). Genes are selected as those identified in the current RNA-seq study as differentially expressed between GM-CSF-positive versus GM-CSF-negative cells and having detectable expression $(\log_2(\text{RPKM} + 1) > 0)$ in at least 4 samples in the data from [26]. (c) Of the 110 established non-MHC MS susceptibility variants [70], two SNPs mapped to consensus peaks from the current ATAC-seq study. Information about these SNPs is shown in the table, along with the differential accessibility analysis in GM-CSF-positive versus GM-CSF-negative CD4 T cells.

the samples correlated more strongly based on dataset than based on cell type (data not shown). Thus, we compared the similarity of the different cell types after batch normalization, and while naïve T cells were similar between the two datasets, the overall transcriptome patterns were not distinguishable based on cytokine expression, neither within the published dataset nor across datasets (Supplementary Figure S4C). This suggests that cytokine-producing CD4 T cell subsets have a largely similar transcriptome and that cell restimulation and isolation procedures dominate the

global gene expression patterns and render it difficult to compare between studies. To further confirm the DEGs in GM-CSF-positive cells in external data and their relevance on the protein level, we asked whether the RNA expression pattern of captured GM-CSF-positive T cells generally agreed with the respective proteins in GM-CSF-positive T cells defined by intracellular cytokine staining. To explore overlap of as many as possible markers, we studied a mass cytometry (CyTOF) dataset [64] which comprises staining of human PBMCs with CD4 and GM-CSF along with other markers measured on the protein level. In pregated CD4-positive T cells of this CyTOF dataset, we gated on GM-CSF+ cells and GM-CSF− cells and determined the relative expression of other available protein markers in these populations. We compared the up- or downregulation of these protein markers in gated GM-CSF+ versus GM-CSF− cells [$\log_2$ (fold change) of the median signal intensity of the two cell populations] with the up- or downregulation of the corresponding protein-coding transcripts of these markers in isolated GM-CSF-positive versus GM-CSF-negative cells from our data [$\log_2$ (fold change) of mRNA expression]. As a result, 16 of the 24 markers (two-thirds) had a fold change with identical directions in the CyTOF and RNA-seq data (Figure 4(c)). According to a binomial distribution, the probability of observing this or greater concordance between the two datasets by chance is 7.6%. This needs to be acknowledged considering that those markers that do not concur might be regulated by protein internalization from the surface, such as the well known for CD3 [65] that was downregulated in the CyTOF data but barely affected in the mRNA data. Also, the total abundance of certain proteins may be regulated on the posttranscriptional level, as transcript levels cannot always predict protein abundance [66, 67]. In addition, PMA and ionomycin stimulation prior to intracellular cytokine staining may have affected some of these markers. Overall, we concluded that the expression profile of the GM-CSF-positive captured T cells matches well with the profile of independently characterized human GM-CSF-positive T cells.

3.3. GM-CSF-Positive CD4 T Cell Transcript Signatures and Chromatin Accessibility Are Associated with Autoimmune Diseases, Especially MS. Next, we asked whether the gene expression pattern of GM-CSF-positive cells was enriched for any diseases by exploring the Open Targets Platform [68]. We ranked the detected genes based on their differential expression in GM-CSF-positive versus negative cells using the $-\log_{10}(\text{FDR}) \times \text{sign}(\log_2(\text{fold change}))$ function for ranking and calculated enrichment scores for diseases. Indeed, among the few significantly enriched diseases (FDR < 0.05), the autoimmune diseases MS and rheumatoid arthritis were represented (Figure 5(a)). Notably, for both diseases, GM-CSF targeting is in clinical trials [16], supporting the relevance of our data. The data also showed enrichment for several other diseases related to the immune system, infection, or metabolism, although it should be noted that some of these disease gene sets contained only few elements (genes) and may thus be less relevant than MS or rheumatoid arthritis, which comprised a large number of genes (Figure 5(a) and Supplementary Table S1A). When performing the same enrichment analysis for the ranked gene list from memory versus naïve CD4 T cells, a large number of diseases were significantly enriched including many diseases involving the immune system, as expected (Supplementary Table S1B).

Due to the relevance of GM-CSF-positive T cells in MS, we studied in more detail whether DEGs identified in GM-CSF-positive cells displayed altered expression in MS patients' T cell samples. T cells recognizing peptides derived from myelin proteins as autoantigen and being activated and migrating to the CNS are thought to be crucial mediators of inflammation in MS [69]. Cao and colleagues have performed RNA-seq of expanded CD4 T cells derived from MS patients and healthy controls, with two subsets of samples each containing those autoreactive to antigenic peptides derived from myelin (tetramer-positive) versus tetramer-negative T cells [26]. The authors discovered that myelin-reactive T cells from patients with MS displayed strongly enhanced production of IFN-γ, IL-17, and GM-CSF compared to those isolated from healthy controls, which instead secreted more anti-inflammatory IL-10 [26]. We studied whether these cells would also display altered expression of the genes we defined as signature genes of GM-CSF-positive cells. Indeed, a subset of these genes was down- and another subset was upregulated in myelin-reactive T cells from MS patients (Figure 5(b)), potentially identifying genes relevant to the disease pathogenesis. Here, the T cells displayed detectable *CSF2* mRNA encoding for GM-CSF, perhaps due to the *in vitro* stimulation and expansion of these T cells. Remarkably, only myelin-reactive cells from MS patients expressed high levels of *CSF2* (Figure 5(b)). Interestingly, this *CSF2* expression pattern strongly resembled the expression patterns of several of the GM-CSF-positive T cell signature DEGs defined here, namely, *DUSP5*, *IL1R1*, *KDM6B*, *EGR1*, and *EGR2* (Figure 5(b)), which may be interesting candidates to explore in the future regarding their role in GM-CSF-positive T cells and MS. While this analysis confirmed the relevance of the GM-CSF-positive T cells' RNA-seq data in MS, we next analyzed whether also the ATAC-seq data could reveal information on those DNA regions most relevant for GM-CSF-positive T cells in the context of MS. To do so, we asked whether the peaks called from our ATAC-seq analysis contained any SNPs associated with MS. Interrogating a list of non-MHC MS susceptibility variants comprising 110 established risk variants from the International Multiple Sclerosis Genetics Consortium [70, 71], we identified two SNPs mapping to the accessible DNA peaks (considering all consensus peaks) from our study. These SNPs were assigned to the protein-coding genes *Regulator Of G Protein Signaling 1* (*RGS1*) and *Engulfment And Cell Motility 1* (*ELMO1*) genes (Figure 5(c)). Importantly, the regions containing these SNPs were significantly differentially accessible (FDR < 0.05) in GM-CSF-positive versus GM-CSF-negative cells (Figure 5(c)), suggesting a putative role of these regions in T cell-mediated MS pathogenesis. It is tempting to speculate that the epigenetic signature

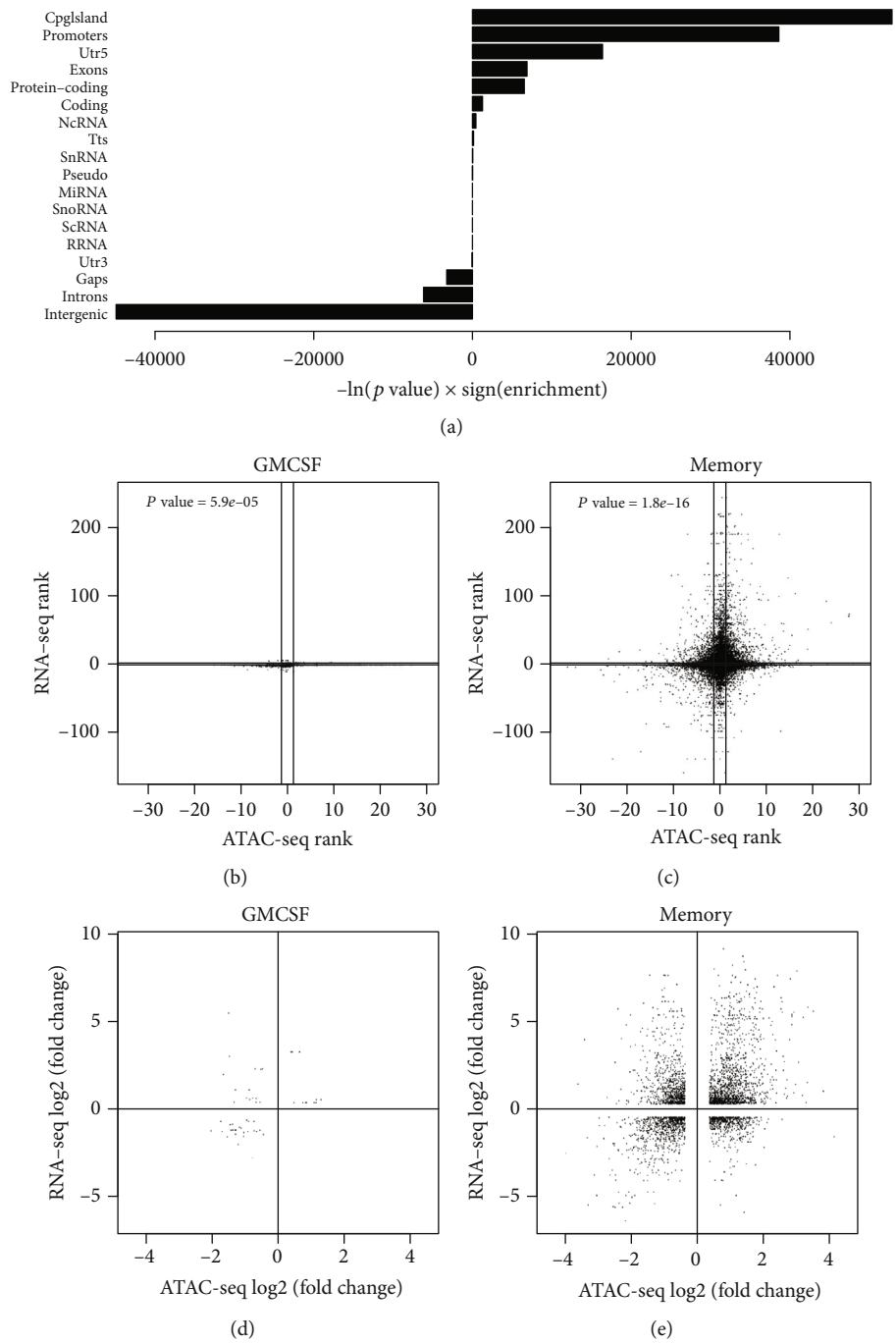

Figure 6: Enrichment of ATAC-seq peaks in regions representing certain genomic features and relationship of ATAC-seq and RNA-seq data. (a) The enrichment of ATAC-seq consensus peaks in different types of genomic regions is shown with bars representing the enrichment significance × direction of enrichment (−ln (*P* value) × sign (enrichment)). (b, c) Genes that were detected on the RNA-seq level and were also assigned to ATAC-seq peaks were ranked using the $-\log_{10}(\text{FDR}) \times \text{sign}(\log_2(\text{fold change}))$ function based on both RNA-seq and ATAC-seq (using values of the assigned peaks) within a given cell type comparison ((b) GM-CSF+ *vs.* GM-CSF−; (c) memory *vs.* naïve). The ranks of genes using ATAC-seq *vs.* RNA-seq for ranking are visualized for both cell type comparisons; lines indicate FDR cutoff 0.05 in the respective comparison. *P* value represents the probability of observing this or more directional agreement between the two data types by chance, using only genes significantly differential (FDR < 0.05) in both data types. *P* values were calculated by Fisher's exact test with Monte Carlo simulation. (d, e) Dot plot representation as in (b, c), but using $\log_2(\text{fold change})$ for ranking and visualizing only (assigned) genes that are significantly differential in both data types.

defined here may be useful as a surrogate signature to define GM-CSF-producing cells, especially in the context of recently available single-cell ATAC-seq methodologies [72, 73] and the instability of *CSF2* mRNA leading to failure to detect GM-CSF-producing cells based on *CSF2* mRNA expression in single-cell RNA-seq studies [61].

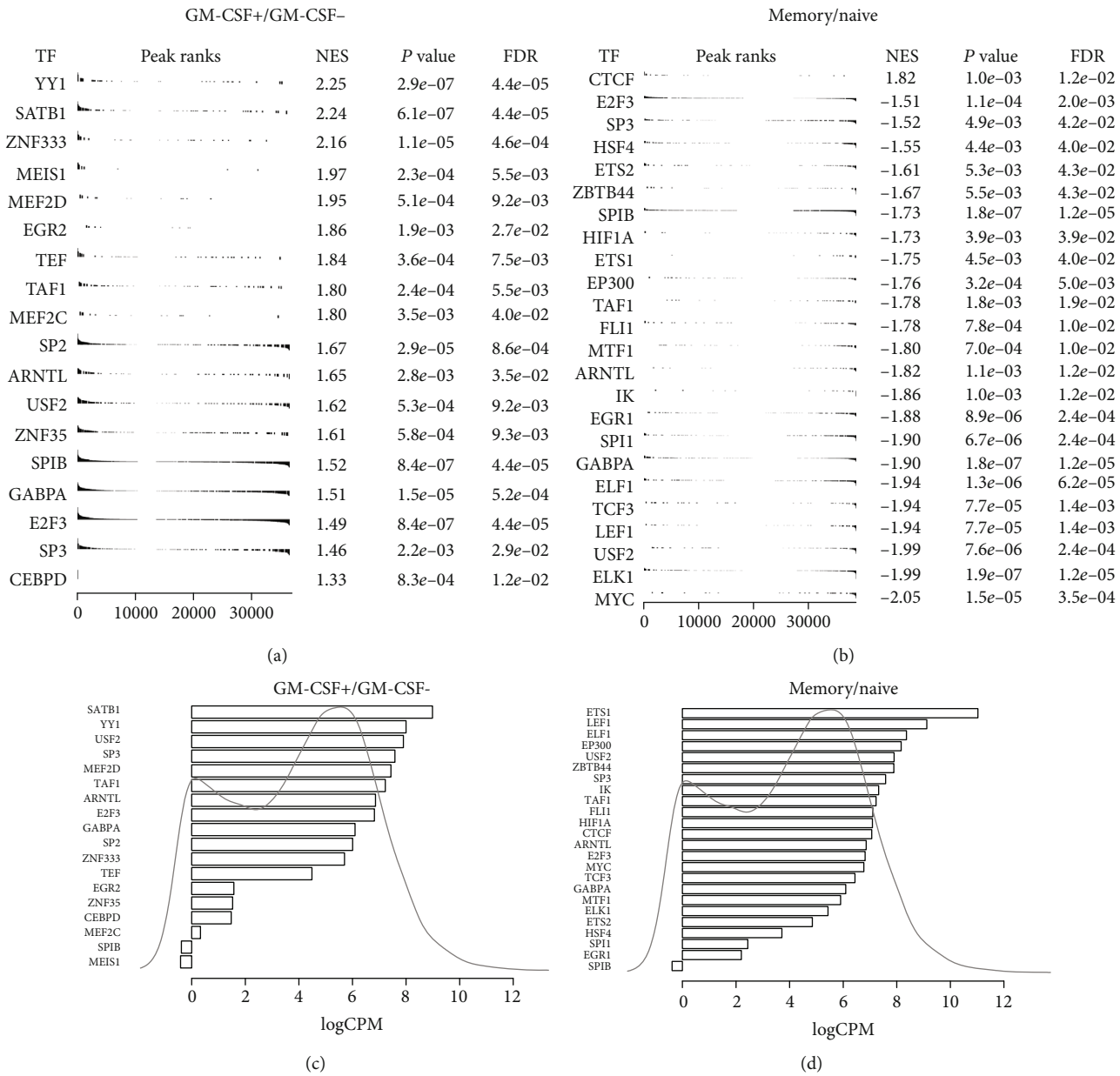

Figure 7: Continued.

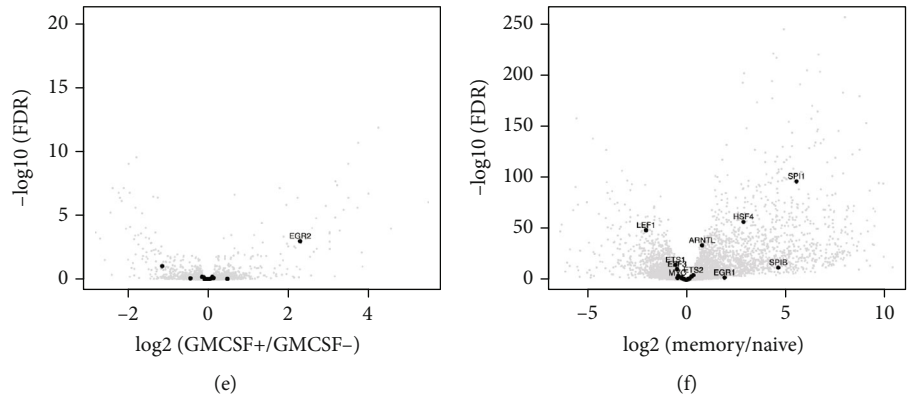

Figure 7: Identification of key TFs with global regulatory effect. (a, b) Rank-based enrichment analysis of TF binding motifs in footprints within peaks that were ranked based on differential accessibility using the $-\log_{10}(\text{FDR}) \times \text{sign}\,(\log_2(\text{fold change}))$ function. The analysis was performed separately for the GM-CSF+/GM-CSF− and memory/naïve cell comparison ((a) and (b), respectively). NES: normalized enrichment score. (c, d) Average expression levels of identified key TFs for both cell comparisons are shown as log (count per million reads). To indicate the relative expression level of these TFs (bars) in view of the spectrum of lowly and highly expressed genes, the scaled kernel density estimate is shown based on the distribution of the average expression of all genes. (e, f) Volcano plots show the differential expression (effect size *vs.* significance) of the TFs identified as key regulators in each of the cell type comparisons (GM-CSF+/GM-CSF− and memory/naïve cell comparison; (e) and (f)). Key TFs are indicated as black dots, and those which are DEGs are labeled with their gene symbol.

3.4. Relationship of Differential Gene Expression and Chromatin Accessibility. Since chromatin accessibility can directly affect gene expression, we next combined the ATAC-seq and RNA-seq data, aiming to identify TFs that may bind to open chromatin regions and hence affect the expression of their target genes. The methods for calling consensus peaks are not trivial. Therefore, we first confirmed that the genes assigned to the consensus peaks defined in this study were enriched for several pathways involved in immune regulation including T cell receptor signaling and Th subset differentiation, as well as for immune-related diseases including MS, RA, and other autoimmune diseases (Supplementary Table S2A, B). Furthermore, the distribution of the consensus peaks (open chromatin regions) defined in our data showed an enrichment for being located in CpG islands, promoters, 5′ UTRs, exons, and protein-coding regions (Figure 6(a)), suggesting that the ATAC-seq data generated here should be well suited to identify TF binding and the expression of corresponding target genes. We first studied the relationship of RNA and chromatin data on a global level: We considered the genes that were both detected on the RNA level and also had an ATAC-seq peak assigned to them. We ranked these genes using the $-\log_{10}(\text{FDR}) \times \text{sign}\,(\log_2(\text{fold change}))$ function separately for the RNA-seq and ATAC-seq data. Next, we visualized the correlation between these two ranks for each contrast (Figures 6(b) and 6(c)). Considering only the genes significantly changing (FDR < 0.05) in the given contrast and assigning them to up- and downregulated categories, we detected more than random coincidence in the direction of the change between the RNA-seq and ATAC-seq data (using Fisher's exact test with Monte Carlo simulation; Figures 6(b) and 6(c)). Increased openness of the chromatin was associated with increased expression of the corresponding gene's RNA for the majority of genes. Less accessible chromatin also coincided with low expression of the corresponding gene in many cases, although a substantial fraction of lowly accessible regions also displayed high expression of the corresponding gene (Figures 6(d) and 6(e)).

3.5. Identification of Key TFs Linked to the Signatures of GM-CSF-Positive and Memory CD4 T Cells. To identify potential TFs that may establish the gene signatures of GM-CSF-positive (versus GM-CSF-negative) and memory (versus naïve) CD4 T cells, we scanned the consensus peaks for footprints, and subsequently, we scanned the identified footprints for TF binding motifs. For motif scanning, we used the TRANSFAC database [47] that contains experimentally validated binding sites, consensus binding sequences (positional weight matrices), and regulated genes of eukaryotic TFs. Confirming the methodology used to identify footprints, they were enriched on the expected ends of the ranked peak lists for the corresponding cell type comparisons (Supplementary Figure S5). Next, we defined the TFs whose binding sites were most enriched in peaks of GM-CSF-positive or memory cells (ranked based on differential accessibility) and identified about 20 TFs each that passed the significance threshold (FDR < 0.05) for enrichment (Figures 7(a) and 7(b)). These lists contained several TFs with a well-known role in T cells, such as SATB1, YY1, ETS, and EGR family TFs, among other factors with a less defined role. Notably, there was only little overlap between the key TFs in GM-CSF-positive and memory cells, suggesting that our strategy may have identified key factors to specifically define the GM-CSF-positive T cell phenotype. The majority of these TFs were highly expressed on the RNA level (Figures 7(c) and 7(d)), falling within the class of highly expressed genes (HEGs) that were suggested to be more likely to be functional than lowly expressed genes [50]. Interestingly however, most of these TFs were not differentially expressed themselves in the cell population comparisons under study (Figures 7(e) and 7(f)), suggesting

that they may be regulated on posttranscriptional levels such as protein phosphorylation and intracellular localization which is well known for many TFs. Hence, with a strategy exploring solely the transcriptome (or even proteome) without integrating ATAC-seq data, several key TFs would likely be missed, while our integrative strategy combining RNA-seq and ATAC-seq data successfully identified such TFs from limited amounts of primary human T cells.

3.6. Integration of RNA-Seq and ATAC-Seq Data Identifies Gene Regulatory Networks of GM-CSF-Positive and Memory CD4 T Cells. Having identified key TFs in GM-CSF-positive and memory CD4 T cells, we were interested whether these factors regulated certain groups of target genes and whether several TFs may act together in a concerted fashion. Some TFs regulated a large number of target genes, and clusters of TFs were grouping together (Supplementary Figure S6A, B). Exploring the cobinding between TFs in more detail showed that certain groups of TFs bound together to the same targets (Supplementary Figure S6C, D). These included the TCF3:LEF1 pair that was always cobinding the same regions, as evident from the memory/naïve CD4 T cell contrast (Supplementary Figure S6B, D). TCF/LEF family proteins act downstream of the Wnt pathway, and it is well known that they often display overlapping expression patterns and functional redundancy [74]. In accordance with our data on human memory and naïve CD4 T cells, binding motifs for TCF family members were recently also determined to be depleted in murine memory CD8 T cells as well as human memory CD4 T cells using ATAC-seq [35, 39].

Finally, by connecting the TFs to the genes assigned to their target regions, we generated a directed gene regulatory network representing GM-CSF-positive (versus negative) and memory (versus naïve) CD4 T cells, respectively (Figure 8). The source nodes were represented by the key TFs as selected above (key TFs from Figures 7(a) and 7(b)), and target nodes were selected when the region was either differentially accessible and/or the mRNA of the assigned gene was differentially expressed in the respective cell population comparisons. Both the GM-CSF and the memory comparisons led to similarly sized networks; however, only some of the target and source nodes were shared between both networks (Figures 8(a)–8(d)).

To quantify the importance of the source nodes in each individual network and to enable comparison of importance between both networks, we calculated scores based on the PageRank algorithm [51]. To do such a calculation on a network where the outgoing edges from a TF reflect its importance, rather than the incoming edges like in the original application of the algorithm, the edges in our networks were inverted (solely for the purpose of calculating the PageRank values). The obtained PageRank values give information on the importance of a node based on the number of other nodes it influences (directly or indirectly). Some of the key TFs that were shared between both networks also had a relatively high PageRank in both networks, such as the TFs E2F3, SPIB, and GABPA (Figures 8(a)–8(d)), and may be general regulators of T cell activation or differentiation. Importantly, we also identified key TFs with a relatively high PageRank in the GM-CSF T cell regulatory network whose PageRank value in the memory/naïve network was 0. These TFs, namely, ZNF35, SP2, SATB1, YY1, TEF, and ZNF333, may, thus, be novel regulators specifically controlling the molecular signatures of GM-CSF-positive CD4 T cells (Figures 8(a)–8(d)).

4. Conclusions and Future Perspectives

In summary, we here provide interpreted high-quality novel RNA-seq and ATAC-seq data from primary human CD4 T cells, with a focus on GM-CSF-positive cells that are known to play an important role in the autoimmune disease MS. We provide a network of key TFs and their targets representing GM-CSF-positive cells and memory CD4 T cells. To our knowledge, this is the first study providing signatures of GM-CSF-secreting cells isolated by capture assay without restimulation, which are likely as similar as currently possible to the state *in vivo* in humans. Recently, others have used a similar approach, capturing IFN-γ, IL-17, and IFN-γ/IL-17 double-positive cells from human donors by cell sorting [75]. Although the authors used restimulation with PMA and ionomycin for 3 hours, the data are especially interesting as they include samples from MS patients [75]. The authors studied only a limited set of 418 genes in the captured IFN-γ- and IL-17-secreting cells, and unfortunately, they did not include GM-CSF-producing cells, while the methods employed in the present work enable genome-wide studies of DNA accessibility and RNA expression patterns in these cells. Nevertheless, the authors obtained important results on the transcriptional signatures of IFN-γ- and IL-17-secreting cells in MS patients, including genes distinguishing clinically stable versus active MS patients. This raises interesting prospects for studying GM-CSF-positive cells specifically from MS patients as well by the methods and comparing to the data resource provided here. This may have important clinical implications given the likely important contribution of GM-CSF-positive CD4 T cells to MS. Future work should also address what distinguishes patterns and contributions of GM-CSF versus IFN-γ- and IL-17-producing T cells, as well as those coproducing GM-CSF and IFN-γ, particularly in MS patients, and ideally even from the affected tissue such as cerebrospinal fluid. However, this is technically challenging due to limitations in the amount of sample. Furthermore, analysis of cytokine producing cells, unfortunately, usually requires artificial restimulation or lengthy cell isolation procedures that may affect the gene signature drastically. Even in our dataset where we avoided artificial restimulation with PMA and ionomycin, dimensionality reduction analysis revealed that the capture assay and column procedure by itself had an effect on the transcriptome, as GM-CSF-positive and negative cells appeared more similar to each other than the GM-CSF-negative cells were to bulk CD4 T cells (which should largely overlap and which also underwent a negative selection for CD4 T cell isolation). On the contrary, ATAC-seq data seemed more robust against such effects, suggesting that the epigenetic signature may be especially suited to reflect *in vivo* patterns less influenced by procedures related to cell

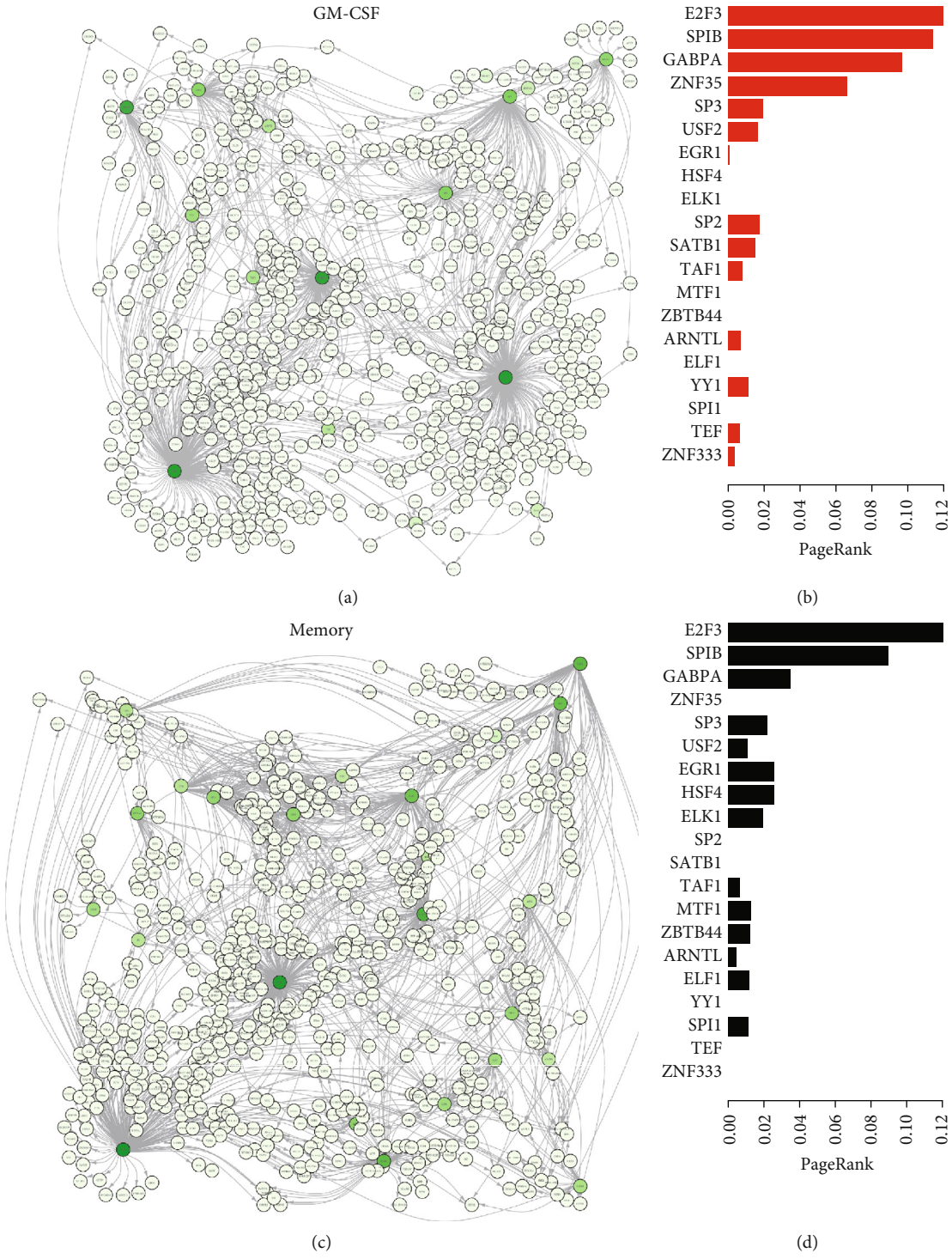

Figure 8: Gene regulatory network of GM-CSF+/GM-CSF− or memory/naïve CD4 T cells. (a, b) Gene regulatory network reflecting the signatures of GM-CSF-positive versus GM-CSF-negative CD4 T cells. (a) A directed network representing binding from source TFs to target peaks assigned to the indicated gene is shown. Source nodes were selected as described (Figure 7, key TFs), and target nodes were selected to be either differentially accessible (as a peak assigned to the respective node gene) and/or to be differentially expressed on the mRNA level in the GM-CSF+/GM-CSF− contrast. To calculate the PageRank [51] as a measure of importance of the TFs (with TFs influencing more genes being more important), the edges were first inverted (not displayed), and the computed PageRank value is represented by the color scale (light to dark green for lower to higher PageRank). (b) Those TFs having a PageRank value higher than the 99-percentile in either the GM-CSF and/or the memory cell network and their corresponding PageRank value in the GM-CSF network are displayed. (c, d) Same as (a, b), but for the memory/naïve CD4 T cell contrast.

sample preparation. Hence, studies on cytokine-producing Th subsets from MS patients should in the future be extended to ATAC-seq and to the GM-CSF-producing Th subset. Interestingly, recent ATAC-seq data from murine GM-CSF versus IFN-γ- and IL-17-producing T cells upon *in vitro* stimulation suggests that while all subsets showed distinct epigenetic profiles, GM-CSF-producing cells were more related to IFN-γ- than to IL-17-producing T cells [10]. With an elegant fate mapping system, that study [10] could also demonstrate that murine GM-CSF-producing T cells display a stable epigenetic imprint. While such fate mapping studies are not possible with human cells, our study provides data from *ex vivo*-isolated human cells that may be most relevant for human diseases and it is tempting to speculate that such epigenetic signatures could be reflected in T cells isolated from MS patients. Together, our data on naïve, memory, and GM-CSF-positive CD4 T cells (and corresponding controls) can be exploited for a multitude of future studies for basic and translational immunology concerning autoimmune diseases. Beyond that, the results may have important implications for other diseases with involvement of GM-CSF-producing cells, such as sepsis and COVID-19. Further, our data can be a testbed for bioinformatics method development for the integration of RNA-seq and ATAC-seq data from the same samples, which may help understanding the basic principles of gene regulation in primary eukaryotic cells.

Data Availability

The datasets are available in the GEO repository under the SuperSeries accession number GSE119734 (with the SubSeries GSE119731 and GSE119732).

Disclosure

The article has been presented as a preprint at bioRxiv, accessible under the following link: https://www.biorxiv.org/content/10.1101/555433v2.

Conflicts of Interest

The authors have no conflict of interest.

Authors' Contributions

S.E. and A.S. designed the project, designed and carried out all the experiments, interpreted results, prepared the figures, and wrote the paper; S.E. designed the computational data analysis pipeline and performed all the data analysis including visualization; D.G.C provided advice for data analysis and feedback on the manuscript; J.T. supervised the research and provided feedback on the manuscript.

Acknowledgments

The authors thank Matilda Eriksson and Peri Noori for performing RNA extractions, library preparation, and quality control for RNA-seq and next-generation sequencing, as well as for their excellent general lab management, Sunjay Jude Fernandes for the reagents and advice for the ATAC-seq protocol, and Gilad Silberberg for the helpful discussions about footprinting and motif scanning (all from Computational Medicine Unit, Karolinska Institute). We thank John Andersson (Translational Immunology Unit, Karolinska Institute) for the helpful suggestions and discussions. This work was supported by Karolinska Institutet's faculty funds for doctoral education (KID funding to S.E.), the Center of Excellence for Research on Inflammation and Cardiovascular Disease (CERIC to A.S. and J.T.), the 7th European Community Framework Programme (FP7-PEOPLE project 326930 to A.S.; FP7-IDEAS-ERC project 617393 to S.E., A.S., J.T., and D.G.C.; and FP7-HEALTH project 306000 to J.T. and D.G.C.), Vetenskapsrådet Medicine and Health (2011-3264 to J.T.), and Torsten Söderberg Foundation (to J.T.).

Supplementary Materials

contain the following Figures and Tables: Supplementary Table S1A: disease enrichment analysis based on the gene list ranked by gene expression in GM-CSF-positive CD4 T cells (versus GM-CSF-negative CD4 T cells). Supplementary Table S1B: disease enrichment analysis based on the gene list ranked by gene expression in memory (versus naïve) CD4 T cells. Supplementary Table S2A: KEGG pathway enrichment analysis of genes assigned to consensus peaks. Supplementary Table S2B: GWAS catalog disease enrichment analysis of genes assigned to consensus peaks. Supplementary Figure S1: purity of cell populations used in this study. Supplementary Figure S2: expression profile and DNA accessibility signatures of human memory CD4 T cells. Supplementary Figure S3: comparison of published and novel naïve and memory T cell transcriptome data. Supplementary Figure S4: cytokine coexpression in GM-CSF-producing T cells. Supplementary Figure S5: enrichment of footprints across peaks ranked based on differential accessibility. Supplementary Figure S6: network structure identifying shared TF binders across peaks and shared targets of key TFs. *(Supplementary Materials)*

References

[1] J. Geginat, M. Paroni, F. Facciotti et al., "The CD4-centered universe of human T cell subsets," *Seminars in Immunology*, vol. 25, no. 4, pp. 252–262, 2013.

[2] J. Geginat, M. Paroni, S. Maglie et al., "Plasticity of human CD4 T cell subsets," *Frontiers in Immunology*, vol. 5, p. 630, 2014.

[3] T. Caza and S. Landas, "Functional and phenotypic plasticity of CD4+ T cell subsets," *BioMed Research International*, vol. 2015, Article ID 521957, 13 pages, 2015.

[4] J. L. McQualter, R. Darwiche, C. Ewing et al., "Granulocyte macrophage colony-stimulating factor: a new putative therapeutic target in multiple sclerosis," *The Journal of Experimental Medicine*, vol. 194, no. 7, pp. 873–882, 2001.

[5] I. A. Ferber, S. Brocke, C. Taylor-Edwards et al., "Mice with a disrupted IFN-gamma gene are susceptible to the induction of experimental autoimmune encephalomyelitis (EAE)," *Journal of Immunology*, vol. 156, pp. 5–7, 1996.

[6] S. Haak, A. L. Croxford, K. Kreymborg et al., "IL-17A and IL-17F do not contribute vitally to autoimmune neuroinflammation in mice," *The Journal of Clinical Investigation*, vol. 119, pp. 61–69, 2009.

[7] E. D. Ponomarev, L. P. Shriver, K. Maresz, J. Pedras-Vasconcelos, D. Verthelyi, and B. N. Dittel, "GM-CSF production by autoreactive T cells is required for the activation of microglial cells and the onset of experimental autoimmune encephalomyelitis," *The Journal of Immunology*, vol. 178, pp. 39–48, 2006.

[8] L. Codarri, G. Gyülvészi, V. Tosevski et al., "RORγt drives production of the cytokine GM-CSF in helper T cells, which is essential for the effector phase of autoimmune neuroinflammation," *Nature Immunology*, vol. 12, no. 6, pp. 560–567, 2011.

[9] W. Sheng, F. Yang, Y. Zhou et al., "STAT5 programs a distinct subset of GM-CSF-producing T helper cells that is essential for autoimmune neuroinflammation," *Cell Research*, vol. 24, no. 12, pp. 1387–1402, 2014.

[10] J. Komuczki, S. Tuzlak, E. Friebel et al., "Fate-mapping of GM-CSF expression identifies a discrete subset of inflammation-driving T helper cells regulated by cytokines IL-23 and IL-1β," *Immunity*, vol. 50, no. 5, pp. 1289–1304.e6, 2019.

[11] R. Noster, R. Riedel, M.-F. Mashreghi et al., "IL-17 and GM-CSF expression are antagonistically regulated by human T helper cells," *Science Translational Medicine*, vol. 6, no. 241, article 241ra80, 2014.

[12] S. M. Restorick, L. Durant, S. Kalra et al., "CCR6 + Th cells in the cerebrospinal fluid of persons with multiple sclerosis are dominated by pathogenic non-classic Th1 cells and GM-CSF-only-secreting Th cells," *Brain, Behavior, and Immunity*, vol. 64, pp. 71–79, 2017.

[13] F. J. Hartmann, M. Khademi, J. Aram et al., "Multiple sclerosis-associated *IL2RA* polymorphism controls GM-CSF production in human T_H cells," *Nature Communications*, vol. 5, no. 1, article 5056, 2014.

[14] E. Galli, F. J. Hartmann, B. Schreiner et al., "GM-CSF and CXCR4 define a T helper cell signature in multiple sclerosis," *Nature Medicine*, vol. 25, no. 8, pp. 1290–1300, 2019.

[15] C. Piper, A. M. Pesenacker, D. Bending et al., "Brief report: T cell expression of granulocyte-macrophage colony-stimulating factor in juvenile arthritis is contingent upon Th17 plasticity," *Arthritis & Rhematology*, vol. 66, no. 7, pp. 1955–1960, 2014.

[16] I. P. Wicks and A. W. Roberts, "Targeting GM-CSF in inflammatory diseases," *Nature Reviews Rheumatology*, vol. 12, no. 1, pp. 37–48, 2016.

[17] H. Huang, S. Wang, T. Jiang et al., "High levels of circulating GM-CSF+CD4+ T cells are predictive of poor outcomes in sepsis patients: a prospective cohort study," *Cellular & Molecular Immunology*, vol. 16, no. 6, pp. 602–610, 2019.

[18] Y. Zhou, B. Fu, X. Zheng et al., "Pathogenic T-cells and inflammatory monocytes incite inflammatory storms in severe COVID-19 patients," *National Science Review*, vol. 7, no. 6, pp. 998–1002, 2020.

[19] Z. Chen and E. John Wherry, "T cell responses in patients with COVID-19," *Nature Reviews Immunology*, vol. 20, no. 9, pp. 529–536, 2020.

[20] N. Vabret, G. J. Britton, C. Gruber et al., "Immunology of COVID-19: current state of the science," *Immunity*, vol. 52, no. 6, pp. 910–941, 2020.

[21] F. M. Lang, K. M. C. Lee, J. R. Teijaro, B. Becher, and J. A. Hamilton, "GM-CSF-based treatments in COVID-19: reconciling opposing therapeutic approaches," *Nature Reviews Immunology*, vol. 20, no. 8, pp. 507–514, 2020.

[22] Y. Lee, A. Awasthi, N. Yosef et al., "Induction and molecular signature of pathogenic TH17 cells," *Nature Immunology*, vol. 13, no. 10, pp. 991–999, 2012.

[23] C. Wu, N. Yosef, T. Thalhamer et al., "Induction of pathogenic TH17 cells by inducible salt-sensing kinase SGK1," *Nature*, vol. 496, no. 7446, pp. 513–517, 2013.

[24] M. el-Behi, B. Ciric, H. Dai et al., "The encephalitogenicity of T_H17 cells is dependent on IL-1- and IL-23-induced production of the cytokine GM-CSF," *Nature Immunology*, vol. 12, no. 6, pp. 568–575, 2011.

[25] C. E. Zielinski, "Autoimmunity beyond Th17: GM-CSF producing T cells," *Cell Cycle*, vol. 13, no. 16, pp. 2489-2490, 2014.

[26] Y. Cao, B. A. Goods, K. Raddassi et al., "Functional inflammatory profiles distinguish myelin-reactive T cells from patients with multiple sclerosis," *Science Translational Medicine*, vol. 7, no. 287, article 287ra74, 2015.

[27] S. Éliás, A. Schmidt, V. Kannan, J. Andersson, and J. Tegnér, "TGF-β affects the differentiation of human GM-CSF$^+$ CD4$^+$ T cells in an activation- and sodium-dependent manner," *Frontiers in Immunology*, vol. 7, p. 603, 2016.

[28] J. D. Buenrostro, P. G. Giresi, L. C. Zaba, H. Y. Chang, and W. J. Greenleaf, "Transposition of native chromatin for fast and sensitive epigenomic profiling of open chromatin, DNA-binding proteins and nucleosome position," *Nature Methods*, vol. 10, no. 12, pp. 1213–1218, 2013.

[29] J. T. Chang, E. J. Wherry, and A. W. Goldrath, "Molecular regulation of effector and memory T cell differentiation," *Nature Immunology*, vol. 15, no. 12, pp. 1104–1115, 2014.

[30] P. Durek, K. Nordström, G. Gasparoni et al., "Epigenomic profiling of human CD4(+) T cells supports a linear differentiation model and highlights molecular regulators of memory development," *Immunity*, vol. 45, no. 5, pp. 1148–1161, 2016.

[31] D. R. Sen, J. Kaminski, R. A. Barnitz et al., "The epigenetic landscape of T cell exhaustion," *Science*, vol. 354, no. 6316, pp. 1165–1169, 2016.

[32] J. P. Scott-Browne, I. F. López-Moyado, S. Trifari et al., "Dynamic changes in chromatin accessibility occur in CD8+ T cells responding to viral infection," *Immunity*, vol. 45, no. 6, pp. 1327–1340, 2016.

[33] G. P. Mognol, R. Spreafico, V. Wong et al., "Exhaustion-associated regulatory regions in CD8$^+$ tumor-infiltrating T cells," *Proceedings of the National Academy of Sciences of the United States of America*, vol. 114, no. 13, pp. E2776–E2785, 2017.

[34] C. D. Scharer, A. P. R. Bally, B. Gandham, and J. M. Boss, "Cutting edge: chromatin accessibility programs CD8 T cell memory," *Journal of Immunology*, vol. 198, no. 6, pp. 2238–2243, 2017.

[35] B. Yu, K. Zhang, J. J. Milner et al., "Epigenetic landscapes reveal transcription factors that regulate CD8+ T cell differentiation," *Nature Immunology*, vol. 18, no. 5, pp. 573–582, 2017.

[36] K. Qu, L. C. Zaba, P. G. Giresi et al., "Individuality and variation of personal regulomes in primary human T cells," *Cell Systems*, vol. 1, no. 1, pp. 51–61, 2015.

[37] E. Gensterblum, P. Renauer, P. Coit et al., "CD4+CD28+KIR+CD11a(hi) T cells correlate with disease activity and are characterized by a pro-inflammatory

epigenetic and transcriptional profile in lupus patients," *Journal of Autoimmunity*, vol. 86, pp. 19–28, 2018.

[38] Y. Kitagawa, N. Ohkura, Y. Kidani et al., "Guidance of regulatory T cell development by Satb1-dependent super-enhancer establishment," *Nature Immunology*, vol. 18, no. 2, pp. 173–183, 2016.

[39] A. T. Satpathy, N. Saligrama, J. D. Buenrostro et al., "Transcript-indexed ATAC-seq for precision immune profiling," *Nature Medicine*, vol. 24, no. 5, pp. 580–590, 2018.

[40] R. E. Gate, C. S. Cheng, A. P. Aiden et al., "Genetic determinants of co-accessible chromatin regions in activated T cells across humans," *Nature Genetics*, vol. 50, no. 8, pp. 1140–1150, 2018.

[41] S. Heinz, C. Benner, N. Spann et al., "Simple combinations of lineage-determining transcription factors prime cis-regulatory elements required for macrophage and B cell identities," *Molecular Cell*, vol. 38, no. 4, pp. 576–589, 2010.

[42] Y. Liao, G. K. Smyth, and W. Shi, "featureCounts: an efficient general purpose program for assigning sequence reads to genomic features," *Bioinformatics*, vol. 30, no. 7, pp. 923–930, 2014.

[43] M. D. Robinson, D. J. McCarthy, and G. K. Smyth, "edgeR: a Bioconductor package for differential expression analysis of digital gene expression data," *Bioinformatics*, vol. 26, no. 1, pp. 139-140, 2010.

[44] K. D. Hansen, R. A. Irizarry, and Z. Wu, "Removing technical variability in RNA-seq data using conditional quantile normalization," *Biostatistics*, vol. 13, no. 2, pp. 204–216, 2012.

[45] J. Piper, M. C. Elze, P. Cauchy, P. N. Cockerill, C. Bonifer, and S. Ott, "Wellington: a novel method for the accurate identification of digital genomic footprints from DNase-seq data," *Nucleic Acids Research*, vol. 41, no. 21, pp. e201–e201, 2013.

[46] S. Neph, J. Vierstra, A. B. Stergachis et al., "An expansive human regulatory lexicon encoded in transcription factor footprints," *Nature*, vol. 489, no. 7414, pp. 83–90, 2012.

[47] V. Matys, O. V. Kel-Margoulis, E. Fricke et al., "TRANSFAC and its module TRANSCompel: transcriptional gene regulation in eukaryotes," *Nucleic Acids Research*, vol. 34, no. 90001, pp. D108–D110, 2006.

[48] A. Subramanian, P. Tamayo, V. K. Mootha et al., "Gene set enrichment analysis: a knowledge-based approach for interpreting genome-wide expression profiles," *Proceedings of the National Academy of Sciences of the United States of America*, vol. 102, no. 43, pp. 15545–15550, 2005.

[49] G. Korotkevich, V. Sukhov, N. Budin, B. Shpak, M. N. Artyomov, and A. Sergushichev, "Fast gene set enrichment analysis," *BioRxiv*, 2021.

[50] D. Hebenstreit, M. Fang, M. Gu, V. Charoensawan, A. van Oudenaarden, and S. A. Teichmann, "RNA sequencing reveals two major classes of gene expression levels in metazoan cells," *Molecular Systems Biology*, vol. 7, no. 1, p. 497, 2011.

[51] L. Page, S. Brin, R. Motwani, and T. Winograd, *The PageRank Citation Ranking: Bringing Order to the Web*, Tech Report, Stanford Digit Libr Technol Proj, 1998.

[52] C. G. Danko, L. A. Choate, B. A. Marks et al., "Dynamic evolution of regulatory element ensembles in primate $CD4^+$ T cells," *Nature Ecology & Evolution*, vol. 2, no. 3, pp. 537–548, 2018.

[53] A. Okhrimenko, J. R. Grun, K. Westendorf et al., "Human memory T cells from the bone marrow are resting and maintain long-lasting systemic memory," *Proceedings of the National Academy of Sciences of the United States of America*, vol. 111, no. 25, pp. 9229–9234, 2014.

[54] K. Westendorf, A. Okhrimenko, J. R. Grün et al., "Unbiased transcriptomes of resting human $CD4^+$ $CD45RO^+$ T lymphocytes," *European Journal of Immunology*, vol. 44, no. 6, pp. 1866–1869, 2014.

[55] L. Maatenvan der and G. Hinton, "Visualizing data using t-SNE," *Journal of Machine Learning Research*, vol. 9, pp. 2579–2605, 2008.

[56] J. Rasouli, B. Ciric, J. Imitola et al., "Expression of GM-CSF in T cells is increased in multiple sclerosis and suppressed by IFN-β therapy," *Journal of Immunology*, vol. 194, no. 11, pp. 5085–5093, 2015.

[57] M. Podtschaske, U. Benary, S. Zwinger, T. Hofer, A. Radbruch, and R. Baumgrass, "Digital NFATc2 activation per cell transforms graded T cell receptor activation into an all-or-none IL-2 expression," *PLoS One*, vol. 2, no. 9, article e935, 2007.

[58] P. Anderson, "Post-transcriptional control of cytokine production," *Nature Immunology*, vol. 9, no. 4, pp. 353–359, 2008.

[59] C. Y. Chen, R. Gherzi, S. E. Ong et al., "AU binding proteins recruit the exosome to degrade ARE-containing mRNAs," *Cell*, vol. 107, no. 4, pp. 451–464, 2001.

[60] G. Shaw and R. Kamen, "A conserved AU sequence from the 3′ untranslated region of GM-CSF mRNA mediates selective mRNA degradation," *Cell*, vol. 46, no. 5, pp. 659–667, 1986.

[61] D. Schafflick, C. A. Xu, M. Hartlehnert et al., "Integrated single cell analysis of blood and cerebrospinal fluid leukocytes in multiple sclerosis," *Nature Communications*, vol. 11, no. 1, p. 247, 2020.

[62] M. H. al-Mossawi, L. Chen, H. Fang et al., "Unique transcriptome signatures and GM-CSF expression in lymphocytes from patients with spondyloarthritis," *Nature Communications*, vol. 8, no. 1, p. 1510, 2017.

[63] N. Beliakova-Bethell, M. Massanella, C. White et al., "The effect of cell subset isolation method on gene expression in leukocytes," *Cytometry. Part A*, vol. 85, no. 1, pp. 94–104, 2014.

[64] M. T. Wong, D. E. H. Ong, F. S. H. Lim et al., "A high-dimensional atlas of human T cell diversity reveals tissue-specific trafficking and cytokine signatures," *Immunity*, vol. 45, no. 2, pp. 442–456, 2016.

[65] H. Liu, M. Rhodes, D. L. Wiest, and D. A. Vignali, "On the dynamics of TCR:CD3 complex cell surface expression and downmodulation," *Immunity*, vol. 13, no. 5, pp. 665–675, 2000.

[66] C. Vogel and E. M. Marcotte, "Insights into the regulation of protein abundance from proteomic and transcriptomic analyses," *Nature Reviews Genetics*, vol. 13, no. 4, pp. 227–232, 2012.

[67] F. Edfors, F. Danielsson, B. M. Hallström et al., "Gene-specific correlation of RNA and protein levels in human cells and tissues," *Molecular Systems Biology*, vol. 12, no. 10, p. 883, 2016.

[68] D. Carvalho-Silva, A. Pierleoni, M. Pignatelli et al., "Open targets platform: new developments and updates two years on," *Nucleic Acids Research*, vol. 47, no. D1, pp. D1056–D1065, 2019.

[69] A. Nylander and D. A. Hafler, "Multiple sclerosis," *The Journal of Clinical Investigation*, vol. 122, no. 4, pp. 1180–1188, 2012.

[70] International Multiple Sclerosis Genetics Consortium (IMSGC), A. H. Beecham, N. A. Patsopoulos et al., "Analysis of immune-related loci identifies 48 new susceptibility variants for multiple sclerosis," *Nature Genetics*, vol. 45, no. 11, pp. 1353–1360, 2013.

[71] International Multiple Sclerosis Genetics Consortium, Wellcome Trust Case Control Consortium 2, S. Sawcer et al., "Genetic risk and a primary role for cell-mediated immune mechanisms in multiple sclerosis," *Nature*, vol. 476, no. 7359, pp. 214–219, 2011.

[72] J. D. Buenrostro, B. Wu, U. M. Litzenburger et al., "Single-cell chromatin accessibility reveals principles of regulatory variation," *Nature*, vol. 523, no. 7561, pp. 486–490, 2015.

[73] D. A. Cusanovich, R. Daza, A. Adey et al., "Multiplex single-cell profiling of chromatin accessibility by combinatorial cellular indexing," *Science*, vol. 348, no. 6237, pp. 910–914, 2015.

[74] D. Hrckulak, M. Kolar, H. Strnad, and V. Korinek, "TCF/LEF transcription factors: an update from the internet resources," *Cancers*, vol. 8, no. 7, article E70, p. 70, 2016.

[75] D. Hu, S. Notarbartolo, T. Croonenborghs et al., "Transcriptional signature of human pro-inflammatory TH17 cells identifies reduced IL10 gene expression in multiple sclerosis," *Nature Communications*, vol. 8, no. 1, p. 1600, 2017.

Hindawi
Journal of Immunology Research
Volume 2021, Article ID 8887437, 10 pages
https://doi.org/10.1155/2021/8887437

Research Article

Hypoxia-Induced Autophagy Enhances Cisplatin Resistance in Human Bladder Cancer Cells by Targeting Hypoxia-Inducible Factor-1α

Xiawa Mao,[1] Nanzhang,[1] Jiaquao Xiao,[1] Huifeng Wu,[1] and Kefeng Ding[2]

[1]*Urology Department, The 2nd Affiliated Hospital of Zhejiang University, School of Medicine, Hangzhou, Zhejiang Province 310000, China*
[2]*Oncology Department, The 2nd Affiliated Hospital of Zhejiang University, School of Medicine, Hangzhou, Zhejiang Province 310000, China*

Correspondence should be addressed to Kefeng Ding; dingkefeng@zju.edu.cn

Received 6 August 2020; Revised 11 December 2020; Accepted 4 February 2021; Published 17 February 2021

Academic Editor: Xinyi Tang

Copyright © 2021 Xiawa Mao et al. This is an open access article distributed under the Creative Commons Attribution License, which permits unrestricted use, distribution, and reproduction in any medium, provided the original work is properly cited.

Purpose. To investigate the effect of hypoxia on chemoresistance and the underlying mechanism in bladder cancer cells. *Methods*. BIU-87 bladder cancer cell line was treated with cisplatin under hypoxic and normoxic conditions and tested using 3-(4,5-dimethylthiazol-2-yl)-2,5-diphenyltetrazolium bromide (MTT) assay, flow cytometry, and Western blotting. All the data were expressed as mean ± standard error from three independent experiments and analyzed by multiple *t*-tests. *Results*. Apoptosis of bladder cancer cells caused by cisplatin was attenuated in hypoxic conditions. Hypoxia enhanced autophagy caused by cisplatin. The autophagy inhibitor and HIF-1α inhibitor can reverse the chemoresistance in hypoxic condition. Apoptosis and autophagy of bladder cancer cells were downregulated by HIF-1α inhibitor YC-1. Hypoxia-induced autophagy enhanced chemoresistance to cisplatin via the HIF-1 signaling pathway. *Conclusion*. Resistance to cisplatin in BIU-87 bladder cancer cells under hypoxic conditions can be explained by activation of autophagy, which is regulated by HIF-1α-associated signaling pathways. The hypoxia–autophagy pathway may be a target for improving the efficacy of cisplatin chemotherapy in bladder cancer.

1. Introduction

Bladder cancer is the second most common genitourinary tumor and the fifth most common cause of cancer-related deaths in men in western countries [1]. Platinum-based systemic chemotherapy is important in the treatment of bladder cancer [2]. However, the general outcome is still unsatisfactory. Drug resistance continues to be a pivotal obstacle that limits the ideal therapeutic effects in patients with bladder cancer. In recent decades, much work has been done to attenuate the drug resistance and develop novel treatments that are less susceptible to resistance [3]. The mechanism for drug resistance can be ascribed to various factors, including altered drug sites, more effective DNA repair mechanisms, drug efflux and metabolism, pharmacokinetics, tumor microenvironment, and stress-induced genetic or epigenetic alterations in response to drug exposure [4]. Among the above reasons, hypoxic tumor microenvironment has to be taken into consideration. Carcinogenesis is closely related to the hypoxic environment within tumor tissues. Hypoxia-inducible factor- (HIF-) 1α, the most elevated protein stimulated by lack of oxygen, is widely expressed in tissues and cells [5]. According to recent literature, chemoresistance is largely due to expression and activation of HIF-1α [6].

Autophagy occurs extensively in eukaryotes and is an evolutionarily conserved process in which intracellular proteins and organelles are sequestered in autophagosomes, which are specialized double-membrane-containing vacuoles [7]. Through autophagy, tumors can counteract different kinds of adverse conditions, including hypoxia [8]. Under starvation or hypoxic conditions, cells are capable of eliminating excessive proteins and organelles, which may

maintain homeostasis and facilitate cycling and reutilization of amino acids. It has been proved that HIF-1α has an intimate relationship with intracellular autophagy caused by a shortage of oxygen. HIF-1α can regulate hypoxia-induced autophagy by manipulating expression of downstream targeting genes BNIP3 and BNIP3L, inducing autophagy by interfering with the interaction between Beclin-1, Bcl-2, and BCL-XL [9, 10].

Bladder urothelial carcinoma is an active metabolic tumor with a higher oxygen consumption than healthy tissue has. As a result, the tumor tissue is partially in a hypoxic environment. However, little work has been performed on the relationship between chemoresistance and hypoxia in bladder cancer. Here, we investigated the influence of low oxygen microenvironment on chemoresistance to cisplatin in bladder cancer cells and tried to explain the underlying mechanism. This study is aimed at revealing how hypoxia and autophagy interact with each other to mediate cisplatin resistance in bladder cancer cells.

2. Materials and Methods

2.1. Cell Culture. The BIU-87 bladder cancer cell line was purchased from Kunming Cell Bank, Chinese Academy of Sciences. BIU-87 cells were initially cultured in RPMI 1640 medium (Gibco, CA, USA) and incubated with 10% fetal bovine serum (Cyclones, Logan, UT, USA) and penicillin/streptomycin (Gibco) at 37°C in 5% CO_2 atmosphere.

2.2. Ethics Statement. Human tissues and samples were not required in this study. All work presented has been performed in well-established, commercially available cell lines.

2.3. Treatment of Cells. BIU-87 cells were treated with different concentrations of cisplatin (Sigma–Aldrich, St. Louis, MO, USA) for hours or days to perform the 3-(4,5-dimethylthiazol-2-yl)-2,5-diphenyltetrazolium bromide (MTT) assay. These cells were grown in 20% or 1% O_2 and 5% CO_2 atmosphere, respectively. To observe the effect of 3-methyladenine (3-MA; Selleck Chemicals, Houston, TX, USA) or lificiguat (YC-1; Selleck Chemicals), BIU-87 cells were first cultured in 96-well or 6-well plates for 24 h and then cisplatin and inhibitors were added for a further 24 h. These cells were cultured in 20% or 1% O_2 and 5% CO_2 atmosphere in hypoxic incubator (Thermo Fisher 3111). Samples were collected and analyzed by Western blotting, as described below.

2.4. MTT Assay. Cell viability after treatment was investigated by MTT assay. Cells (5000/well, 100 μl medium) were cultured in a 96-well plate (Corning, Corning, NY, USA), and after treatment, 20 μl MTT was added (5 mg/mL in PBS) and incubated for 4 h at 37°C. We removed the medium and MTT solution, added 100 μl dimethyl sulfoxide (Sigma–Aldrich), and measured at 490 nm by ELISA Plate Readers (BioTek, Winooski, VT, USA).

2.5. Flow Cytometry. Cells after treatment were collected and washed in PBS 3 times. They were resuspended in loading buffer (Sangon Biotech, Shanghai, China) to 2×105 to 5×105 cells/mL. For apoptosis and autophagy analysis, Annexin V-FITC/PI kit (Sangon Biotech) and monodansylcadaverine (MDC) kit (Beijing Solarbio Science & Technology Co. Ltd., Beijing, China) were utilized, respectively. BD FACSCanto™ II system (BD Biosciences, San Jose, CA, USA) was utilized to detect cell surface markers. All the results were analyzed by the FlowJo software.

2.6. MDC Fluorescence Staining. BIU-87 cells grown on coverslips were used for MDC fluorescence staining. The cells were cultured in 20% or 1% O_2 and 5% CO_2 atmosphere. Coverslips were soaked in 75% ethanol overnight and washed in PBS (Sangon Biotech) 3 times. The coverslips were put in 6-well plates (Corning), and cell suspension was added. One day later, we added cisplatin and inhibitors to the cells for a further day and removed the coverslips with the cells and washed in PBS 3 times. Cells were fixed with 4% paraformaldehyde (Sangon Biotech) for 30 min at room temperature and washed in PBS 3 times. The cells were incubated with 10% MDC for 30 min and washed in PBS 3 times. All the images were photographed by Leica DM4000B microscope (Leica, IL, USA).

2.7. Western Blotting. Cells were lysed in RIPA buffer (Beyotime Biotechnology, Shanghai, China) containing protease and phosphatase inhibitor cocktails (Thermo Fisher Scientific, Waltham, MA, USA). The protein concentration of the samples was quantified by the BCA assay kit (Beyotime Biotechnology), and equal amounts of protein were loaded on 10% SDS-PAGE and transferred to polyvinylidene difluoride membrane (Millipore, Billerica, MA, USA). The membranes were blocked with 5% nonfat milk for 1 h and incubated with primary antibody overnight at 4°C. The following primary antibodies were used to detect proteins: rabbit anti-Beclin-1 polyclonal antibody (1 : 500; Affinity, Canal Fulton, OH, USA), rabbit anti-ATG 5 polyclonal antibody (1 : 500, Affinity, OH, USA), mouse anti-HIF-1A monoclonal antibody (1 : 500; Affinity), and rabbit anti-caspase-3 polyclonal antibody (1 : 500; Proteintech, Wuhan, China). The membranes were incubated with a goat anti-rabbit IgG conjugated to horseradish peroxidase (1 : 1000; Beyotime) or a goat anti-mouse IgG conjugated to horseradish peroxidase (1 : 1000; Beyotime) for 1 h. Incubation with a mouse anti-β-actin monoclonal antibody (1 : 1000; Abcam, Cambridge, UK) was performed as the loading sample control. The blots were detected using Clarity MAX™ Western ECL Substrate (BioRad, Hercules, CA, USA) by ChemiDoc™ XRS+ System (BioRad).

2.8. Statistical Analysis. All the data were expressed as mean ± standard error from three independent experiments and analyzed by multiple t-tests. Data were graphically displayed using GraphPad Prism version 6.0 (GraphPad Software, La Jolla, CA, USA). A p value <0.05 was considered statistically significant for all the analyses.

3. Results

3.1. Hypoxia Induced Chemoresistance in BIU-87 Bladder Cancer Cells. Resistance to chemotherapeutic agents is a pivotal obstacle that is encountered in the chemotherapy of

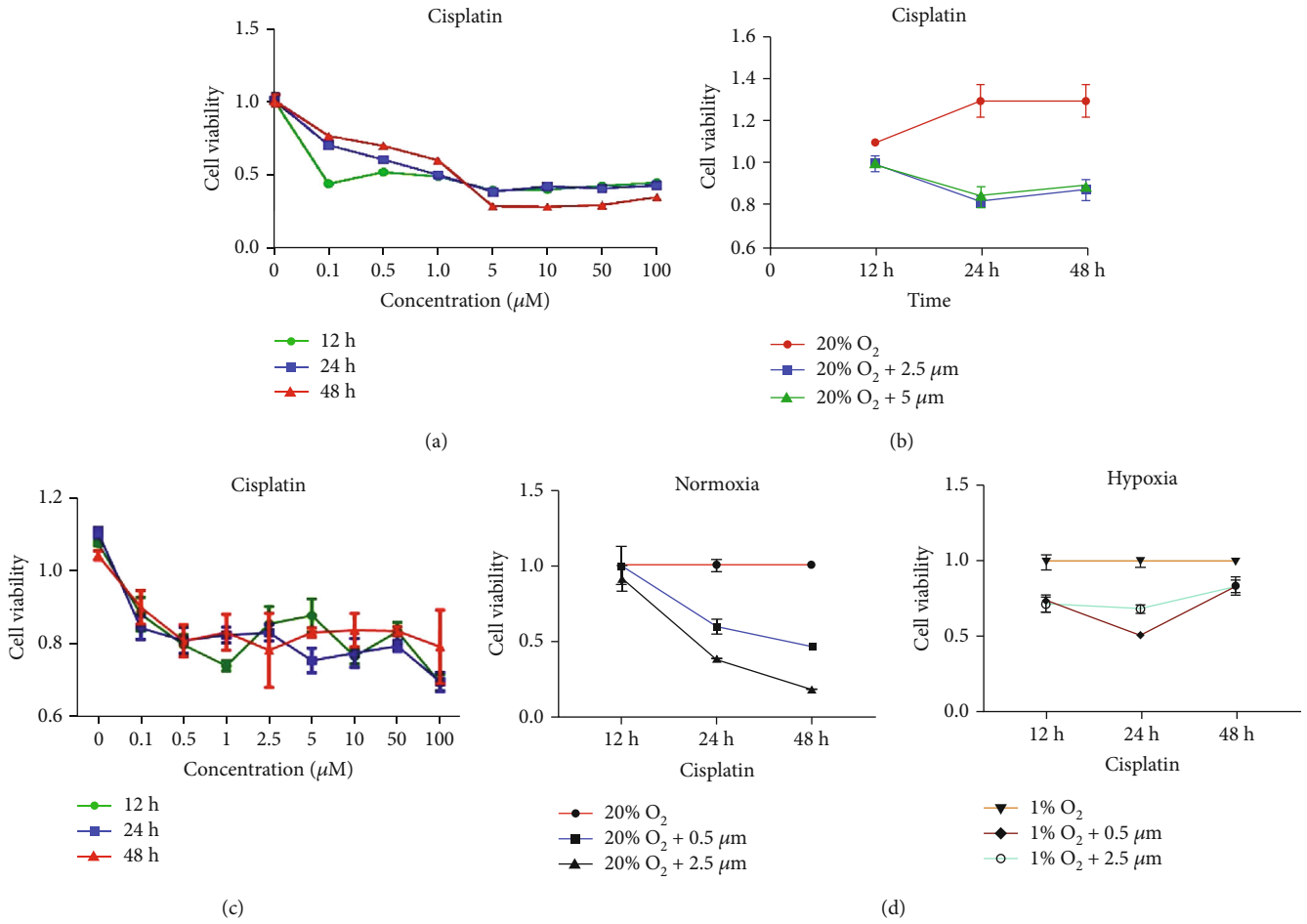

Figure 1: Hypoxia reduced chemosensitivity of bladder cancer cells to cisplatin. (a) Viability of bladder cancer cells was measured after treatment with graded concentrations of cisplatin at 12, 24, and 48 h. (b) Cell viability was further observed after treatment with 2.5 and 5.0 μm cisplatin under normoxia. (c) BIU-87 cancer cells were cultured under hypoxic conditions with different concentrations of cisplatin for 12, 24, and 48 h. (d) Viability of cells incubated with cisplatin was reversed under hypoxia compared with that under normoxia.

urological tumors [11]. To explore the exact mechanisms behind this resistance, we designed experiments to observe the difference in cell growth in normoxic and hypoxic conditions, which were defined as 5% CO_2 with 20% O_2 and 5% CO_2 with 1% O_2, respectively. BIU-87 cancer cells were maintained in complete medium under normoxia and hypoxia and incubated with graded concentrations of cisplatin. At 12 h, the cell proliferation rate was decreased by cisplatin, but the trend was not apparent with the increase in drug concentration. At 24 and 48 h, the cell inhibition rate was increased in a dose-dependent manner after cisplatin treatment. The trend became more evident at concentrations above 5 μM cisplatin and influencing cell proliferation (Figure 1(a)). Due to the significant change in inhibition rates, the concentration refinement experiments at 2.5 μM and 5 μM were further performed. The inhibition rates of BIU-87 cells were similar between 2.5 and 5 μM cisplatin (Figure 1(b)). Therefore, 2.5 μM was selected for the next experiment.

The inhibition rate of cisplatin fluctuated about 20% with increase in concentration when BIU-87 cells were cultured under hypoxic conditions (Figure 1(c)). However, little changes at 100 μM concentration and irregular changes at 12 h were observed simultaneously. With the same concentration of cisplatin, the inhibition rate of BIU-87 cells under hypoxia was significantly downregulated compared with that under normoxia (Figure 1(d)), indicating that cisplatin resistance may have been induced by hypoxia in BIU-87 cells.

3.2. Flow Cytometry Verified Chemoresistance of BIU-87 Cells to Cisplatin. Cisplatin-induced death in bladder cancer cells involves multiple signaling pathways. Among these pathways, mitochondrial apoptosis plays a central role. The MTT assay inferred that chemotherapeutic agents and hypoxia have definite effects on the viability of BIU-87 cells. To elucidate the cause of this phenomenon, we investigated the effects of drugs on apoptosis. Flow cytometry demonstrated that apoptosis rate was significantly increased (16.2–31.3% at 24 h to 9–14.6% at 48 h) with increase of drug concentration under normoxia. In contrast, the apoptosis rate increased slightly with increase of drug concentration (36–46.7% at 24 h to 32.6–34.2% at 48 h) under hypoxia. After 48 h treatment, the apoptosis rate was not significantly different from that under normoxia. After treatment

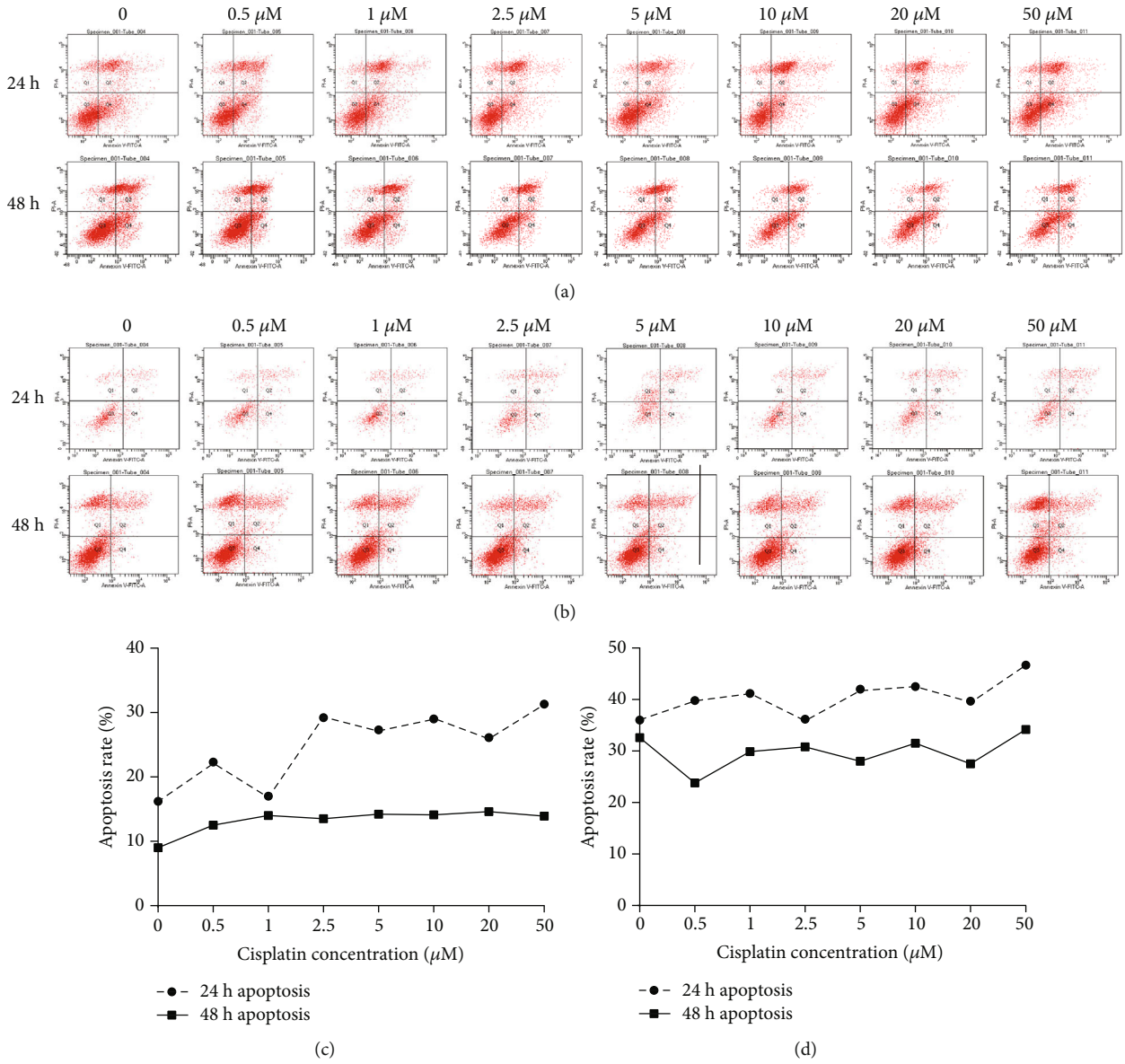

Figure 2: Effects of cisplatin on apoptosis of bladder cancer cells under normoxic and hypoxic conditions. (a, c) Under normoxia, the apoptosis rate was significantly increased with increase of drug concentration, from 16.2% to 31.3% at 24 h and 9% to 14.6% at 48 h. (b, d) Under hypoxia, the apoptosis rate was slightly increased with increase of drug concentration, from 36% to 46.7% at 24 h and 32.6% to 34.2% at 48 h.

with 2.5 μM cisplatin at 24 h, the apoptosis rate was higher than that of control cells under normoxic conditions (28.6% vs. 16.2%) (Figures 2(a) and 2(c)). However, a similar change was not detected under hypoxic conditions (36% vs. 36.7%). This suggests that drug toxicity to cancer cells under normoxia is enhanced with increase of drug concentration, and such an effect is impaired by hypoxia (Figures 2(b) and 2(d)). The results at 48 h may be attributed to drug deactivation at this point.

3.3. Effects of Autophagy Inhibitor and HIF-1 Inhibitor on Chemoresistance of BIU-87 Cells under Normoxia and Hypoxia. The above results proved that hypoxia induced resistance to chemotherapy, and apoptosis was related to this procedure. It is reported that cancer cells make themselves more adaptive through autophagy in adverse conditions. Therefore, we hypothesized that autophagy played an essential role in this process. To test this hypothesis, we inhibited autophagy by 3-MA and HIF-1 by YC-1 under hypoxic and normoxic conditions. According to the MTT assay, after incubation with 3-MA and HIF-1α inhibitor YC-1, cisplatin cytotoxicity was strengthened with increased concentration of 3-MA and YC-1 (Figures 3(a) and 3(b)). We chose 5 mM 3-MA and 100 μm YC-1 for the following experiments.

In order to investigate the effect of 3-MA and YC-1, we examined the expression of HIF-1α by qRT-PCR. The results showed that under hypoxia, 5 mM 3-MA and 100 μm YC-1 could inhibit the expression of HIF-1α effectively in BIU-87

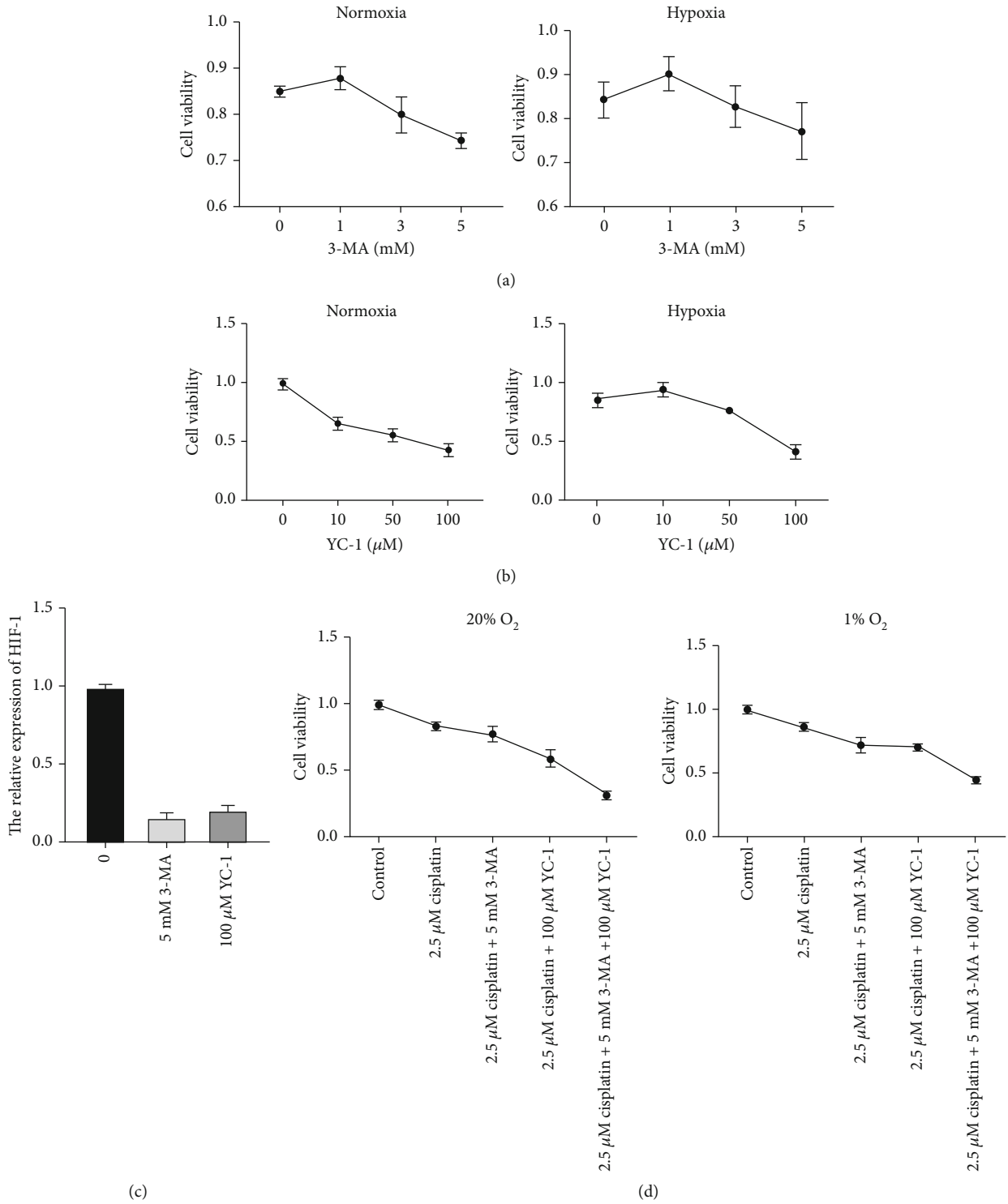

Figure 3: Effect of autophagy inhibitor and HIF-1 inhibitor on BIU-87 bladder cancer cell chemoresistance under hypoxia and normoxia. (a) Under normoxic and hypoxic, toxicity of cisplatin in BIU-87 cells was increased with the increased concentration of 3-MA. (b) Under normoxic and hypoxic, toxicity of cisplatin in BIU-87 cells was increased with increased concentration of YC-1. (c) The relative expression of HIF-1 in BIU-87 cells treated with 100 μM YC-1. (d) Under normoxic and hypoxic conditions, viability of BIU-87 cells was observed in different groups.

cells (Figure 3(c)). Under normoxic conditions, inhibition of the autophagy pathway could decrease cell activity. This environment causes autophagy and thus shows resistance to cisplatin. To verify the above assumption, we continued the relevant tests under hypoxic conditions. The trend under hypoxia was similar to that under normoxia (Figure 3(d)).

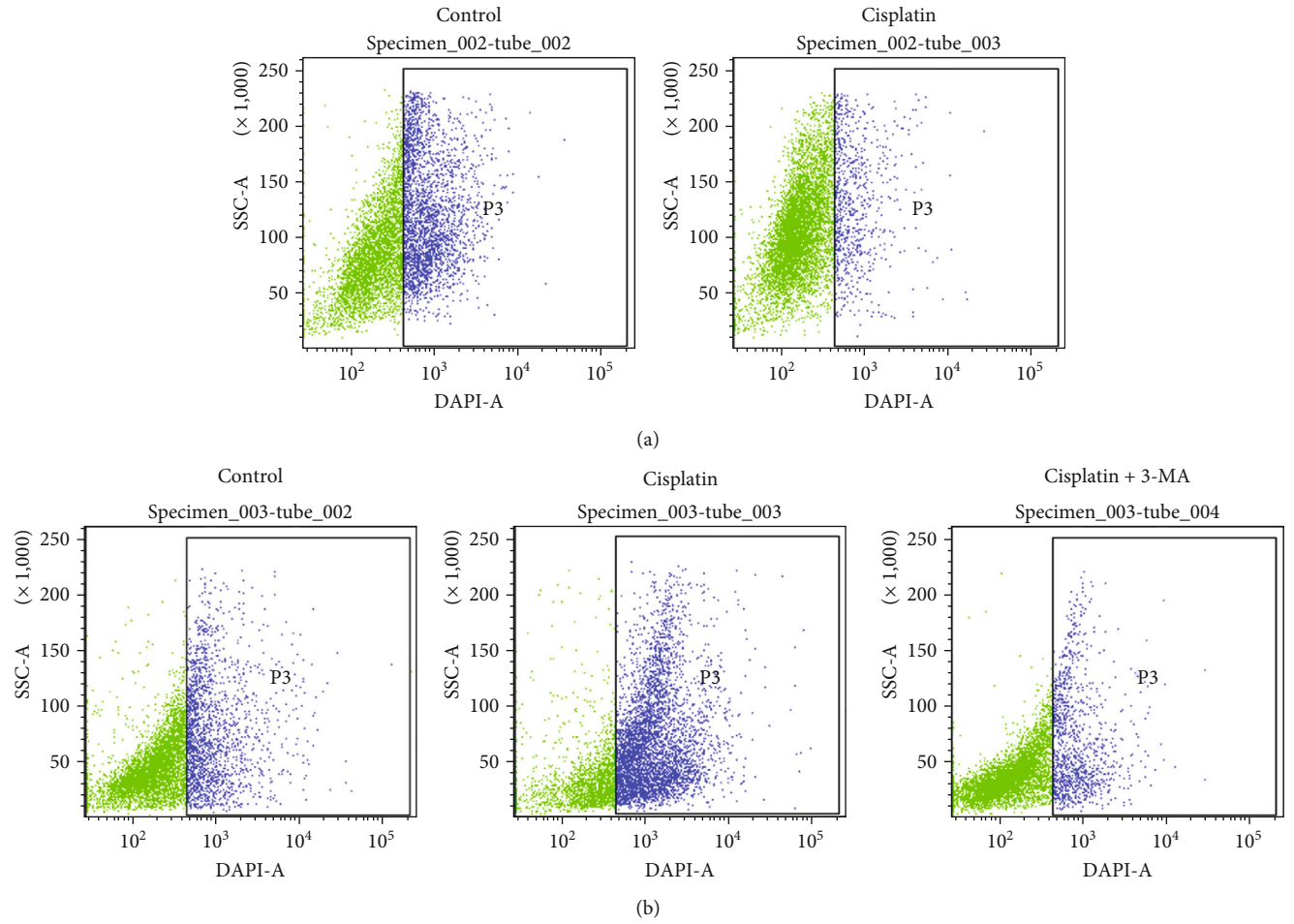

Figure 4: Autophagy analysis of BIU-87 bladder cancer cells. (a) Under normoxia, flow cytometry revealed that autophagy was not activated in the cisplatin group (8%) compared with the control group (27.7%). (b) Under hypoxia, flow cytometry showed that autophagy was 19.4% in the control group, significantly increased in the cisplatin group (48.1%) and downregulated after incubation with autophagy inhibitor 3-MA.

It is worth noting that this trend under hypoxia was less than that under normoxia (relative viability of cells under normoxic conditions, cisplatin: 83.9%, cisplatin+3-MA: 77.0%, cisplatin+YC-1: 59.2%, and cisplatin+3-MA+YC-1: 31.5%; relative viability under hypoxic conditions, cisplatin: 86.0%, cisplatin+3-MA: 72.5%, cisplatin+YC-1: 71.0%, and cisplatin+3-MA+YC-1: 45.2%). This result suggests that autophagy and the HIF-1α gene are likely involved in the hypoxic resistance to cisplatin in BIU-87 cancer cells.

3.4. Autophagy Analysis in the Drug Resistance Process. MDC is a fluorescent compound that is incorporated into multilamellar bodies by an ion-trapping mechanism and interaction with membrane lipids and is a probe for detection of autophagic vacuoles in cultured cells [12]. Flow cytometry showed that the control group had 27.7% autophagy while the cisplatin group had only 8% under normoxic conditions, suggesting that the cells could not undergo autophagy under normoxic conditions to counteract drug toxicity (Figure 4(a)). Compared with the control group (19.4%), autophagy was increased significantly (48.1%) in the drug group and dramatically reduced after addition of 3-MA (11.3%). This indicated that drug resistance of the cells in the hypoxic environment was indeed achieved through autophagy regulation (Figure 4(b)).

The above results proved that under hypoxic conditions, cisplatin induced autophagy in cancer cells, which was in accordance with the results of MDC detection.

3.5. Autophagy and Apoptosis Were Involved in Chemoresistance to Cisplatin under Hypoxic Conditions as Proved by Molecular Tests. The MTT assay (Figure 2) showed that apoptosis was involved in drug resistance. To confirm this, we designed experiments to detect several major marker proteins and genes related to the process.

Beclin-1 is used as a marker protein of cell autophagy. Under normoxia, expression of Beclin-1 in the cisplatin group was lower than that in the control group and similar to that in the autophagy inhibitor group (Figure 5(a)). In contrast, expression of Beclin-1 under hypoxia was significantly increased after treatment with cisplatin and obviously decreased after incubation with 3-MA. These results were similar to those of the MTT assay and MDC test, suggesting that hypoxia promotes autophagy, making cells more adaptive to chemotherapy.

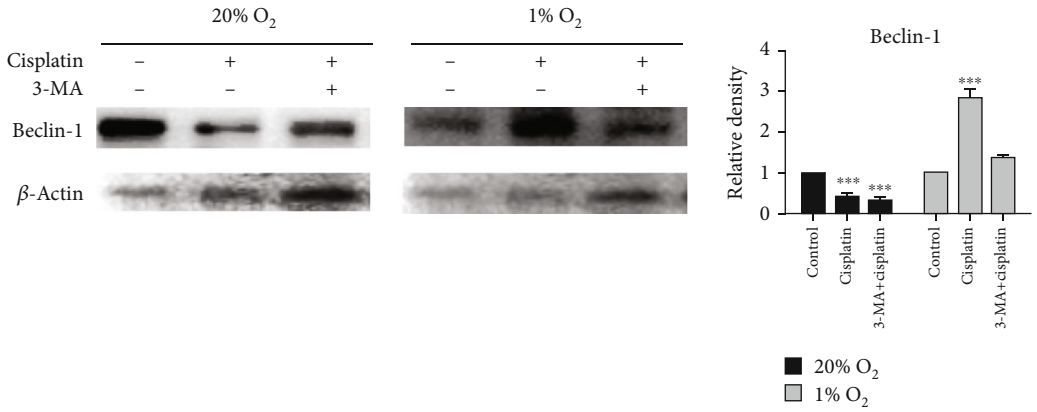

(a)

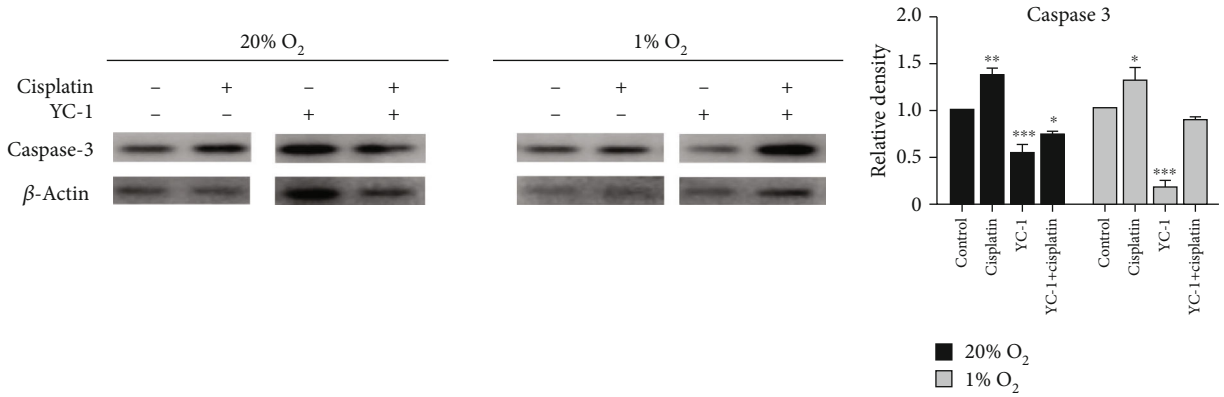

(b)

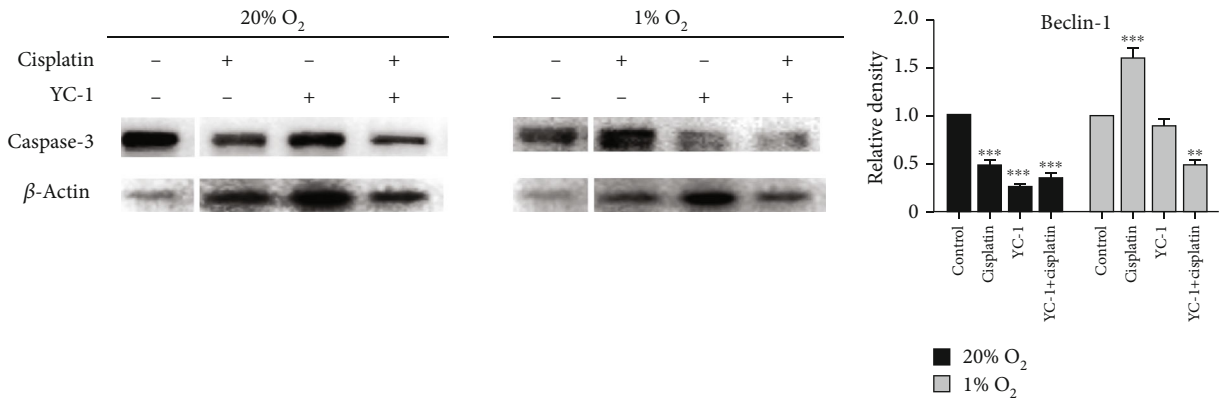

(c)

Figure 5: Continued.

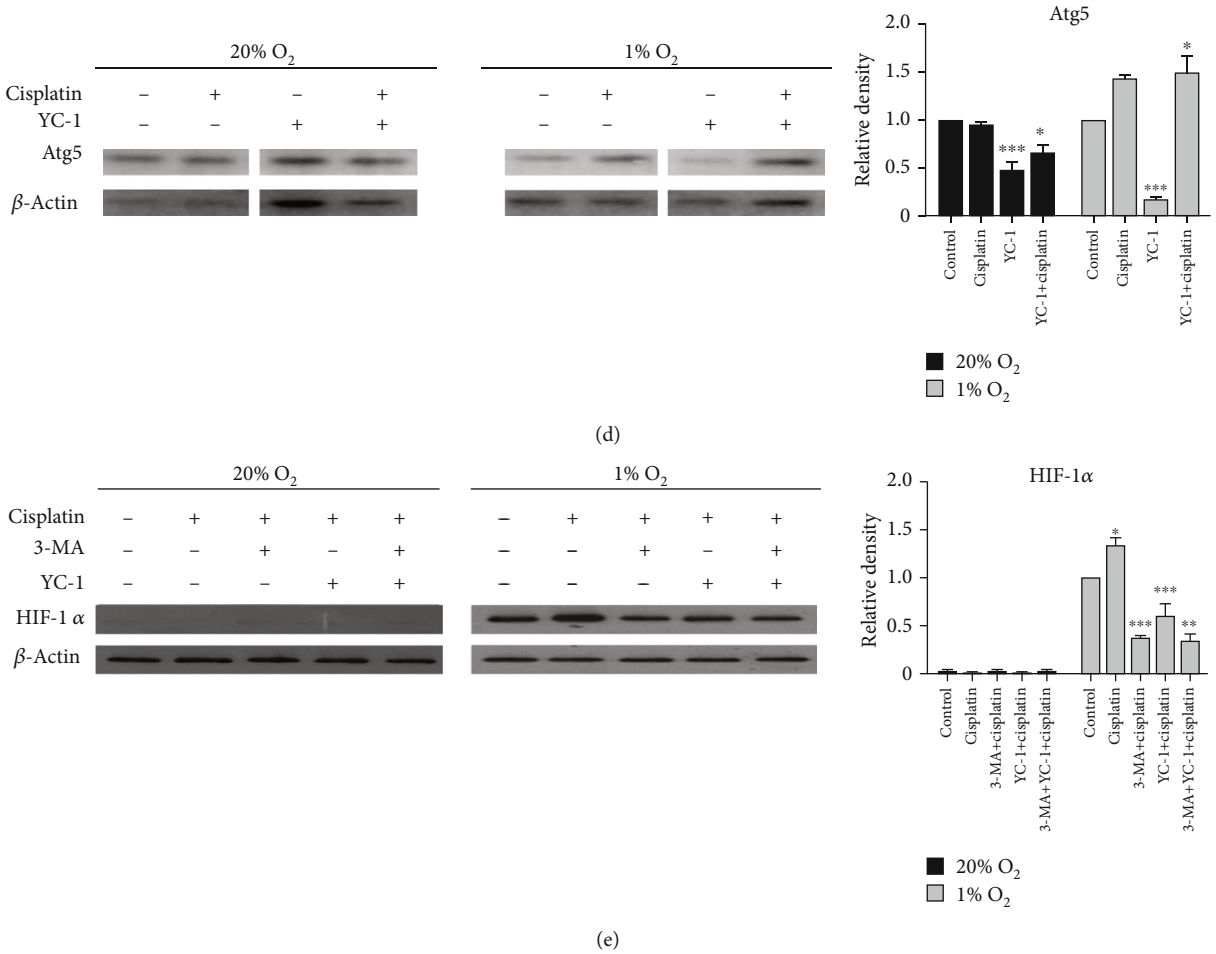

Figure 5: Expression of related marker proteins and genes under normoxic and hypoxic conditions by Western blotting. (a) Beclin-1 was measured by immunoblotting under normoxia and hypoxia. (b) Caspase-3 was measured by immunoblotting when incubated with HIF-1α inhibitor YC-1. The results indicate that hypoxia might induce cell chemoresistance through the HIF-1α signaling pathway. (c) Beclin-1 was measured by immunoblotting under normoxia and hypoxia. (d) Atg5 was measured by Western blotting and showed a similar trend to caspase-3. (e) HIF-1α was measured with Western blotting. The result revealed that HIF was involved in targeting apoptosis induced by autophagy.

Under normoxia, expression of caspase-3 was downregulated after treatment with YC-1 and the downward trend was alleviated when followed by cisplatin. Under hypoxic conditions, expression of caspase-3 did not change much in the study group compared with that in the control group, indicating that apoptosis in the two groups was similar (Figure 5(b)). This result demonstrated that hypoxia might induce drug resistance in cells by targeting the HIF-1α signaling pathway.

Under hypoxia, expression of Beclin-1 was significantly upregulated after treatment with cisplatin, downregulated by YC-1, and lowest after treatment with both agents (Figure 5(c)). This suggests that hypoxia may cause autophagy in cells, and decreased expression of HIF-1α may attenuate autophagy. This suggests that a lower oxygen environment produces cell autoregulation by targeting HIF-1α expression. This pathway is responsible for drug resistance.

Atg5, a molecule involved in autophagy, is known to be regulated via various stress-induced transcription factors and protein kinases [13]. Expression of Atg5 was similar to that of caspase-3 (Figure 5(d)), supporting the hypothesis at the molecular level that hypoxic conditions may cause autophagy in cells by targeting HIF-1α.

Based on previous results, HIF-1α has been confirmed to be involved in this process. Consequently, it is necessary to investigate how it changes and works. Expression of HIF-1α could not be detected under normoxia. It was upregulated under hypoxia, significantly downregulated after adding 3-MA and cisplatin, and similarly reduced after adding YC-1 and cisplatin compared with that in the negative control group (Figure 5(e)). We conclude that cisplatin may induce apoptosis in BIU-87 cells under hypoxic conditions by targeting HIF-1α-mediated autophagy.

4. Discussion

Hypoxia has been proved as one of the important factors in promoting chemoresistance of cancers cells. Autophagy has been extensively studied as a cytoprotective mechanism

against chemotherapy [14]. During the past decade, there has been an increasing interest in the relationship between hypoxia and autophagy [15, 16]. However, little work has been performed on bladder cancer [17]. The present study demonstrated that cisplatin was lethal to BIU-87 cells under normoxic conditions, but hypoxia reversed the cytotoxicity of chemotherapy by mediating autophagy through targeting HIF-1α.

It has been reported that cancer cells undergo a series of complex molecular changes that allow them to be more adaptive to chemotherapeutic agents [18–20]. Similar to this, our study showed that cisplatin was less toxic to bladder cancer cells under hypoxic compared with normoxic conditions. One of the principal factors attributed to the difference is HIF [21, 22]. Researches have proved that HIF-1α is involved in hypoxia-induced chemoresistance [23–25]. Our results supported the finding that hypoxia decreased sensitization to cisplatin in bladder cancer cells by targeting apoptosis. We also showed that HIF-1α was hardly expressed under normoxia but highly upregulated under hypoxia and downregulated when treated with HIF inhibitor YC-1. The underlying mechanisms of hypoxia-induced chemoresistance are manifold, including MDR gene expression, reduced reactive oxygen species levels, cell cycle arrest, gene mutations, and drug concentration decreases [26–30].

Autophagy is one of the decisive factors that assist cancer cells to counteract various adverse conditions. Hypoxia can activate autophagy and hypoxia-induced autophagy may protect cells from apoptosis induced by chemotherapeutic agents [31–34]. Consistent with the above reports, our study demonstrated that MDC and Beclin-1 were increased under hypoxia, and simultaneously, bladder cancer cells were less sensitive to cisplatin. However, when incubated with 3-MA, a popular inhibitor of autophagy that inhibits conversion of LC3-I to LC3-II by targeting PI3K [34], hypoxia-induced autophagy was significantly attenuated, suggesting that autophagy induced under hypoxic conditions contributes to chemoresistance of bladder cancer. Therefore, 3-MA can be used to enhance apoptosis when combined with chemotherapeutic agents under hypoxic conditions [35, 36]. When incubated with YC-1, a typical HIF inhibitor, caspase-3 was upregulated under hypoxic conditions, indicating that the regulatory effect of cisplatin on apoptosis may be achieved by targeting the HIF-1α signaling pathway. Furthermore, expression of Beclin-1 and Atg5 showed no change under normoxia, increased under hypoxia, and was downregulated when treated with YC-1 sequentially, suggesting that autophagy induced by hypoxia may be achieved by regulating expression of HIF-1α. Sun et al. thought HIF-1α/MDR1 pathway confers the chemoresistance to cisplatin in bladder cancer [37]. Combined with our results, it indicates that a variety of mechanisms are involved in the chemoresistance of bladder cancer. Future study could be focused on combined experiments of HIF-1a/MDR1 and autophage.

It should be noted that our study examined only one bladder cancer cell line and a single chemotherapeutic agent. Future research should focus on multiple bladder cancer cell lines and more chemotherapeutic drugs. Additionally, in vivo experiments will make the results more convincing and acceptable.

5. Conclusions

To sum up, the present study revealed that resistance to cisplatin in BIU-87 bladder cancer cells under hypoxic conditions could be explained by the activation of autophagy, which was regulated by HIF-1α-associated signaling pathways. Accordingly, the hypoxia–autophagy pathway may be a target for improving the efficacy of cisplatin chemotherapy in bladder cancer.

Data Availability

The data used to support the findings of this study are included within the article.

Conflicts of Interest

The authors declare that they have no competing interests.

Authors' Contributions

Xiawa Mao wrote the manuscript, and Nanzhang and Kefeng Ding revised the manuscript.

Acknowledgments

This work was supported by grants from the Natural Science Foundation of Zhejiang Province, LY18H050002 and Y21H050008. We thank the authors of those references for their excellent work.

References

[1] R. L. Siegel, K. D. Miller, and A. Jemal, "Cancer statistics, 2018," *CA: a Cancer Journal for Clinicians*, vol. 68, no. 1, pp. 7–30, 2019.

[2] J. A. Witjes, E. Compérat, N. C. Cowan et al., "EAU guidelines on muscle-invasive and metastatic bladder cancer: summary of the 2013 guidelines," *European Urology*, vol. 65, no. 4, pp. 778–792, 2014.

[3] R. Ojha, S. K. Singh, and S. Bhattacharyya, "JAK-mediated autophagy regulates stemness and cell survival in cisplatin resistant bladder cancer cells," *Biochimica et Biophysica Acta (BBA) - General Subjects*, vol. 1860, no. 11, pp. 2484–2497, 2016.

[4] M. M. Gottesman, "Mechanisms of cancer drug resistance," *Annual Review of Medicine*, vol. 53, no. 1, pp. 615–627, 2002.

[5] E. Clottes, "Hypoxia-inducible factor 1: regulation, involvement in carcinogenesis and target for anticancer therapy," *Bulletin du Cancer*, vol. 92, no. 2, pp. 119–127, 2005.

[6] Y.-A. Tang, Y.-f. Chen, Y. Bao et al., "Hypoxic tumor microenvironment activates GLI2 via HIF-1alpha and TGF-beta2 to promote chemoresistance in colorectal cancer," *Proceedings of the National Academy of Sciences of the United States of America*, vol. 115, no. 26, pp. E5990–E5999, 2018.

[7] J. Mani, S. Vallo, S. Rakel et al., "Chemoresistance is associated with increased cytoprotective autophagy and diminished apoptosis in bladder cancer cells treated with the BH3 mimetic

(−)-Gossypol (AT-101)," *BMC Cancer*, vol. 15, no. 1, p. 224, 2015.

[8] L. Galluzzi, I. Vitale, J. M. Abrams et al., "Molecular definitions of cell death subroutines: recommendations of the Nomenclature Committee on Cell Death 2012," *Cell Death & Differentiation*, vol. 19, no. 1, pp. 107–120, 2012.

[9] N. Pore, Z. Jiang, A. Gupta, G. Cerniglia, G. D. Kao, and A. Maity, "EGFR tyrosine kinase inhibitors decrease VEGF expression by both hypoxia-inducible factor (HIF)-1-independent and HIF-1-dependent mechanisms," *Cancer Research*, vol. 66, no. 6, pp. 3197–3204, 2006.

[10] M. C. Maiuri, A. Criollo, E. Tasdemir et al., "BH3-only proteins and BH3 mimetics induce autophagy by competitively disrupting the interaction between Beclin 1 and Bcl-2/Bcl-XL," *Autophagy*, vol. 3, no. 4, pp. 374–376, 2014.

[11] M. Babjuk, M. Burger, R. Zigeuner et al., "EAU guidelines on non-muscle-invasive urothelial carcinoma of the bladder: update 2013," *European Urology*, vol. 64, no. 4, pp. 639–653, 2013.

[12] A. L. Contento, Y. Xiong, and D. C. Bassham, "Visualization of autophagy in Arabidopsis using the fluorescent dye monodansylcadaverine and a GFP-AtATG8e fusion protein," *The Plant Journal*, vol. 42, no. 4, pp. 598–608, 2005.

[13] R. Höcker, A. Walker, and I. Schmitz, "Inhibition of autophagy through MAPK14-mediated phosphorylation of ATG5," *Autophagy*, vol. 9, no. 3, pp. 426–428, 2014.

[14] A. Notte, N. Ninane, T. Arnould, and C. Michiels, "Hypoxia counteracts taxol-induced apoptosis in MDA-MB-231 breast cancer cells: role of autophagy and JNK activation," *Cell Death & Disease*, vol. 4, no. 5, article e638, 2013.

[15] S. Owada, H. Endo, Y. Shida et al., "Autophagy-mediated adaptation of hepatocellular carcinoma cells to hypoxia-mimicking conditions constitutes an attractive therapeutic target," *Oncology Reports*, vol. 39, no. 4, pp. 1805–1812, 2018.

[16] Y. Sun, X. Xing, Q. Liu et al., "Hypoxia-induced autophagy reduces radiosensitivity by the HIF-1α/miR-210/Bcl-2 pathway in colon cancer cells," *International Journal of Oncology*, vol. 46, no. 2, pp. 750–756, 2015.

[17] X. Yang, H. Yin, Y. Zhang et al., "Hypoxia-induced autophagy promotes gemcitabine resistance in human bladder cancer cells through hypoxia-inducible factor 1α activation," *International Journal of Oncology*, vol. 53, no. 1, pp. 215–224, 2018.

[18] J. P. Cosse and C. Michiels, "Tumour hypoxia affects the responsiveness of cancer cells to chemotherapy and promotes cancer progression," *Anti-Cancer Agents in Medicinal Chemistry*, vol. 8, no. 7, pp. 790–797, 2008.

[19] M. Hockel and P. Vaupel, "Tumor hypoxia: definitions and current clinical, biologic, and molecular aspects," *Journal of the National Cancer Institute*, vol. 93, no. 4, pp. 266–276, 2001.

[20] J. Zhou, T. Schmid, S. Schnitzer, and B. Brune, "Tumor hypoxia and cancer progression," *Cancer Letters*, vol. 237, no. 1, pp. 10–21, 2006.

[21] C. Wohlkoenig, K. Leithner, A. Deutsch, A. Hrzenjak, A. Olschewski, and H. Olschewski, "Hypoxia-induced cisplatin resistance is reversible and growth rate independent in lung cancer cells," *Cancer Letters*, vol. 308, no. 2, pp. 134–143, 2011.

[22] G. L. Semenza, "HIF-1: upstream and downstream of cancer metabolism," *Current Opinion in Genetics & Development*, vol. 20, no. 1, pp. 51–56, 2010.

[23] D. Hussein, E. J. Estlin, C. Dive, and G. W. J. Makin, "Chronic hypoxia promotes hypoxia-inducible factor-1α–dependent resistance to etoposide and vincristine in neuroblastoma cells," *Molecular Cancer Therapeutics*, vol. 5, no. 9, pp. 2241–2250, 2006.

[24] G. Melillo, "Inhibiting hypoxia-inducible factor 1 for cancer therapy," *Molecular Cancer Research*, vol. 4, no. 9, pp. 601–605, 2006.

[25] L. M. Brown, R. L. Cowen, C. Debray et al., "Reversing hypoxic cell chemoresistance in vitro using genetic and small molecule approaches targeting hypoxia inducible factor-1," *Molecular Pharmacology*, vol. 69, no. 2, pp. 411–418, 2006.

[26] H. Yasuda, "Solid tumor physiology and hypoxia-induced chemo/radio-resistance: novel strategy for cancer therapy: nitric oxide donor as a therapeutic enhancer," *Nitric Oxide*, vol. 19, no. 2, pp. 205–216, 2008.

[27] X.-l. Guo, D. Li, K. Sun et al., "Inhibition of autophagy enhances anticancer effects of bevacizumab in hepatocarcinoma," *Journal of Molecular Medicine*, vol. 91, no. 4, pp. 473–483, 2013.

[28] Q. Wang, Y. Yang, L. Wang, P. Z. Zhang, and L. Yu, "Acidic domain is indispensable for MDM2 to negatively regulate the acetylation of p53," *Biochemical and Biophysical Research Communications*, vol. 374, no. 3, pp. 437–441, 2008.

[29] M. Wartenberg, E. Hoffmann, H. Schwindt et al., "Reactive oxygen species-linked regulation of the multidrug resistance transporter P-glycoprotein in Nox-1 overexpressing prostate tumor spheroids," *FEBS Letters*, vol. 579, no. 20, pp. 4541–4549, 2005.

[30] W. L. Chen, C. C. Wang, Y. J. Lin, C. P. Wu, and C. H. Hsieh, "Cycling hypoxia induces chemoresistance through the activation of reactive oxygen species-mediated B-cell lymphoma extra-long pathway in glioblastoma multiforme," *Journal of Translational Medicine*, vol. 13, no. 1, 2015.

[31] G. Bellot, R. Garcia-Medina, P. Gounon et al., "Hypoxia-induced autophagy is mediated through hypoxia-inducible factor induction of BNIP3 and BNIP3L via their BH3 domains," *Molecular and Cellular Biology*, vol. 29, no. 10, pp. 2570–2581, 2009.

[32] N. M. Mazure and J. Pouyssegur, "Hypoxia-induced autophagy: cell death or cell survival?," *Current Opinion in Cell Biology*, vol. 22, no. 2, pp. 177–180, 2010.

[33] X. Song, X. Liu, W. Chi et al., "Hypoxia-induced resistance to cisplatin and doxorubicin in non-small cell lung cancer is inhibited by silencing of HIF-1alpha gene," *Cancer Chemotherapy and Pharmacology*, vol. 58, no. 6, pp. 776–784, 2006.

[34] H. Li, P. Wang, Q. Sun et al., "Following cytochrome c release, autophagy is inhibited during chemotherapy-induced apoptosis by caspase 8-mediated cleavage of Beclin 1," *Cancer Research*, vol. 71, no. 10, pp. 3625–3634, 2011.

[35] H. M. Wu, Z. F. Jiang, P. S. Ding, L. J. Shao, and R. Y. Liu, "Hypoxia-induced autophagy mediates cisplatin resistance in lung cancer cells," *Scientific Reports*, vol. 5, no. 1, 2015.

[36] X. W. Liu, Y. Su, H. Zhu et al., "HIF-1α-dependent autophagy protects HeLa cells from fenretinide (4-HPR)-induced apoptosis in hypoxia," *Pharmacological Research*, vol. 62, no. 5, pp. 416–425, 2010.

[37] Y. Sun, Z. Guan, L. Liang et al., "HIF-1α/MDR1 pathway confers chemoresistance to cisplatin in bladder cancer," *Oncology Reports*, vol. 35, no. 3, pp. 1549–1556, 2016.

Hindawi
Journal of Immunology Research
Volume 2021, Article ID 8816041, 14 pages
https://doi.org/10.1155/2021/8816041

Review Article

Th17 Cells in Inflammatory Bowel Disease: Cytokines, Plasticity, and Therapies

Junjun Zhao,[1,2] **Qiliang Lu**,[3] **Yang Liu**,[3] **Zhan Shi**,[4] **Linjun Hu**,[3] **Zhi Zeng**,[3] **Yifeng Tu**,[4] **Zunqiang Xiao**,[4] **and Qiuran Xu**[2]

[1]*Graduate Department, Bengbu Medical College, Bengbu, Anhui 233030, China*
[2]*The Key Laboratory of Tumor Molecular Diagnosis and Individualized Medicine of Zhejiang Province, Zhejiang Provincial People's Hospital (People's Hospital of Hangzhou Medical College), Hangzhou, Zhejiang 310014, China*
[3]*The Medical College of Qingdao University, Qingdao, Shandong 266071, China*
[4]*The Second Clinical Medical College of Zhejiang Chinese Medical University, Hangzhou, Zhejiang 310014, China*

Correspondence should be addressed to Qiuran Xu; windway626@sina.com

Received 13 August 2020; Revised 15 December 2020; Accepted 12 January 2021; Published 22 January 2021

Academic Editor: Xinyi Tang

Copyright © 2021 Junjun Zhao et al. This is an open access article distributed under the Creative Commons Attribution License, which permits unrestricted use, distribution, and reproduction in any medium, provided the original work is properly cited.

Autoimmune diseases (such as rheumatoid arthritis, asthma, autoimmune bowel disease) are a complex disease. Improper activation of the immune system or imbalance of immune cells can cause the immune system to transform into a proinflammatory state, leading to autoimmune pathological damage. Recent studies have shown that autoimmune diseases are closely related to CD4+ T helper cells (Th). The original CD4 T cells will differentiate into different T helper (Th) subgroups after activation. According to their cytokines, the types of Th cells are different to produce lineage-specific cytokines, which play a role in autoimmune homeostasis. When Th differentiation and its cytokines are not regulated, it will induce autoimmune inflammation. Autoimmune bowel disease (IBD) is an autoimmune disease of unknown cause. Current research shows that its pathogenesis is closely related to Th17 cells. This article reviews the role and plasticity of the upstream and downstream cytokines and signaling pathways of Th17 cells in the occurrence and development of autoimmune bowel disease and summarizes the new progress of IBD immunotherapy.

1. Introduction

Inflammatory bowel disease (IBD) is a chronic idiopathic inflammatory disease of the digestive tract, including Crohn's disease (CD) and ulcerative colitis (UC). Their clinical manifestations have common characteristics, such as diarrhea, abdominal pain, and bloody stools. Ulcerative colitis is a continuous inflammation of the colonic mucosa and submucosa. Crohn's disease can involve the full digestive tract and is a discontinuous full-thickness inflammation. Although the incidence of IBD in the United States and other developed countries is only about 1.3%, the cost to the health system and society is also increasing [1].

At present, the pathogenic factors of IBD are mainly attributed to the patient's genetic susceptibility, intestinal flora, lifestyle problems, and the patient's immune system [2]. The immune system, including the innate immune system and the adaptive immune system, plays a key role in IBD [3]. Traditionally, the pathogenesis of CD and UC is considered to be Th1 and Th2 cell-mediated, respectively; however, with the development of immunology, more and more Th cell subtypes have been discovered, such as Th17, Th9, and Treg cell [4]. Among them, due to the immune response in the intestinal mucosa and participation in autoimmune diseases, Th17 cells have received special attention in recent years.

T helper cell 17 (Th17) is a newly discovered subset of T cells that can secrete interleukin 17 (IL-17). Th17 is a helper T cell differentiated from naive T cells under the stimulation of IL6 and IL23. It mainly secretes proinflammatory factors such as IL17 and IL22 and plays an important role in inflammatory diseases. Retinoic acid orphan receptor g γ(RORγ) is

preferentially expressed in Th17 cells and is essential for the differentiation and development of Th17 cells [5]. Th17 cells are involved in the pathogenesis of the most common autoimmune diseases, including psoriasis, rheumatoid arthritis (RA), inflammatory bowel disease (IBD), and multiple sclerosis (MS) [6, 7]. With more in-depth research on Th17 cells, people have found that Th17 cells are at the core of autoimmune diseases (especially IBD). Since it was discovered in 2005, Th17 cells have been strongly associated with the pathogenesis of IBD [8]. Under physiological conditions, mucosal Th17 cells regulate the integrity of the physical barrier of epithelial cells through the chemotaxis of neutrophils and macrophages and stimulate epithelial cells to produce antimicrobial peptides, which play an important role in the intestinal mucosal barrier [9]. However, under pathological conditions, Th17 will secrete proinflammatory mediators to aggravate disease progression and prognosis; this shows that Th17 cells are not only related to the mucosal barrier but also related to inflammation.

This article reviews many previous studies on Th17 and IBD, aiming to clarify the influence of Th17 from differentiation to pathogenesis on IBD and try to bring new ideas to researchers in the immunotherapy of IBD.

2. Th17 Differentiation

The proinflammatory effect of Th17 cells in the pathogenesis of IBD mainly depends on the imbalance of cytokine differentiation in the process of differentiation. In addition, the connection between them is based on the induction and maintenance of Th17 cells. In view of the important connection between Th17 cells and IBD, here, it is necessary to explain the differentiation process of Th17 (especially in the intestinal mucosal immunity).

CD4+ T helper cells are an important part of the immune system. After contact with activated antigen-presenting cells (APC) and binding to Th cell histocompatibility complex molecules, the naive CD4+ T cells turn from a resting state to clonal expansion and are differentiated into different effector cell subtypes under the stimulation of cytokines in the environment. Interleukin 12 (IL12) and interferon γ (IFN-γ) initiate downstream signals and activate the differentiation of Th1 cells [10]. The T-box transcription factor (T-bet) is the main regulator of Th1 differentiation [11], and mature Th1 cells participate in the elimination of pathogens in cells and are related to organ-specific autoimmunity [12]. IL-4 is the lineage driving factor of Th2 cells, which is characterized by expressing GATA3 and producing IL-4, IL-5, and IL-13. Th2 plays an important role in the immune response of worms, asthma, and other allergic diseases [13]. Treg cells produce IL-10, TGF-β, and other cytokines under the stimulation of TGF-β, which play an important role in immune regulation. The most important transcription factor for Treg cell differentiation is FOXP3 [14]. Although Th1, Th2, and Treg also play an important role in inflammatory bowel disease, Th17 cells are indeed at the core of the pathogenesis of IBD [15–17] (Figure 1).

The development of Th17 cells starts with the differentiation of naive T helper cells (Th0) after receiving appropriate stimulation. In the differentiation process from Th0 to Th17, the corresponding cytokines play a decisive role. These cytokines mainly include interleukin-23 (IL-23), interleukins-6 (IL-6), interleukin-21 (IL-21), transforming growth factor-β (TGF-β), and interleukin-1β [5].

IL-23 is a member of the IL-12 cytokine family. It is a heterodimer structure composed of IL-23's p40 subunit (shared with IL-12) and p19 subunit connected by disulfide bonds. The genes encoding p40/19 subunits are located on human chromosome 5/12; these two subunits alone are not biologically active, and only when the two are combined into a heterodimer can they perform corresponding functions. The cells that produce IL-23 mainly include dendritic cells (DC cells), macrophages, B cells, or endothelial cells [18–20]. Since the discovery of IL-23 in 2000, it has shown its characteristics as an important inflammatory factor in the intestinal tract, and more importantly, it can stimulate the differentiation and proliferation of Th17 cells and participate in a wide range of inflammatory diseases [21]. IL-23 works by binding to its receptor (IL-23); IL-23R is also a heterodimer structure, consisting of IL-12Rβ1 subunit (shared by IL-12p40 subunit) and its own unique IL-23R subunit [22]. IL-23R via downstream signals Janus kinase (JAK) 2 and tyrosine kinase (Tyk) 2 and further activates downstream effectors such as STAT, MAPK, and PI3K signaling pathways and then induces the production of RORC, IL-17A, and IL-23R. Among them, IL-23R seems to stabilize RORC induction and Th17 phenotype through a positive feedback loop [23]. In addition, the T cells of naive mice do not express IL-23R, but can be induced by RORC. IL-23R-/- mice lose Th17 cells, indicating that IL-23 may be necessary for the maintenance of Th17 cells [24]. IL-23 can induce the proliferation of Th17 cells and the production of inflammatory mediators (such as IL-17). Currently, IL-23/Th17 axis is important for maintaining Th17 cells, and IL-23 signaling has been shown to significantly promote the pathogenicity of Th17 subsets in mouse models [25, 26]. IL-23 mainly promotes the occurrence of IBD by inducing the proliferation of pathogenic Th17 cells and producing IL-17 and other inflammatory factors. Studies have also shown that IL-23 induces Th17 cells to produce INF-γ and aggravates the progression of IBD [27]. In addition, IL-23 promotes the production of IBD by regulating the Th17/Treg balance. In patients with IBD, the number of Treg cells in peripheral blood decreased, while the Th17 cells increased [28, 29]. The single nucleotide polymorphism of the IL-23R gene in the subgroup of IBD patients affects the susceptibility to IBD [30]. Salt concentration-dependent SGK1 promotes IL-23R expression, promotes the differentiation of Th17 cells, and promotes the development of autoimmunity [31].

IL-6 is a glycoprotein composed of 184 amino acids. Its gene has been located on chromosome 7p21 and can be synthesized by a variety of cells, including monocytes, macrophages, lymphocytes, fibroblasts, endothelial cells, intestinal epithelial cells (IEC), and some tumor cells [32]. The receptors of IL-6 mainly include IL-6R and its soluble receptor (sIL-6R). The IL-6/IL-6R complex activates the receptor cell membrane transduction chain gp130. The activation of gp130 in lymphocytes leads to the JAK/STAT3 pathway

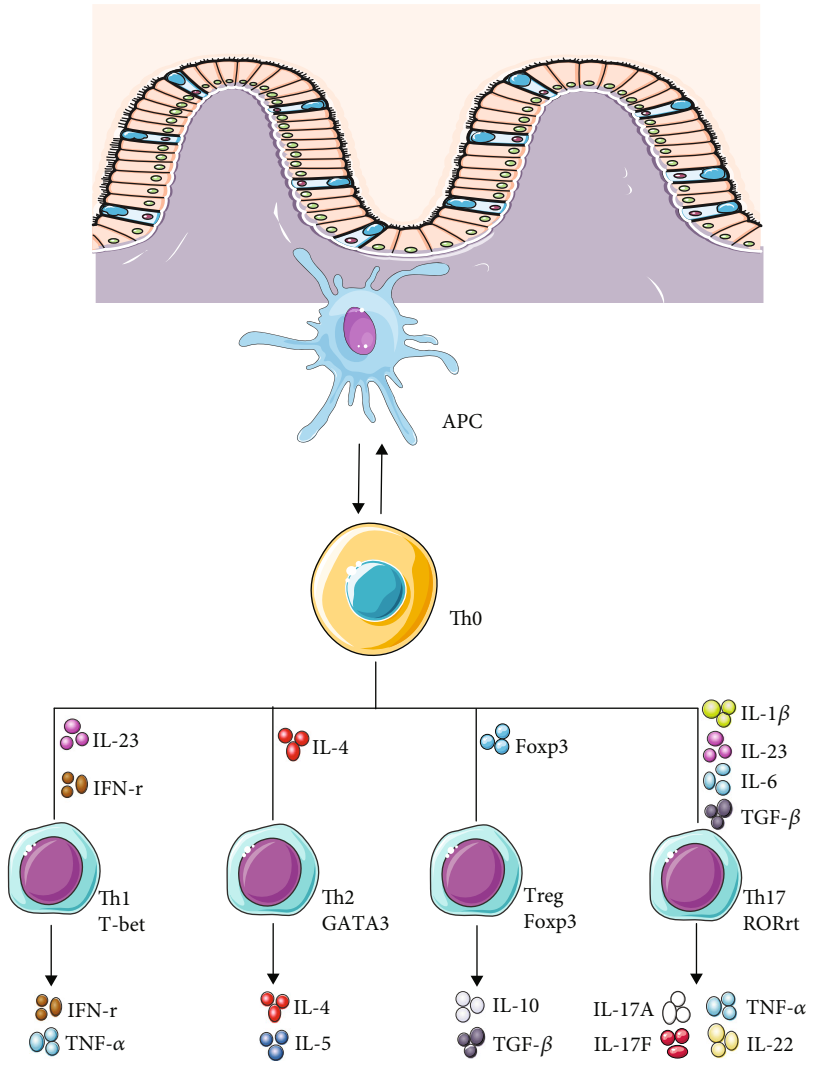

Figure 1: Differentiation of Th17 cell.

and initiates the antiapoptotic response through bcl-2 and bcl-xL. IL-6R produces sIL-6R under proteolysis or splicing and combines with IL-6 to produce an IL-6/sIL-6R complex. The IL-6/sIL-6R complex can stimulate the expression of only the gp130 but not IL-6R cells. In the absence of sIL-6R, such cells will not be able to respond to the cytokine IL-6 (known as IL-6 *trans*-signaling) [33, 34]. IL-6 is a pleiotropic cytokine that induces the production of acute-phase proteins such as CRP and serum amyloid A in the early stage of inflammation and promotes the development of immune cells such as Th17 cells [35]. In inflammatory bowel disease, IL-6 produced by macrophages mediates apoptosis resistance and abnormal accumulation of T cells in the intestinal mucosa through its classical and trans-signals and promotes the differentiation of Th17 cells [34, 36]. TGF-β and IL6 are considered to be critical for the production of pathogenic IL-17, but studies have shown that pathogenic Th17 cells are mediated by IL-23, not by TGF-β and IL-6 [37]. In addition, the IL-6 signal plays an important role in Th17/Treg differentiation balance. The IL-6 signal blocks the inhibitory signal of FoxP3 on RORγt and finally leads to the differentiation of naive T cells to Th17 cells [38].

IL-21 is a member of the IL-2 cytokine family. The human IL-21 gene is located at 4q26-q27. It is an important effector cytokine in the T cell-dependent inflammatory process. IL-21 acts on natural killer T (NKT) cells, various CD4 T cell subsets (including Th17 cells, follicular helper T cells (Tfh)), and CD8+ T cell [39, 40]. IL-21R is a complex composed of IL-21R subunit and γ-chain (γc); IL-21R subunit is located at 16p11, among which IL-21R subunit is the ligand recognition binding site, and γc is the signal transduction unit [41, 42]. IL-21R can be expressed on a variety of cells, including B cells, T cells, natural killer (NK) cells, and dendritic cells (DC) [40]. After IL-21 binds to IL-21R, it activates the JAK1/STAT3 pathway, as well as the phosphatidylinositol kinase (PI3K)/AKT and mitogen-activated protein kinase (MAPK) pathways, thereby playing an important role in mediating cell proliferation effect [43]. Many studies have shown that IL-21 also controls the production of Th17 cells. When IL-21 is combined with transforming

growth factor-β, it can induce naive T cells to differentiate into Th17 cells, accompanied by the acquired expression of RORγt and IL-23R. IL-21 can induce Th17 cells to produce IL-21 by themselves. The autocrine method of IL-21 amplifies the production and maintenance of Th17 cells induced by IL-2 [44–47]. IL-21 and TGF-β synergistically induce Th17 cells in the original IL-6-/- T cells, and IL-21 receptor-deficient T cells are defective in producing Th17 responses [44]. Although the proinflammatory effects of IL-21 in IBD have been extensively studied, some studies have shown that IL-21 improves DSS-induced colitis [48, 49]. The different effects of IL-21/IL-21R signals in the intestine may be related to the type of IBD disease and different backgrounds of experimental subjects.

Interleukin 1 beta (IL-1β), also known as leukocyte pyrogen, is a member of the interleukin 1 cytokine family and is a cytokine protein encoded by the IL1B gene. This cytokine is produced by activated macrophages in the form of the original protein, which is proteolyzed and processed into its active form by caspase 1 (CASP1). This cytokine is an important mediator of the inflammatory response [50, 51]. In most inflammatory bowel diseases, IL-1β acts together with other proinflammatory cytokines such as IL-6 and tumor necrosis factor-α or IL-23 in the inflammatory process, and treatment alone against the proinflammatory effects of IL-1β has little effect. Under inflammatory conditions, the inflammasomes in the intestinal mucosal macrophages are activated and further induce the production of IL-1β. The produced IL-1β and IL-6 and other cytokines jointly induce the production of IL-17-Th17 cells and the differentiation of downstream T cells that produce INF-γ and aggravate intestinal inflammation [52]. In addition, IL-1β can also induce the expression of transcription factor IRF4, which is necessary for RORγt expression [53].

In addition, transforming growth factor β (TGF-β) is also involved in the differentiation of Th17 cells. High concentrations of TGF-β inhibited the induction of RORC, which encodes the main transcription factor RORγt of Th17 cells, indicating that there is an optimal range for TGF-β to induce Th17 cells [54].

Retinoic acid-related orphan receptor-γt (ROR-γt) is the main transcription factor for Th17 cell differentiation [55]. Th17 cells are effective inducers of tissue inflammation, and dysregulated expression of IL-17 appears to trigger organ-specific autoimmunity. Th17 cell differentiation requires the lineage-specific transcription factor retinoic acid-related orphan receptor-γt (human known as RORC), which activates primary T cells in the presence of cytokines TGF-β and IL-6 to upregulate the expression of ROR-γt and induce its differentiation into Th17 cells [56]. In addition, transcription coactivator (TAZ) acts as a cell fate switch between immunosuppressive Treg cells and inflammatory Th17 cells. TAZ acts as a coactivator of RORγt to promote the differentiation of TH17. TEAD1 inhibits TH17 by antagonizing TAZ and thus plays a positive role in regulating the growth and development of Treg cells. The possible mechanism is that TAZ directly binds and activates RORγt, blocks Foxp3's inhibitory effect on RORγt, increases the expression of Th17-specific genes, and promotes the development of Th17 [57]. In other signaling pathways, such as the TNF-β signaling pathway, Smad3 reduces the RORγt activity of Th17 cells, thereby reducing the development of TH17 cells [58]. In the metabolic pathway, the study found that Roquin protein inhibits the PI3K-mTOR pathway at multiple levels, thereby controlling protein biosynthesis and thus inhibiting the differentiation and transformation of Th17 [59]. Phosphatase DUSP2 controls the activity of the transcription activator STAT3 and regulates the differentiation of TH17. The experimental colitis model found that the lack of DUSP2 directly enhances the transcriptional activity of STAT3, thereby inducing TH17 differentiation. Further research identified DUSP2 as a negative regulator of STAT3 signal transduction and participated in the development of the Th17 lineage [60]. The abovementioned pathways play an important role in inflammatory bowel disease by promoting the differentiation of Th17 to produce IL17 and other inflammatory mediators.

3. Th17 Cell in IBD

Inflammatory bowel disease (IBD) is a chronic nonspecific disease of the intestinal mucosa, and many factors affect its development. At present, the specific mechanism of the onset of IBD is unclear, and innate or adaptive immune response may be involved [61, 62]. Th17 cells and their cytokines are generally considered to play a proinflammatory role in human autoimmune diseases. A large number of studies have clarified the role of Th17 cells in inflammatory diseases such as type I diabetes (T1D), rheumatoid arthritis (RA), multiple sclerosis (MS), systemic lupus erythematosus (SLE), asthma, and IBD [63–66] (Figure 2).

Traditionally, CD is considered to be related to Th1 cells and UC is related to Th2 [67]. However, with the development of immunology, we have known that there are a large number of Th17 cells and their cytokines in the mucosa of IBD patients, which has changed people's understanding of IBD, but it is precisely this way that Th17 cells have entered the study of IBD core. The gastrointestinal tract is necessary for the absorption of nutrients and is also the human body's largest immune organ. It is an important barrier to protect the host from pathogens. The bacterial microbiota in the intestine can regulate and maintain the dynamic balance of the intestinal immune system. However, when this balancing behavior is disrupted, chronic inflammation may occur, such as IBD [68]. Experiments have shown that mice in a sterile state will not have gastrointestinal inflammation, while T cells that respond to intestinal flora are different [69, 70]. Th17 cells are mainly distributed in the small intestine. Th17 cells in the intestine are affected by coliforms to activate the immune system and stimulate the development and migration of Th17 cells to the small intestine. The majority of gut Th17 cells are specific for microbial antigens [71]. Segmental filamentous bacteria (SFB) and other bacteria with the same ability, such as Citrobacter and Escherichia coli, can attach to intestinal epithelial cells (IEC) and play an important role in maintaining the integrity of the intestinal barrier. Under inflammatory conditions, these bacteria can also induce dendritic cells to produce IL-6 and IL-1β to

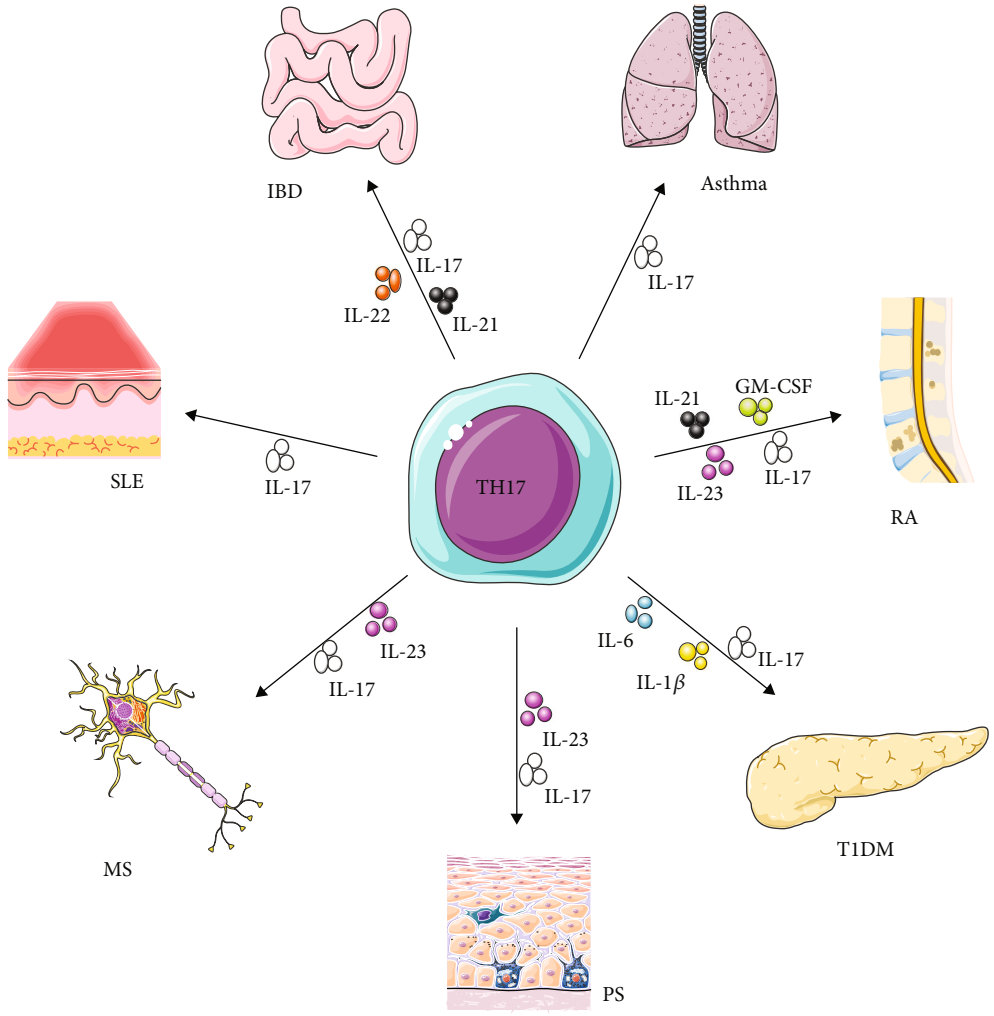

Figure 2: Functions of Th17 cell.

induce the differentiation of pathogenic Th17 and the production of inflammatory cytokines [72–74]. It has been found that Th17 and Th17 cell-related cytokines accumulate in the inflammatory lesions of patients with Crohn's disease and ulcerative colitis [75–77]. In the intestinal mucosa of patients with active IBD, Th17-related cytokines (IL-17, IL-21, and IL-22) increase, suggesting that Th17 cells may play an important role in disease activity and mucosal damage [78]. External factors such as a high-salt diet stimulate the intestinal Th17 cell response and aggravate the colitis induced by trinitrobenzene sulfonic acid (TNBS) [79]. However, Th17 cells in the small intestine of nonimmune pathogen-free mice are thought to promote intestinal barrier function by stimulating the formation of tight junctions and antimicrobial peptides [80, 81]. The pathogenicity of Th17 cells in inflammatory bowel disease is certain, but the role of Th17 in the intestine is heterogeneous, which may be protective or harmful. An interesting finding was that S1p receptor-1-dependent intestinal Th17 cells migrated to the kidneys and exacerbated autoimmune nephropathy, while oral administration of vancomycin reduced microbial-induced intestinal Th17 cells and Th17 responses in the kidneys, thereby improving the course of treatment for crescent glomerulonephritis (cGN) without any significant side effects [82]; these findings broaden the new understanding of Th17 cells.

In addition to the regulation of intestinal flora, Th17 cells play a central role in IBD, and their role depends on the production of their downstream effector cytokines. These cytokines mainly include IL-17A, IL-17F, IL-22, IL-21, and TNF-α [5].

IL-17 plays a key role in immune diseases. IL-17A is mainly produced by Th17 cells, but there are also many other types of cells that produce IL-17A, including CD8+ T cells, $\gamma\delta$ T cells, NK cells, and natural lymphoid cells (ILC). It plays an important role in adaptive and innate immune regulation. It mainly includes IL-17A-F, and its receptors mainly include IL-17RA-RE. IL-17A can exist as a homodimer, or it can pair with IL-17F to form a heterodimer, both of which are present in the colon of hapten-induced colitis mice [83, 84]. In the IL-17 family, IL-17A and IL-17F are considered to be the main cytokines that drive inflammation and autoimmunity. IL-17A and IL-17F can not only form a homodimer each but also can combine to form a heterodimer [84, 85]. IL-

17A mainly induces the production of a series of inflammatory mediators by activating the NF-κB and MAPK pathways, thereby recruiting a variety of immune cells to cause or aggravate the inflammation of colon tissue [86]. The effects of IL-17A and IL-17F in inflammatory mice are different. Studies have shown that IL17A-induced response is 10-30 times stronger than IL-17F in terms of downstream gene activation, and IL-17A-IL-17F heterologous two aggregate action at the intermediate level; this also explains that IL-17F knockout mice exhibit less severe DSS-induced colitis compared with the data obtained using IL-17A knockout mice [81, 87, 88]. Compared with normal mucosa, the levels of IL-17A and IL-17A mRNA in serum and diseased intestinal mucosa tissue of IBD patients are higher than that of normal people. In addition, the number of peripheral blood mononuclear cells (PBMCs) that produce IL-17A is similar to that of UC patients. The severity of the disease is related to the severity of the disease, which shows that IL-17 in the intestine plays a role in IBD patients [89]. In addition, IL-17A also induces the recruitment and activation of neutrophils and locally promotes the production of other proinflammatory cytokines, such as TNF-α and IL-6 [90]. However, this is contrary to the known positive effects of IL-17 in the formation of intestinal antimicrobial peptides and the defense against bacteria and fungi [91, 92]. In general, the immune function of IL-17 in the intestine has two sides. How to balance this two-sidedness is worthy of our in-depth study.

IL-22 is a member of the IL-10 family of cytokines, which can be produced by a variety of immune cells, including CD4+ (Th1, Th17, Th22), CD8+ T cells, $\gamma\delta$ T cells, NK cells, NKT cells, and innate lymphoid cell group ILC; due to its role in connecting inflammation and regeneration, it has received considerable attention in the past few years [93–97]. Among them, the third group of ILC represents a subgroup of natural lymphoid cells and is widely considered to be the innate counterpart of Th17 cells. IL-22 exerts its biological function mainly by binding to the IL-22 receptor (IL-22R). The receptor complex consists of two subunits, IL-22R1 and IL-10R2. In addition, soluble single-chain IL-22 binding receptor (IL-22 binding protein, IL-22BP), which can compete with IL-22R1, is considered an antagonist of IL-22 [98]. The ligation of IL-22-IL-22R1-IL-10R2 complex leads to the activation of JAK1/TYK2 kinase, which in turn leads to phosphorylation of STAT protein. In addition to the activation of STAT3, it seems that phosphorylation of STAT1 and STAT5 has also been observed [99–101]. IL-22 is mainly regulated by IL-23. Other promoting and regulating factors include IL-1β, IL-7, AhR, and Notch, and inhibitory factors mainly include IL-22BP, TGF-β, ICOS, and c-Maf [101]. In the intestinal immune response, IL-22 has been shown to be highly upregulated in the serum of patients with Crohn's disease or ulcerative colitis and is associated with poor prognosis [102]. During homeostasis, TH17 cells and ILC3 are induced to produce IL-17A and IL-22 by the intestinal symbiotic microflora, which plays an important role in promoting the integrity of the epithelial barrier, mucus production, and the release of antimicrobial peptides [103, 104]. In the acute inflammatory phase, Th17 cells and ILC3 proliferate and trigger the elimination of antigenic substances by neutrophils. In this process, IL-17A and IL-22 promote the proliferation and migration of intestinal cells, thereby promoting mucosal healing and maintaining the intestinal immune system. If the balance cannot be maintained for a long time, it will lead to chronic inflammation. In inflammatory bowel disease, highly pathogenic Th17 cells expand and secrete proinflammatory cytokines, such as IL-17A and IL-22, which can cause a wide range of inflammatory responses. In addition, long-term elevated IL-17A and IL-22 levels can promote cancer [105].

TNF-α is a member of the TNF superfamily, which is mainly produced by activated macrophages, Th cells, NK cells, neutrophils, and eosinophils [106, 107]. As a trimer, TNF-α exerts many functions by binding to cell membrane receptors TNFR-1 and TNFR-2, both of which belong to the so-called TNF receptor superfamily [108]. TNF-α is a powerful proinflammatory cytokine, which plays an important role in the pathogenesis of graft-versus-host disease and chronic inflammatory diseases (such as rheumatoid arthritis (RA) and inflammatory bowel disease) [109, 110]. TNF-α includes the transmembrane type and secreted type, among which transmembrane type TNF plays a more important role in inflammatory bowel disease. Experiments show that transmembrane TNF induces the activation of TNFR2, which intensifies the activity of colitis, and inhibits its function to improve the severity of colitis [111, 112]. Therefore, targeted transmembrane TNF may benefit more in clinical inflammatory bowel disease and have more promising treatments.

In addition to cytokines, transcription factors also play an important role in Th17 cells. The transcription factor IRF4 is involved in the occurrence of chronic inflammatory diseases. IRF4 can directly bind to the IL-17 promoter and induce mucosal RORγt levels and IL-17 gene expression, thereby controlling Th17-dependent colitis [113]. In the mouse model of colitis, HAO472 significantly improved the clinical symptoms of mice and reduced the severity of inflammation. These changes involved changes in many cytokines and decreased expression and activity of NF-κB [114]. Batf is an important transcription factor for Th17 cell development, and it is strongly upregulated in the tissues of IBD. Targeting Batf is a promising method for the treatment of IBD, which not only causes the loss of pathogenic T cell activity but also retains the off-target effect of the intestinal epithelial cell compartment [115]. In addition, ATF3 signals through IL-22-pSTAT3 in epithelial cells and IL-6-pSTAT3 in Th17 cells to maintain mucosal homeostasis [116].

Genome-wide association studies (GWAS) on IBD still provide strong evidence linking IBD to the Th17 pathway. Dangerous alleles in Th17 pathway-specific genes, such as NOD2, IL23R, CARD9, STAT3, RORC, JAK2, TYK2, and CCR6, enhance people's understanding of disease-related biological pathways, and these biological pathways which affect intestinal inflammation development are crucial [117, 118]. Recent studies have focused on small nuclear molecules that can broadly regulate gene expression, such as epigenetic markers (including DNA methylation, histone modifications that regulate chromatin structure, microRNA

(miRNA) interference that regulates posttranscriptional steps, and nucleosome localization), microRNAs (such as miR-802, miR-425, miR-301a), and noncoding RNAs, all of which participate in the pathogenesis of IBD through different pathways [117, 123].

4. Th17 Cell Plasticity

Polarized T cells have the ability to change their phenotype and repolarize toward different fates. This inherent flexibility is usually called plasticity. It is affected by the cytokine environment, microbial products, and metabolites. Among Th cells, Th17 cells are not one of the most stable cells and can be transformed into other Th subgroups under various influences. The plasticity of Th1-Th17 and Th17-Treg plays an important role in regulating the intestinal immune response [124].

4.1. Th1/Th17 Plasticity. A large number of studies suggest that the occurrence of inflammatory bowel disease is related to both Th1 and Th17. T cells accumulate in the inflamed gut of IBD patients, accompanied by higher levels of IFN-γ and IL-17, when compared with healthy individuals. IFN-γ^+ IL-17^+ double expressing cells are considered to be Th17 transformed into Th1 lymphocyte precursor cells, showing the indispensability of Th17/Th1 plasticity in the pathogenesis of colitis [125–127]. Retinoic acid (RA) signaling pathway is essential for restricting Th1 cells to transform into Th17 effectors and preventing pathogenic Th17 responses in vivo [128]. Likewise, IL-23 signaling can promote conversion from Th17 to Th1 by switching secretion from IL-17A to IFN-γ in vivo [129] a lineage marker of progenitor Th17 cells; CD161 is still sustained in Th1 cells converted from Th17 in humans [130]. This serves as evidence for the transdifferentiating of Th17 cells into Th1 cells because the conventional Th1 population does not express CD161. Besides, some "Th1-like" cells which coexpress RORγt and T-bet are functional in humans and mice and associated with potential pathogenicity [131]. The above research shows that Th17/Th1 is playing an increasingly important role in the development of IBD.

4.2. Treg/Th17 Plasticity. Several studies have described an imbalance between regulatory T cells and Th17 that may be associated with chronic inflammation and autoimmune diseases [132, 133]. Treg cells are known as an anti-inflammatory culture and include natural regulatory cells of thymus origin (nTregs) and peripheral regulatory cells (iTregs). According to reports, the developmental pathways of Th17 and tires are closely related, that is, they regulate and differentiate each other to maintain balance, thereby affecting the outcome of inflammatory bowel disease [134]. iTreg cells coexist with Th17 cells in the intestinal mucosa, where they play a role in controlling excessive effector T cell responses that may affect the host tissue [135]. Regulatory T cell therapy is a safe and well-tolerated potential approach for treating refractory Crohn's disease [136]. The ability to control inflammatory lesions with transferred Treg cells has been demonstrated in several IBD models [137]. In mouse models, it has been shown that transferring Tregs into mice can improve the clinical outcome and histological status of colitis [138, 139]. A similar result was that the expanded Tregs of rapamycin improved the colitis model of SCID mice [140]. For Treg therapy to be effective in IBD, expanded Tregs must have the ability to home to the gut [141]. The results of a multicenter phase I/IIa clinical trial indicate that the change in the balance between Foxp3 + CD4 + Treg cells and T effector cells in the intestinal microenvironment may be the cause of inflammatory bowel disease [142]. These results indicate that Th17 and Treg are closely related to inflammatory bowel disease, and there may be an antagonistic relationship; patients with IBD exhibit reduced numbers of peripheral Treg cells, and increased numbers of peripheral Th17 cells corroborated this [28]. Recent studies have demonstrated that Foxp3+ Treg cells express retinoic acid receptor-related orphan receptor gamma t and are thus able to differentiate into Th17 cells, a process that is associated with a decreased suppressive Treg cell function in patients with IBD. Treg cells were found to suppress colonic inflammation by downregulating Th17 responsiveness via TGF-β in an adoptive transfer mouse model of colitis [15, 16]. In addition, FoxP3 and RORγt regulate each other in the intestine [134], and double-expressing cells are well-documented in the large and small intestines [143]. Besides, a study showed evidence of plasticity between Treg and Th17 in the inflamed intestine of CD patients [144]. Further study shows the presence of circulating IL-17+Foxp3+ CD4+ T cells in IBD patients, suggesting increased plasticity between Th17 and Treg cells compared to healthy controls [15].

4.3. Microbiotas/Th17 Plasticity. In mouse models of IBD, components of IBD-associated microbiotas can induce Th17-biased effector T cell responses and exacerbate disease severity [145]. Recent clinical trials have demonstrated the potential of fecal microbiota transplantation (FMT) for treating individuals with ulcerative colitis [146]. Transfer of IBD microbiotas into germ-free mice increased the number of intestinal Th17 cells and decreased the number of RORγt+ Treg cells [147]. In mice, the resident intestinal Th17 cells almost completely recognized by symbiotic segmented filamentous bacteria (SFB) are in a noninflammatory barrier protection state and do not participate in systemic inflammatory reactions. However, citric acid Th17 cells induced by Bacillus have high plasticity to inflammatory cytokines; these findings indicate that the cellular microenvironment of Th17 cells may induce different inflammatory microenvironments, resulting in different epigenetic characteristics [148]. Taken together, the microbiome can induce Th17 development and further plasticity in the context of healthy and IBD conditions.

5. Treatment of IBD

In view of the key role of Th17 cells in intestinal inflammation, targeting Th17 cells may bring therapeutic hope for controlling intestinal inflammation. The traditional treatment of inflammatory bowel disease mainly uses 5-ASA, hormones, and immunosuppressive agents to control the

Table 1: Therapies targeting Th17 cells in IBD.

Drug	Targeted cytokine	Phase	Ref.
Ustekinumab	IL-12/23p40	III	[165]
Infliximab, adalimumab/golimumab, certolizumab pegol	TNF-α	Used in clinical	[166–168]
CT-P13/AVX-470	TNF-α	III/I	[156, 169]
Brazikumab/risankizumab/brazikumab/guselkumab/mirkizumab	IL-23p19	III/II	[151–154]
Tocilizumab	IL-6R	II	[170]
Secukinumab	*IL-17A*	II	[164]
Vedolizumab	$\alpha 4\beta 7$	Used in clinical	[160]
Tofacitinib	*JAK*	III	[159]
ABX464	*miR-124*	II	[163]

inflammatory symptoms, but it cannot be cured. Long-term treatment will also bring many adverse reactions. At present, new biological agents are more targeted and effective. It can bring more treatment options for IBD patients who are resistant to traditional treatment. The treatment of Th17 cells and related cytokines in patients has made some progress, which brings new ideas for the further treatment of IBD. Here, we focus on the progress of Th17 cells and important cytokines in their signaling pathways in the treatment of IBD [149](Table 1).

5.1. Anti-IL-23/12. The rise of anti-IL-23 therapies targeting the p40 subunit shared between IL-12 and IL-23, the p19 subunit of IL-23 alone, and JAK inhibitors that transmit IL-23R signals is all in the treatment of IBD with a display base. Ustekinumab is a humanized monoclonal IgG1 antibody that binds to the common subunit p40 of IL-12 and IL-23. Ustekinumab is currently the only anti-IL-23 therapy approved by the FDA for IBD. Early results showed that in the 8th week of the treatment group (130 mg IV or 6 mg/kg IV), about 16% of patients reported clinical remission, compared with 5% in the placebo group [150]. In addition, the strategy of targeting IL-23p19 also showed clinical benefits, including endoscopic remission and mucosal healing. Antibodies targeting IL-23p19 mainly include risankizumab, brazikumab, guselkumab, and mirikizumab. These targeted treatments are currently undergoing clinical trials [151–154].

5.2. Anti-TNF. At present, 4 TNF-α inhibitors have been approved for clinical use. They are infliximab (infliximab, IFX), adalimumab (ADA), golimumab (golimumab), and Sai Tocilizumab (certolizumab pegol, CZP). Therapeutic drugs that antagonize TNF-α mainly antagonize transmembrane TNF, while the effect of mainly blocking secreted TNF is not ideal [155]. Therefore, the interaction between transmembrane TNF-TNFR2 is expected to achieve better therapeutic effects. In addition, AVX-470 is a polyclonal antibody extracted from cows immunized with recombinant human TNF, which can exert certain effects in patients with IBD by targeting TNF-α in the gastrointestinal tract [156]. Although anti-TNF-α therapy shows clinical effectiveness, 10%-30% of patients with inflammatory bowel disease do not respond to antitumor necrosis factor-α therapy, and 20%-40% of patients lose their response over time [157, 158].

5.3. Anti-JAK-STAT Signaling. Since the JAK-STAT signaling pathway is involved in the pathogenesis of IBD, blocking JAK preparations can be an option for the treatment of IBD, such as the JAK inhibitor tofacitinib. A phase 3 clinical trial showed that compared with the placebo group, patients who took tofacitinib within 3 days had significantly improved symptoms [159].

Vedolizumab (vedolizumab) is a humanized anti-$\alpha 4\beta 7$ integrin Ig G1 monoclonal antibody that targets $\alpha 4\beta 7$ integrin, thereby reducing the intestinal immunity of patients with IBD. It was awarded the European Medicines Agency and FDA approval for the treatment of moderate to severe UC and CD [160].

Other treatments including RORrt, gene therapy, and fecal microbiota transplantation (FMT) have made corresponding research progress, which broadens people's understanding of IBD treatment [161–163].

6. Conclusion

IBD is a type of autoimmune disease. With the recent decades of research, it has been discovered that immune cells play an important role in the occurrence and development of IBD. As an important part of the immune pathological response, helper T cells are closely related to a variety of autoimmune diseases. With the deepening of research, Th17 cells, a subgroup of T helper cells, gradually appear in front of the people. A large number of studies have shown that Th17 cells are mainly related to autoinflammatory response, and its downstream cytokines and related immune mediators play a role in promoting the development of the disease, and this promotion is unfavorable to the body. Current research shows that Th17 cells are at the center of the occurrence and development of IBD. The effect of cytokines upstream and downstream of Th17 cells on IBD has been extensively studied. In addition, it includes transcription factors, intestinal flora, external environment, and other factors. The interaction with Th17 cells has a corresponding effect on IBD. The plasticity and heterogeneity of Th117 cells have opened new doors for Th17 cells. These new understandings provide new ideas for immunotherapy of autoimmune diseases including IBD. IBD is an autoimmune disease. With the recent decades of research, it has been found that the immune system has made great progress in revealing the role of Th17 cells in

the intestinal inflammation process, and attempts to target Th17 cells have shown encouraging results. However, there are still many problems in clinical treatment. For example, anti-IL-17 drugs have a good effect on psoriasis, but they are not effective in CD patients or aggravate the condition of CD patients [164]. Therefore, a better understanding of Th17 cells can lay a solid foundation for the development of new and effective IBD therapeutic biological agents.

Individualized drug therapy, the use of multifactor blockers, gene therapy, FMT, and other combined treatment programs are expected to become new methods for the treatment of IBD. Maintaining the balance of Th17/Treg cells is the basis of treatment for the balance of proinflammatory and anti-inflammatory in the body. This method provides a bright vision for the current treatment of IBD.

Conflicts of Interest

The authors declare that there is no conflict of interest regarding the publication of this paper.

Authors' Contributions

Junjun Zhao, Qiliang Lu, Yang Liu, and Zhan Shi equally contributed to this work.

Acknowledgments

The supporting grants from funds are as follows: the National Natural Science Foundation of China (81672474, 81874049), the Coconstruction of Provincial and Department Project (WKJ-ZJ-1919), and the National Science and Technology Major Project for New Drug (No. 2017ZX09302003004).

References

[1] R. Voelker, "Inflammatory bowel disease is more common than earlier studies showed," *JAMA*, vol. 316, no. 24, p. 2590, 2016.

[2] A. Kaser, S. Zeissig, and R. S. Blumberg, "Inflammatory bowel disease," *Annual Review of Immunology*, vol. 28, no. 1, pp. 573–621, 2010.

[3] A. Geremia, P. Biancheri, P. Allan, G. R. Corazza, and A. di Sabatino, "Innate and adaptive immunity in inflammatory bowel disease," *Autoimmunity Reviews*, vol. 13, no. 1, pp. 3–10, 2014.

[4] Z.-J. Liu, P. K. Yadav, J.-L. Su, J.-S. Wang, and K. Fei, "Potential role of Th17 cells in the pathogenesis of inflammatory bowel disease," *World Journal of Gastroenterology*, vol. 15, no. 46, pp. 5784–5788, 2009.

[5] A. Raza, W. Yousaf, R. Giannella, and M. T. Shata, "Th17 cells: interactions with predisposing factors in the immunopathogenesis of inflammatory bowel disease," *Expert Review of Clinical Immunology*, vol. 8, no. 2, pp. 161–168, 2014.

[6] J. Yang, M. S. Sundrud, J. Skepner, and T. Yamagata, "Targeting Th17 cells in autoimmune diseases," *Trends in Pharmacological Sciences*, vol. 35, no. 10, pp. 493–500, 2014.

[7] K. Yasuda, Y. Takeuchi, and K. Hirota, "The pathogenicity of Th17 cells in autoimmune diseases," *Seminars in Immunopathology*, vol. 41, no. 3, pp. 283–297, 2019.

[8] L. E. Harrington, R. D. Hatton, P. R. Mangan et al., "Interleukin 17-producing CD4+ effector T cells develop via a lineage distinct from the T helper type 1 and 2 lineages," *Nature Immunology*, vol. 6, no. 11, pp. 1123–1132, 2005.

[9] C. Blaschitz and M. Raffatellu, "Th17 cytokines and the gut mucosal barrier," *Journal of Clinical Immunology*, vol. 30, no. 2, pp. 196–203, 2010.

[10] G. Trinchieri, S. Pflanz, and R. A. Kastelein, "The IL-12 family of heterodimeric cytokines: new players in the regulation of T cell responses," *Immunity*, vol. 19, no. 5, pp. 641–644, 2003.

[11] S. J. Szabo, S. T. Kim, G. L. Costa, X. Zhang, C. G. Fathman, and L. H. Glimcher, "A novel transcription factor, T-bet, directs Th1 lineage commitment," *Cell*, vol. 100, no. 6, pp. 655–669, 2000.

[12] G. Del Prete, "Human Th1 and Th2 lymphocytes: their role in the pathophysiology of atopy," *Allergy*, vol. 47, no. 5, pp. 450–455, 1992.

[13] J. Zhu, "T helper 2 (Th2) cell differentiation, type 2 innate lymphoid cell (ILC2) development and regulation of interleukin-4 (IL-4) and IL-13 production," *Cytokine*, vol. 75, no. 1, pp. 14–24, 2015.

[14] E. M. Shevach and A. M. Thornton, "tTregs, pTregs, and iTregs: similarities and differences," *Immunological Reviews*, vol. 259, no. 1, pp. 88–102, 2014.

[15] A. Ueno, H. Jijon, R. Chan et al., "Increased prevalence of circulating novel IL-17 secreting Foxp3 expressing CD4+ T cells and defective suppressive function of circulating Foxp3+ regulatory cells support plasticity between Th17 and regulatory T cells in inflammatory bowel disease patients," *Inflammatory Bowel Diseases*, vol. 19, no. 12, pp. 2522–2534, 2013.

[16] O. J. Harrison, N. Srinivasan, J. Pott et al., "Epithelial-derived IL-18 regulates Th17 cell differentiation and Foxp3$^+$ Treg cell function in the intestine," *Mucosal Immunology*, vol. 8, no. 6, pp. 1226–1236, 2015.

[17] J. Galvez, "Role of Th17 cells in the pathogenesis of human IBD," *ISRN Inflammation*, vol. 2014, Article ID 928461, 14 pages, 2014.

[18] C. L. Langrish, Y. Chen, W. M. Blumenschein et al., "IL-23 drives a pathogenic T cell population that induces autoimmune inflammation," *The Journal of Experimental Medicine*, vol. 201, no. 2, pp. 233–240, 2005.

[19] C. A. Murphy, C. L. Langrish, Y. Chen et al., "Divergent pro- and antiinflammatory roles for IL-23 and IL-12 in joint autoimmune inflammation," *The Journal of Experimental Medicine*, vol. 198, no. 12, pp. 1951–1957, 2003.

[20] G. Hou and S. Bishu, "Th17 cells in inflammatory bowel disease: an update for the clinician," *Inflammatory Bowel Diseases*, vol. 26, no. 5, pp. 653–661, 2020.

[21] B. Oppmann, R. Lesley, B. Blom et al., "Novel p19 protein engages IL-12p40 to form a cytokine, IL-23, with biological activities similar as well as distinct from IL-12," *Immunity*, vol. 13, no. 5, pp. 715–725, 2000.

[22] C. Parham, M. Chirica, J. Timans et al., "A receptor for the heterodimeric cytokine IL-23 is composed of IL-12Rbeta1 and a novel cytokine receptor subunit, IL-23R," *Journal of Immunology*, vol. 168, no. 11, pp. 5699–5708, 2002.

[23] T. Korn, E. Bettelli, M. Oukka, and V. K. Kuchroo, "IL-17 and Th17 cells," *Annual Review of Immunology*, vol. 27, no. 1, pp. 485–517, 2009.

[24] M. J. McGeachy, Y. Chen, C. M. Tato et al., "The interleukin 23 receptor is essential for the terminal differentiation of interleukin 17-producing effector T helper cells in vivo," *Nature Immunology*, vol. 10, no. 3, pp. 314–324, 2009.

[25] M. C. Kullberg, D. Jankovic, C. G. Feng et al., "IL-23 plays a key role in Helicobacter hepaticus-induced T cell-dependent colitis," *Journal of Experimental Medicine*, vol. 203, no. 11, pp. 2485–2494, 2006.

[26] A. Peters, Y. Lee, and V. K. Kuchroo, "The many faces of Th17 cells," *Current Opinion in Immunology*, vol. 23, no. 6, pp. 702–706, 2011.

[27] T. Feng, H. Qin, L. Wang, E. N. Benveniste, C. O. Elson, and Y. Cong, "Th17 cells induce colitis and promote Th1 cell responses through IL-17 induction of innate IL-12 and IL-23 production," *Journal of Immunology*, vol. 186, no. 11, pp. 6313–6318, 2011.

[28] N. Eastaff-Leung, N. Mabarrack, A. Barbour, A. Cummins, and S. Barry, "Foxp3+ regulatory T cells, Th17 effector cells, and cytokine environment in inflammatory bowel disease," *Journal of Clinical Immunology*, vol. 30, no. 1, pp. 80–89, 2010.

[29] X. M. Zhu, Y. Z. Shi, M. Cheng, D. F. Wang, and J. F. Fan, "Serum IL-6, IL-23 profile and Treg/Th17 peripheral cell populations in pediatric patients with inflammatory bowel disease," *Pharmazie*, vol. 72, no. 5, pp. 283–287, 2017.

[30] M. F. Neurath, "IL-23 in inflammatory bowel diseases and colon cancer," *Cytokine & Growth Factor Reviews*, vol. 45, pp. 1–8, 2019.

[31] C. Wu, N. Yosef, T. Thalhamer et al., "Induction of pathogenic TH17 cells by inducible salt-sensing kinase SGK1," *Nature*, vol. 496, no. 7446, pp. 513–517, 2013.

[32] M. Allocca, M. Jovani, G. Fiorino, S. Schreiber, and S. Danese, "Anti-IL-6 treatment for inflammatory bowel diseases: next cytokine, next target," *Current Drug Targets*, vol. 14, no. 12, pp. 1508–1521, 2013.

[33] S. A. Jones and S. Rose-John, "The role of soluble receptors in cytokine biology: the agonistic properties of the sIL-6R/IL-6 complex," *Biochimica et Biophysica Acta*, vol. 1592, no. 3, pp. 251–263, 2002.

[34] J. Mudter and M. F. Neurath, "Il-6 signaling in inflammatory bowel disease: pathophysiological role and clinical relevance," *Inflammatory Bowel Diseases*, vol. 13, no. 8, pp. 1016–1023, 2007.

[35] T. Tanaka, M. Narazaki, and T. Kishimoto, "IL-6 in inflammation, immunity, and disease," *Cold Spring Harbor Perspectives in Biology*, vol. 6, no. 10, p. a016295, 2014.

[36] S. N. Harbour, D. F. DiToro, S. J. Witte et al., "TH17 cells require ongoing classic IL-6 receptor signaling to retain transcriptional and functional identity," *Science Immunology*, vol. 5, no. 49, 2020.

[37] M. J. McGeachy, K. S. Bak-Jensen, Y. Chen et al., "TGF-β and IL-6 drive the production of IL-17 and IL-10 by T cells and restrain TH-17 cell-mediated pathology," *Nature Immunology*, vol. 8, no. 12, pp. 1390–1397, 2007.

[38] Y. Chen, C. . J. Haines, I. Gutcher et al., "Foxp3(+) regulatory T cells promote T helper 17 cell development in vivo through regulation of interleukin-2," *Immunity*, vol. 34, no. 3, pp. 409–421, 2011.

[39] J. M. Coquet, K. Kyparissoudis, D. G. Pellicci et al., "IL-21 is produced by NKT cells and modulates NKT cell activation and cytokine production," *Journal of Immunology*, vol. 178, no. 5, pp. 2827–2834, 2007.

[40] D. S. Mehta, A. L. Wurster, and M. J. Grusby, "Biology of IL-21 and the IL-21 receptor," *Immunological Reviews*, vol. 202, no. 1, pp. 84–95, 2004.

[41] J. Parrish-Novak, S. R. Dillon, A. Nelson et al., "Interleukin 21 and its receptor are involved in NK cell expansion and regulation of lymphocyte function," *Nature*, vol. 408, no. 6808, pp. 57–63, 2000.

[42] K. Ozaki, K. Kikly, D. Michalovich, P. R. Young, and W. J. Leonard, "Cloning of a type I cytokine receptor most related to the IL-2 receptor beta chain," *Proceedings of the National Academy of Sciences of the United States of America*, vol. 97, no. 21, pp. 11439–11444, 2000.

[43] Y. Tian and A. J. Zajac, "IL-21 and T cell differentiation: consider the context," *Trends in Immunology*, vol. 37, no. 8, pp. 557–568, 2016.

[44] T. Korn, E. Bettelli, W. Gao et al., "IL-21 initiates an alternative pathway to induce proinflammatory T_H17 cells," *Nature*, vol. 448, no. 7152, pp. 484–487, 2007.

[45] R. Nurieva, X. O. Yang, G. Martinez et al., "Essential autocrine regulation by IL-21 in the generation of inflammatory T cells," *Nature*, vol. 448, no. 7152, pp. 480–483, 2007.

[46] L. Zhou, I. I. Ivanov, R. Spolski et al., "IL-6 programs T(H)-17 cell differentiation by promoting sequential engagement of the IL-21 and IL-23 pathways," *Nature Immunology*, vol. 8, no. 9, pp. 967–974, 2007.

[47] E. K. Deenick and S. G. Tangye, "Autoimmunity: IL-21: a new player in Th17-cell differentiation," *Immunology and Cell Biology*, vol. 85, no. 7, pp. 503–505, 2007.

[48] Y. Wang, X. Jiang, J. Zhu et al., "IL-21/IL-21R signaling suppresses intestinal inflammation induced by DSS through regulation of Th responses in lamina propria in mice," *Scientific Reports*, vol. 6, article 31881, 2016.

[49] A. Yeste, I. D. Mascanfroni, M. Nadeau et al., "IL-21 induces IL-22 production in CD4+ T cells," *Nature Communications*, vol. 5, no. 1, p. 3753, 2014.

[50] P. E. Auron, A. C. Webb, L. J. Rosenwasser et al., "Nucleotide sequence of human monocyte interleukin 1 precursor cDNA," *Proceedings of the National Academy of Sciences of the United States of America*, vol. 81, no. 24, pp. 7907–7911, 1984.

[51] A. S. Yazdi and K. Ghoreschi, "The interleukin-1 family," *Advances in Experimental Medicine and Biology*, vol. 941, pp. 21–29, 2016.

[52] L. Mao, A. Kitani, W. Strober, and I. J. Fuss, "The role of NLRP3 and IL-1β in the pathogenesis of inflammatory bowel disease," *Frontiers in Immunology*, vol. 9, p. 2566, 2018.

[53] Y. Chung, S. H. Chang, G. J. Martinez et al., "Critical regulation of early Th17 cell differentiation by interleukin-1 signaling," *Immunity*, vol. 30, no. 4, pp. 576–587, 2009.

[54] N. Manel, D. Unutmaz, and D. R. Littman, "The differentiation of human TH-17 cells requires transforming growth factor-β and induction of the nuclear receptor RORγt," *Nature Immunology*, vol. 9, no. 6, pp. 641–649, 2008.

[55] R. K. Ramakrishnan, S. Al Heialy, and Q. Hamid, "Role of IL-17 in asthma pathogenesis and its implications for the clinic," *Expert Review of Respiratory Medicine*, vol. 13, no. 11, pp. 1057–1068, 2019.

[56] I. I. Ivanov, B. S. McKenzie, L. Zhou et al., "The orphan nuclear receptor RORγt directs the differentiation program of proinflammatory IL-17+ T helper cells," *Cell*, vol. 126, no. 6, pp. 1121–1133, 2006.

[57] J. Geng, S. Yu, H. Zhao et al., "The transcriptional coactivator TAZ regulates reciprocal differentiation of T17 cells and T cells," *Nature Immunology*, vol. 18, no. 7, pp. 800–812, 2017.

[58] G. J. Martinez, Z. Zhang, Y. Chung et al., "Smad3 differentially regulates the induction of regulatory and inflammatory T cell differentiation," *Journal of Biological Chemistry*, vol. 284, no. 51, pp. 35283–35286, 2009.

[59] K. Essig, D. Hu, J. C. Guimaraes et al., "Roquin suppresses the PI3K-mTOR signaling pathway to inhibit T helper cell differentiation and conversion of Treg to Tfr cells," *Immunity*, vol. 47, no. 6, pp. 1067–1082.e12, 2017.

[60] D. Lu, L. Liu, X. Ji et al., "The phosphatase DUSP2 controls the activity of the transcription activator STAT3 and regulates TH17 differentiation," *Nature Immunology*, vol. 16, no. 12, pp. 1263–1273, 2015.

[61] D. Shi, J. Das, and G. Das, "Inflammatory bowel disease requires the interplay between innate and adaptive immune signals," *Cell Research*, vol. 16, no. 1, pp. 70–74, 2006.

[62] D. K. Podolsky, "Inflammatory bowel disease," *New England Journal of Medicine*, vol. 347, no. 6, pp. 417–429, 2002.

[63] Y. Li, Y. Liu, and C.-Q. Chu, "Th17 cells in type 1 diabetes: role in the pathogenesis and regulation by gut microbiome," *Mediators of Inflammation*, vol. 2015, Article ID 638470, 7 pages, 2015.

[64] C. Sie, T. Korn, and M. Mitsdoerffer, "Th17 cells in central nervous system autoimmunity," *Experimental Neurology*, vol. 262, pp. 18–27, 2014.

[65] S. Kotake, T. Yago, T. Kobashigawa, and Y. Nanke, "The plasticity of Th17 cells in the pathogenesis of rheumatoid arthritis," *Journal of Clinical Medicine*, vol. 6, no. 7, 2017.

[66] S. J. Allison, "Autoimmune disease: egress of intestinal T17 cells in autoimmune renal disease," *Nature Reviews Nephrology*, vol. 13, no. 2, p. 61, 2017.

[67] C. Abraham and J. H. Cho, "Inflammatory bowel disease," *The New England Journal of Medicine*, vol. 361, no. 21, pp. 2066–2078, 2009.

[68] S. K. Mazmanian, J. L. Round, and D. L. Kasper, "A microbial symbiosis factor prevents intestinal inflammatory disease," *Nature*, vol. 453, no. 7195, pp. 620–625, 2008.

[69] J. D. Taurog, J. A. Richardson, J. T. Croft et al., "The germfree state prevents development of gut and joint inflammatory disease in HLA-B27 transgenic rats," *The Journal of Experimental Medicine*, vol. 180, no. 6, pp. 2359–2364, 1994.

[70] Y. Cong, S. L. Brandwein, R. P. McCabe et al., "CD4+ T cells reactive to enteric bacterial antigens in spontaneously colitic C3H/HeJBir mice: increased T helper cell type 1 response and ability to transfer disease," *The Journal of Experimental Medicine*, vol. 187, no. 6, pp. 855–864, 1998.

[71] T. G. Tan, E. Sefik, N. Geva-Zatorsky et al., "Identifying species of symbiont bacteria from the human gut that, alone, can induce intestinal Th17 cells in mice," *Proceedings of the National Academy of Sciences*, vol. 113, no. 50, pp. E8141–E8150, 2016.

[72] I. I. Ivanov, K. Atarashi, N. Manel et al., "Induction of intestinal Th17 cells by segmented filamentous bacteria," *Cell*, vol. 139, no. 3, pp. 485–498, 2009.

[73] W. Reinisch, C. Gasche, W. Tillinger et al., "Clinical relevance of serum interleukin-6 in Crohn's disease: single point measurements, therapy monitoring, and prediction of clinical relapse," *The American Journal of Gastroenterology*, vol. 94, no. 8, pp. 2156–2164, 1999.

[74] J.-Y. Lee, J. A. Hall, L. Kroehling et al., "Serum amyloid A proteins induce pathogenic Th17 cells and promote inflammatory disease," *Cell*, vol. 180, no. 1, pp. 79–91.e16, 2020.

[75] L. Rovedatti, T. Kudo, P. Biancheri et al., "Differential regulation of interleukin 17 and IFN-γ production in inflammatory bowel disease," *Gut*, vol. 58, no. 12, pp. 1629–1636, 2009.

[76] I. J. Fuss, M. Neurath, M. Boirivant et al., "Disparate CD4+ lamina propria (LP) lymphokine secretion profiles in inflammatory bowel disease. Crohn's disease LP cells manifest increased secretion of IFN-gamma, whereas ulcerative colitis LP cells manifest increased secretion of IL-5," *The Journal of Immunology*, vol. 157, no. 3, pp. 1261–1270, 1996.

[77] S. Fujino, A. Andoh, S. Bamba et al., "Increased expression of interleukin 17 in inflammatory bowel disease," *Gut*, vol. 52, no. 1, pp. 65–70, 2003.

[78] W. Jiang, J. Su, X. Zhang et al., "Elevated levels of Th17 cells and Th17-related cytokines are associated with disease activity in patients with inflammatory bowel disease," *Inflammation Research*, vol. 63, no. 11, pp. 943–950, 2014.

[79] Y. Wei, C. Lu, J. Chen et al., "High salt diet stimulates gut Th17 response and exacerbates TNBS-induced colitis in mice," *Oncotarget*, vol. 8, no. 1, pp. 70–82, 2017.

[80] T. Kinugasa, T. Sakaguchi, X. Gu, and H. C. Reinecker, "Claudins regulate the intestinal barrier in response to immune mediators," *Gastroenterology*, vol. 118, no. 6, pp. 1001–1011, 2000.

[81] H. Ishigame, S. Kakuta, T. Nagai et al., "Differential roles of interleukin-17A and -17F in host defense against mucoepithelial bacterial infection and allergic responses," *Immunity*, vol. 30, no. 1, pp. 108–119, 2009.

[82] C. . F. Krebs, H.-J. Paust, S. Krohn et al., "Autoimmune renal disease is exacerbated by S1P-receptor-1-dependent intestinal Th17 cell migration to the kidney," *Immunity*, vol. 45, no. 5, pp. 1078–1092, 2016.

[83] P. Miossec and J. K. Kolls, "Targeting IL-17 and T_H17 cells in chronic inflammation," *Nature Reviews. Drug Discovery*, vol. 11, no. 10, pp. 763–776, 2012.

[84] J. F. Wright, F. Bennett, B. Li et al., "The human IL-17F/IL-17A heterodimeric cytokine signals through the IL-17RA/IL-17RC receptor complex," *Journal of Immunology*, vol. 181, no. 4, pp. 2799–2805, 2008.

[85] R. E. Kuestner, D. W. Taft, A. Haran et al., "Identification of the IL-17 receptor related molecule IL-17RC as the receptor for IL-17F," *The Journal of Immunology*, vol. 179, no. 8, pp. 5462–5473, 2007.

[86] J. C. Brazil, N. A. Louis, and C. A. Parkos, "The role of polymorphonuclear leukocyte trafficking in the perpetuation of inflammation during inflammatory bowel disease," *Inflammatory Bowel Diseases*, vol. 19, no. 7, pp. 1556–1565, 2013.

[87] S. L. Gaffen, "Structure and signalling in the IL-17 receptor family," *Nature Reviews. Immunology*, vol. 9, no. 8, pp. 556–567, 2009.

[88] S. L. Gaffen, J. M. Kramer, J. J. Yu, and F. Shen, "The IL-17 cytokine family," *Vitamins and Hormones*, vol. 74, pp. 255–282, 2006.

[89] H. Rafa, H. Saoula, M. Belkhelfa et al., "IL-23/IL-17A axis correlates with the nitric oxide pathway in inflammatory bowel disease: immunomodulatory effect of retinoic acid," *Journal of Interferon & Cytokine Research*, vol. 33, no. 7, pp. 355–368, 2013.

[90] Y. Iwakura, H. Ishigame, S. Saijo, and S. Nakae, "Functional specialization of interleukin-17 family members," *Immunity*, vol. 34, no. 2, pp. 149–162, 2011.

[91] S. Ho, C. Pothoulakis, and H. W. Koon, "Antimicrobial peptides and colitis," *Current Pharmaceutical Design*, vol. 19, no. 1, pp. 40–47, 2013.

[92] P. Kumar, L. Monin, P. Castillo et al., "Intestinal interleukin-17 receptor signaling mediates reciprocal control of the gut microbiota and autoimmune inflammation," *Immunity*, vol. 44, no. 3, pp. 659–671, 2016.

[93] L. Dumoutier, J. Louahed, and J. C. Renauld, "Cloning and characterization of IL-10-related T cell-derived inducible factor (IL-TIF), a novel cytokine structurally related to IL-10 and inducible by IL-9," *Journal of Immunology*, vol. 164, no. 4, pp. 1814–1819, 2000.

[94] S. Trifari, C. D. Kaplan, E. H. Tran, N. K. Crellin, and H. Spits, "Identification of a human helper T cell population that has abundant production of interleukin 22 and is distinct from T(H)-17, T(H)1 and T(H)2 cells," *Nature Immunology*, vol. 10, no. 8, pp. 864–871, 2009.

[95] H. Hamada, M. . . L. Garcia-Hernandez, J. B. Reome et al., "Tc17, a unique subset of CD8 T cells that can protect against lethal influenza challenge," *Journal of Immunology*, vol. 182, no. 6, pp. 3469–3481, 2009.

[96] P. L. Simonian, F. Wehrmann, C. L. Roark, W. K. Born, R. L. O'Brien, and A. P. Fontenot, "$\gamma\delta$ T cells protect against lung fibrosis via IL-22," *The Journal of Experimental Medicine*, vol. 207, no. 10, pp. 2239–2253, 2010.

[97] N. Satoh-Takayama, C. A. J. Vosshenrich, S. Lesjean-Pottier et al., "Microbial flora drives interleukin 22 production in intestinal NKp46+ cells that provide innate mucosal immune defense," *Immunity*, vol. 29, no. 6, pp. 958–970, 2008.

[98] K. Wolk, S. Kunz, E. Witte, M. Friedrich, K. Asadullah, and R. Sabat, "IL-22 increases the innate immunity of tissues," *Immunity*, vol. 21, no. 2, pp. 241–254, 2004.

[99] D. Lejeune, L. Dumoutier, S. Constantinescu, W. Kruijer, J. J. Schuringa, and J. C. Renauld, "Interleukin-22 (IL-22) activates the JAK/STAT, ERK, JNK, and p38 MAP kinase pathways in a rat hepatoma cell line," *The Journal of Biological Chemistry*, vol. 277, no. 37, pp. 33676–33682, 2002.

[100] A. Mitra, S. K. Raychaudhuri, and S. P. Raychaudhuri, "IL-22 induced cell proliferation is regulated by PI3K/Akt/mTOR signaling cascade," *Cytokine*, vol. 60, no. 1, pp. 38–42, 2012.

[101] J. A. Dudakov, A. M. Hanash, and M. R. van den Brink, "Interleukin-22: immunobiology and pathology," *Annual Review of Immunology*, vol. 33, pp. 747–785, 2015.

[102] A. Andoh, Z. Zhang, O. Inatomi et al., "Interleukin-22, a member of the IL-10 subfamily, induces inflammatory responses in colonic subepithelial myofibroblasts," *Gastroenterology*, vol. 129, no. 3, pp. 969–984, 2005.

[103] G. Pickert, C. Neufert, M. Leppkes et al., "STAT3 links IL-22 signaling in intestinal epithelial cells to mucosal wound healing," *The Journal of Experimental Medicine*, vol. 206, no. 7, pp. 1465–1472, 2009.

[104] C. J. Kim, A. Nazli, O. L. Rojas et al., "A role for mucosal IL-22 production and Th22 cells in HIV-associated mucosal immunopathogenesis," *Mucosal Immunology*, vol. 5, no. 6, pp. 670–680, 2012.

[105] J. Kempski, L. Brockmann, N. Gagliani, and S. Huber, "TH17 cell and epithelial cell crosstalk during inflammatory bowel disease and carcinogenesis," *Frontiers in Immunology*, vol. 8, p. 1373, 2017.

[106] L. C. Gahring, N. G. Carlson, R. A. Kulmer, and S. W. Rogers, "Neuronal expression of tumor necrosis factor alpha in the murine brain," *Neuroimmunomodulation*, vol. 3, no. 5, pp. 289–303, 1996.

[107] M. B. Olszewski, A. J. Groot, J. Dastych, and E. F. Knol, "TNF trafficking to human mast cell granules: mature chain-dependent endocytosis," *Journal of Immunology*, vol. 178, no. 9, pp. 5701–5709, 2007.

[108] H. T. Idriss and J. H. Naismith, "TNF alpha and the TNF receptor superfamily: structure-function relationship(s)," *Microscopy Research and Technique*, vol. 50, no. 3, pp. 184–195, 2000.

[109] J. R. Bradley, "TNF-mediated inflammatory disease," *The Journal of Pathology*, vol. 214, no. 2, pp. 149–160, 2008.

[110] S. H. Murch, C. P. Braegger, J. A. Walker-Smith, and T. T. MacDonald, "Location of tumour necrosis factor alpha by immunohistochemistry in chronic inflammatory bowel disease," *Gut*, vol. 34, no. 12, pp. 1705–1709, 1993.

[111] C. Perrier, G. de Hertogh, J. Cremer et al., "Neutralization of membrane TNF, but not soluble TNF, is crucial for the treatment of experimental colitis," *Inflammatory Bowel Diseases*, vol. 19, no. 2, pp. 246–253, 2013.

[112] T. Horiuchi, H. Mitoma, S. I. Harashima, H. Tsukamoto, and T. Shimoda, "Transmembrane TNF-α: structure, function and interaction with anti-TNF agents," *Rheumatology (Oxford)*, vol. 49, no. 7, pp. 1215–1228, 2010.

[113] J. Mudter, J. Yu, C. Zufferey et al., "IRF4 regulates IL-17A promoter activity and controls RORγt-dependent Th17 colitis in vivo," *Inflammatory Bowel Diseases*, vol. 17, no. 6, pp. 1343–1358, 2011.

[114] Q. Q. Liu, H. L. Wang, K. Chen et al., "Oridonin derivative ameliorates experimental colitis by inhibiting activated T-cells and translocation of nuclear factor-kappa B," *Journal of Digestive Diseases*, vol. 17, no. 2, pp. 104–112, 2016.

[115] K. Hildner, E. Punkenburg, B. Abendroth, and M. F. Neurath, "Immunopathogenesis of IBD: Batf as a key driver of disease activity," *Digestive Diseases*, vol. 34, Supplement 1, pp. 40–47, 2016.

[116] D. Glal, J. N. Sudhakar, H.-H. Lu et al., "ATF3 sustains IL-22-induced STAT3 phosphorylation to maintain mucosal immunity through inhibiting phosphatases," *Frontiers in Immunology*, vol. 9, article 2522, 2018.

[117] Y. Z. Zhang and Y. Y. Li, "Inflammatory bowel disease: pathogenesis," *World Journal of Gastroenterology*, vol. 20, no. 1, pp. 91–99, 2014.

[118] D. P. McGovern, S. Kugathasan, and J. H. Cho, "Genetics of inflammatory bowel diseases," *Gastroenterology*, vol. 149, no. 5, pp. 1163–1176.e2, 2015.

[119] G. P. Ramos and K. A. Papadakis, "Mechanisms of disease: inflammatory bowel diseases," *Mayo Clinic Proceedings*, vol. 94, no. 1, pp. 155–165, 2019.

[120] J. Yao, R. Gao, M. Luo et al., "miR-802 participates in the inflammatory process of inflammatory bowel disease by suppressing SOCS5," *Bioscience Reports*, vol. 40, no. 4, 2020.

[121] X. Yang, Q. He, Z. Guo et al., "MicroRNA-425 facilitates pathogenic Th17 cell differentiation by targeting forkhead box O1 (Foxo1) and is associated with inflammatory bowel disease," *Biochemical and Biophysical Research Communications*, vol. 496, no. 2, pp. 352–358, 2018.

[122] C. He, Y. Shi, R. Wu et al., "miR-301a promotes intestinal mucosal inflammation through induction of IL-17A and TNF-α in IBD," *Gut*, vol. 65, no. 12, pp. 1938–1950, 2016.

[123] R. Yarani, A. H. Mirza, S. Kaur, and F. Pociot, "The emerging role of lncRNAs in inflammatory bowel disease," *Experimental & Molecular Medicine*, vol. 50, no. 12, pp. 1–14, 2018.

[124] A. Ueno, L. Jeffery, T. Kobayashi, T. Hibi, S. Ghosh, and H. Jijon, "Th17 plasticity and its relevance to inflammatory bowel disease," *Journal of Autoimmunity*, vol. 87, pp. 38–49, 2018.

[125] S. N. Harbour, C. L. Maynard, C. L. Zindl, T. R. Schoeb, and C. T. Weaver, "Th17 cells give rise to Th1 cells that are required for the pathogenesis of colitis," *Proceedings of the National Academy of Sciences*, vol. 112, no. 22, pp. 7061–7066, 2015.

[126] M. Esposito, F. Ruffini, A. Bergami et al., "IL-17- and IFN-γ-secreting Foxp3+ T cells infiltrate the target tissue in experimental autoimmunity," *The Journal of Immunology*, vol. 185, no. 12, pp. 7467–7473, 2010.

[127] J. Verdier, B. Begue, N. Cerf-Bensussan, and F. M. Ruemmele, "Compartmentalized expression of Th1 and Th17 cytokines in pediatric inflammatory bowel diseases," *Inflammatory Bowel Diseases*, vol. 18, no. 7, pp. 1260–1266, 2012.

[128] C. . C. Brown, D. Esterhazy, A. Sarde et al., "Retinoic acid is essential for Th1 cell lineage stability and prevents transition to a Th17 cell program," *Immunity*, vol. 42, no. 3, pp. 499–511, 2015.

[129] K. Hirota, J. H. Duarte, M. Veldhoen et al., "Fate mapping of IL-17-producing T cells in inflammatory responses," *Nature Immunology*, vol. 12, no. 3, pp. 255–263, 2011.

[130] L. Cosmi, R. De Palma, V. Santarlasci et al., "Human interleukin 17-producing cells originate from a CD161+CD4+ T cell precursor," *Journal of Experimental Medicine*, vol. 205, no. 8, pp. 1903–1916, 2008.

[131] V. Brucklacher-Waldert, C. Ferreira, S. Innocentin et al., "Tbet or continued RORγt expression is not required for Th17-associated immunopathology," *The Journal of Immunology*, vol. 196, no. 12, pp. 4893–4904, 2016.

[132] A. Bai, N. Lu, Y. Guo, and Z. Peng, "All-trans retinoic acid down-regulates inflammatory responses by shifting the Treg/Th17 profile in human ulcerative and murine colitis," *Journal of Leukocyte Biology*, vol. 86, no. 4, pp. 959–969, 2009.

[133] L. Li and V. A. Boussiotis, "The role of IL-17-producing Foxp3+ CD4+ T cells in inflammatory bowel disease and colon cancer," *Clinical Immunology*, vol. 148, no. 2, pp. 246–253, 2013.

[134] L. Zhou, J. E. Lopes, M. M. W. Chong et al., "TGF-β-induced Foxp3 inhibits T(H)17 cell differentiation by antagonizing RORγt function," *Nature*, vol. 453, no. 7192, pp. 236–240, 2008.

[135] L. L. Xu, A. Kitani, I. Fuss, and W. Strober, "Cutting edge: regulatory T cells induce CD4+CD25-Foxp3- T cells or are self-induced to become Th17 cells in the absence of exogenous TGF-βeta," *The Journal of Immunology*, vol. 178, no. 11, pp. 6725–6729, 2007.

[136] A. McLarnon, "Regulatory T-cell therapy is a safe and well-tolerated potential approach for treating refractory Crohn's disease," *Nature Reviews Gastroenterology & Hepatology*, vol. 9, no. 10, p. 559, 2012.

[137] A. Mizoguchi, "Animal models of inflammatory bowel disease," in *Progress in Molecular Biology and Translational Science*, vol. 105, pp. 263–320, Elsevier, 2012.

[138] C. Mottet, H. H. Uhlig, and F. Powrie, "Cutting edge: cure of colitis by CD4+CD25+ regulatory T cells," *The Journal of Immunology*, vol. 170, no. 8, pp. 3939–3943, 2003.

[139] J. L. Coombes, N. J. Robinson, K. J. Maloy, H. H. Uhlig, and F. Powrie, "Regulatory T cells and intestinal homeostasis," *Immunological Reviews*, vol. 204, pp. 184–194, 2005.

[140] H. Ogino, K. Nakamura, T. Iwasa et al., "Regulatory T cells expanded by rapamycin in vitro suppress colitis in an experimental mouse model," *Journal of Gastroenterology*, vol. 47, no. 4, pp. 366–376, 2012.

[141] C. J. Voskens, A. Fischer, S. Roessner et al., "Characterization and expansion of autologous GMP-ready regulatory T cells for TREG-based cell therapy in patients with ulcerative colitis," *Inflammatory Bowel Diseases*, vol. 23, no. 8, pp. 1348–1359, 2017.

[142] P. Desreumaux, A. Foussat, M. Allez et al., "Safety and efficacy of antigen-specific regulatory T-cell therapy for patients with refractory Crohn's disease," *Gastroenterology*, vol. 143, no. 5, pp. 1207–1217.e2, 2012.

[143] T. Tanoue, K. Atarashi, and K. Honda, "Development and maintenance of intestinal regulatory T cells," *Nature Reviews Immunology*, vol. 16, no. 5, pp. 295–309, 2016.

[144] Z. Hovhannisyan, J. Treatman, D. R. Littman, and L. Mayer, "Characterization of interleukin-17-producing regulatory T cells in inflamed intestinal mucosa from patients with inflammatory bowel diseases," *Gastroenterology*, vol. 140, no. 3, pp. 957–965, 2011.

[145] J. Hansen, A. Gulati, and R. B. Sartor, "The role of mucosal immunity and host genetics in defining intestinal commensal bacteria," *Current Opinion in Gastroenterology*, vol. 26, no. 6, pp. 564–571, 2010.

[146] S. Paramsothy, M. A. Kamm, N. O. Kaakoush et al., "Multidonor intensive faecal microbiota transplantation for active ulcerative colitis: a randomised placebo-controlled trial," *The Lancet*, vol. 389, no. 10075, pp. 1218–1228, 2017.

[147] G. J. Britton, E. J. Contijoch, I. Mogno et al., "Microbiotas from humans with inflammatory bowel disease alter the balance of gut Th17 and RORγt regulatory T cells and exacerbate colitis in mice," *Immunity*, vol. 50, no. 1, pp. 212–224.e4, 2019.

[148] S. Omenetti, C. Bussi, A. Metidji et al., "The intestine harbors functionally distinct homeostatic tissue-resident and inflammatory Th17 cells," *Immunity*, vol. 51, no. 1, pp. 77–89.e6, 2019.

[149] T. Velikova, D. Kyurkchiev, Z. Spassova et al., "Retracted:alterations in cytokine gene expression profile in colon mucosa of inflammatory bowel disease patients on different therapeutic regimens," *Cytokine*, vol. 92, pp. 12–19, 2017.

[150] R. Panaccione, S. Danese, W. J. Sandborn et al., "Ustekinumab is effective and safe for ulcerative colitis through 2 years of maintenance therapy," *Alimentary Pharmacology & Therapeutics*, vol. 52, no. 11-12, pp. 1658–1675, 2020.

[151] W. J. Sandborn, M. Ferrante, B. R. Bhandari et al., "Efficacy and safety of mirikizumab in a randomized phase 2 study of

patients with ulcerative colitis," *Gastroenterology*, vol. 158, no. 3, pp. 537–549.e10, 2020, e10.

[152] B. G. Feagan, W. J. Sandborn, G. D'Haens et al., "Induction therapy with the selective interleukin-23 inhibitor risankizumab in patients with moderate-to-severe Crohn's disease: a randomised, double-blind, placebo-controlled phase 2 study," *The Lancet*, vol. 389, no. 10080, pp. 1699–1709, 2017.

[153] B. E. Sands, J. Chen, B. G. Feagan et al., "Efficacy and safety of MEDI2070, an antibody against interleukin 23, in patients with moderate to severe Crohn's disease: a phase 2a study," *Gastroenterology*, vol. 153, no. 1, pp. 77–86.e6, 2017, e6.

[154] U. Wong and R. K. Cross, "Expert opinion on interleukin-12/23 and interleukin-23 antagonists as potential therapeutic options for the treatment of inflammatory bowel disease," *Expert Opinion on Investigational Drugs*, vol. 28, no. 5, pp. 473–479, 2019.

[155] R. Atreya, M. Zimmer, B. Bartsch et al., "Antibodies against tumor necrosis factor (TNF) induce T-cell apoptosis in patients with inflammatory bowel diseases via TNF receptor 2 and intestinal $CD14^+$ macrophages," *Gastroenterology*, vol. 141, no. 6, pp. 2026–2038, 2011.

[156] M. S. Harris, D. Hartman, B. R. Lemos et al., "AVX-470, an orally delivered anti-tumour necrosis factor antibody for treatment of active ulcerative colitis: results of a first-in-human trial," *Journal of Crohn's & Colitis*, vol. 10, no. 6, pp. 631–640, 2016.

[157] D. Sorrentino, P. Nash, M. Viladomiu, R. Hontecillas, and J. Bassaganya-Riera, "Stopping anti-TNF agents in patients with Crohn's disease in remission," *Inflammatory Bowel Diseases*, vol. 20, no. 4, pp. 757–766, 2014.

[158] G. Roda, B. Jharap, N. Neeraj, and J.-F. Colombel, "Loss of response to anti-TNFs: definition, epidemiology, and management," *Clinical and Translational Gastroenterology*, vol. 7, article e135, 2016.

[159] S. Hanauer, R. Panaccione, S. Danese et al., "Tofacitinib induction therapy reduces symptoms within 3 days for patients with ulcerative colitis," *Clinical Gastroenterology and Hepatology*, vol. 17, no. 1, pp. 139–147, 2019.

[160] D. Soler, T. Chapman, L. L. Yang, T. Wyant, R. Egan, and E. R. Fedyk, "The binding specificity and selective antagonism of vedolizumab, an anti-$\alpha 4\beta 7$Integrin therapeutic antibody in development for inflammatory bowel diseases," *The Journal of Pharmacology and Experimental Therapeutics*, vol. 330, no. 3, pp. 864–875, 2009.

[161] S. Vermeire, "Oral SMAD7 antisense drug for Crohn's disease," *The New England Journal of Medicine*, vol. 372, no. 12, pp. 1166-1167, 2015.

[162] D. R. Withers, M. R. Hepworth, X. Wang et al., "Transient inhibition of ROR-γt therapeutically limits intestinal inflammation by reducing TH17 cells and preserving group 3 innate lymphoid cells," *Nature Medicine*, vol. 22, no. 3, pp. 319–323, 2016.

[163] K. Chebli, L. Papon, C. Paul et al., "The anti-Hiv candidate Abx464 dampens intestinal inflammation by triggering Il-22 production in activated macrophages," *Scientific Reports*, vol. 7, no. 1, p. 4860, 2017.

[164] W. Hueber, B. E. Sands, S. Lewitzky et al., "Secukinumab, a human anti-IL-17A monoclonal antibody, for moderate to severe Crohn's disease: unexpected results of a randomised, double-blind placebo-controlled trial," *Gut*, vol. 61, no. 12, pp. 1693–1700, 2012.

[165] B. E. Sands, W. J. Sandborn, R. Panaccione et al., "Ustekinumab as induction and maintenance therapy for ulcerative colitis," *New England Journal of Medicine*, vol. 381, no. 13, pp. 1201–1214, 2019.

[166] A. Hemperly and N. V. Casteele, "Clinical pharmacokinetics and pharmacodynamics of infliximab in the treatment of inflammatory bowel disease," *Clinical Pharmacokinetics*, vol. 57, no. 8, pp. 929–942, 2018.

[167] M. Chaparro, A. Garre, E. Ricart et al., "Short and long-term effectiveness and safety of vedolizumab in inflammatory bowel disease: results from the ENEIDA registry," *Alimentary Pharmacology & Therapeutics*, vol. 48, no. 8, pp. 839–851, 2018.

[168] Y. Bouhnik, F. Carbonnel, D. Laharie et al., "Efficacy of adalimumab in patients with Crohn's disease and symptomatic small bowel stricture: a multicentre, prospective, observational cohort (CREOLE) study," *Gut*, vol. 67, no. 1, pp. 53–60, 2018.

[169] B. D. Ye, M. Pesegova, O. Alexeeva et al., "Efficacy and safety of biosimilar CT-P13 compared with originator infliximab in patients with active Crohn's disease: an international, randomised, double-blind, phase 3 non-inferiority study," *The Lancet*, vol. 393, no. 10182, pp. 1699–1707, 2019.

[170] H. Ito, M. Takazoe, Y. Fukuda et al., "A pilot randomized trial of a human anti-interleukin-6 receptor monoclonal antibody in active Crohn's disease," *Gastroenterology*, vol. 126, no. 4, pp. 989–996, 2004.

Hindawi
Journal of Immunology Research
Volume 2020, Article ID 8813558, 8 pages
https://doi.org/10.1155/2020/8813558

Review Article

The Function and Role of the Th17/Treg Cell Balance in Inflammatory Bowel Disease

Jun-bin Yan, Min-min Luo, Zhi-yun Chen, and Bei-hui He

The Second Central Laboratory, Key Laboratory of Integrative Chinese and Western Medicine for the Diagnosis and Treatment of Circulatory Diseases of Zhejiang Province, The First Affiliated Hospital of Zhejiang Chinese Medical University, Hangzhou 310006, China

Correspondence should be addressed to Bei-hui He; graf303@sina.com

Received 13 August 2020; Revised 28 September 2020; Accepted 9 December 2020; Published 15 December 2020

Academic Editor: Jie Tian

Copyright © 2020 Jun-bin Yan et al. This is an open access article distributed under the Creative Commons Attribution License, which permits unrestricted use, distribution, and reproduction in any medium, provided the original work is properly cited.

Inflammatory bowel disease (IBD) is a chronic, inflammatory, and autoimmune disorder. The pathogenesis of IBD is not yet clear. Studies have shown that the imbalance between T helper 17 (Th17) and regulatory T (Treg) cells, which differentiate from $CD4^+$ T cells, contributes to IBD. Th17 cells promote tissue inflammation, and Treg cells suppress autoimmunity in IBD. Therefore, Th17/Treg cell balance is crucial. Some regulatory factors affecting the production and maintenance of these cells are also important for the proper regulation of the Th17/Treg balance; these factors include T cell receptor (TCR) signaling, costimulatory signals, cytokine signaling, bile acid metabolites, and the intestinal microbiota. This article focuses on our understanding of the function and role of the balance between Th17/Treg cells in IBD and these regulatory factors and their clinical significance in IBD.

1. Introduction

IBD is a disorder that involves chronic and recurrent nonspecific intestinal inflammation with unknown aetiology and pathogenesis. The types of IBD include ulcerative colitis (UC), which can cause long-lasting inflammation and ulcers in the colon, and Crohn's disease (CD), which is characterized by inflammation of the lining of the digestive tract, which can spread into other tissues [1]. IBD can lead to life-threatening complications, including primary sclerosing cholangitis, blood clots, and even colon cancer [2].

The pathogenesis of IBD is still unclear, and the aetiology of IBD may include the host immune system, genetic variability, and environmental factors [3]. In recent years, it has been found that the abnormal intestinal mucosal immune system plays a crucial role in the occurrence, development, and prognosis of IBD, in which the influence of the imbalance in Th17 and Treg cells has been confirmed by previous studies [4, 5]. Multiple factors are involved in the Th17 and Treg cell balance and mainly include TCR signaling, costimulatory signals, cytokine signaling, bile acid metabolites, and the intestinal microbiota.

This paper will discuss the roles of these factors in regulating the balance in Th17/Treg cells and their subsequent influence of IBD, which will provide new perspectives for the treatment of IBD.

2. Th17 Cells

As a $CD4^+$ T cell subset, Th17 cells play dual roles in the pathogenesis of IBD (mainly a proinflammatory role) [6]. Th17 cells can not only protect the intestinal mucosa by keeping the balance of the immune microenvironment but also exacerbate the intestinal inflammatory response through proinflammatory cytokines. The differentiation process of Th17 cells can be divided into three stages: IL-6 and TGF-β initiate the differentiation of Th17 cells, IL-21 expands the differentiation state of Th17 cells, and IL-23 maintains the stable maturation of Th17 cells during the later stage of differentiation [7].

3. Treg Cells

Treg cells are a subset of $CD4^+$ T cells that play a negative immunomodulatory role and play an essential role in maintaining immune tolerance and balance. Considerable evidence indicates that Treg cells in the intestinal microenvironment contribute to the pathogenesis of IBD [8]. Treg cells mainly participate in various immune diseases by secreting anti-inflammatory cytokines, such as TGF-β and IL-10, suppressing the activity of immune cells and thereby controlling inflammation [9]. According to their origin, natural regulatory T (nTreg) cells are primarily generated in the thymus (tTreg) or be generated extrathymically in the periphery (pTreg) in vivo. On the other hand, Tregs generated from naive T cells in vitro, in the presence of transforming growth factor-β (TGF-β) and IL-2, are called induced Treg (iTreg) cells. Murine studies have shown that tTreg cells exhibit strong lineage fidelity, whereas pTreg cells can revert into conventional CD4+ T cells [10]. Tregs are characterized by forkhead box protein P3 (Foxp3) expression, and Helios is a marker of tTreg for distinguishing tTreg cells from pTreg cells [11].

4. Th17/Treg Cell Balance in IBD

Th17 and Treg cells are related through differentiation and in the inhibition of function. They share a common signal pathway mediated by TGF-β. Studies have shown that in the presence of IL-6 or IL-21 (with TGF-β), naïve $CD4^+$ T cells differentiate into Th17 cells; however, in the absence of proinflammatory cytokines, naive $CD4^+$ T cells differentiate into Treg cells [12]. Once this balance is broken, a number of autoimmune diseases, including IBD, will occur.

Th17 cells play an important role in the pathogenesis of IBD. Studies have shown that compared with those of healthy controls, Th17 cells infiltrate the intestinal mucosa of IBD patients, and the amount of the cytokine IL-17 that is specifically secreted by Th17 cells increases [13]. In the UC mouse model, Th17 cells in the peripheral blood of mice also increased [14].

Compared with Th17 cells, Treg cells not only suppress the occurrence of autoimmune diseases but also control intestinal inflammation. In the UC mouse model, Treg cells in the peripheral blood of mice decreased [15], and by increasing the secretion of IL-10 and TGF-β, the symptoms of diarrhoea in mice were significantly improved [16]. Therefore, Treg cells may be regulated by IL-10, TGF-β, and other anti-inflammatory factors that are secreted to suppress the intestinal inflammation cascade and amplify the response, thereby improving the clinical symptoms of IBD. Relevant clinical observations and animal experiments have shown that Treg cells and their inhibitory mechanism are essential for inhibiting spontaneous intestinal inflammation [17]. Therefore, Treg cell deficiency may be the central link in the pathogenesis of IBD.

The regulation of Th17/Treg cell balance is prospective to be a new target for the treatment of IBD. The vitamin A metabolite such as retinoic acid (RA) is the main regulator of the TGF-β-dependent immune response, which can prevent IL-6 from inducing proinflammatory Th17 cells and differentiate into anti-inflammatory Treg cells. RA may be helpful in the treatment of IBD [18].

5. Factors Affecting the Th17/Treg Cell Balance in IBD

5.1. TCR and Costimulatory Signals. The TCR can bind to peptide-major histocompatibility complex (MHC) molecules on the surface of antigen-presenting cells (APCs). In the immune system, the TCR recognizes antigens, transmits signals, and determines the differentiation of T cells [19]. When the TCR-peptide-MHC is on the surface of APCs with the coreceptor CD4 or CD8, it activates the tyrosine-based activation motif (ITAM) at the end of the CD3 chain. Finally, TCR activation enables the differentiation of naive $CD4^+$ T cells [20].

TCR signal strength could alter the balance of Th17 and Treg cells [21]. IL-2 inducible T cell kinase (ITK), a critical regulator of intracellular signaling downstream of the TCR, positively regulates the differentiation of Th17 and negatively regulates the differentiation of Treg cells [22]. Studies have shown that attenuated TCR signaling in ITK-/- cells induced immature T lymphocytes to preferentially differentiate into Treg cells but not Th17 cells by inhibiting the Akt/mTOR signaling pathway [23]. Attenuated TCR signals caused by mutations in particular components of the TCR signaling pathway, such as Zap70 [23], DAGs [24], Raf [25], and NF-κB [26], will affect the development of tTreg cells [27]. Studies have shown that attenuated TCR signals did not only promote the growth of tTreg cells but also inhibit [28], such as naïve T cells require weak TCR signals to differentiate into Treg cells [29]. Additionally, aminoacyl tRNA synthetase-(ARS-) interacting multifunctional protein 1 (AIMP1) affects the balance of Th17 and Treg cells directly by downregulating TCR signal complex formation and inducing CD4+ T cells differentiate into Treg cells. In contrast, the differentiation of Th17 cells was not now affected [29]. Bach2, a transcription factor of downstream of TCR signaling, balances TCR signal-induced transcriptional activity of IRF4 to maintain homeostasis of tTreg and pTreg cells and shapes the balance of Th17/Treg cells [30, 31].

The TCR is not sufficient for the complete activation and differentiation of T cells. TCR stimulation in the absence of costimulation will induce anergy or cell apoptosis instead of activation [32]. Therefore, secondary signals are required. Costimulatory signals produced by the interaction of different costimulatory molecules and their ligands could accelerate the differentiation of naïve T cells [33]. CD28 is a costimulatory molecule expressed on the surface of T lymphocytes and plays a crucial role in the activation of T cells. Studies have shown that the costimulatory molecule CD28 participates in the induction of Th17 differentiation [34]. CD28 can also, together with the TCR, upregulate the expression of OX40 [35]. The T cell costimulatory molecule OX40 and its cognate ligand OX40L collectively play an essential role in keeping the growth of Th17 and Treg cells. It was found that the activation of OX40 enhanced Th17 function while blocking OX40L decreased Treg proliferation [36,

Table 1: The role of cytokines in Th17/Treg balance.

Cytokines	Mechanism	Changes
TGF-β	The stimulation of naïve CD4+ T cells with TGF-β induces SMAD2 and SMAD3, which in turn activate the transcription factor Foxp3	Treg↑ [45, 46]
HIF-1α	HIF-1α promotes Th17 differentiation by directly inducing RORγt transcription. Also, HIF-1α inhibits Treg differentiation through an active process that targets Foxp3 protein for degradation	Th17↑ [42]
IL-2	IL-2 phosphorylates STAT5, which binds to the Foxp3 locus and upregulate the expression of Foxp3	Treg↑ [54]
IL-6	IL-6 drives naïve CD4+ T cells to differentiate into Th17 by phosphorylating STAT3, which then induces the upregulation of Th17-specific genes, such as RORγt, IL-17, and IL-23	Th17↑ [42]
IL-15	IL-15 upregulates the expression of Foxp3 by activating STAT5 and inhibits the differentiation of Th17 by reducing the secretion of IL-17	Treg↑ [55]
IL-18	IL-18 inhibits the MyD88-dependent downstream signal IL-1R, which in turn reduces the differentiation of Th17	Treg↑ [53]
IL-21	IL-21 induces the differentiation of Th17 by activating STAT3, which then upregulate the expression of RORγt	Th17↑ [51, 52]
IL-23	IL-23 maintains the differentiation of Th17 by enhancing the transcription of Th17 signature cytokines, such as RORγt	Th17↑ [50]

37]. However, the effect of costimulatory signals on the balance of Th17 and Treg cells is mainly realized by acting as the second signals of TCR signals.

There are also some coinhibitory receptors, which inhibit the strength of TCR signals. Among them, cytotoxic T lymphocyte antigen 4 (CTLA4) has received much attention. CTLA4, a highly homologous receptor of CD28, competes with CD28 for the same ligands (CD80 and CD86). CTLA4 binds the ligands with a high affinity allowing CTLA4 to inhibit T cell responses by competing with CD28 [38]. Studies have shown that CD28 and CTLA4 have opposing influences on T cell stimulation, and CD28 provides an activating signal, while CTLA4 delivers an inhibitory signal [39]. Costimulatory and coinhibitory signals coassist TCR signals in regulating the balance of Th17 and Treg cells.

5.2. Cytokines. Cytokines, small peptides secreted by cells in autocrine and paracrine manners, are the most potent determinants of the fate of T cells. It has been found that the cytokines, which involve in regulating the balance of Th17 cells and Treg cells, are mainly inflammation cytokines, mainly including transforming growth factor-β (TGF-β), IL-2, IL-6, IL-15, IL-18, IL-2, and IL-23 [40].

TGF-β acts on the naive $CD4^+$ T cells to induce the development of Th17 cells and Treg cells, while IL-6 induces specific genes in Th17 cells by phosphorylating STAT3, which drives the upregulation of Th17-specific genes, such as RORγt, Il-17, and IL-23 receptor (IL-23R) [41, 42]. In patients with IBD, TGF-β is highly expressed, but TGF-β-mediated immunosuppression is significantly impaired. Researchers have found that this effect is related to Smad7, an intracellular protein that binds to the receptors of TGF-β and inhibits the Smad-dependent signal transduction driven by TGF-β1 [43]. Silencing Smad7 with specific antisense oligodeoxynucleotides can restore TGF-β1/Smad signal transduction, downregulate the expression of inflammatory cytokines, and improve experimental UC in mice [44]. The stimulation of naive $CD4^+$ T cells with TGF-β induces SMAD2 and SMAD3, which in turn activate the transcription factor Foxp3, which could facilitate the differentiation of Treg cells [45, 46]. Unlike IL-6 and TGF-β, IL-23 does not directly induce Th17 cell differentiation because of the absence of IL-23R in naive T cells [47]. In mice, T cell receptors engage and bind with specific cytokines, such as TGF-β, inducing a network of transcription factors, of which retinoid-related orphan receptor-γt (RORγt) is the primary regulator and promotes IL-23R expression [48]. IL-23 could thus activate signal transducer and activator of transcription 3 (STAT3) by interacting with IL-23R [49], which promotes the expression of IL-23R and RORγt, supporting a positive feedback loop that stabilizes the gene expression required for the activation of Th17 cells [50]. IL-21 can also induce the differentiation of Th17 by activating STAT3, which then upregulates the expression of RORrt [51, 52]. IL-18 inhibits the MyD88-dependent downstream signal IL-1R, which in turn reduces the differentiation of Th17 [53]. IL-2 and IL-15 all could upregulate the expression of Foxp3 by activating STAT5, thus promote the differentiation of Treg cells [54]. In addition, IL-15 could inhibit the differentiation of Th17 by reducing the secretion of IL-17 [55]. In addition to inflammation cytokines, HIF-1α could promote Th17 differentiation by directly inducing RORγt transcription as well. HIF-1α inhibits Treg differentiation through an active process that targets Foxp3 protein for degradation [42] (Table 1).

5.3. Bile Acid Metabolites. Bile acids (BAs) are natural surfactants derived from cholesterol that is produced in the liver and secreted into the duodenum. BAs play a significant role in lipid digestion, antibacterial defense, and glucose metabolism [56]. Through enterohepatic circulation, bacteria

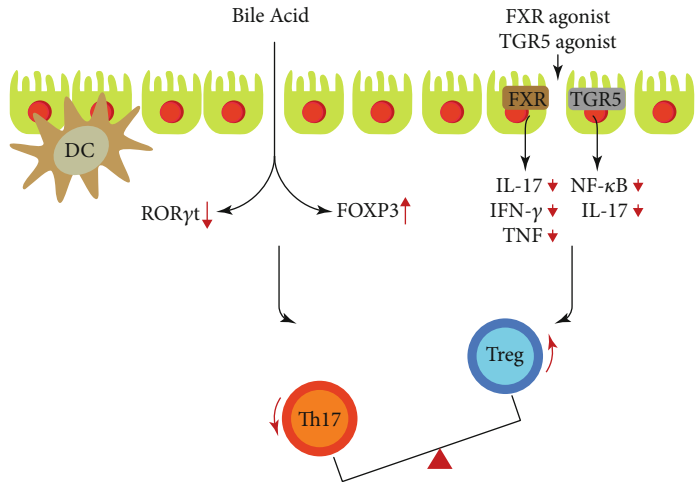

Figure 1: The role of bile acid and bile acid receptor FXR/TGR5 agonist in Th17/Treg balance.

convert hundreds of milligrams of bile acid into secondary bile acid with unique chemical structures. Appropriate concentrations of secondary bile acids have immunomodulatory effects [57]. BAs have emerged as modulators of innate immunity and gut inflammation [58].

Compared with that of healthy people, the decrease in the abundance of Firmicum in IBD patients leads to a reduction in the level of secondary bile acids, which weakens the anti-inflammatory effect of secondary bile acids and delays the resolution of inflammation [59]. Studies have shown that the expression of bile acid transporter (ASBT) is decreased in TNBS-induced colitis rats and rabbit models of intestinal inflammation [60]. A recent study reported that bile acids control Th17 cell functions by modulating RORγt activity [61]. Farnesoid-X-receptor (FXR) and transmembrane G protein-coupled receptor 5 (TGR5), the bile acid receptors, regulate innate immunity and the Th17/Treg balance [62, 63]. FXR expression in the inflammatory tissue of Crohn's disease patients was decreased [64]. Clinical observation of using FXR agonist to stimulate IBD patients showed that the secretion of proinflammatory cytokines IL-17, IFN-γ, and TNF in lamina propria mononuclear cells was significantly decreased [65]. TGR5 activation of macrophages, which was cocultured with $CD4^+$ T cells, inhibited the release of IL-17 in the culture supernatant [66]. FXR and TGR5 agonists may be used to treat IBD (Figure 1).

5.4. The Intestinal Microbiota. There are many microorganisms in the gastrointestinal tract that are near related to human health. With the in-depth study of the intestinal microbiota, it has been found that the incidence of IBD is closely related to intestinal microbiota imbalance. Chu et al. [63] noted that intestinal microbiota dysbiosis is the leading cause of immune imbalance and intestinal diseases such as IBD.

Studies have shown that the intestinal microbiota and its metabolites can affect Th17/Treg differentiation. A recent study showed that the microbiotas of humans with IBD could affect the balance of gut Th17 and $ROR\gamma t^+$ Treg cells in mice [67]. By using GF mice and antibiotic treatment models, various researchers have found that colonic Th17 cells and Treg cells are significantly decreased in GF mice [68, 69]. Recently, it has been found that ATP and SCFAs, the metabolites derived from the intestinal microbiota, respectively, stimulate the differentiation of Th17 cells and Treg cells [70, 71].

Intestinal microbes and their bacterial products directly act on TLRs and other innate immune receptors to mediate Th17 cell differentiation. A study showed that in the presence of TLR9, intestinal flora DNA can directly induce and promote the differentiation of Th17 cells, inhibit Treg cells, and exacerbate intestinal inflammation [72]. In addition, apoptotic intestinal epithelial cells infected with bacteria also provide ligands for TLRs and activate dendritic cells to secrete IL-6 and TGF-β, leading to increased Th17 cell differentiation [73]. The specific role of each TLR in Th17 cell differentiation induction remains to be further explored. One type of filamentous bacteria, *segmented filamentous bacteria* (SFB), induced naive $CD4^+$ T cells to differentiate into Th17 cells. Many kinds of research have shown that SFB promotes the differentiation of Th17 cells through serum amyloid A protein (SAA) and dendritic cells (DCs) in intestinal epithelial cells. The cytokine IL-23 secreted by DCs, in turn, can promote an increase in SAA and enhance the secretion of IL-17, thus enhancing the differentiation of Th17 cells and maintaining the intestinal inflammation [74, 75].

Studies on the relationship between the intestinal flora and Treg cells have mostly focused on short-chain fatty acids (SCFAs) and Treg cells. SCFAs can act on intestinal epithelial mucosal cells through TGF-β1 to facilitate the differentiation of nTreg cells. SCFAs can also inhibit the activity of histone deacetylase in order to make histones highly acetylated, regulate the expression of related genes, produce anti-inflammatory factors, or lead to growth inhibition and the apoptosis of associated cells, which generates immune tolerance [76]. SCFAs can also affect the ATP level via G protein-coupled receptors (GPCRs) (such as GPR43) or mammalian target of rapamycin (mTOR), thereby influencing the differentiation of Treg cells [77]. In addition, some intestinal flora has been found to alter the Th17/Treg cell balance towards Treg cells by releasing polysaccharide A (PSA);

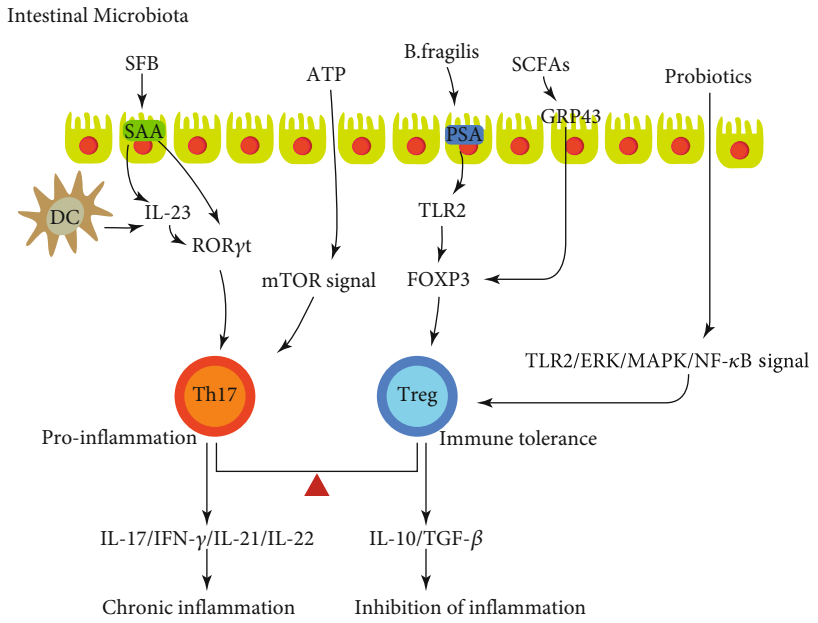

Figure 2: The role of intestinal microbiota in Th17/Treg balance.

Bacteroides fragilis upregulates Foxp3 expression and promotes Treg cell differentiation. Clostridium IV and the XIV flora also induce Foxp3 expression and Treg cell differentiation [78].

A study showed that probiotics could reduce the secretion of TNF-α and IL-23 in the serum of mice with oxazolidone-induced colitis. IL-23 is a crucial factor in maintaining the survival, proliferation, and stability of Th17 cells. Therefore, probiotics can inhibit the production and function of IL-17 by reducing the secretion of IL-23, which confirms that probiotics can improve intestinal inflammation in this way [79]. Studies have shown that probiotic *B. adolescentis* can transmit probiotic-mediated adaptive immune regulation to the Treg/Th17 axis through the trl2/ERK/-MAPK/NF-κB signaling pathway, stimulate immunosuppressive polarization of macrophages, and secrete the cytokine IL-10 [16]. Probiotics may be used in the treatment of IBD (Figure 2).

6. Conclusions

The imbalance of Th17/Treg cells is a vital factor, which influences the occurrence and development of IBD. Th17 cells promote the occurrence of intestinal inflammation and induce autoimmune diseases, while Treg cells inhibit intestinal inflammation. The balance is mainly affected by TCR signaling, costimulatory signals, cytokines, bile acid metabolites, intestinal microbiomes, and other factors. The study of the mutual transformational mechanism of Th17/Treg cells has deepened the understanding of the immune mechanisms of IBD and may provide new research directions of IBD in the future.

Data Availability

All data generated or analyzed during this study are included in this article.

Conflicts of Interest

The authors declare that they have no conflicts of interest.

Acknowledgments

This study was supported by the Zhejiang Provincial Natural Science Foundation of China (Grant No. LY17H290007), the Research Project of the Health Commission of Zhejiang Province (Grant No. 2018KY550), the Research Project of Zhejiang Traditional Chinese Medicine Administration (CN) (Grant No. 2020ZB081), and Research Project of Zhejiang Chinese Medical University (No. 2019ZG03) and the Zhejiang Provincial Key Lab of Diagnosis and Treatment of Circulatory Diseases (Grant No. 2019E10012).

References

[1] N. A. Molodecky, I. S. Soon, D. M. Rabi et al., "Increasing incidence and prevalence of the inflammatory bowel diseases with time, based on systematic review," *Gastroenterology*, vol. 142, no. 1, pp. 46–54.e42, 2012.

[2] A. N. Ananthakrishnan, "Epidemiology and risk factors for IBD," *Nature Reviews Gastroenterology & Hepatology*, vol. 12, no. 4, pp. 205–217, 2015.

[3] A. N. Ananthakrishnan, C. N. Bernstein, D. Iliopoulos et al., "Environmental triggers in IBD: a review of progress and evidence," *Nature Reviews Gastroenterology & Hepatology*, vol. 15, no. 1, pp. 39–49, 2018.

[4] G. Iacomino, V. Rotondi Aufiero, N. Iannaccone et al., "IBD: role of intestinal compartments in the mucosal immune response," *Immunobiology*, vol. 225, no. 1, article 151849, 2020.

[5] F. A. Silva, B. L. Rodrigues, M. L. Ayrizono, and R. F. Leal, "The immunological basis of inflammatory bowel disease," *Gastroenterology research and practice*, vol. 2016, Article ID 2097274, 11 pages, 2016.

[6] M. A. Daniels and E. Teixeiro, "TCR signaling in T cell memory," *Frontiers in Immunology*, vol. 6, 2015.

[7] A. Ueno, L. Jeffery, T. Kobayashi, T. Hibi, S. Ghosh, and H. Jijon, "Th17 plasticity and its relevance to inflammatory bowel disease," *Journal of Autoimmunity*, vol. 87, pp. 38–49, 2018.

[8] J. Gálvez, "Role of Th17 cells in the pathogenesis of human IBD," *ISRN inflammation*, vol. 2014, Article ID 928461, 14 pages, 2014.

[9] C. G. Mayne and C. B. Williams, "Induced and natural regulatory T cells in the development of inflammatory bowel disease," *Inflammatory Bowel Diseases*, vol. 19, no. 8, pp. 1772–1788, 2013.

[10] E. M. Shevach and A. M. Thornton, "tTregs, pTregs, and iTregs: similarities and differences," *Immunological Reviews*, vol. 259, no. 1, pp. 88–102, 2014.

[11] K. Singh, M. Hjort, L. Thorvaldson, and S. Sandler, "Concomitant analysis of Helios and Neuropilin-1 as a marker to detect thymic derived regulatory T cells in naive mice," *Scientific Reports*, vol. 5, no. 1, 2015.

[12] E. Bettelli, Y. Carrier, W. Gao et al., "Reciprocal developmental pathways for the generation of pathogenic effector T_H17 and regulatory T cells," *Nature*, vol. 441, no. 7090, pp. 235–238, 2006.

[13] M. Veldhoen, R. J. Hocking, C. J. Atkins, R. M. Locksley, and B. Stockinger, "TGFβ in the context of an inflammatory cytokine milieu supports de novo differentiation of IL-17-producing T cells," *Immunity*, vol. 24, no. 2, pp. 179–189, 2006.

[14] S. Fujino, A. Andoh, S. Bamba et al., "Increased expression of interleukin 17 in inflammatory bowel disease," *Gut*, vol. 52, no. 1, pp. 65–70, 2003.

[15] S. Acharya, M. Timilshina, L. Jiang et al., "Amelioration of experimental autoimmune encephalomyelitis and DSS induced colitis by NTG-A-009 through the inhibition of Th1 and Th17 cells differentiation," *Scientific Reports*, vol. 8, no. 1, 2018.

[16] R. Yu, F. Zuo, H. Ma, and S. Chen, "Exopolysaccharide-producing Bifidobacterium adolescentis strains with similar adhesion property induce differential regulation of inflammatory immune response in Treg/Th17 axis of DSS-colitis mice," *Nutrients*, vol. 11, no. 4, p. 782, 2019.

[17] T. V. Velikova, L. Miteva, N. Stanilov, Z. Spassova, and S. A. Stanilova, "Interleukin-6 compared to the other Th17/Treg related cytokines in inflammatory bowel disease and colorectal cancer," *World Journal of Gastroenterology*, vol. 26, no. 16, pp. 1912–1925, 2020.

[18] G. Tejón, V. Manríquez, J. de Calisto et al., "Vitamin A impairs the reprogramming of Tregs into IL-17-producing cells during intestinal inflammation," *BioMed Research International*, vol. 2015, Article ID 137893, 8 pages, 2015.

[19] J. E. Smith-Garvin, G. A. Koretzky, and M. S. Jordan, "T cell activation," *Annual Review of Immunology*, vol. 27, no. 1, pp. 591–619, 2009.

[20] N. R. Gascoigne, V. Rybakin, O. Acuto, and J. Brzostek, "TCR signal strength and T cell development," *Annual Review of Cell and Developmental Biology*, vol. 32, no. 1, pp. 327–348, 2016.

[21] H. S. Kim, S. W. Jang, W. Lee et al., "PTEN drives Th17 cell differentiation by preventing IL-2 production," *The Journal of Experimental Medicine*, vol. 214, no. 11, pp. 3381–3398, 2017.

[22] J. P. Elmore, M. C. McGee, N. F. Nidetz, O. Anannya, W. Huang, and A. August, "Tuning T helper cell differentiation by ITK," *Biochemical Society Transactions*, vol. 48, no. 1, pp. 179–185, 2020.

[23] S. Tanaka, S. Maeda, M. Hashimoto et al., "Graded attenuation of TCR signaling elicits distinct autoimmune diseases by altering thymic T cell selection and regulatory T cell function," *Journal of immunology*, vol. 185, no. 4, pp. 2295–2305, 2010.

[24] R. P. Joshi, A. M. Schmidt, J. Das et al., "The ζ isoform of diacylglycerol kinase plays a predominant role in regulatory T cell development and TCR-mediated ras signaling," *Science signaling*, vol. 6, no. 303, 2013.

[25] X. Chen, J. J. Priatel, M. T. Chow, and H. S. Teh, "Preferential development of CD4 and CD8 T regulatory cells in RasGRP1-deficient mice," *Journal of immunology*, vol. 180, no. 9, pp. 5973–5982, 2008.

[26] M. Schmidt-Supprian, J. Tian, E. P. Grant et al., "Differential dependence of CD4+CD25+ regulatory and natural killer-like T cells on signals leading to NF-kappaB activation," *Proceedings of the National Academy of Sciences of the United States of America*, vol. 101, no. 13, pp. 4566–4571, 2004.

[27] S. Hwang, K. D. Song, R. Lesourne et al., "Reduced TCR signaling potential impairs negative selection but does not result in autoimmune disease," *The Journal of Experimental Medicine*, vol. 209, no. 10, pp. 1781–1795, 2012.

[28] R. H. Schwartz, "A cell culture model for T lymphocyte clonal anergy," *Science*, vol. 248, no. 4961, pp. 1349–1356, 1990.

[29] M. O. Li and A. Y. Rudensky, "T cell receptor signalling in the control of regulatory T cell differentiation and function," *Nature Reviews Immunology*, vol. 16, no. 4, pp. 220–233, 2016.

[30] L. Yang, S. Chen, Q. Zhao, Y. Sun, and H. Nie, "The critical role of Bach2 in shaping the balance between $CD4^+$ T cell subsets in immune-mediated diseases," *Mediators of inflammation*, vol. 2019, Article ID 2609737, 9 pages, 2019.

[31] M. Sasikala, V. V. Ravikanth, K. Murali Manohar et al., "Bach2 repression mediates Th17 cell induced inflammation and associates with clinical features of advanced disease in chronic pancreatitis," *United European Gastroenterology Journal*, vol. 6, no. 2, pp. 272–282, 2018.

[32] I. Vogel, A. Kasran, J. Cremer et al., "CD28/CTLA-4/B7 costimulatory pathway blockade affects regulatory T-cell function in autoimmunity," *European Journal of Immunology*, vol. 45, no. 6, pp. 1832–1841, 2015.

[33] S. Bhatia, M. Edidin, S. C. Almo, and S. G. Nathenson, "Different cell surface oligomeric states of B7-1 and B7-2: implications for signaling," *Proceedings of the National Academy of Sciences of the United States of America*, vol. 102, no. 43, pp. 15569–15574, 2005.

[34] H. Park, Z. Li, X. O. Yang et al., "A distinct lineage of CD4 T cells regulates tissue inflammation by producing interleukin 17," *Nature Immunology*, vol. 6, no. 11, pp. 1133–1141, 2005.

[35] J. J. Engelhardt, T. J. Sullivan, and J. P. Allison, "CTLA-4 overexpression inhibits T cell responses through a CD28-B7-dependent mechanism," *Journal of immunology*, vol. 177, no. 2, pp. 1052–1061, 2006.

[36] Z. Zhang, W. Zhong, D. Hinrichs et al., "Activation of OX40 augments Th17 cytokine expression and antigen-specific uveitis," *The American Journal of Pathology*, vol. 177, no. 6, pp. 2912–2920, 2010.

[37] D. Odobasic, A. J. Ruth, V. Oudin, S. R. Holdsworth, and S. R. Holdsworth, "OX40 ligand is inhibitory during the effector

phase of crescentic glomerulonephritis," *Nephrology Dialysis Transplantation*, vol. 34, no. 3, pp. 429–441, 2019.

[38] M. F. Krummel and J. P. Allison, "CD28 and CTLA-4 have opposing effects on the response of T cells to stimulation," *The Journal of Experimental Medicine*, vol. 182, no. 2, pp. 459–465, 1995.

[39] N. Manel, D. Unutmaz, and D. R. Littman, "The differentiation of human TH-17 cells requires transforming growth factor-β and induction of the nuclear receptor RORγt," *Nature Immunology*, vol. 9, no. 6, pp. 641–649, 2008.

[40] L. Durant, W. T. Watford, H. L. Ramos et al., "Diverse targets of the transcription factor STAT3 contribute to T cell pathogenicity and homeostasis," *Immunity*, vol. 32, no. 5, pp. 605–615, 2010.

[41] M. Boirivant, F. Pallone, C. di Giacinto et al., "Inhibition of Smad7 with a specific antisense oligonucleotide facilitates TGF-β1-mediated suppression of colitis," *Gastroenterology*, vol. 131, no. 6, pp. 1786–1798, 2006.

[42] E. V. Dang, J. Barbi, H. Y. Yang et al., "Control of T_H17/Treg balance by hypoxia-inducible factor 1," *Cell*, vol. 146, no. 5, pp. 772–784, 2011.

[43] S. Sedda, I. Marafini, V. Dinallo, D. di Fusco, and G. Monteleone, "The TGF-β/Smad system in IBD pathogenesis," *Inflammatory Bowel Diseases*, vol. 21, no. 12, pp. 2921–2925, 2015.

[44] C. L. Langrish, Y. Chen, W. M. Blumenschein et al., "IL-23 drives a pathogenic T cell population that induces autoimmune inflammation," *The Journal of Experimental Medicine*, vol. 201, no. 2, pp. 233–240, 2005.

[45] M. Kanamori, H. Nakatsukasa, M. Okada, Q. Lu, and A. Yoshimura, "Induced regulatory T cells: their development, stability, and applications," *Trends in Immunology*, vol. 37, no. 11, pp. 803–811, 2016.

[46] S. Sakaguchi, T. Yamaguchi, T. Nomura, and M. Ono, "Regulatory T cells and immune tolerance," *Cell*, vol. 133, no. 5, pp. 775–787, 2008.

[47] I. Ivanov, B. S. McKenzie, L. Zhou et al., "The orphan nuclear receptor RORγt directs the differentiation program of proinflammatory IL-17$^+$ T helper cells," *Cell*, vol. 126, no. 6, pp. 1121–1133, 2006.

[48] C. Parham, M. Chirica, J. Timans et al., "A receptor for the heterodimeric cytokine IL-23 is composed of IL-12Rbeta1 and a novel cytokine receptor subunit, IL-23R," *Journal of immunology*, vol. 168, no. 11, pp. 5699–5708, 2002.

[49] M. W. Teng, E. P. Bowman, J. J. McElwee et al., "IL-12 and IL-23 cytokines: from discovery to targeted therapies for immune- mediated inflammatory diseases," *Nature Medicine*, vol. 21, no. 7, pp. 719–729, 2015.

[50] P. A. Dawson and S. J. Karpen, "Intestinal transport and metabolism of bile acids," *Journal of Lipid Research*, vol. 56, no. 6, pp. 1085–1099, 2015.

[51] L. Zhou, J. E. Lopes, M. M. Chong et al., "TGF-β-induced Foxp3 inhibits TH17 cell differentiation by antagonizing RORγt function," *Nature*, vol. 453, no. 7192, pp. 236–240, 2008.

[52] T. J. Harris, J. F. Grosso, H. R. Yen et al., "Cutting edge: an in vivo requirement for STAT3 signaling in TH17 development and TH17-dependent autoimmunity," *Journal of immunology*, vol. 179, no. 7, pp. 4313–4317, 2007.

[53] Q. Dai, Y. Li, H. Yu, and X. Wang, "Suppression of Th1 and Th17 responses and induction of Treg responses by IL-18-expressing plasmid gene combined with IL-4 on collagen-induced arthritis," *BioMed research international*, vol. 2018, Article ID 5164715, 8 pages, 2018.

[54] W. Liao, J. X. Lin, and W. J. Leonard, "Interleukin-2 at the crossroads of effector responses, tolerance, and immunotherapy," *Immunity*, vol. 38, no. 1, pp. 13–25, 2013.

[55] C. Apert, P. Romagnoli, and J. P. M. Van Meerwijk, "IL-2 and IL-15 dependent thymic development of Foxp3-expressing regulatory T lymphocytes," *Protein & Cell*, vol. 9, no. 4, pp. 322–332, 2018.

[56] J. M. Ridlon, D. J. Kang, and P. B. Hylemon, "Bile salt biotransformations by human intestinal bacteria," *Journal of Lipid Research*, vol. 47, no. 2, pp. 241–259, 2006.

[57] W. Jia, G. Xie, and W. Jia, "Bile acid-microbiota crosstalk in gastrointestinal inflammation and carcinogenesis," *Nature Reviews Gastroenterology & Hepatology*, vol. 15, no. 2, pp. 111–128, 2018.

[58] H. Duboc, S. Rajca, D. Rainteau et al., "Connecting dysbiosis, bile-acid dysmetabolism and gut inflammation in inflammatory bowel diseases," *Gut*, vol. 62, no. 4, pp. 531–539, 2013.

[59] L. R. Fitzpatrick and P. Jenabzadeh, "IBD and bile acid absorption: focus on pre-clinical and clinical observations," *Frontiers in Physiology*, vol. 11, 2020.

[60] S. Hang, D. Paik, L. Yao et al., "Bile acid metabolites control T(H)17 and T(reg) cell differentiation," *Nature*, vol. 576, no. 7785, pp. 143–148, 2019.

[61] L. Ding, L. Yang, Z. Wang, and W. Huang, "Bile acid nuclear receptor FXR and digestive system diseases," *Acta Pharmaceutica Sinica B*, vol. 5, no. 2, pp. 135–144, 2015.

[62] S. Fiorucci, M. Biagioli, A. Zampella, and E. Distrutti, "Bile acids activated receptors regulate innate immunity," *Frontiers in Immunology*, vol. 9, 2018.

[63] H. Chu, A. Khosravi, I. P. Kusumawardhani et al., "Gene-microbiota interactions contribute to the pathogenesis of inflammatory bowel disease," *Science*, vol. 352, no. 6289, pp. 1116–1120, 2016.

[64] P. Vavassori, A. Mencarelli, B. Renga, E. Distrutti, and S. Fiorucci, "The bile acid receptor FXR is a modulator of intestinal innate immunity," *Journal of immunology*, vol. 183, no. 10, pp. 6251–6261, 2009.

[65] R. M. Gadaleta, K. J. van Erpecum, B. Oldenburg et al., "Farnesoid X receptor activation inhibits inflammation and preserves the intestinal barrier in inflammatory bowel disease," *Gut*, vol. 60, no. 4, pp. 463–472, 2011.

[66] J. Yang, J. Hu, L. Feng et al., "Decreased expression of TGR5 in Vogt-Koyanagi-Harada (VKH) disease," *Ocular Immunology and Inflammation*, vol. 28, no. 2, pp. 200–208, 2020.

[67] G. J. Britton, E. J. Contijoch, I. Mogno et al., "Microbiotas from humans with inflammatory bowel disease alter the balance of gut Th17 and RORγt$^+$ regulatory T cells and exacerbate colitis in mice," *Immunity*, vol. 50, no. 1, pp. 212–24.e4, 2019.

[68] Y. Mishima, B. Liu, J. J. Hansen, and R. B. Sartor, "Resident bacteria-stimulated IL-10-secreting B cells ameliorate T cell-mediated colitis by inducing Tr-1 cells that require IL-27-signaling," *Cellular and Molecular Gastroenterology and Hepatology*, vol. 1, no. 3, pp. 295–310, 2015.

[69] K. M. Telesford, W. Yan, J. Ochoa-Reparaz et al., "A commensal symbiotic factor derived from *Bacteroides fragilis* promotes human CD39$^+$Foxp3$^+$ T cells and T_{reg} function," *Gut Microbes*, vol. 6, no. 4, pp. 234–242, 2015.

[70] C. B. Larmonier, K. W. Shehab, F. K. Ghishan, and P. R. Kiela, "T lymphocyte dynamics in inflammatory bowel diseases: role of the microbiome," *BioMed research international*, vol. 2015, Article ID 504638, 9 pages, 2015.

[71] P. M. Smith, M. R. Howitt, N. Panikov et al., "The microbial metabolites, short-chain fatty acids, regulate colonic Treg cell homeostasis," *Science*, vol. 341, no. 6145, pp. 569–573, 2013.

[72] P. Hemarajata and J. Versalovic, "Effects of probiotics on gut microbiota: mechanisms of intestinal immunomodulation and neuromodulation," *Therapeutic Advances in Gastroenterology*, vol. 6, no. 1, pp. 39–51, 2013.

[73] R. Rogier, M. I. Koenders, and S. Abdollahi-Roodsaz, "Toll-like receptor mediated modulation of T cell response by commensal intestinal microbiota as a trigger for autoimmune arthritis," *Journal of immunology research*, vol. 2015, Article ID 527696, 8 pages, 2015.

[74] I. Ivanov, K. Atarashi, N. Manel et al., "Induction of intestinal Th17 cells by segmented filamentous bacteria," *Cell*, vol. 139, no. 3, pp. 485–498, 2009.

[75] Y. Goto, C. Panea, G. Nakato et al., "Segmented filamentous bacteria antigens presented by intestinal dendritic cells drive mucosal Th17 cell differentiation," *Immunity*, vol. 40, no. 4, pp. 594–607, 2014.

[76] D. Parada Venegas, M. K. de la Fuente, G. Landskron et al., "Short chain fatty acids (SCFAs)-mediated gut epithelial and immune regulation and its relevance for inflammatory bowel diseases," *Frontiers in Immunology*, vol. 10, 2019.

[77] A. Luo, S. T. Leach, R. Barres, L. B. Hesson, M. C. Grimm, and D. Simar, "The microbiota and epigenetic regulation of T helper 17/regulatory T cells: in search of a balanced immune system," *Frontiers in Immunology*, vol. 8, 2017.

[78] S. Omenetti and T. T. Pizarro, "The Treg/Th17 axis: a dynamic balance regulated by the gut microbiome," *Frontiers in Immunology*, vol. 6, 2015.

[79] K. Wang, H. Dong, Y. Qi et al., "*Lactobacillus casei* regulates differentiation of Th17/Treg cells to reduce intestinal inflammation in mice," *Journal of Veterinary Research*, vol. 81, no. 2, pp. 122–128, 2017.

Hindawi
Journal of Immunology Research
Volume 2020, Article ID 3757015, 8 pages
https://doi.org/10.1155/2020/3757015

Research Article

Increased Circulating Th1 and Tfh1 Cell Numbers Are Associated with Disease Activity in Glucocorticoid-Treated Patients with IgG4-Related Disease

Changsheng Xia,[1] **Caoyi Liu**,[2] **Yanying Liu**,[3] **Yan Long**,[1] **Lijuan Xu**,[4] **and Chen Liu**[1]

[1]*Department of Clinical Laboratory, Peking University People's Hospital, Beijing, China*
[2]*Institute of Blood Transfusion, Chinese Academy of Medical Sciences, Chengdu, China*
[3]*Department of Rheumatology and Immunology, Peking University People's Hospital, Beijing, China*
[4]*Department of Immunology, School of Basic Medicine Sciences, Peking University Health Science Center, Beijing, China*

Correspondence should be addressed to Changsheng Xia; xiachangsheng@bjmu.edu.cn and Chen Liu; liuchen-best@pku.edu.cn

Received 18 July 2020; Revised 24 October 2020; Accepted 3 November 2020; Published 30 November 2020

Academic Editor: Dawei Cui

Copyright © 2020 Changsheng Xia et al. This is an open access article distributed under the Creative Commons Attribution License, which permits unrestricted use, distribution, and reproduction in any medium, provided the original work is properly cited.

Background. This study is aimed at exploring the changes and significance of circulating Th and Tfh cell subsets in glucocorticoid-treated IgG4-RD patients. *Methods*. 39 glucocorticoid-treated IgG4-RD patients and 22 healthy controls (HC) were enrolled. Peripheral blood mononuclear cells were separated, and circulating Th and Tfh cell subsets were examined by flow cytometry according to the surface and intranuclear markers. Disease activity was accessed by the IgG4-RD responder index (RI) score. Correlation analyses were conducted between Th/Tfh subset numbers and clinical indicators. The receiver operating characteristic (ROC) curve was used to evaluate the efficacy of Th and Tfh subsets to distinguish active IgG4-RD patients from remission IgG4-RD patients. *Results*. Circulating Th1, Th17, Tfh1, and Tfh17 cells were significantly increased in active IgG4-RD patients compared with HC. Th1 and Tfh1 numbers were positively correlated with serum IgG4 levels in patients with IgG4-RD. Meanwhile, the absolute numbers of circulating Th1 and Tfh1 cells were positively correlated with IgG4-RD RI scores. The areas under the curve (AUC) were 0.8276 for Th1 and 0.7310 for Tfh1, 0.5862 for Tfh2, and 0.6810 for Tfh17. *Conclusion*. Increased circulating Th1 and Tfh1 subsets are related to elevated serum IgG4 levels in active IgG4-RD patients during glucocorticoid treatment, which may play an important role in the course of IgG4-RD disease, and could be potential biomarkers for monitoring disease activity of IgG4-RD.

1. Introduction

IgG4-related disease (IgG4-RD) is a chronic immune-mediated fibroinflammatory disorder characterized by tumefactive lesions, a dense lymphoplasmacytic infiltration rich in IgG4-positive plasma cells, storiform fibrosis, and frequently elevated serum IgG4 concentrations [1]. The majority of infiltrating cells are small lymphocytes that are composed predominantly of T cells distributed diffusely throughout the lesion and intermingled with plasma cells [2]. Infiltrating T cells in the lesion are primarily activated $CD4^+$ T cells, which play an important role in the course of IgG4-RD [3].

Previous studies have reported that $CD4^+$ cytotoxic T lymphocytes (CTLs) and follicular helper T (Tfh) cells that infiltrated tissue lesions were the main $CD4^+$ T cells at disease sites in IgG4-RD [4–8]. Circulating $CD4^+$ CTLs and Tfh cells were found to be expanded in patients with IgG4-RD [5, 6, 9]. Circulating CD4 T helper (Th) cells can be divided into Th1 cells ($CXCR3^+CCR6^-$), Th2 plus naïve $CD4^+$ cells ($CXCR3^-CCR6^-$, $CXCR3^-CCR6^-CCR4^+$ cells represent Th2, and $CXCR3^-CCR6^-CCR4^-$ cells belong to naïve CD4), and Th17 cells ($CXCR3^-CCR6^+$) [10, 11]. $CD4^+$ CTLs, which express the transcription factors of ThPOK, Runx3, and T-bet, are mainly differentiated from Th1 cells [12, 13]. Accordingly, the expansion of circulating $CD4^+$ CTLs may lead to elevated Th1 cells in the peripheral blood of IgG4-RD patients. Tfh cells represent a distinct $CD4^+$ T cell subset providing key signals to B cells for their differentiation into

plasma cells which secrete high-affinity antibodies in the germinal center [14, 15]. Peripheral blood $CD4^+CXCR5^+$ T cells are considered to be a circulating pool of memory Tfh cells, which can be divided into Tfh1 ($CXCR3^+CCR6^-$), Tfh2 ($CXCR3^-CCR6^-$), and Tfh17 ($CXCR3^-CCR6^+$) cells, and they have different capabilities to help the differentiation of B cell subsets [16, 17]. Some studies have investigated the role of circulating $CD4^+$ T cell subsets in IgG4-RD. However, most previous studies have focused on untreated IgG4-RD patients. Few studies have explored the relationship between circulating $CD4^+$ T cell subsets and disease activity in treated IgG4-RD patients.

In this study, we aim to determine the relationship between circulating Th and Tfh cell subsets and serum IgG4 levels as well as disease activity in glucocorticoid-treated IgG4-RD patients. We intend to clarify the changes and clinical significance of circulating Th and Tfh cell subsets in treated IgG4-RD patients.

2. Results

2.1. Clinical Characteristics of the Patients with IgG4-RD. We involved 39 patients with IgG4-RD including the diagnosis of definite ($n = 25$), possible ($n = 12$), and probable ($n = 2$) IgG4-RD diagnosis results, and the clinical and demographic characteristics of the patients are described in Supplementary Table 1. Of those subjects, 38 (97.4%) were presented with ≥2 organs involved. Frequent sites of initial organ involvement included the submandibular glands (13 cases, 33.3%), lacrimal glands (7 cases, 17.9%), parotid gland (1 case, 2.6%), pancreas (10 cases, 25.6%), bile ducts (1 case, 2.6%), lymph nodes (2 cases, 5.1%), retroperitoneum (3 cases, 7.7%), sinus (1 case, 2.6%), and mesentery (1 case, 2.6%). The median RI score of these IgG4-RD patients was 5. These patients were divided into active ($n = 29$) and remission ($n = 10$) IgG4-RD patients according to RI scores.

We measured and compared levels of IgG4, IgG, IgE, C3, C4, and CRP in the serum of active IgG4-RD patients, remission IgG4-RD patients, and HC. As shown in Supplementary Figure 1, the concentrations of serum IgG4 were significantly higher in active IgG4-RD patients than in HC and remission patients (3.01 g/L versus 0.46 g/L and 0.85 g/L; $P < 0.0001$ and $P = 0.0153$, respectively). Similarly, IgE was significantly elevated in active IgG4-RD patients compared with HC and remission patients (103.40 IU/mL versus 24.94 IU/mL and 38.13 IU/mL; $P = 0.0001$ and $P = 0.0483$, respectively). In contrast, serum C4 levels were significantly decreased in patients with active IgG4-RD compared with HC (0.209 g/L versus 0.268 g/L, $P = 0.0032$). We also analyzed levels of lymphocytes and $CD4^+$ T cell percentages and found elevated lymphocyte concentrations and $CD4^+$ T cell percentages in active IgG4-RD patients compared to HC or remission patients (not shown).

2.2. Increased Th1 and Th17 Cells in Patients with Active IgG4-RD. We next measured Th cell levels in IgG4-RD patients and HC according to surface markers. Circulating Th cells were defined as $CD3^+CD4^+CXCR5^-Foxp3^-$ cells because we want to exclude the influence of $Foxp3^+$ regulatory T cells. Th1, Th2 plus naïve CD4, and Th17 cell subsets were defined as $CXCR3^+CCR6^-$ cells, $CXCR3^-CCR6^-$ cells, and $CXCR3^-CCR6^+$ cells within the $CD3^+CD4^+CXCR5^-Foxp3^-$ Th cells, respectively. As shown in Figure 1, the absolute number (per μL) of circulating Th1 cells was significantly increased in active IgG4-RD patients compared with HC and remission patients (111.9 cells/μL versus 76.4 cells/μL and 57.4 cells/μL; $P = 0.0376$ and $P = 0.0047$, respectively). Moreover, the absolute numbers (per μL) and frequencies of circulating Th17 cells were significantly higher in patients with active IgG4-RD than in HC (76.4 cells/μL versus 30.6 cells/μL, 0.107 versus 0.070; $P = 0.0007$ and $P = 0.0067$, respectively). Interestingly, the absolute numbers (per μL) of circulating Th2 plus naïve CD4 cells were significantly lower in remission IgG4-RD patients than in active patients and HC (197.9 cells/μL versus 400.9 cells/μL and 374.6 cells/μL; $P = 0.0264$ and $P = 0.0474$, respectively). The frequencies of circulating Th2 plus naïve CD4 cells were significantly lower in active IgG4-RD than in HC (0.611 versus 0.745; $P = 0.0007$).

2.3. Tfh1 and Tfh17 Cells in Patients with Active IgG4-RD Were Increased. We next analyzed circulating Tfh cell changes in these IgG4-RD patients. Circulating Tfh cells were defined as $CD3^+CD4^+CXCR5^+Foxp3^-$ cells. $Foxp3^+$ cells were also excluded because we want to exclude the influence of follicular regulatory T cells. Tfh1, Tfh2, and Tfh17 cell subsets were defined as $CXCR3^+CCR6^-$ cells, $CXCR3^-CCR6^-$ cells, and $CXCR3^-CCR6^+$ cells within $CD3^+CD4^+CXCR5^+Foxp3^-$ Tfh cells, respectively. As shown in Figure 2, the absolute number (per μL) of circulating Tfh1 cells was significantly increased in active IgG4-RD patients compared with HC (26.2 cells/μL versus 17.4 cells/μL; $P = 0.0172$). Moreover, the absolute numbers (per μL) and frequencies of circulating Tfh17 cells were also significantly increased in patients with active IgG4-RD compared with HC (25.8 cells/μL versus 10.4 cells/μL, 0.226 versus 0.145; $P = 0.0009$ and $P = 0.0027$, respectively). Conversely, the frequencies of circulating Tfh2 cells were significantly decreased in active IgG4-RD patients compared with HC and remission patients (0.424 versus 0.612 and 0.572; $P < 0.0001$ and $P = 0.0091$, respectively).

2.4. Circulating Th1 Cells Are Positively Correlated with IgG4 Levels and RI Scores in IgG4-RD Patients. To determine the associations of Th cell subsets with clinical indicators, the correlations of Th cell subsets with serum IgG4 and RI scores in IgG4-RD patients were conducted. As shown in Figure 3, the absolute number (per μL) of Th1 cells was found to be positively correlated with serum IgG4 levels and IgG4-RD RI scores ($r = 0.8134$ and 0.4457; $P < 0.0001$ and $P = 0.0045$, respectively). Similarly, the correlations of Tfh cell subsets with serum IgG4 and RI scores in IgG4-RD patients were also analyzed, respectively (Figure 4). Interestingly, we found that the number of Tfh1 cells was also positively correlated with serum IgG4 levels and IgG4-RD RI scores ($r = 0.6424$ and 0.3568; $P < 0.0001$ and $P = 0.0257$, respectively).

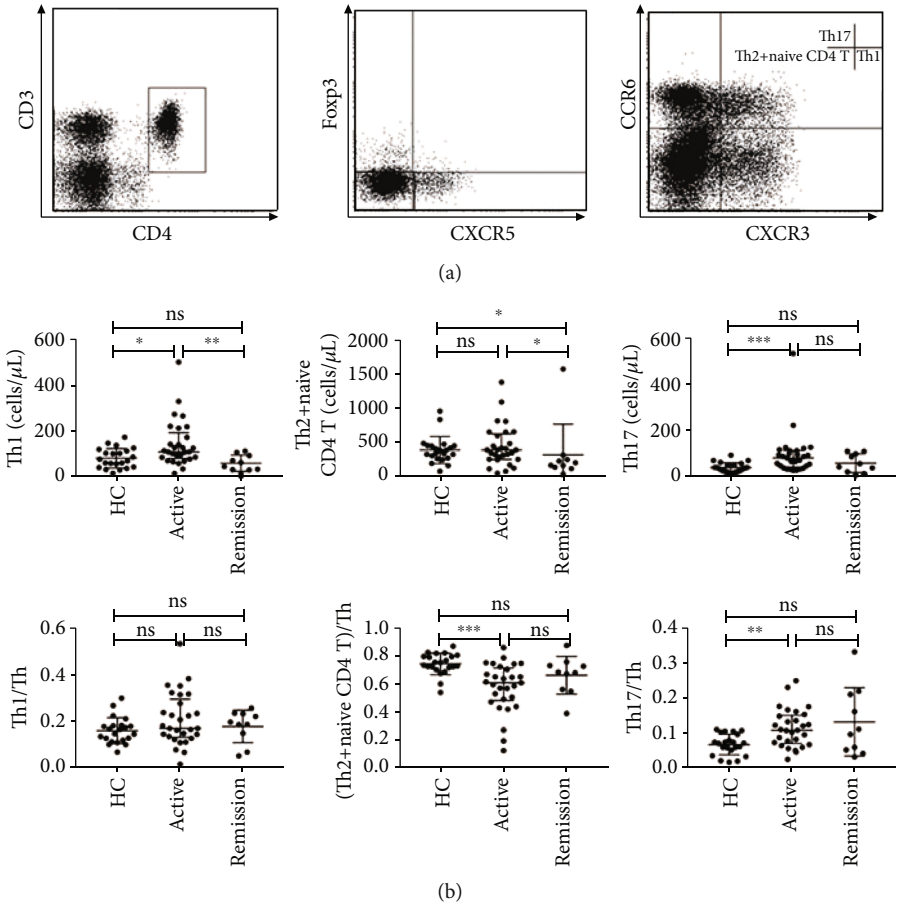

Figure 1: Analyses of Th cell subsets in active IgG4-RD patients, remission IgG4-RD patients, and healthy controls. Th and Tfh cells in PBMCs were analyzed by FCM. Circulating Th cells were defined as $CD3^+CD4^+CXCR5^-Foxp3^-$ cells. Th1, Th2 plus naïve CD4, and Th17 cell subsets were defined as $CXCR3^+CCR6^-$ cells, $CXCR3^-CCR6^-$ cells, and $CXCR3^-CCR6^+$ cells within Th cells. Circulating Tfh cells were defined as $CD3^+CD4^+CXCR5^+Foxp3^-$ cells. Tfh1, Tfh2, and Tfh17 cell subsets were defined as $CXCR3^+CCR6^-$ cells, $CXCR3^-CCR6^-$ cells, and $CXCR3^-CCR6^+$ cells among Tfh cells. (a) Representative dot plots of flow cytometry analysis and Th1, Th2 plus naïve CD4, and Th17 subsets were shown. (b) The absolute numbers (per μL) and frequencies of circulating Th cell subsets in active IgG4-RD patients ($n = 29$), remission IgG4-RD patients ($n = 10$), and HC ($n = 22$). The error bars represented the median and interquartile range. The Mann–Whitney test was used to compare the subset levels. ns, $P \geq 0.05$ (not significant); $^*P < 0.05$; $^{**}P < 0.01$; $^{***}P < 0.001$.

2.5. Th1 and Tfh1 Cell Numbers Can Be Used as Potential Biomarkers for IgG4-RD Disease Activity Monitoring. Since Th1 and Tfh1 subset numbers are significantly increased in active IgG4-RD patients and have significant positive correlations with disease activity, we further explored whether they could be used as potential markers for IgG4-RD disease activity monitoring. As shown in Figure 5, we used Tfh1 and Th1 cell numbers to distinguish active IgG4-RD from remission IgG4-RD and generated ROC curves. The areas under the curve (AUC) were 0.8276 for Th1 cells and 0.7310 for Tfh1 cells. We also analyzed the efficacy of using other cell subsets for diagnosis. The areas under the curve (AUC) were 0.7586 for Th2 plus naïve CD4 cells and 0.6517 for Th17 cells, and AUC were 0.5862 for Tfh2 cells and 0.6810 for Tfh17 cells (Figure 5).

3. Discussion

In this research, we studied the changes and significance of circulating Th and Tfh cell subsets in glucocorticoid-treated IgG4-RD patients. We found that circulating Th1 and Tfh1 subsets were increased and were related to serum IgG4 levels and RI scores in active IgG4-RD patients, which may play an important role in IgG4-RD, and could be potential biomarkers for monitoring disease activity of IgG4-RD during treatment.

IgG4-RD is often featured by elevated levels of serum IgG4 [18, 19]. Serum IgE concentrations are also increased in some patients [20]. In the present study, we also found that the concentrations of serum IgG4 and IgE were significantly increased in active IgG4-RD patients. Conversely, serum C4 levels were significantly lower in active IgG4-RD patients than in HC. The reduction in serum C4 levels in these active patients may indicate that specific antibodies bind to the target antigen and the activated complement system is common in the disease.

Expanded $CD4^+$ CTLs have been reported to play an important role in the pathogenesis of IgG4-RD [4, 20–23]. $CD4^+$ CTLs differentiate mainly from Th1 cells. Accordingly, we investigated circulating Th subsets in patients with IgG4-

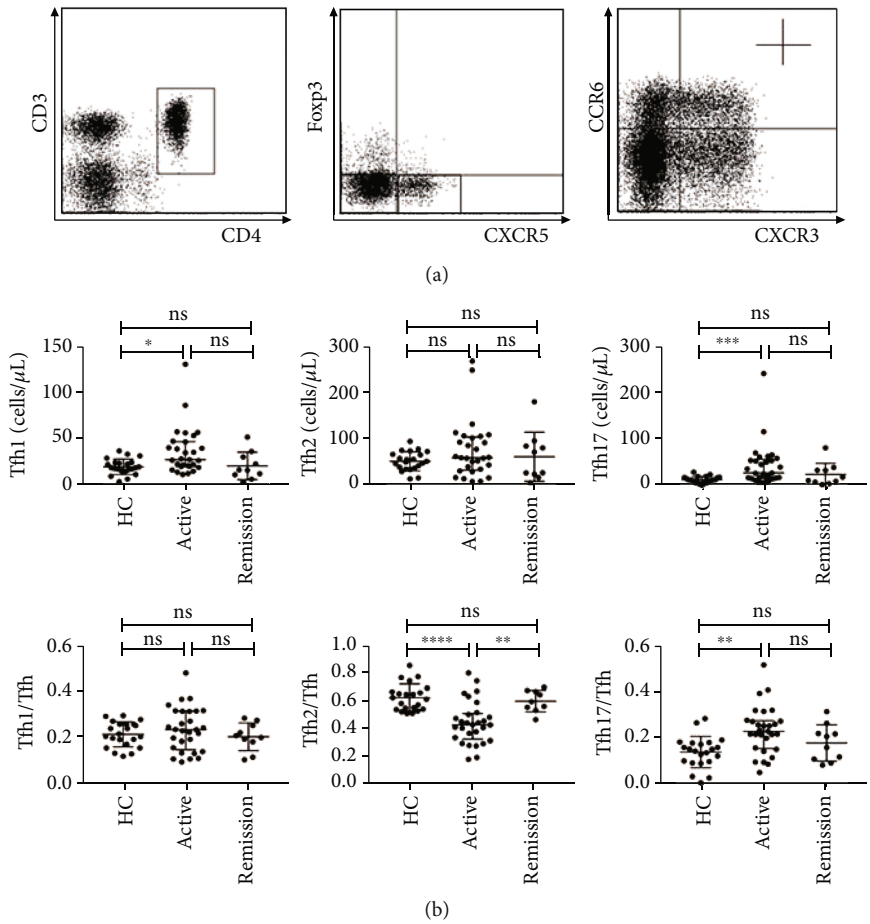

Figure 2: Tfh cell subset analysis in active IgG4-RD patients, remission IgG4-RD patients, and healthy controls. (a) Representative dot plots for FCM analysis. Tfh1, Tfh2, and Tfh17 were defined as $CD4^+CXCR5^+Foxp3^-CXCR3^+CCR6^-$ cells, $CD4^+CXCR5^+Foxp3^-CXCR3^-$ $CCR6^-$ cells, and $CD4^+CXCR5^+Foxp3^-CXCR3^-CCR6^+$ cells, respectively. (b) The absolute numbers (per μL) and frequencies of circulating Tfh subsets in active IgG4-RD patients ($n = 29$), remission IgG4-RD patients ($n = 10$), and HC ($n = 22$). The error bars represented the median and interquartile range. The Mann–Whitney test was used to compare the subset levels. ns, $P \geq 0.05$ (not significant); $^*P < 0.05$; $^{**}P < 0.01$; $^{***}P < 0.001$; $^{****}P < 0.0001$.

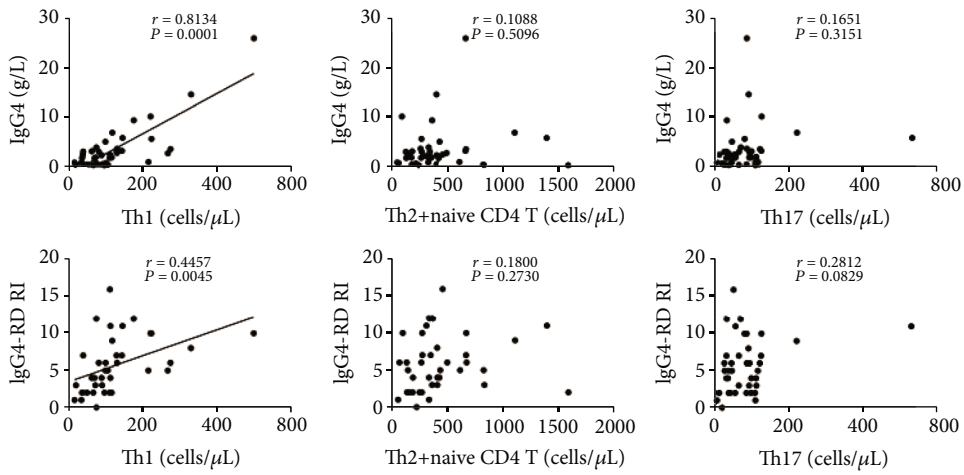

Figure 3: Correlation analysis of circulating Th cell subsets with serum IgG4 and IgG4-RD RI in IgG4-RD patients. Serum IgG4 concentrations of all IgG4-RD patients ($n = 39$) were measured. Correlation analyses were conducted between absolute numbers (per μL) of Th subsets and serum IgG4 (up) or IgG4-RD RI scores (down) in IgG4-RD patients. Each plot represented the data of a patient. The Spearman test's r and P values for each parameter were listed. The r values were Spearman's correlation coefficients. For P values less than 0.05, data were presented as scatter plots with a linear fit.

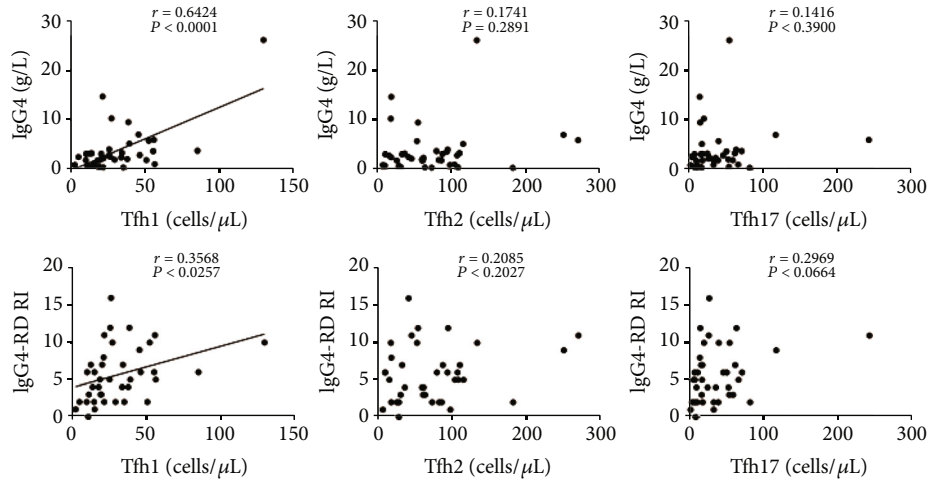

Figure 4: The correlations of circulating Tfh cell subsets with serum IgG4 and IgG4-RD RI in IgG4-RD patients. Correlation analyses were conducted between absolute numbers (per μL) of Tfh subsets and serum IgG4 levels (up) or IgG4-RD RI scores (down) in IgG4-RD patients ($n = 39$). Each plot represented the data of one patient. The Spearman test's correlation coefficient r and P values were listed, and the P values less than 0.05 were linearly regressed to show relevant trends.

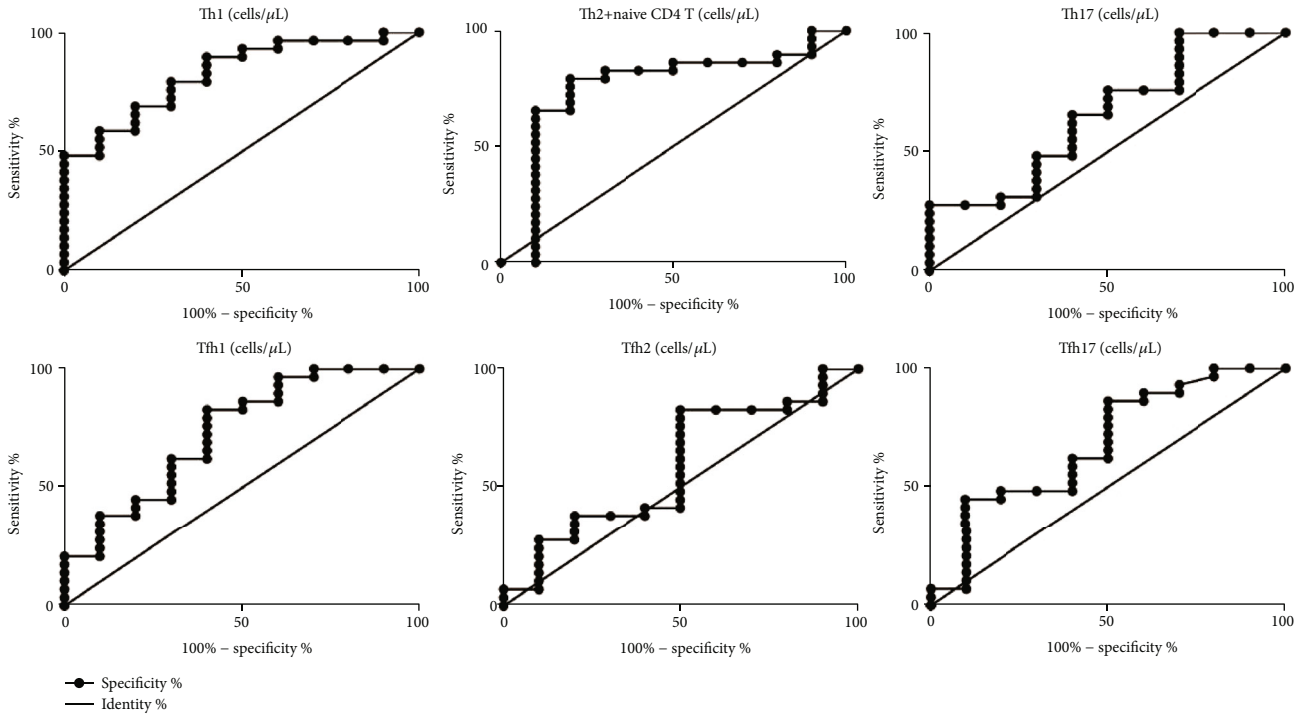

Figure 5: ROC analysis of the values of Tfh and Th subsets in the diagnosis of active IgG4-RD. Th (up) and Tfh (down) subset levels in 39 cases of IgG4-RD patients were analyzed, including 29 active and 10 remission IgG4-RD patients. The receiver operating characteristic (ROC) curves were performed to evaluate the efficacy of Th or Tfh subsets to distinguish active IgG4-RD from remission IgG4-RD patients. The areas under the curve (AUC) were 0.8276 for Th1 cells, 0.7586 for Th2 plus naïve CD4 cells, and 0.6517 for Th17 cells, and AUC were 0.7310 for Tfh1 cells, 0.5862 for Tfh2 cells, and 0.6810 for Tfh17 cells.

RD. The numbers of circulating Th1 cells were significantly increased in active IgG4-RD patients. In line with our results, increased circulating Th1 cells in IgG4-related sialadenitis patients have already been reported by Ohta et al. and Higashioka et al. [24, 25]. Here, we used surface molecules to characterize the Th subgroup for providing potential diagnostic applications in the future. We also found that the numbers of circulating Th1 cells were well correlated with serum IgG4 levels, which suggests that expanded Th1 cells may be involved in the elevation of serum IgG4. Similarly, Maehara et al. reported that the ratio of $CD4^+$ CTLs in lesion tissues from patients with IgG4-related dacryoadenitis and sialoadenitis was positively correlated with serum IgG4 concentrations [4]. Upregulation of Th1 cells or $CD4^+$ CTLs will

result in the production of more IFN-γ, and excessive IFN-γ is thought to lead to the pathogenic accumulation of Tfh cells, which in turn leads to the formation of abnormal germinal centers and the production of autoantibodies [26]. This indirect effect may be the explanation for the positive correlation between Th1 cells and IgG4. Besides, we found that the numbers of circulating Th1 cells were positively correlated with the IgG4-RD RI scores. This means that circulating Th1 cells reflect the disease activity of IgG4-RD. The reason may be because the Th1 cells can produce inflammatory cytokines (IFN-γ, etc.) and cytolytic molecules (perforin and granzyme), which were associated with the disease activity.

Previous studies investigated the role of Tfh cell subsets in IgG4-RD. However, the results remain controversial. Akiyama et al. reported that activated circulating Tfh1 and Tfh2 cells were increased in IgG4-RD and the number of Tfh2 cells was associated with serum IgG4 levels [27, 28]. Chen et al. reported that frequencies of circulating Tfh1 and Tfh2 cells were significantly increased in IgG4-RD patients [8]. Grados et al. found that circulating T cells polarized toward Th2/Tfh2 and Th17/Tfh17 in patients with IgG4-RD [29]. A recent study showed that all circulating PD-1^+ Tfh cell subsets were expanded in IgG4-related sclerosing cholangitis and pancreatitis, but only activated Tfh2 cells were associated with disease activity [30]. IL-4^+ Tfh cells were reported to be significantly increased in secondary lymphoid organs and lesion tissues in IgG4-RD [7], and these IL-4^+ Tfh cells express BATF, rather than GATA-3, which was identified as a master transcriptional factor of circulating Tfh2 [10]. CXCR3 and CCR6 were found to be upregulated on $CD4^+$ Tfh cells in lesion tissues of IgG4-RD patients [4], suggesting that increased Tfh in IgG4-RD might be $CXCR3^+$ Tfh and $CCR6^+$ Tfh cells. Here, we found that the number of circulating Tfh1 cells was significantly higher in patients with active IgG4-RD. Moreover, the number and proportion of circulating Tfh17 cells were significantly higher in patients with active IgG4-RD than in HC. In contrast, the proportion of circulating Tfh2 cells was significantly decreased in active IgG4-RD patients. Also, the numbers of circulating Tfh1 cells were positively correlated with serum IgG4 levels and IgG4-RD RI scores, which suggests that increased Tfh1 cells may be associated with the elevated IgG4 and might contribute to IgG4-RD.

One of the reasons for the inconsistent conclusions is the different criteria for the inclusion of patients. We included patients in this study who were undergoing glucocorticoid therapy. The changes in Th and Tfh subpopulations in these patients during the treatment process were very different from those of new onset or after treatment. Since most IgG4-RD patients are often in the state of starting treatment, it is difficult to collect new-onset patients, but our results are more of reference significance because it reflects the situation of most patients who come to the hospital. This is also the first time to systematically study the changes of Th and Tfh subsets in patients treated with glucocorticoid. We suspect that glucocorticoid can have an effect on circulating T cell subsets, and changes in T cell subsets can also reflect the effects of treatment.

Based on this, we also conducted a preliminary exploration of the diagnostic value of the Th and Tfh subsets and used ROC curves to evaluate the effectiveness of these subsets for distinguishing the active from remission status of IgG4-RD patients during glucocorticoid treatment. According to our results, the areas under the curve (AUC) were 0.8276 for Th1 and 0.7310 for Tfh1, suggesting that Th1 and Tfh1 numbers could be potential diagnosis makers in monitoring IgG4-RD disease activity. Our research uses flow cytometry to detect molecules on the surface of peripheral blood cells. If it can achieve the purpose of evaluating the treatment of patients, it will have a good application prospect. However, because the sample size is not large enough, it is necessary to expand the sample size in the future to clarify the diagnostic value of Th1 and Tfh1.

In summary, our study demonstrates that active IgG4-RD is characterized by circulating T cell polarization toward Th1/Tfh1 and Th17/Tfh17 during glucocorticoid treatment. Circulating Th1 and Tfh1 levels positively correlate with serum IgG4 levels and disease activity in patients with IgG4-RD, which might play an important role in the course of IgG4-RD, and could be the potential biomarkers for disease activity monitoring in IgG4-RD.

4. Materials and Methods

4.1. Subjects. A total of 39 patients with IgG4-RD (24 males, 15 females; median age: 62 years) and 22 healthy controls (HC) (13 males, 9 females; median age: 66 years) were recruited from outpatient and inpatient sections of Peking University People's Hospital between December 2018 and May 2019. The diagnosis of IgG4-RD was performed according to the 2011 comprehensive diagnostic criteria [31]. All IgG4-RD patients were receiving glucocorticoid therapy. Most patients have been standardized to dosing: prednisolone 0.6 mg/kg/d for 2–4 weeks and then dose reduction to 5 mg/d after 3-6 months, with the expected cessation of treatment by 2–3 years. The IgG4-RD responder index (RI) score was used for the assessment of disease activity [32]. Each affected organ was scored separately, and all individual organ scores were summed to calculate the overall RI. All RI scores in this present study were calculated with the inclusion of serum IgG4 levels. IgG4-RD RI score ≥ 3 was considered an active disease, and <3 was classified as remission [21]. This research was approved by the Ethics Committee of Peking University People's Hospital and was performed following the ethical standards of the Declaration of Helsinki.

4.2. Clinical Indicator Measurement. Serum levels of IgG4 were measured by nephelometry using a Siemens BN II Nephelometer (Siemens Healthcare Diagnostics; Malburg, Germany) and Siemens reagents. Serum concentrations of IgG, C3, and C4 were measured by nephelometry using a Beckman Coulter Immage 800 Nephelometer (Beckman Coulter Ireland Inc.; CA, USA) and Beckman Coulter reagents. CRP in serum was tested by immunoturbidimetry using a Beckman Coulter Chemistry Analyzer AU5800

(Beckman Coulter Ireland Inc.; CA, USA) and Beckman Coulter reagents. Serum IgE levels were tested by a Cobas e601 Electrochemiluminescence Immunoassay Analyzer (Roche; Mannheim, Germany). WBC and lymphocyte counts were determined by Sysmex XE-2100 (TOA Medical Electronics; Kobe, Japan).

4.3. Flow Cytometry. Peripheral blood mononuclear cells (PBMCs) were separated by gradient centrifugation with a human lymphocyte separation medium (Dakewei Biotech Co., Ltd.; Shenzhen, China) and then washed twice with PBS. Enriched PBMCs were immediately stained for 30 minutes with the following antibodies: CD3-APC, CD4-PerCP/Cy5.5, CXCR5-APC/Cy7, CXCR3-PE, and CCR6-PE/Cy7. Intracellular staining for Foxp3 was performed using a transcription factor staining buffer kit (Thermo Fisher Scientific-eBioscience; San Diego, CA, USA), according to the manufacturer's instructions. After fixation and permeabilization, cells were incubated with anti-Foxp3 allophycocyanin for 30 minutes. All fluorescent antibodies were purchased from BioLegend (San Diego, CA, USA). Samples were analyzed on FACSCanto using Diva software (BD Biosciences; San Jose, CA, USA). Based on the number of lymphocytes in the complete blood count and the proportion of each subgroup of lymphocytes determined by flow cytometry, the absolute count (per μL) of each subgroup was calculated.

4.4. Statistics. Continuous variables are shown as median with 25^{th}-75^{th} percentiles. Multiple group comparisons were analyzed using the Kruskal–Wallis test. The Mann–Whitney *U* test was used for comparison between two groups. Also, receiver operating characteristic (ROC) curve analyses were performed to explore the efficiency of parameters in evaluating IgG4-RD disease activity and the AUC values were determined. Statistical significance was determined using GraphPad Prism software V.7.0 (GraphPad Software; San Diego, CA, USA). Statistics with *P* values less than 0.05 were considered to be significant.

Abbreviations

AUC: Area under the curve
FCM: Flow cytometry
IgG4-RD: IgG4-related disease
RI: Responder index
HC: Healthy controls
CTLs: Cytotoxic T lymphocytes
ROC: Receiver operating characteristic
Th: T helper cells
Tfh: Follicular helper T cells
PBMCs: Peripheral blood mononuclear cells
WBC: White blood cell.

Data Availability

The data used to support the findings of this study may be released upon application to Dr. Changsheng Xia, who can be contacted at xiachangsheng@bjmu.edu.cn.

Conflicts of Interest

There are no competing financial interests in relation to the work described.

Authors' Contributions

CS. X. and C. L. designed the study; CY. L., Y. L., and LJ. X. performed the experiments; YY. L. was responsible for subject recruitment; CS. X. and C. L. wrote the paper.

Acknowledgments

This work was supported by grants from the National Natural Science Foundation of China (81871230), the Doctoral Fund of Ministry of Education of China (20120001120053), the Peking University People's Hospital Scientific Research Development Funds (RDT2020-01), and the Beijing Natural Science Foundation (7163228).

Supplementary Materials

Supplementary Figure 1: the levels of serological markers in active IgG4-RD patients, remission IgG4-RD patients, and healthy controls. Supplementary Table 1: clinical characteristics of the patients with IgG4-RD. *(Supplementary Materials)*

References

[1] J. H. Stone, Y. Zen, and V. Deshpande, "IgG4-related disease," *The New England Journal of Medicine*, vol. 366, no. 6, pp. 539–551, 2012.

[2] V. Deshpande, Y. Zen, J. K. Chan et al., "Consensus statement on the pathology of IgG4-related disease," *Modern Pathology*, vol. 25, no. 9, pp. 1181–1192, 2012.

[3] T. Kamisawa, Y. Zen, S. Pillai, and J. H. Stone, "IgG4-related disease," *The Lancet*, vol. 385, no. 9976, pp. 1460–1471, 2015.

[4] T. Maehara, H. Mattoo, M. Ohta et al., "Lesional CD4+IFN-γ+cytotoxic T lymphocytes in IgG4-related dacryoadenitis and sialoadenitis," *Annals of the Rheumatic Diseases*, vol. 76, no. 2, pp. 377–385, 2017.

[5] R. Kamekura, K. Takano, M. Yamamoto et al., "Cutting edge: a critical role of lesional T follicular helper cells in the pathogenesis of IgG4-related disease," *Journal of Immunology*, vol. 199, pp. 2624–2629, 2017.

[6] H. Mattoo, V. S. Mahajan, T. Maehara et al., "Clonal expansion of CD4(+) cytotoxic T lymphocytes in patients with IgG4-related disease," *The Journal of Allergy and Clinical Immunology*, vol. 138, no. 3, pp. 825–838, 2016.

[7] T. Maehara, H. Mattoo, V. S. Mahajan et al., "The expansion in lymphoid organs of IL-4^+ $BATF^+$ T follicular helper cells is linked to IgG4 class switching in vivo," *Life Science Alliance*, vol. 1, 2018.

[8] Y. Chen, W. Lin, H. Yang et al., "Aberrant expansion and function of follicular helper T cell subsets in IgG4-related disease," *Arthritis & Rheumatology*, vol. 70, no. 11, pp. 1853–1865, 2018.

[9] S. Kubo, S. Nakayamada, J. Zhao et al., "Correlation of T follicular helper cells and plasmablasts with the development of organ involvement in patients with IgG4-related disease," *Rheumatology*, vol. 57, no. 3, pp. 514–524, 2018.

[10] R. Morita, N. Schmitt, S. E. Bentebibel et al., "Human blood CXCR5(+)CD4(+) T cells are counterparts of T follicular cells and contain specific subsets that differentially support antibody secretion," *Immunity*, vol. 34, no. 1, pp. 108–121, 2011.

[11] A. Gosselin, P. Monteiro, N. Chomont et al., "Peripheral blood $CCR4^+$ $CCR6^+$ and $CXCR3^+$ CCR6+ $CD4^+$ T cells are highly permissive to HIV-1 infection," *The Journal of Immunology*, vol. 184, no. 3, pp. 1604–1616, 2010.

[12] B. Bengsch, T. Ohtani, R. S. Herati, N. Bovenschen, K. M. Chang, and E. J. Wherry, "Deep immune profiling by mass cytometry links human T and NK cell differentiation and cytotoxic molecule expression patterns," *Journal of Immunological Methods*, vol. 453, pp. 3–10, 2018.

[13] Y. Serroukh, C. Gu-Trantien, B. Hooshiar Kashani et al., "The transcription factors Runx3 and ThPOK cross-regulate acquisition of cytotoxic function by human Th1 lymphocytes," *eLife*, vol. 7, 2018.

[14] D. Breitfeld, L. Ohl, E. Kremmer et al., "Follicular B helper T cells express CXC chemokine receptor 5, localize to B cell follicles, and support immunoglobulin production," *The Journal of Experimental Medicine*, vol. 192, no. 11, pp. 1545–1552, 2000.

[15] C. H. Kim, L. S. Rott, I. Clark-Lewis, D. J. Campbell, L. Wu, and E. C. Butcher, "Subspecialization of CXCR5+ T cells: B helper activity is focused in a germinal center-localized subset of CXCR5+ T cells," *The Journal of Experimental Medicine*, vol. 193, no. 12, pp. 1373–1382, 2001.

[16] H. Ueno, "Human circulating T follicular helper cell subsets in health and disease," *Journal of Clinical Immunology*, vol. 36, no. S1, pp. 34–39, 2016.

[17] M. M. Figueiredo, P. A. C. Costa, S. Q. Diniz et al., "T follicular helper cells regulate the activation of B lymphocytes and antibody production during *Plasmodium vivax* infection," *PLoS Pathogens*, vol. 13, no. 7, article e1006484, 2017.

[18] C. S. Xia, C. H. Fan, and Y. Y. Liu, "Diagnostic performances of serum IgG4 concentration and IgG4/IgG ratio in IgG4-related disease," *Clinical Rheumatology*, vol. 36, no. 12, pp. 2769–2774, 2017.

[19] W. L. Xu, Y. C. Ling, Z. K. Wang, and F. J. S. R. Deng, "Diagnostic performance of serum IgG4 level for IgG4-related disease: a meta-analysis," *Scientific Reports*, vol. 6, no. 1, article 32035, 2016.

[20] Z. S. Wallace, H. Mattoo, V. S. Mahajan et al., "Predictors of disease relapse in IgG4-related disease following rituximab," *Rheumatology*, vol. 55, no. 6, pp. 1000–1008, 2016.

[21] H. Mattoo, J. H. Stone, and S. Pillai, "Clonally expanded cytotoxic CD4(+) T cells and the pathogenesis of IgG4-related disease," *Autoimmunity*, vol. 50, no. 1, pp. 19–24, 2017.

[22] E. Della-Torre, E. Bozzalla-Cassione, C. Sciorati et al., "A CD8α− subset of CD4+SLAMF7+ cytotoxic T cells is expanded in patients with IgG4-related disease and decreases following glucocorticoid treatment," *Arthritis & Rheumatology*, vol. 70, no. 7, pp. 1133–1143, 2018.

[23] C. A. Perugino, N. Kaneko, T. Maehara et al., "$CD4^+$ and $CD8^+$ cytotoxic T lymphocytes may induce mesenchymal cell apoptosis in IgG_4-related disease," *The Journal of Allergy and Clinical Immunology*, 2020.

[24] N. Ohta, S. Makihara, M. Okano et al., "Roles of IL-17, Th1, and Tc1 cells in patients with IgG4-related sclerosing sialadenitis," *Laryngoscope*, vol. 122, no. 10, pp. 2169–2174, 2012.

[25] K. Higashioka, Y. Ota, T. Maehara et al., "Association of circulating SLAMF7(+)Tfh1 cells with IgG4 levels in patients with IgG4-related disease," *BMC Immunology*, vol. 21, no. 1, p. 31, 2020.

[26] S. K. Lee, D. G. Silva, J. L. Martin et al., "Interferon-γ excess leads to pathogenic accumulation of follicular helper T cells and germinal centers," *Immunity*, vol. 37, no. 5, pp. 880–892, 2012.

[27] M. Akiyama, K. Suzuki, K. Yamaoka et al., "Number of circulating follicular helper 2 T cells correlates with IgG4 and interleukin-4 levels and plasmablast numbers in IgG4-related disease.," *Arthritis & Rheumatology*, vol. 67, no. 9, pp. 2476–2481, 2015.

[28] M. Akiyama, H. Yasuoka, K. Yamaoka et al., "Enhanced IgG4 production by follicular helper 2 T cells and the involvement of follicular helper 1 T cells in the pathogenesis of IgG4-related disease," *Arthritis Research & Therapy*, vol. 18, no. 1, p. 167, 2016.

[29] A. Grados, M. Ebbo, C. Piperoglou et al., "T cell polarization toward TH2/TFH2 and TH17/TFH17 in patients with IgG4-related disease," *Frontiers in Immunology*, vol. 8, 2017.

[30] T. Cargill, M. Makuch, R. Sadler et al., "Activated T-follicular helper 2 cells are associated with disease activity in IgG4-related sclerosing cholangitis and pancreatitis," *Clinical and Translational Gastroenterology*, vol. 10, no. 4, article e00020, 2019.

[31] H. Umehara, K. Okazaki, Y. Masaki et al., "Comprehensive diagnostic criteria for IgG4-related disease (IgG4-RD), 2011," *Modern Rheumatology / the Japan Rheumatism Association*, vol. 22, pp. 21–30, 2012.

[32] M. N. Carruthers, J. H. Stone, V. Deshpande, and A. Khosroshahi, "Development of an IgG4-RD responder index," *International Journal of Rheumatology*, vol. 2012, Article ID 259408, 7 pages, 2012.

Hindawi
Journal of Immunology Research
Volume 2020, Article ID 6027361, 8 pages
https://doi.org/10.1155/2020/6027361

Research Article

Th1/Th2 Cells and Associated Cytokines in Acute Hepatitis E and Related Acute Liver Failure

Jian Wu,[1,2] Yurong Guo,[3] Xuan Lu,[1] Fen Huang,[4] Feifei Lv,[5] Daqiao Wei,[4] Anquan Shang,[6] Jinfeng Yang,[1] Qiaoling Pan,[1] Bin Jiang,[7] Jiong Yu,[1] Hongcui Cao,[1,8] and Lanjuan Li[1]

[1]*State Key Laboratory for Diagnosis and Treatment of Infectious Diseases, National Clinical Research Center for Infectious Diseases, The First Affiliated Hospital, Zhejiang University School of Medicine, 79 Qingchun Rd., Hangzhou 310003, China*
[2]*Department of Laboratory Medicine, Yancheng Clinical Medical College of Nanjing Medical University, Yancheng 224001, China*
[3]*Department of Laboratory Medicine, Yancheng Hospital of Traditional Chinese Medicine, Affiliated to Nanjing University of Traditional Chinese Medicine, Yancheng 224000, China*
[4]*Medical School, Kunming University of Science and Technology, 727 Jing Ming South Road, Kunming 650031, China*
[5]*Department of Laboratory Medicine, The First Affiliated Hospital, College of Medicine, Zhejiang University, Hangzhou, China*
[6]*Department of Clinical Laboratory, Shanghai Tongji Hospital, Tongji University School of Medicine, 389 Xincun Road, Shanghai 200065, China*
[7]*Department of Laboratory Medicine, The Central Blood Station of Yancheng City, Yancheng, 224000 Jiangsu, China*
[8]*Zhejiang Provincial Key Laboratory for Diagnosis and Treatment of Aging and Physic-chemical Injury Diseases, 79 Qingchun Rd, Hangzhou 310003, China*

Correspondence should be addressed to Hongcui Cao; hccao@zju.edu.cn

Received 5 June 2020; Revised 8 September 2020; Accepted 30 October 2020; Published 19 November 2020

Academic Editor: Xinyi Tang

Copyright © 2020 Jian Wu et al. This is an open access article distributed under the Creative Commons Attribution License, which permits unrestricted use, distribution, and reproduction in any medium, provided the original work is properly cited.

Background and Aims. The involvement of cellular immunity in the development of hepatitis E virus (HEV) infection is rare. We aimed to study the roles of viral load and Th cell responses in acute hepatitis E (AHE) and HEV-related acute liver failure (HEV-ALF). *Methods*. We evaluated viral load and Th1/Th2 cytokine levels in 34 patients with HEV infection, including 17 each with AHE or HEV-ALF. Seventeen healthy controls (HCs) were also included who were negative for anti-HEV IgM and IgG. *Results*. There was no significant difference in viral load and HEV RNA in the AHE and HEV-ALF groups (both $P > 0.05$). The Th lymphocyte levels (CD3+, CD4+) in the AHE and HEV-ALF groups were significantly higher than those in the HC group (both $P < 0.05$), but there was no significant difference between the AHE and HEV-ALF groups ($P > 0.05$). Both IFN-γ and IL-10 showed gradual upward trend from the HC group to the AHE (both $P < 0.01$), but IFN-γ showed a sharp downward trend from the AHE group to the HEV-ALF group ($P < 0.01$) and IL-4 showed gradual upward trend from the AHE group to the HEV-ALF group ($P < 0.01$).There was no significant difference in Th1 and Th2 cytokines between the HEV RNA(+) group and HEV RNA(-) group (all $P > 0.05$). Th2 bias was observed from the AHE (ratio = 58.65) to HEV-ALF (ratio = 1.20) groups. The level of IFN-γ was associated with the outcome of HEV-ALF patients. *Conclusions*. HEV viral load was not associated with aggravation of AHE, and the HEV-ALF patients showed significant Th2 bias, which may be involved in the aggravation of AHE.

1. Introduction

Hepatitis E is an infectious disease of the digestive tract caused by hepatitis E virus (HEV) [1, 2]. It is mainly spread by the fecal–oral route, which is one of the main routes of transmission of hepatitis worldwide, and has become an important public health problem [3, 4]. Hepatitis E mainly occurs in developing countries and regions with backward sanitation conditions, which can spread infection [5]. In recent years, some developed countries, such as North America, Europe, and Japan, have also reported nonimported sporadic cases of hepatitis E [6]. There are four HEV genotypes, and those in China are mainly concentrated in types I and IV [7]. So far, only one serotype of HEV has been found. HEV

Table 1: Characteristics of study subjects.

	HC group ($n = 17$)	AHE group ($n = 17$)	HEV-ALF group ($n = 17$)	P value
Age (y)	43.4 ± 14.9	45.7 ± 15.3	55.8 ± 7.3	0.018
Gender (F/M)	9/8	7/10	3/14	0.095
Pregnant woman	0	0	0	—
Fever	0	4 (23.53)	7 (41.18)	0.014
Jaundice	0	15 (88.24)	17 (100.00)	≤0.001
Nausea/vomit	0	5 (29.41)	9 (52.94)	0.002
Severity of hepatic encephalopathy	0	0	4 (23.53)	0.013
Hepatorenal syndrome	0	2 (11.76)	1 (5.88)	0.352
Ascites	0	2 (11.76)	8 (47.06)	≤0.001
IgM(+)	0	17 (100.00)	17 (100.00)	≤0.001
HEV-RNA (IU/ml)	0	34.84 (29.18-38.73)	33.44 (30.55-37.74)	≤0.001
ALT (U/l)	18 (9-31)	535 (128-834)	750 (392-1027)	≤0.001
TBIL (μmol/l)	12.4 (8.4-14.2)	58.0 (12.2-141.6)	206.6 (92.0-263.4)	≤0.001
Length of stay (day)	0	7 (5-11)	12 (8-23)	≤0.001
Mortality rate	0	0	8 (47.06)	≤0.001

The P value was for the difference among the three groups.

can cause subclinical, acute, chronic, or severe infections in people of all ages and sexes [8, 9].

A large number of studies have confirmed that humoral and cellular immunity both play an important role in viral infection [10, 11]. In previous studies, Shen et al. [12] showed that CD8 of patients with hepatitis B virus-associated acute-on-chronic liver failure (HBV-ACLF) had obvious clonal expansion in the course of disease progression. The higher the degree of CD8 T cell clone expansion, the better the prognosis of HBV-ACLF patients. Han et al. [13] showed that patients with hepatitis C virus (HCV) infection had defective T cell function, and the direct effect of antiviral therapy improved the proliferation of HCV-specific CD8+ T cells. In a study by Shin et al. [14], providing nutritional education and food supplements to human immunodeficiency virus-(HIV-) infected women significantly increased weight and CD4+ T cells, and these interventions can be integrated into HIV care programs in low-income areas. Schlosse et al. [15] inoculated C57BL/6 mice, BALB/C nude mice, Wistar rats, and European rabbits with wild boar-derived HEV-3 strain, and monitored the replication and shedding of the virus and the humoral immune response to it. Remarkably, immunosuppressive dexamethasone treatment did not increase the susceptibility of rats to HEV infection. In rabbits, recombinant HEV-3 and rat HEV capsid protein induced a protective effect against HEV-3 infection. However, the involvement of cellular immunity in the development of HEV infection is rare. Although hepatitis E is self-limited, a growing number of cases of chronic infection or HEV-related liver failure have been reported [16, 17], especially in elderly people and pregnant women. It is important to investigate further the role of cellular immunity in hepatitis E development.

Hence, we conducted a correlation study in 34 patients with HEV infection, including 17 each with acute hepatitis E (AHE) or HEV-related acute liver failure (HEV-ALF). The study was carried out in response to the changes in T helper cell immune status and viral load in patients. To the best of our knowledge, this is the first study to characterize the immune mechanism of Th cells during HEV infection.

2. Materials and Methods

2.1. Study Population. We enrolled 34 patients with HEV infection, including 17 with AHE and 17 with HEV-ALF, who were referred to the First Affiliated Hospital, College of Medicine, Zhejiang University, between 10 September 2018 and 10 March 2019. The follow-up period ended in 9 March 2020. Another 17 healthy controls (HCs) were from the Health Examination Center of the First People's Hospital of Yancheng City. The present study was performed in accordance with the Declaration of Helsinki and was approved by the Ethics Committee of the First Affiliated Hospital, Zhejiang University (approval number: 2011013).

2.2. Definition and Clinical Classification of Cases. We defined AHE and HEV-ALF according to the King's College criteria as previously described [18]: AHE: (1) positive serum anti-HEV IgM and/or a greater than twofold increase in anti-HEV IgG titer and/or detectable HEV RNA and (2) combined with clinical presentation of acute viral hepatitis (e.g., elevated liver enzymes and/or jaundice and/or nonspecific symptoms, such as sudden onset of fever, vomiting, and nausea). HEV-ALF: (1) evidence of abnormal liver synthetic function (prothrombin activity ≤ 40% or international normalized ratio ≥ 1.5), jaundice, and hepatic atrophy over a 2-week period; (2) presence of stage 2 or 3 encephalopathy complicating end-stage disease manifestations; and (3) no chronic liver disease. Hepatitis A virus, HBV, HCV, and HIV infections were excluded from all enrolled patients and HCs, and HEV infection was also excluded from the HC group.

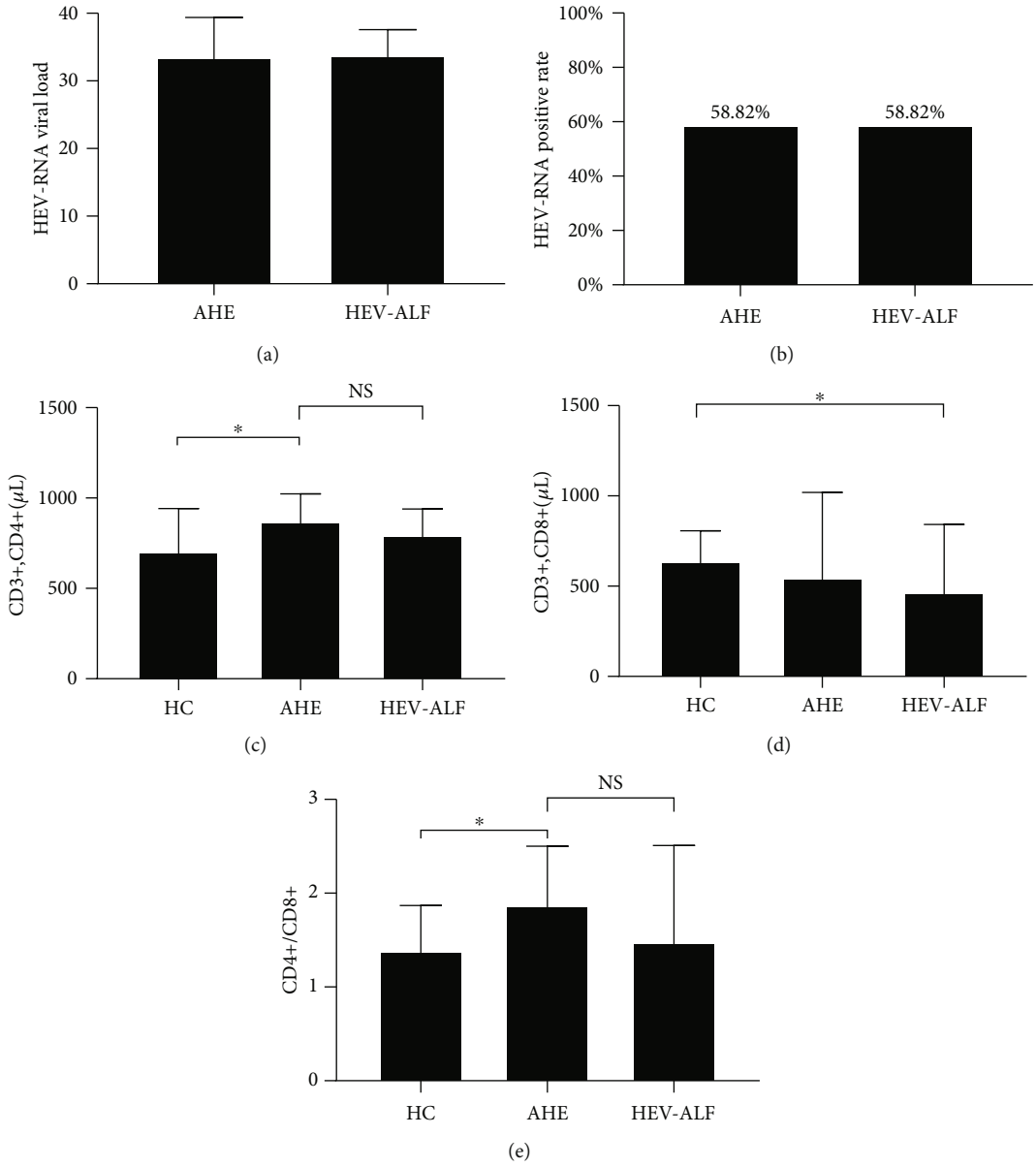

Figure 1: Viral load and lymphocyte levels in the AHE group and HEV-ALF group. (a, b) The viral load and positive rates of HEV-RNA in the AHE group and HEV-ALF group. (c–e) The CD3+CD4+, CD3+CD8+, and CD4+/CD8+ among the HC, AHE, and HEV-ALF groups.

2.3. Data Collection. We collected all the data from the patients' medical records, including clinical baseline parameters, laboratory parameters, length of stay, and prognosis. The follow-up data were collected through medical records or by direct contact with the patients or their families, with death or liver transplantation as an endpoint.

2.4. HEV-Specific Antibody Detection. Diagnosis of hepatitis E was based on the presence of anti-HEV-IgM and IgG antibodies by ELISA, and only IgM- and IgG-positive cases were included. The presence of anti-HEV IgM and IgG antibodies was detected using commercially available HEV ELISA kits (Wantai, Beijing, China). The positive samples had optical density > 1.1.

2.5. HEV RNA Detection. HEV RNA was detected by internally controlled, quantitative real-time reverse transcription polymerase chain reaction (PCR), as previously described [18]. Total RNA was extracted and purified from serum using a viral nucleic acid purification kit (Aikang, Hangzhou, China). Nested PCR amplified a 348-nucleotide fragment of the HEV open reading frame 2, and the fragment of the HEV was sequenced to identify the genotype. The viral load of each sample was estimated by quantitative PCR, using a diagnostic kit for Hepatitis E Virus RNA (Aikang), with the following conditions: 30 min at 50°C, 2 min at 94°C, and 50 cycles of 30 s at 94°C, 30 s at 55°C, and 2 min 30 s at 68°C.

2.6. Isolation of Peripheral Blood Mononuclear Cells. At 4 days after initiation of detoxification treatment, peripheral

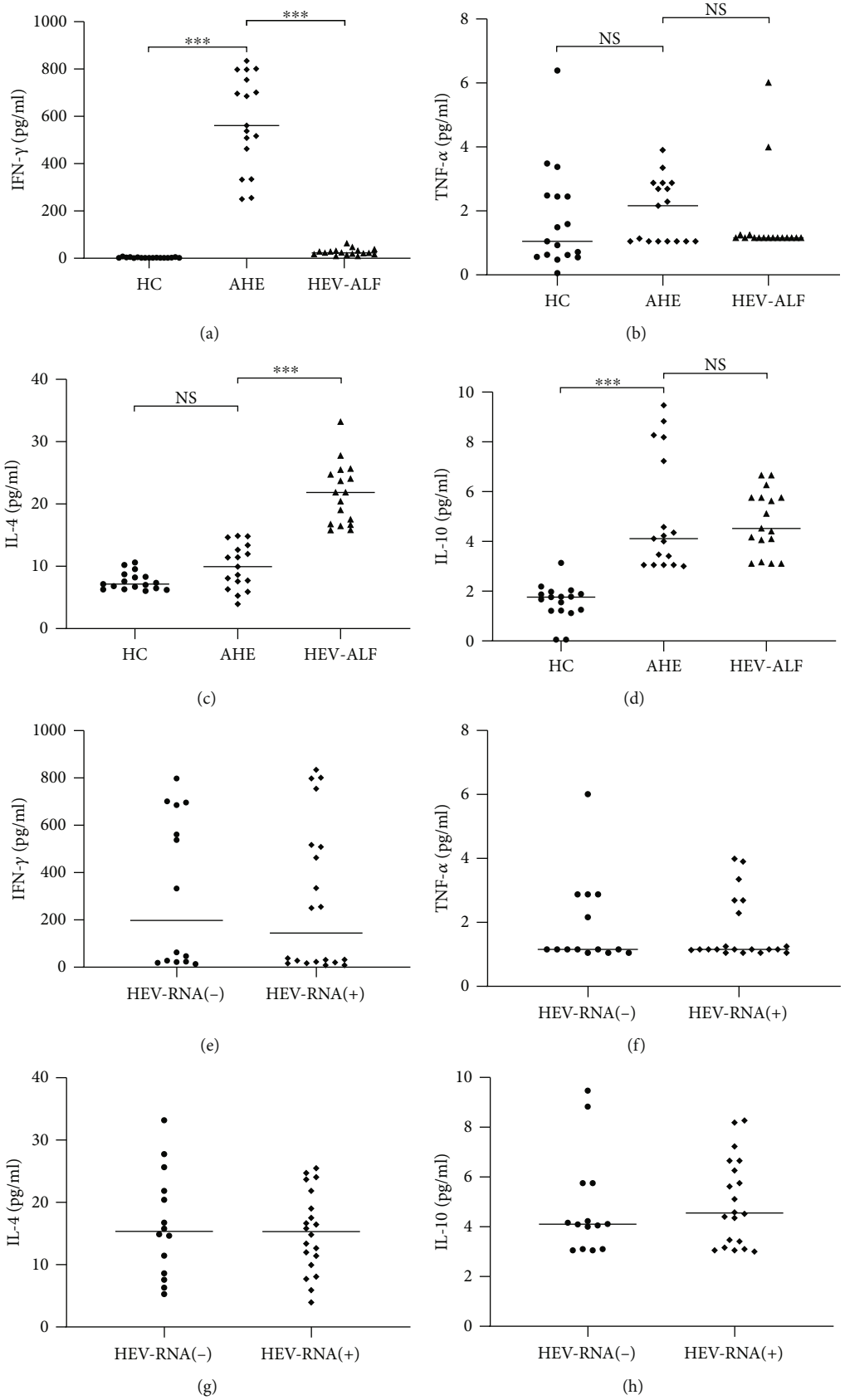

Figure 2: Compared with Th1/Th2 cytokines among the HC group, AHE group, and HEV-ALF group. (a, b) Th1 cytokines (IFN-γ and TNF-α) and (c, d) Th2 cytokines (IL-4 and IL-10) among the HC group, AHE group, and HEV-ALF group. (e, f) Th1 cytokines (IFN-γ and TNF-α) and (g, h) Th2 cytokines (IL-4 and IL-10) between the HEV RNA(+) group and HEV RNA(-) group.

Table 2: Th1/Th2 (IFN-γ/IL4) ratios in the AHE group and HEV-ALF group.

Categories	IFN-γ (pg/ml)	IL-4 (pg/ml)	IFN-γ/IL-4 ratio
HC group	2.94	7.63	0.39
AHE group	578.24	9.86	58.65
HEV-ALF group	25.78	21.57	1.20

blood samples (10 ml) were collected by venipuncture and placed in EDTA tubes. Peripheral blood mononuclear cells were isolated from fresh blood collected in K3 EDTA tubes using Ficoll density gradient centrifugation (GE Healthcare Life Sciences, Marlborough, MA, USA) for 30 min at $900 \times g$. Under a microscope (100x), cells were counted, and viability was always >95%, as determined by trypan blue exclusion (Sigma-Aldrich, St. Louis, MO, USA).

2.7. Immunophenotyping. A comprehensive panel of lymphocyte subsets was identified using multicolor flow cytometry. Peripheral blood mononuclear cells were washed in flow cytometry buffer (phosphate-buffered saline containing 1% fetal calf serum and 0.01% sodium azide) and then treated with flow cytometry blocking solution for 20 min. The cells were stained with combinations of anti-CD3, anti-CD8, anti-CD4, anti-CD56, and anti-CD16 monoclonal antibodies for 30 min at 4°C. Fluorescein isothiocyanate, phycoerythrin, and allophycocyanin were the fluorescent dyes, and all antibodies were purchased from BD Biosciences (San Jose, CA, USA). By using a FACS Canto II flow cytometer (BD Biosciences), at least 20,000 stained lymphocytes were identified by granularity and size. Data were analyzed by FlowJo version 7.2.5 software. CD3+ T cells were gated and displayed through histogram plots for other surface markers, and the percentage of cells showed the levels (mean ± SE).

2.8. Cytokine Measurements. ProcartaPlex Analyst 1.00 (eBioscience, San Diego, CA, USA) was used to determine the levels of plasma cytokines. By using a MILLIPLEX MAP Kit to analyze statistical data according to manufacturer's instructions, the value of samples was less than 0.2 pg/ml showing undetectable concentrations.

2.9. Statistical Analysis. All statistical analyses were performed with SPSS version 25 (IBM SPSS Statistics, Armonk, NY, USA). The continuous variables with normal distribution were expressed as the mean ± standard deviation and tested with independent sample t-test. The variables with nonnormal distribution were expressed as median (IQR) and tested with the nonparameter test. The Mann–Whitney U test was used for group comparisons. The classified variables were tested by the chi-square test. A value of $P < 0.05$ was considered statistically significant.

3. Results

3.1. Characteristics of Study Subjects. The characteristics of the study subjects are summarized in Table 1. There was no significant difference among the three groups ($P = 0.095$), but the average age was 55.8 ± 7.3 years in the HEV-ALF group, which was significantly higher than in the AHE (45.7 ± 15.3 years) and HC (43.4 ± 14.9 years) groups. All enrolled 34 HEV patients were genotype 4. The average hospitalization time in the HEV-ALF group was 12 (8–23) days, which was significantly longer than in the AHE group (7 (5–11) days). Nine of the 17 patients in the HEV-ALF group recovered and eight died. All 17 patients in the HEV-ALF group had jaundice, eight (47.06%) had ascites, four (23.53%) had severity of hepatic encephalopathy, and 1 (5.88%) patient had hepatorenal syndrome. There were no pregnant women in the AHE and HEV-ALF groups.

3.2. Viral Load in the AHE and HEV-ALF Groups. Both the positive rates for HEV RNA in the AHE and HEV-ALF groups were 58.82%, and there was no significant difference in the viral load between the two groups (33.56 ± 5.81 vs. 33.85 ± 3.72; $P > 0.05$) (Figures 1(a) and 1(b)).

3.3. Th Lymphocytes and Th1/Th2 Cytokines. We measured the lymphocyte levels with anti-CD3, anti-CD4, and anti-CD8 antibodies in the HC, AHE, and HEV-ALF groups. The Th lymphocyte levels (CD3+, CD4+) in the AHE and HEV-ALF groups were significantly higher than in the HC group (both $P < 0.05$), but there was no significant difference between the AHE and HEV-ALF groups ($P > 0.05$). For cytotoxic T lymphocytes (CD3+, CD8+), there was no significant difference between the AHE and HC groups ($P > 0.05$), with similar conclusion between the HEV-ALF and AHE groups ($P > 0.05$), while cytotoxic T lymphocytes (CD3+, CD8+) in the HEV-ALF group were significantly lower than those in the HC group ($P < 0.05$) (Figures 1(c)–1(e)).

Compared with Th1/T2 cytokines between the HC group and AHE group, both IFN-γ and IL-10 showed gradual upward trend from the HC group to the AHE (both $P < 0.01$), and there was no significant difference for TNF-α and IL-4 between the AHE and HC groups (both $P > 0.05$). Compared with Th1/Th2 cytokines between the AHE group and HEV-ALF group, IFN-γ showed a sharp downward trend from the AHE group to the HEV-ALF group ($P < 0.01$), while IL-4 showed gradual upward trend from the AHE group to the HEV-ALF group ($P < 0.01$), and there was no significant difference for TNF-α and IL-10 between the AHE and HEV-ALF groups (both $P > 0.05$; Figures 2(a)–2(d)).

In order to study the relationship between viral load and Th1/Th2 cytokines, we regrouped the 34 patients in the AHE and HEV-ALF groups according to whether HEV RNA was positive or not (HEV RNA(+) and HEV RNA(-) groups). There was no significant difference in Th1 (IFN-γ and TNF-α) and Th2 (IL-4 and IL-10) cytokines between the two groups (all $P > 0.05$; Figures 2(e)–2(h)).

3.4. Th1/Th2 Cytokine Production in the AHE and HEV-ALF Groups. To characterize the immune mechanism of Th cells during HEV infection, we compared Th1/Th2 (IFN-γ/IL-4) ratios among the groups (Table 2). Compared with the HC group, the AHE group showed Th1 bias (ratio = 58.65). Compared with the AHE group, there was a Th2 bias (ratio = 1.20) in the HEV-ALF group.

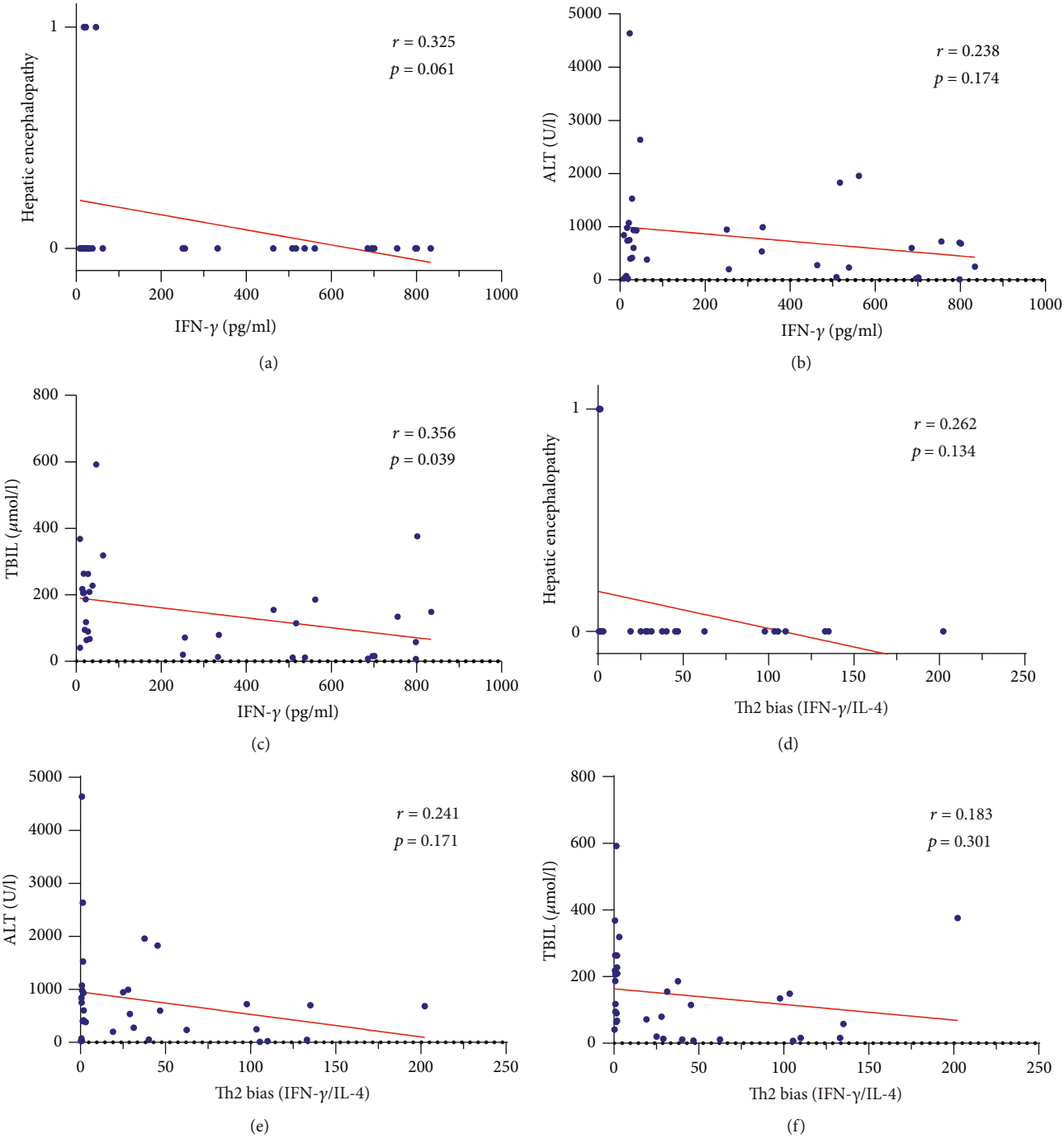

Figure 3: Correlation of ALT, TBIL, and severity of hepatic encephalopathy with Th2 bias and IFN-γ. (a–c) Correlation of severity of hepatic encephalopathy, ALT, and TBIL with the level of IFN-γ. (d–f) Correlation of severity of hepatic encephalopathy, ALT, and TBIL with Th2 bias.

3.5. Correlation of ALT and TBIL and Severity of Hepatic Encephalopathy with Th2 Bias and IFN-γ. We evaluated correlation of ALT and TBIL and severity of hepatic encephalopathy with Th2 bias and IFN-γ in the HEV-ALF group. The levels of severity of hepatic encephalopathy and ALT were weakly correlated with IFN-γ in the HEV-ALF groups ($r = 0.325$, $P = 0.061$; $r = 0.238$, $P = 0.174$; Figures 3(a) and 3(b)). The level of TBIL was strongly correlated with IFN-γ bias in the HEV-ALF group ($r = 0.356$, $P = 0.039$; Figure 3(c)). The level of ALT, severity of hepatic encephalopathy, and TBIL were weakly correlated with Th2 bias in the HEV-ALF groups ($r = 0.262$, $P = 0.134$; $r = 0.241$, $P = 0.171$; $r = 0.183$, $P = 0.301$; Figures 3(d)–3(f)).

3.6. Relationship between Th1/Th2 Cytokine Levels and Patient Outcome. We compared Th1/Th2 cytokine levels in 28 recovered patients and six patients who died. Only the level of IFN-γ in dead patients was significantly lower than

Table 3: Relationship between Th1/Th2 cytokine levels and outcome of patients.

Th1/Th2 cytokines	Recovered patients ($N = 26$)	Dead patients ($N = 8$)	P value
IFN-γ	399.03 (34.35-697.22)	25.84 (16.63-30.23)	0.006
TNF-α	1.16 (0.05-2.88)	1.16 (1.16-0.25)	0.205
IL-4	12.31 (8.48-23.78)	16.70 (15.98-18.64)	0.167
IL-10	4.23 (3.78-5.00)	5.36 (3.42-5.75)	0.393

in recovered patients (25.84 (16.63-30.23) vs. 399.03 (34.35-697.22); $P = 0.006$), while there were no significant differences for TNF-α, IL-4, and IL-10 between recovered and dead patients (all $P > 0.05$) (Table 3).

4. Discussion

The cellular immune response plays an important role in HEV infection [19, 20]. Although hepatitis E is an acute self-limited disease, chronic hepatitis E and hepatic failure caused by hepatitis E have been reported in recent years. A subset of immunosuppressed patients infected with HEV may develop chronic infection. The study by Ramdasi et al. [21] showed that HEV infection during pregnancy was highly correlated with the level of T regulatory cells and Th1 to Th2 shift. In cellular immunity, Th cells are normally in the precursor state. Under the influence of the virus, T cells differentiate and proliferate in different directions. Th1 cells mainly secrete cytokines such as IFN-γ and IL-2, which play an important role in antiviral and bacterial immune responses, while Th2 cells mainly secrete cytokines such as IL-4 and IL-10, which play a role in parasitic infection [22, 23].

In this study, we compared the changes in Th cell subsets by cell surface molecular staining. The numbers of Th lymphocyte levels (CD3+, CD4+) in the AHE group and HEV-ALF group were significantly higher than those in the HC group, but there was no significant difference between the AHE group and HEV-ALF group. Although the level of cytotoxic T lymphocytes (CD3+, CD8+) in the HEV-ALF group was significantly lower than that in the HC group, there was no significant change in the levels of Th2 cells between the AHE group and HEV-ALF group. We analyzed the changes in the levels of Th cell-related factors. The level of IFN-γ in the AHE group was significantly increased. Although IL-10 also showed a significant increase, we considered that Th1 cells were involved in HEV infection and virus clearance. It should be noted that IFN-γ decreased sharply from AHE to HEV-ALF. At the same time, this process is accompanied by increased level of IL-4. Significant Th2 bias was observed from AHE to HEV-ALF. We inferred that hepatocyte damage was aggravated due to the persistent imbalance of immune status in the body. This result is consistent with Ravi and Arankalle [24] and Majumdar et al. [25].

We compared the HEV positive rates and viral loads in the AHE and HEV-ALF groups. There was no significant difference in the HEV positive rate or viral load between the two groups, suggesting that HEV viral load was not associated with disease severity. There was no significant difference in Th1/Th2 cytokines between the HEV or HEV-ALF groups. All the above results may indicate that the HEV viral load has little effect on Th1/Th2 cytokines, but it may also be related to the positive feedback of Th1/Th2 cell proliferation on immunity. Sex and age should be excluded, and the results were verified in more samples.

Both IFN-γ and Th1 bias were negatively correlated with ALT, and severity of hepatic encephalopathy, especially for TBIL. Although HEV was cleared in many patients, ALT and bilirubin levels indicated further hepatocyte damage, and we speculate that hepatocyte damage may not be directly caused by HEV, but rather by Th2 bias caused by restraint of Th1 cells. HEV-ALF patients had a high mortality rate. Hence, we evaluated the relationship between Th1/Th2 cytokine levels and outcome of HEV-ALF patients, and only the level of IFN-γ was associated with outcome.

Cytokines are important immune messenger molecules, which are secreted in the blood, and they are affected by a variety of viruses and bacteria. The study cohort excluded interference by other infectious diseases, tumors, age, sex, and other factors. Our research also considered the effect of lifestyle, environment, and other factors. None of these could completely exclude the influence of other organs and factors, which needs to be confirmed by a large multicenter study.

In summary, HEV viral load was not associated with aggravation of AHE. The IFN-γ levels showed a gradual upward trend from the HC group to the AHE group, while it showed a sharp downward trend from the AHE group to the HEV-ALF group and the HEV-ALF patients showed significant Th2 bias. The level of IFN-γ was associated with the outcome of HEV-ALF patients. We consider that Th2 bias may be involved in the aggravation of AHE.

Abbreviations

HE: Hepatitis E
HEV: Hepatitis E virus
AHE: Acute hepatitis E
HEV-ALF: HEV-related acute liver failure
HC: Healthy controls
ELISA: Enzyme-linked immunosorbent assay
Th: Helper T cell
ALT: Alanine aminotransferase
TBIL: Total bilirubin.

Data Availability

All data relevant to the study are included in the article.

Conflicts of Interest

All the authors declare no competing interests.

Authors' Contributions

J.W. and Y.G. contributed to the study concept and design, conducted the literature search, and wrote the manuscript. F.H., A.S., and D.W. contributed to the data analysis and made the tables and figures. F.L., J.Y., and Q.P. contributed to the collection of patients' samples and medical information. B.J., X.L., and J.Y. contributed to the acquisition and analysis of data. H.C. and L.L. contributed to the study concept, obtained funding, and critically revised the manuscript. Jian Wu and Yurong Guo contributed equally to this work.

Acknowledgments

This study was supported by the National Science and Technology Major Project for Infectious Diseases (No. 2012ZX10002004).

References

[1] N. Kamar, F. Abravanel, P. Behrendt et al., "Ribavirin for hepatitis E virus infection after organ transplantation: a large European retrospective multicenter study," *Clinical Infectious Diseases*, vol. 71, no. 5, pp. 1204–1211, 2020.

[2] H. Sooryanarain and X.-J. Meng, "Hepatitis E virus: reasons for emergence in humans," *Current Opinion in Virology*, vol. 34, pp. 10–17, 2019.

[3] M. Li, S. Li, Q. He et al., "Hepatitis E-related adverse pregnancy outcomes and their prevention by hepatitis E vaccine in a rabbit model," *Emerging Microbes & Infections*, vol. 8, no. 1, pp. 1066–1075, 2019.

[4] H. Fenaux, M. Chassaing, S. Berger, C. Gantzer, I. Bertrand, and E. Schvoerer, "Transmission of hepatitis E virus by water: an issue still pending in industrialized countries," *Water Research*, vol. 151, pp. 144–157, 2019.

[5] J. Wu, N. Guo, L. Zhu et al., "Seroprevalence of AIH-related autoantibodies in patients with acute hepatitis E viral infection: a prospective case-control study in China," *Emerg Microbes Infect*, vol. 9, no. 1, pp. 332–340, 2020.

[6] V. Suin, S. E. Klamer, V. Hutse et al., "Epidemiology and genotype 3 subtype dynamics of hepatitis E virus in Belgium, 2010 to 2017,," *Euro Surveillance*, vol. 24, no. 10, 2019.

[7] S. Sridhar, V. C. C. Cheng, S.-C. Wong et al., "Donor-derived genotype 4 hepatitis E virus infection, Hong Kong, China, 2018," *Emerging Infectious Diseases*, vol. 25, no. 3, pp. 425–433, 2019.

[8] R. Shirazi, P. Pozzi, M. Wax et al., "Hepatitis E in pigs in Israel: seroprevalence, molecular characterisation and potential impact on humans," *Euro Surveillance*, vol. 23, no. 49, 2018.

[9] S. Sridhar, C. C. Y. Yip, S. Wu et al., "Rat hepatitis E virus as cause of persistent hepatitis after liver transplant," *Emerging Infectious Diseases*, vol. 24, no. 12, pp. 2241–2250, 2018.

[10] K.-H. Ng, S. L. Zhang, H. C. Tan et al., "Persistent dengue infection in an immunosuppressed patient reveals the roles of humoral and cellular immune responses in virus clearance," *Cell Host & Microbe*, vol. 26, no. 5, pp. 601–605.e3, 2019.

[11] E. Gonçalves, O. Bonduelle, A. Soria et al., "Innate gene signature distinguishes humoral versus cytotoxic responses to influenza vaccination," *The Journal of Clinical Investigation*, vol. 129, no. 5, pp. 1960–1971, 2019.

[12] G. Shen, S. Sun, J. Huang et al., "Dynamic changes of T cell receptor repertoires in patients with hepatitis B virus-related acute-on-chronic liver failure," *Hepatology International*, vol. 14, no. 1, pp. 47–56, 2020.

[13] J. W. Han, P. S. Sung, K. H. Kim et al., "Dynamic changes in ex vivo T-cell function after viral clearance in chronic HCV infection," *The Journal of Infectious Diseases*, vol. 220, no. 8, pp. 1290–1301, 2019.

[14] S. S. Shin, V. A. Satyanarayana, M. L. Ekstrand et al., "The effect of community-based nutritional interventions on children of women living with Human Immunodeficiency Virus in rural India: a 2 × 2 factorial intervention trial," *Clinical Infectious Diseases*, vol. 71, no. 6, pp. 1539–1546, 2020.

[15] J. Schlosser, L. Dähnert, P. Dremsek et al., "Different outcomes of experimental hepatitis E virus infection in diverse mouse strains, Wistar rats, and rabbits," *Viruses*, vol. 11, no. 1, p. 1, 2019.

[16] S. J. Wallace, R. Swann, M. Donnelly et al., "Mortality and morbidity of locally acquired hepatitis E in the national Scottish cohort: a multicentre retrospective study," *Alimentary Pharmacology & Therapeutics*, vol. 51, no. 10, pp. 974–986, 2020.

[17] Y. Wang, H. Liu, S. Liu et al., "Incidence, predictors and prognosis of genotype 4 hepatitis E related liver failure: a tertiary nested case-control study," *Liver International*, vol. 39, no. 12, pp. 2291–2300, 2019.

[18] J. Wu, N. Guo, X. Zhang et al., "HEV-LFS: a novel scoring model for patients with hepatitis E virus-related liver failure," *Journal of Viral Hepatitis*, vol. 26, no. 11, pp. 1334–1343, 2019.

[19] M. R. Edwards, M. Hoad, S. Tsimbalyuk et al., "Henipavirus W proteins interact with 14-3-3 to modulate host gene expression," *Journal of Virology*, vol. 94, no. 14, 2020.

[20] W. Wang, Y. Wang, C. Qu et al., "The RNA genome of hepatitis E virus robustly triggers an antiviral interferon response," *Hepatology*, vol. 67, no. 6, pp. 2096–2112, 2018.

[21] A. Y. Ramdasi, R. P. Arya, and V. A. Arankalle, "Effect of pregnancy on anti-HEV antibody titres, plasma cytokines and the corresponding gene expression levels in the PBMCs of patients presenting with self-recovering clinical and subclinical hepatitis E," *PLoS One*, vol. 9, no. 8, article e103257, 2014.

[22] N. Alvarez, W. Aguilar-Jimenez, and M. T. Rugeles, "The potential protective role of vitamin D supplementation on HIV-1 infection," *Frontiers in Immunology*, vol. 10, 2019.

[23] Z. Zhang, X. Zhang, M. J. Carr et al., "A neonatal murine model of coxsackievirus A4 infection for evaluation of vaccines and antiviral drugs," *Emerging Microbes & Infections*, vol. 8, no. 1, pp. 1445–1455, 2019.

[24] R. P. Arya and V. A. Arankalle, "Phenotypic analysis of monocytes and CD4+ T cells in hepatitis E patients with or without pregnancy," *Human Immunology*, vol. 80, no. 10, pp. 855–862, 2019.

[25] M. Majumdar, R. K. Ratho, Y. Chawla, and M. P. Singh, "Role of TLR gene expression and cytokine profiling in the immunopathogenesis of viral hepatitis E," *Journal of Clinical Virology*, vol. 73, pp. 8–13, 2015.

Hindawi
Journal of Immunology Research
Volume 2020, Article ID 5679254, 6 pages
https://doi.org/10.1155/2020/5679254

Review Article

The Function of T Follicular Helper Cells in the Autoimmune Liver Diseases

Lin Li,[1] **Panyang Xu**,[1] **Qi Zhou**,[2] **and Jiancheng Xu**[1]

[1]*Department of Laboratory Medicine, First Hospital of Jilin University, Changchun 130021, China*
[2]*Department of Pediatrics, First Hospital of Jilin University, Changchun 130021, China*

Correspondence should be addressed to Jiancheng Xu; jianchengxu@yeah.net

Received 3 August 2020; Revised 29 October 2020; Accepted 31 October 2020; Published 19 November 2020

Academic Editor: Dawei Cui

Copyright © 2020 Lin Li et al. This is an open access article distributed under the Creative Commons Attribution License, which permits unrestricted use, distribution, and reproduction in any medium, provided the original work is properly cited.

T follicular helper (TFH) cells are recognized as a subtype of T cells that are involved in the germinal center formation and B cell development. When dysregulated, TFH cells may represent an important mechanism that contributes to a heightened humoral response and autoantibody production in autoimmune liver diseases (AILDs). TFH cells participate in the immune response associated with AILDs by expressing surface receptors such as programmed cell death protein-1, C-X-C motif chemokine receptor 5, and inducible T cell costimulators, as well as cytokines such as interleukin-21. TFH cells also downregulate chemokine (C-C motif) receptor 7 and promote the dysregulation of the T follicular regulatory/TFH axis. This review highlights the importance of TFH cells in AILDs.

1. Introduction

Autoimmune liver disease is a group of chronic hepatobiliary inflammatory diseases mediated by autoimmune response, mainly consist of autoimmune hepatitis (AIH), primary biliary cholangitis (PBC), primary sclerosing cholangitis (PSC), and IgG4-related sclerosing cholangitis (IgG4-SC) [1]. T follicular helper (TFH) cells are special subtypes of $CD4^+$ T cells that have evolved appropriate mechanisms to induce B cell activation and differentiation into immunoglobulin (Ig-) secreting cells (plasma cells) [2]. In secondary lymphoid tissues, TFH cells have an important influence on the formation of the germinal center (GC) and the development of T cell-dependent B cell responses [3]. One distinctive feature of TFH is that they have the high surface expression of C-X-C motif chemokine receptor 5 (CXCR5), which can induce TFH cells to transfer to the follicular area of B cells expressing CXCL13 (the ligand of CXCR5). TFH cells can also regulate humoral immune response through secretion and expression of various cytokines, including the signal transcription factor B cell lymphoma 6 (BCL-6), programmed cell death protein-1 (PD-1), CD40 ligand, and the cytokine interleukins IL-21, IL-10, and IL-6 [4–6]. Circulating TFH cells can be classified into three different subsets (TFH17, TFH1, and TFH2) in view of the subtype cytokine profiles and effectiveness in supporting B cells [7] (see Figure 1). We also introduce a T cell subtype that is closely related to TFH cells: T follicular regulatory (TFR) cells, which are in the germinal center and have the same phenotypic traits as TFH cells. The differentiation of TFR cells is an extremely complex process. The differentiation of TFR cells was initiated by dendritic cells; development and expansion required the help of B cells, costimulatory signals, such as CD28 and ICOS, and the expression of transcription factors such as BCL-6 [8–12].TFR cells play a negative regulatory role in germinal center reaction. TFR cells may inhibit plasma cells by inhibiting the GC reaction. When plasma cells migrate from secondary lymphoid organs to bone marrow, TFR cells will lose the inhibitory effect on plasma cells [13]. More evidence indicated that the imbalance between circulating TFR and TFH cells might cause the immune system's tolerance disorders and the production of abnormal autoantibodies. These pathogenic mechanisms are considered a crucial development of autoimmune responses [14]. This article will investigate the

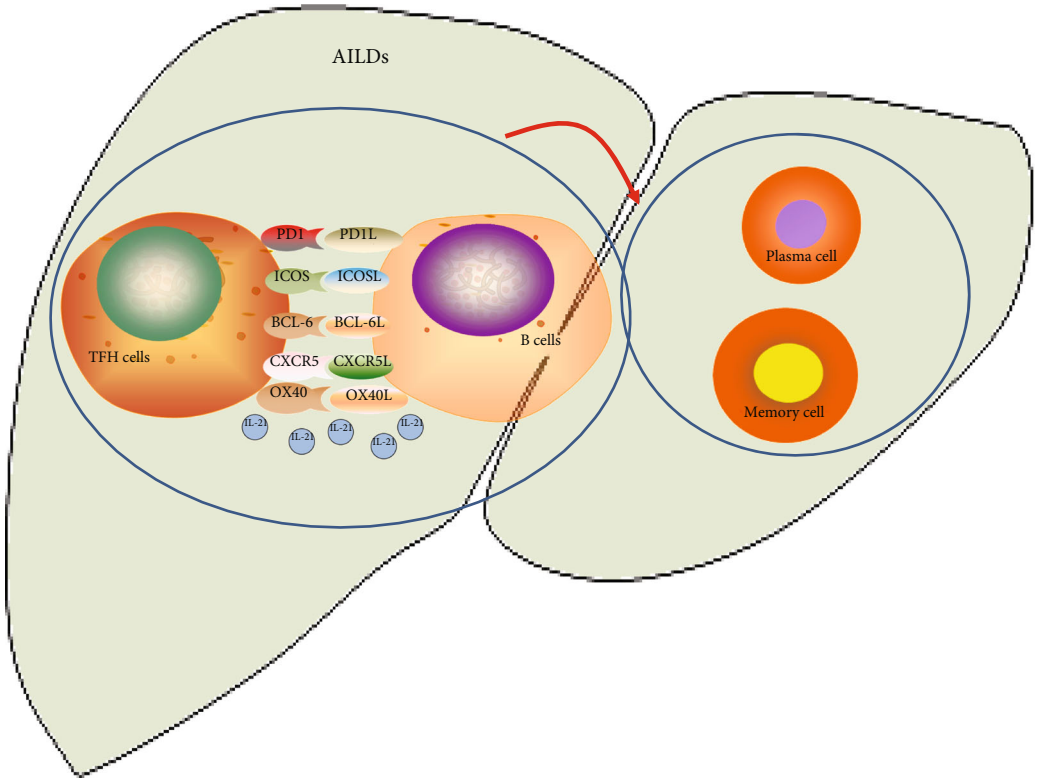

Figure 1: AILDs: autoimmune liver diseases; PD-1: programmed cell death protein-1; CXCR5: CXC chemokine receptor 5; ICOS: inducible T cell costimulator; IL-21: cytokine interleukin- (IL-) 21; BCL-6: B cell lymphoma 6; OX40: tumor necrosis factor receptor. TFH plays a key role in assisting B cells. Autoimmune diseases are characterized by excessive activation of B cells, leading to the production of autoantibodies and attacking their normal tissues. This suggests that TFH cells may have an important influence on the pathogenesis of autoimmune diseases.

contribution of TFH cells to the disease pathogenesis in AILDs.

2. Autoimmune Hepatitis (AIH)

AIH is a chronic inflammatory liver disease induced by decreased immunological tolerance to liver autoantigens. The clinical features of AIH include the detection of autoantibodies via liver histology, hyperglobulinemia, and lymphocytic plasma infiltration of interface hepatitis [15]. In a prospective population-based study, Lamba et al. found that the incidence of AIH in New Zealand tended to increase annually [16]. However, the reason for the change in the incidence of AIH has not yet been discovered. Evidence in recent years has shown that B cells have an important influence on autoimmune diseases. During the pathogenesis and development of AIH autoimmunity, TFH cells provided the B cells in the GC area with a key signal to produce autoantibodies [17]. Over expanded TFH cells could lead to overreactions of the GC, such as the disordered proliferation of self-reactive B cells, excessive differentiation of long-lived plasma cells, and the mass secretion of high-affinity pathogenic autoantibodies. The pathological enrichment of TFH cells could be critical for the survival of homologous self-reactive B cells and the tolerance check of escaping the GC area [3]. These observations indicated the contribution of TFH cells in autoimmune hepatitis, and TFH cells are mainly affected by three substances: interleukin-21, programmed cell death protein-1, and T follicular regulatory cells.

2.1. Interleukin-21 (IL-21). TFH cells express high levels of IL-21 that influence B cell differentiation and antibody production [3]. IL-21 belongs to the type I cytokine family; type I cytokines have massive effects on the immune system, including B cell activation in the GC of the secondary lymphoid organs, plasma cell differentiation, and immunoglobulin production [2, 18]. Although the data on IL-21-induced direct antibody-mediated cytotoxicity is limited, the circumstantial evidence shows that IL-21 may mediate the production of autoantibodies and has an important influence on the pathogenesis of AIH. Ma et al. found that patients with new-onset AIH had higher serum IL-21 levels, which was accompanied by plasma cells, activated B cells, TFH cells, and serum immunoglobulins [19]. Subsequently, researchers explored whether TFH cells participated in AIH autoimmunity through the elevated secretion of IL-21. Using coculture experiments, Morita et al. reported that TFH2 and TFH17, but not TFH1, induced naive B cells to produce immunoglobulin by secreting IL-21 [7]. Meanwhile, in the mouse model of AIH, blocking IL-21 secretion effectively inhibited the production of TFH cells and prevented the development of AIH in the mice [20, 21]. Abe et al. found that serum levels of IL-21 were prominently higher among AIH patients contrasted to nonsevere liver disease patients; this increase was positively correlated with necrotizing inflammatory activity

[18]. Serum IL-21 levels are expected to be an indicator for predicting the evolution of necrotizing inflammatory activity in liver histology, providing important evidences regarding AIH diagnosis, and identifying necessary therapeutic targets [18]. In summary, researchers found that TFH cells were involved in the pathogenesis of AIH by secreting IL-21, and the serum concentration of IL-21 in severe AIH patients is significantly increased through animal and human studies. These studies indirectly prove that TFH cells involve in the pathogenesis of AIH by secreting IL-21 cytokines, which has severity with the disease.

2.2. Programmed Cell Death Protein-1 (PD-1). The TFH cell surface receptor PD-1 inhibits the adaptive immune response by binding to its ligand, programmed cell death ligand-(PDL-) 1, or PDL-2 [22]. The role of chemokine (C-C motif) receptor 7 (CCR7) is the opposite of PD-1 and promotes a variety of adaptive immune functions [23]. The researchers found that there were $CCR7^{-}PD\text{-}1^{+}$ TFH cell subtypes in the peripheral blood of AIH patients. Quantifying $CCR7^{-}PD\text{-}1^{+}$ TFH cells in the peripheral blood of AIH patients might be used to the auxiliary diagnosis of AIH, which thus also confirming that TFH cells participated in the pathogenesis of AIH [24, 25].

The chemokine receptor CXCR5, the nuclear transcriptional repressor BCL-6 [12], and the surface receptor-inducible T cell costimulator (ICOS) [3] may also control TFH cell transcription. However, whether TFH cells participate in the pathogenesis of AIH through CXCR5 and ICOS has not yet been confirmed, and more basic researches are needed to support this hypothesis.

2.3. T Follicular Regulatory (TFR) Cells. The dysregulation of TFR and TFH cells is closely related to the pathological mechanisms of autoimmune diseases. Liang et al. closely followed the relationship between the dysregulation of TFR and TFH cells and the pathogenesis of AIH. Studies found that in AIH patients, TFR cell counts were negatively related to TFH cell numbers and IL-21 levels but positively related to the inhibitory factors IL-10 and TGF-β1. Collectively, the decrease of CTLA-4 and TFR-related factor IL-10/TGF-β1 and the increase of PD-1/ICOS in AIH patients lead to the decrease of TFR cells, while the increase of TFH-related factor IL-21 increases the number of TFH cells and the decrease of TFR/TFH ratio, thus promoting the differentiation of B cells and the production of immunoglobulin.

3. Primary Biliary Cholangitis (PBC)

PBC, which is once described as primary biliary cirrhosis, is an autoimmune disease that occurs more frequently among women. PBC is characterized by chronic cholestasis, which leads to the injury of small hepatic bile ducts, inflammation, and eventually progressive fibrosis [15]. Because of genetic risk factors and decreased environmental tolerance, PBC is often correlated with autoimmune diseases (such as chronic thyroiditis and Sjogren's syndrome). Liver transplantation is often required because of liver failure; however, PBS often reoccurs after liver transplantation [26]. Studies have shown that the pathogenesis of PBC is closely related to TFH cells. The following sections will focus on the relationships between TFH cells and PBC. Similarly, in PBS, TFH cell count was associated with TFR cells. Besides, CXCR5 and other cytokines affected TFH cell levels.

3.1. CXCR5. CXCR5 is a TFH-related factor that is also considered a risk factor for PBC [27]. Circulating $CD4^{+}CXCR5^{+}$ TFH cells are a subtype of memory TFH cells that may exist in the blood for a long time [7]. When antigenic stimulation occurs, these memory TFH cell subsets can quickly transform into TFH cells to promote the GC response [28]. When the production of circulating TFH cells is out of control, it reflects GC imbalance and causes an abnormal elevation in the number of autoreactive B cells as well as the production of pathogenic autoantibodies. At this time, clinical symptoms often appear. When the immune response continues, irreversible tissue damage will eventually occur [29]. Wang et al. detected circulating of $CD4^{+}CXCR5^{+}$ TFH cells in the peripheral blood of PBC patients [6]. They also found that elevated numbers of TFH in PBC patients were correlated with B cell activation, disease severity, and response to ursodeoxycholic acid treatment [6]. The above reports give us a deeper understanding of the immune pathogenesis of PBC. $CD4^{+}CXCR5^{+}$ TFH cells may become a marker for monitoring the effect of treatment in PBC patients. However, it is still unknown why high numbers of $CD4^{+}CXCR5^{+}$ TFH cells are positively correlated to the disease severity in PBC patients [30]. Researches are still needed to be explored for its fundamental mechanism.

3.2. Other Cytokines. Wang et al. demonstrated that elevated numbers of circulating ICOS+ TFH, IL-21+ TFH [31], and PD-1+ TFH2 cells [32] might be found in PBC patients. Adam et al. also confirmed that PBC patients had significantly higher numbers of CXCR5+PD-1+ and CD4+ TFH cells [33]. Additionally, the activation marker OX40 and inducible T cell costimulatory factors were highly expressed in PBC and were related to the titers of antimitochondrial antibody M2 and IgM. When PBC patients developed cirrhosis, its serological level was detected that there was a significant upward trend [33].

Significant increases in concentrations of OX40, CXCR5, PD-1, ICOS, and IL-21 have been observed in PBC patients. These previous studies showed that TFH cells were closely associated with the pathogenesis of PBC and provided an important tool for the diagnosis and treatment of PBC. However, these molecular mechanisms are not yet fully understood; more researches are still needed.

3.3. TFR Cells. The roles of dysregulated TFR and TFH cells in the immune systems of PBC patients are controversial. Zheng et al. pointed out that the serum TFR/TFH ratio of PBC patients was remarkably lower than that of the normal control group [34]. This study also indirectly proved that the dysregulation of the circulating TFR/TFH ratio was involved in the pathogenesis of PBC. Therefore, this ratio might be used as a serological marker for developing new therapies and evaluated therapeutic efficacy in PBC patients

Table 1: Influence of follicular helper T cells (TFH) in human and mouse AILDs.

Disease	ICOS	IL-21	PD-1	CXCR5	BCL-6	OX40	TFR/TFH ratio	References	
								Mouse	Human
AIH	-	Pathogenic	Pathogenic	-	-	-	Pathogenic	[20, 21]	[19] [7] [18] [24, 25] [17]
PBC	Pathogenic	Pathogenic	Pathogenic	-	-	Pathogenic	Controversial	-	[6] [31] [32] [33] [34]
PSC	-	-	Controversial	Controversial	-	-	-	-	[33]
IgG4-SC	-	-	Pathogenic	-	-	-	-	-	[32]

AILDs: autoimmune liver diseases; AIH: autoimmune hepatitis; PBC: primary biliary cholangitis; PSC: primary sclerosing cholangitis; IgG4-SC: IgG4-related sclerosing cholangitis; PD-1: programmed cell death protein-1; CXCR5: CXC chemokine receptor 5; ICOS: inducible T cell costimulator; IL-21: cytokine interleukin- (IL-) 21; BCL-6: B cell lymphoma 6; OX40: tumor necrosis factor receptor; TFR: T follicular regulatory.

[34]. However, Adam et al. found that although PBC patients showed a higher count of TFR cells, the TFH/TFR ratio was not remarkably different from that of healthy people [33]. Therefore, more researches are required to confirm whether there is a significant change in the circulating TFR/TFH ratio in PBC.

4. Primary Sclerosing Cholangitis (PSC)

PSC is an uncommon illness whose distinguishing features are multifocal bile duct strictures and progressive liver disease [35]. There are no clinical manifestations during the disease; rather, the pathophysiological mechanism manifests as anterior cholestasis. Subsequently, PSC will develop progressive biliary strictures, which lead to recurrent cholangitis, biliary cirrhosis, and end-stage liver disease [36]. Therapy will not slow the disease progression of this disease. Many patients require liver transplantation, after which there is a risk of recurring disease [36]. Although significant progress has been made in defining the immunological features related to the deficiency of tolerance, there is little information on the biological effects of biliary injury [26]. Furthermore, the pathogenesis of PSC has not been precisely defined. Perinuclear antineutrophil cytoplasmic antibodies may be detected in most PSC patients, which suggest that its pathogenesis may be related to immune disorders. However, various studies indicated that the pathogenesis of PSC did not support its classification as an autoimmune disease. For example, PSC patients had male dominance, and lack of clear autoantigens and immunosuppressants did not affect the disease process [26]. By detecting $CXCR5^{+}PD\text{-}1^{+}CD4^{+}$ TFH cells in patients, Adam et al. found that TFH cells affected the occurrence of PSC to a lesser extent, which supported the above hypothesis [33]. However, there are numerous debates over whether PSC can be regarded as a true autoimmune disease.

5. IgG4-Related Sclerosing Cholangitis (IgG4-SC)

IgG4-SC, the biliary manifestation of the systemic fibroinflammatory condition, is featured by the enrichment of IgG4-positive plasma cells and CD4+ T cells in associated tissues [37]. IgG4-SC has been gradually valued because of its high rate of organ dysfunction and failure, high rate of recurrence, and high mortality rate [38]. Although serum concentrations of IgG4 and IgE are elevated in mass PSC patients, they are not enough to be diagnosed and monitored with disease activity [39, 40]. Studies have found that PD-1 may be associated with the proliferation and activation of TFH cells, leading to IgG4-SC.

5.1. PD-1. PD-1 is a milestone of cell activation in TFH cells, which is important to the selection of B cells and survival in GCs, along with the transformation of B cells into antibody-secreting cells [7]. Cargill et al. found that circulating and tissue-activated TFH cells were expanded in IgG4-SC, correlated with disease activity, and drove the class switch and proliferation of IgG4-committed B cells. $PD\text{-}1^{+}$ TFH2 cells are possible to be a marker of activating disease and a latent target for immunotherapy [32].

Previous studies paid attention to the immune mechanism of the disease found that TFH cells were closely correlated with the immune mechanism of IgG4-SC. However, new literature is still needed to support this argument.

6. Conclusion

TFH cells have an important influence on the pathogenesis of AILDs, especially in AIH, PBC, and IgG4-SC. Whether TFH cells participated in the pathogenesis of PSC remains to be discussed (Table 1). In summary, the literature on the contribution of TFH cells in the pathogenesis of AILDS is still in its infancy. The immune system is a complex and well-regulated network. Furthermore, the discovery and correct understanding of TFH cells provide insight into the pathogenesis of autoimmune diseases. TFH cells may be used as a new diagnostic marker and treatment point in the clinic, thus bringing new hope to the treatment of AILDs.

Conflicts of Interest

The authors declare that there is no conflict of interest regarding the publication of this paper.

Acknowledgments

This work was supported by grants from Jilin Science and Technology Development Program (no. 20170623092TC-09, to Dr. Jiancheng Xu; no. 20190304110YY to Dr.

Jiancheng Xu) and The First Hospital Translational Funding for Scientific &Technological Achievements (no. JDYYZH-1902002 to Dr. Jiancheng Xu).

References

[1] S. P. Liu, Z. H. Bian, Z. B. Zhao et al., "Animal models of autoimmune liver diseases: a comprehensive review," *Clinical Reviews in Allergy and Immunology*, vol. 58, no. 2, pp. 252–271, 2020.

[2] C. S. Ma and E. K. Deenick, "Human T follicular helper (Tfh) cells and disease," *Immunology and Cell Biology*, vol. 92, no. 1, pp. 64–71, 2014.

[3] D. Mesquita Jr., W. M. Cruvinel, L. S. Resende et al., "Follicular helper T cell in immunity and autoimmunity," *Brazilian Journal of Medical and Biological Research*, vol. 49, no. 5, article e5209, 2016.

[4] D. Breitfeld, L. Ohl, E. Kremmer et al., "Follicular B helper T cells express CXC chemokine receptor 5, localize to B cell follicles, and support immunoglobulin production," *Journal of Experimental Medicine*, vol. 192, no. 11, pp. 1545–1552, 2000.

[5] M. D. Gunn, V. N. Ngo, K. M. Ansel, E. H. Ekland, J. G. Cyster, and L. T. Williams, "A B-cell-homing chemokine made in lymphoid follicles activates Burkitt's lymphoma receptor-1," *Nature*, vol. 391, no. 6669, pp. 799–803, 1998.

[6] L. Wang, Y. Sun, Z. Zhang et al., "CXCR5+ CD4+ T follicular helper cells participate in the pathogenesis of primary biliary cirrhosis," *Hepatology*, vol. 61, no. 2, pp. 627–638, 2015.

[7] R. Morita, N. Schmitt, S. E. Bentebibel et al., "Human blood CXCR5(+)CD4(+) T cells are counterparts of T follicular cells and contain specific subsets that differentially support antibody secretion," *Immunity*, vol. 34, no. 1, pp. 108–121, 2011.

[8] P. T. Sage, L. M. Francisco, C. V. Carman, and A. H. Sharpe, "The receptor PD-1 controls follicular regulatory T cells in the lymph nodes and blood," *Nature Immunology*, vol. 14, no. 2, pp. 152–161, 2013.

[9] Y. Chung, S. Tanaka, F. Chu et al., "Follicular regulatory T cells expressing Foxp3 and Bcl-6 suppress germinal center reactions," *Nature Medicine*, vol. 17, no. 8, pp. 983–988, 2011.

[10] M. Y. Gerner, P. Torabi-Parizi, and R. N. Germain, "Strategically localized dendritic cells promote rapid T cell responses to lymph-borne particulate antigens," *Immunity*, vol. 42, no. 1, pp. 172–185, 2015.

[11] P. T. Sage, D. Alvarez, J. Godec, U. H. von Andrian, and A. H. Sharpe, "Circulating T follicular regulatory and helper cells have memory-like properties," *Journal of Clinical Investigation*, vol. 124, no. 12, pp. 5191–5204, 2014.

[12] Y. Zhu, L. Zou, and Y. C. Liu, "T follicular helper cells, T follicular regulatory cells and autoimmunity," *International Immunology*, vol. 28, no. 4, pp. 173–179, 2016.

[13] M. J. Shlomchik and F. Weisel, "Germinal center selection and the development of memory B and plasma cells," *Immunological Reviews*, vol. 247, no. 1, pp. 52–63, 2012.

[14] M. A. Linterman, W. Pierson, S. K. Lee et al., "Foxp3+ follicular regulatory T cells control the germinal center response," *Nature Medicine*, vol. 17, no. 8, pp. 975–982, 2011.

[15] S. A. Taylor, D. N. Assis, and C. L. Mack, "The contribution of B cells in autoimmune liver diseases," *Seminars in Liver Disease*, vol. 39, no. 4, pp. 422–431, 2019.

[16] M. Lamba, N. J. Hieng, and C. Stedman, "Trends in incidence of autoimmune liver diseases and increasing incidence of autoimmune hepatitis," *Clinical Gastroenterology and Hepatology*, 2020.

[17] M. Liang, Z. Liwen, D. Juan, Z. Yun, D. Yanbo, and C. Jianping, "Dysregulated TFR and TFH cells correlate with B-cell differentiation and antibody production in autoimmune hepatitis," *Journal of Cellular and Molecular Medicine*, vol. 24, no. 7, pp. 3948–3957, 2020.

[18] K. Abe, A. Takahashi, H. Imaizumi et al., "Interleukin-21 plays a critical role in the pathogenesis and severity of type I autoimmune hepatitis," *Springerplus*, vol. 5, no. 1, p. 777, 2016.

[19] L. Ma, J. Qin, H. Ji, P. Zhao, and Y. Jiang, "Tfh and plasma cells are correlated with hypergammaglobulinaemia in patients with autoimmune hepatitis," *Liver International*, vol. 34, no. 3, pp. 405–415, 2014.

[20] N. Aoki, M. Kido, S. Iwamoto et al., "Dysregulated generation of follicular helper T cells in the spleen triggers fatal autoimmune hepatitis in mice," *Gastroenterology*, vol. 140, no. 4, pp. 1322–1333.e5, 2011.

[21] L. Ma, L. W. Zhang, Y. Zhuang, Y. B. Ding, and J. P. Chen, "Exploration the significance of Tfh and related molecules on C57BL/6 mice model of experimental autoimmune hepatitis," *Journal of Microbiology, Immunology and Infection*, 2019.

[22] G. Mallett, A. Laurence, and S. Amarnath, "Programmed cell death-1 receptor (PD-1)-mediated regulation of innate lymphoid cells," *International Journal of Molecular Sciences*, vol. 20, no. 11, p. 2836, 2019.

[23] I. Comerford, Y. Harata-Lee, M. D. Bunting, C. Gregor, E. E. Kara, and S. R. McColl, "A myriad of functions and complex regulation of the CCR7/CCL19/CCL21 chemokine axis in the adaptive immune system," *Cytokine & Growth Factor Reviews*, vol. 24, no. 3, pp. 269–283, 2013.

[24] N. Kimura, S. Yamagiwa, T. Sugano et al., "Possible involvement of chemokine C-C receptor 7(-) programmed cell death-1(+) follicular helper T-cell subset in the pathogenesis of autoimmune hepatitis," *Journal of Gastroenterology and Hepatology*, vol. 33, no. 1, pp. 298–306, 2018.

[25] N. Kimura, S. Yamagiwa, T. Sugano et al., "Usefulness of chemokine C-C receptor 7−/programmed cell death-1+follicular helper T cell subset frequencies in the diagnosis of autoimmune hepatitis," *Hepatology Research*, vol. 49, no. 9, pp. 1026–1033, 2019.

[26] E. J. Carey, A. H. Ali, and K. D. Lindor, "Primary biliary cirrhosis," *Lancet*, vol. 386, no. 10003, pp. 1565–1575, 2015.

[27] G. F. Mells, J. A. Floyd, K. I. Morley et al., "Genome-wide association study identifies 12 new susceptibility loci for primary biliary cirrhosis," *Nature Genetics*, vol. 43, no. 4, pp. 329–332, 2011.

[28] G. Papp, K. Szabo, Z. Szekanecz, and M. Zeher, "Follicular helper T cells in autoimmune diseases," *Rheumatology (Oxford)*, vol. 53, no. 7, pp. 1159-1160, 2014.

[29] N. Simpson, P. A. Gatenby, A. Wilson et al., "Expansion of circulating T cells resembling follicular helper T cells is a fixed phenotype that identifies a subset of severe systemic lupus erythematosus," *Arthritis and Rheumatism*, vol. 62, no. 1, pp. 234–244, 2010.

[30] Z. Q. Zhou, D. N. Tong, J. Guan et al., "Circulating follicular helper T cells presented distinctively different responses toward bacterial antigens in primary biliary cholangitis," *International Immunopharmacology*, vol. 51, pp. 76–81, 2017.

[31] L. Wang, X. Sun, J. Qiu et al., "Increased numbers of circulating ICOS(+) follicular helper T and CD38(+) plasma cells in

patients with newly diagnosed primary biliary cirrhosis," *Digestive Diseases and Sciences*, vol. 60, no. 2, pp. 405–413, 2015.

[32] T. Cargill, M. Makuch, R. Sadler et al., "Activated T-follicular helper 2 cells are associated with disease activity in IgG4-related sclerosing cholangitis and pancreatitis," *Clinical and Translational Gastroenterology*, vol. 10, no. 4, p. e00020, 2019.

[33] L. Adam, K. Zoldan, M. Hofmann et al., "Follicular T helper cell signatures in primary biliary cholangitis and primary sclerosing cholangitis," *Hepatology Communications*, vol. 2, no. 9, pp. 1051–1063, 2018.

[34] J. Zheng, T. Wang, L. Zhang, and L. Cui, "Dysregulation of circulating Tfr/Tfh ratio in primary biliary cholangitis," *Scandinavian Journal of Immunology*, vol. 86, no. 6, pp. 452–461, 2017.

[35] T. H. Karlsen, T. Folseraas, D. Thorburn, and M. Vesterhus, "Primary sclerosing cholangitis - a comprehensive review," *Journal of Hepatology*, vol. 67, no. 6, pp. 1298–1323, 2017.

[36] G. M. Hirschfield, T. H. Karlsen, K. D. Lindor, and D. H. Adams, "Primary sclerosing cholangitis," *Lancet*, vol. 382, no. 9904, pp. 1587–1599, 2013.

[37] E. L. Culver and R. W. Chapman, "IgG4-related hepatobiliary disease: an overview," *Nature Reviews. Gastroenterology & Hepatology*, vol. 13, no. 10, pp. 601–612, 2016.

[38] M. T. Huggett, E. L. Culver, M. Kumar et al., "Type 1 autoimmune pancreatitis and IgG4-related sclerosing cholangitis is associated with extrapancreatic organ failure, malignancy, and mortality in a prospective UK cohort," *American Journal of Gastroenterology*, vol. 109, no. 10, pp. 1675–1683, 2014.

[39] E. L. Culver, R. Sadler, A. C. Bateman et al., "Increases in IgE, eosinophils, and mast cells can be used in diagnosis and to predict relapse of IgG4-related disease," *Clinical Gastroenterology and Hepatology*, vol. 15, no. 9, pp. 1444–1452.e6, 2017.

[40] E. L. Culver, R. Sadler, D. Simpson et al., "Elevated serum IgG4 levels in diagnosis, treatment response, organ involvement, and relapse in a prospective IgG4-related disease UK cohort," *American Journal of Gastroenterology*, vol. 111, no. 5, pp. 733–743, 2016.

Hindawi
Journal of Immunology Research
Volume 2020, Article ID 9236234, 7 pages
https://doi.org/10.1155/2020/9236234

Research Article

Identification of Long Noncoding RNAs lnc-DC in Plasma as a New Biomarker for Primary Sjögren's Syndrome

Yanhong Chen, Yongqiang Chen, Beibei Zu, Jia Liu, Li Sun, Chen Ding, Duping Wang, Xing Cheng, DeLiang Yang, and Guoping Niu

Department of Clinical Laboratory, XuZhou Central Hospital, China

Correspondence should be addressed to Guoping Niu; xz70707@163.com

Received 28 May 2020; Revised 12 August 2020; Accepted 28 September 2020; Published 16 October 2020

Academic Editor: Dawei Cui

Copyright © 2020 Yanhong Chen et al. This is an open access article distributed under the Creative Commons Attribution License, which permits unrestricted use, distribution, and reproduction in any medium, provided the original work is properly cited.

Objective. To evaluate the plasma levels of lnc-DC in primary Sjögren's syndrome (pSS) patients and investigate the potential associations between lnc-DC and disease activity. *Methods*. In this study, we recruited 358 enrollments, including 127 pSS patients without immune thrombocytopenia (ITP), 22 pSS patients with ITP, 50 systemic lupus erythematosus (SLE) patients, and 50 patients with rheumatoid arthritis (RA) and 109 healthy individuals, from Xuzhou Central Hospital. The expression of anti-SSA and anti-SSB was detected by enzyme-linked immunosorbent assay (ELISA). Spearman rank correlation test was used to analyze the relationship between lnc-DC and pSS activity. pSS activity was measured by anti-SSA, anti-SSB antibody, erythrocyte sedimentation rate (ESR), and β_2-microglobulin levels. The receiver operating characteristic (ROC) curve was used to determine the diagnostic performance of plasma lnc-DC for pSS. *Results*. Compared with healthy controls, SLE and RA patients, the lnc-DC expression levels were significantly elevated in pSS patients ($P < 0.001$), especially in pSS patients with ITP ($P < 0.001$). As expected, we also found that the lnc-DC expression positively correlated with anti-SSA ($R^2 = 0.290$, $P < 0.001$), anti-SSB ($R^2 = 0.172$, $P < 0.001$), ESR level ($R^2 = 0.076$, $P = 0.002$), and β_2-microglobulin level ($R^2 = 0.070$, $P = 0.003$) in pSS patients. ROC curves showed that plasma lnc-DC in pSS patients had an AUC 0.80 with a sensitivity of 0.75 and specificity of 0.85 at the optimum cutoff 1.06 in discriminating SLE and RA patients. In addition, the combination of lnc-DC and anti-SSA/SSB (AUC: 0.84, sensitivity: 0.79, specificity: 0.90) improved significantly the diagnostic ability of pSS patients from SLE and RA patients. In the efficacy monitoring study, levels of plasma lnc-DC were dramatically decreased after treatment ($P < 0.001$). *Conclusion*. These findings highlight that plasma lnc-DC as a novel biomarker for the diagnosis of pSS and can be used to evaluate the therapeutic efficacy of pSS underwent interventional therapy.

1. Introduction

Primary Sjögren's syndrome (pSS), more often seen in women, is a multifactor and organ-specific autoimmune disease [1, 2]. The main clinical symptoms of pSS are eye and oral dryness, following with other manifestations such as skin dryness and immune thrombocytopenia (ITP) [3, 4]. Like other autoimmune diseases, both environmental and genetic factors contribute to the onset of pSS [5, 6]. Accumulating evidence has demonstrated that multiple molecules including and development of pSS [7, 8]. ITP is an immune-mediated disease that characterized by impaired platelet production or platelet more destruction, resulting in platelet decreased and varying degree of bleeding risk [9]. ITP is commonly associated with autoimmune diseases such as systemic lupus erythematosus (SLE) [10, 11]. However, the pathogenesis and molecular diagnosis of pSS with or without ITP are yet to be elucidated. Our study explores the clinical and immunological characteristics of ITP in patients with pSS, suggesting that pSS patients with ITP expressed higher level of lnc-DC compared to pSS patients without ITP. And we aim to explore plasma biomarkers in pSS patients which could contribute to better diagnosis and prognosis.

Characterized as a subtype of noncoding RNAs with more than 200 nucleotides in length [12, 13], long noncoding RNAs (lncRNAs) are widely involved in various physiological and pathological processes mostly by functioning at transcriptional or posttranscriptional control [14, 15], including

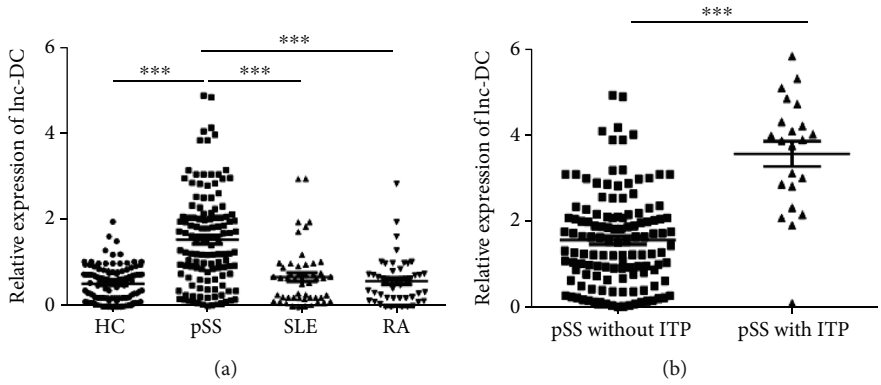

Figure 1: The relative expression of lnc-DC in HCs and pSS with or without ITP, SLE, and RA patients that was determined by qRT-PCR. $^{*}P < 0.05$; $^{***}P < 0.001$, by one-way ANOVA with Bonferroni's test and 2-tailed unpaired t-test.

Table 1: The basic characteristics, clinical manifestations and laboratory findings of pSS patients with and without ITP.

Characteristic	pSS without ITP ($n = 127$)	pSS with ITP ($n = 22$)	t/χ^2/Z	P value
Basic characteristics				
Age (years)	48.59 ± 12.98	49.34 ± 15.72	-0.242 [a]	0.809
Gender (female/male)	121/6	20/2	0.107[b]	0.744
Clinical manifestations				
Dry mouth (%)	85/118 (72.03)	11/20 (55.00)	2.344[b]	0.126
Dry eye (%)	60/118 (50.85)	6/20 (30.00)	2.979[b]	0.084
Arthritis (%)	41/110 (37.27)	3/19 (15.79)	3.327[b]	0.068
Interstitial lung disease (%)	58/108 (53.70)	5/17 (29.41)	3.467[b]	0.063
ESSDAI	4.00 (2.00–6.00)	5.00 (3.00–7.00)	-2.135[c]	0.033
Laboratory findings				
lnc-DC, IU/mL	1.57 ± 0.09	3.56 ± 0.28	-33.041[a]	<0.001
Platelet, ×109/L	234.00 ± 186.00	37.00 ± 33.00	22.384[c]	<0.001
Hemoglobin, g/L	124.00 ± 102.00	117.00 ± 110.00	0.522[c]	0.602
Leukocyte, ×109/L	5.77 ± 3.83	6.05 ± 4.01	-0.776[c]	0.438
Creatinine, mg/dL	46.20 ± 37.20	42.50 ± 29.80	1.985[c]	0.047
ALT, U/L	19.00 ± 16.00	22.00 ± 15.00	-0.950[c]	0.342
AST, U/L	19 ± 13.00	24.00 ± 15.00	-1.232[c]	0.218
Positive ANA (%)	93/116 (80.17)	15/20 (75.00)	0.052[b]	0.819
Positive AHA (%)	2/121 (16.67)	2/18 (11.11)	—	0.081[d]

Data are presented as mean ± SD (standard deviation) or median with 25–75th percentiles, positive number/tested number (%). ESSDAI: European League Against Rheumatism Sjögren's Syndrome Disease Activity Index; ALT: alanine aminotransferase; AST: aspartate aminotransferase; Anna: antinuclear antibody; aha: anti-histone antibody. $P < 0.05$ was considered statistically significant. [a]Independent sample t-test; [b]chi-squared test; [c]Mann–Whitney U test; [d]Fisher exact probability method.

cancers [16], immune diseases [17], cardiovascular diseases [18–20], and cardio-metabolic diseases [21]. Piling evidence showed that lncRNAs exist stably in human body fluids including urine and plasma, thereby acting as sensitive prognostic and diagnostic biomarkers in cancers and cardiovascular diseases [22–24]. lnc-DC, identified by Wang et al., is a specific lncRNA that exclusively expressed in dendritic cells (DCs) which mediates the differentiation of DCs and the activation of T cells [25]. However, it remains uncertain whether lnc-DC in plasma can effectively diagnose pSS. Thus, in this study, we evaluate the plasma levels of lnc-DC in pSS patients and investigate their potential value for pSS diagnosis.

2. Materials and Methods

2.1. Study Subjects. A total of 127 primary Sjögren's syndrome (pSS) patients, 22 pSS patients with immune thrombocytopenia (ITP), and 109 healthy controls were collected in the physical examination central of XuZhou Central Hospital, June 1, 2018, to December 1, 2019. All pSS patients were according to the 2002 US-EU Consensus Group criteria

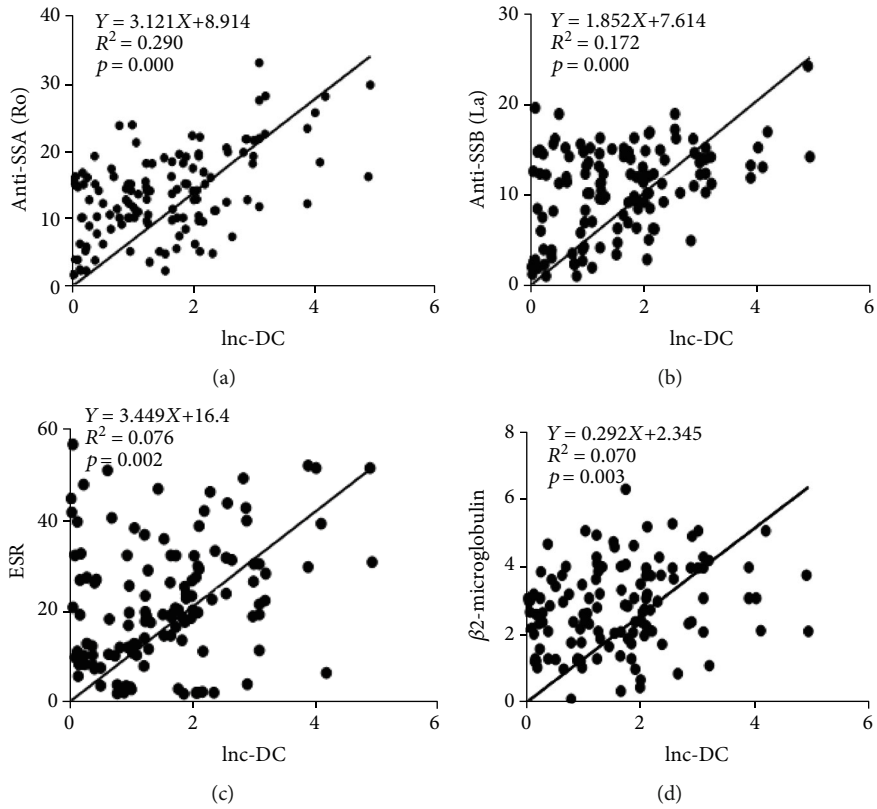

Figure 2: lnc-DC and the correlativity of pSS patients with certain clinical characteristics, lnc-DC, and 127 patients with pSS in the correlation between some clinical characteristics, including anti-SSA (a), anti-SSB (b), the ESR (c), and β_2-microglobulin (d). The correlation analysis used the Spearman rank correlation coefficient test.

[26], and all ITP patients fulfilled the diagnosis criteria according to the American Society of Hematology guidelines [9]. Healthy controls have no history of autoimmune diseases and have never been treated with immunosuppressive drugs. The sampling method was biopsy sampling. In order to analyze the specificity of lnc-DC in patients, 100 patients from our hospital were selected as a control group, including 50 systemic lupus erythematosus (SLE) patients and 50 rheumatoid arthritis (RA) patients, and their lnc-DC expression levels were analyzed. This study has been approved by relevant agencies and is feasible for implementation.

2.2. Extraction of Plasma. Use ethylenediaminetetraacetic acid anticoagulation tube as the collection device to collect 7 ~ 10 mL of peripheral blood of patients. Blood samples were centrifuged at 1500 g for 10 min, and 12000 g, 4°C for 10 min. The plasma samples were divided into several parts and then placed at -80°C for storage.

2.3. Enzyme-Linked Immunosorbent Assay (ELISA). Anti-SSA and anti-SSB in the plasma were quantified using the ELISA kits (Sterlitech co, Beijing, China) according to the manufacturer's protocol. The absorbance of the samples at 405 nm is using a microplate reader (Biotek USA).

2.4. Quantitative Reverse Transcription Polymerase Chain (qRT-PCR) Reaction. Total RNA was extracted using PrimeScript™ RT regent kit (Invitrogen), while scientific cDNA reverse transcription was performed, followed by qRT-PCR according to the biological system protocol. The primers of lnc-DC are as follows: R-CCCTAAGATCGTCCCTTCC, F-CAACCCCTCTTCCCTGCC. The reactions involved were 96-optical plates treated at 95°C for 5 minutes, followed by 42 cycles at 95°C for 10 seconds, 30 seconds at 60°C, and 72°C for 20 seconds. lnc-DC is calculated using the relative expression of the endogenous$2^{-\Delta\Delta ct}$ control method of standardization.

2.5. Data Collection. The clinical data involved in this study include specific laboratory test results, patient medical history information, specific treatment methods, and other medical records. The clinical performance of the patient is analyzed, including symptoms related to skin bleeding and mucous petechiae in pSS patients. When conducting an immunological characteristic test, the detection analysis indicators involved include the following several parts: C-reactive protein (CRP), erythrocyte sedimentation rate (ESR), complement 3 (C3), and complement 4 (C4), at the same time, the patients with analysis of antibody and immune globulin, disease activity in patients with pSS evaluation theoretical basis for the European anti rheumatoid glen syndrome disease activity index (ESSDAI) evaluation way [27]. Patients with hemorrhagic manifestations of the severity of bleeding are described by the ITP-specific assessment tools (ITP-bat) [28].

2.6. Statistical Analysis. Analysis of variance (ANOVA) was used for statistical analysis of data. This method can be

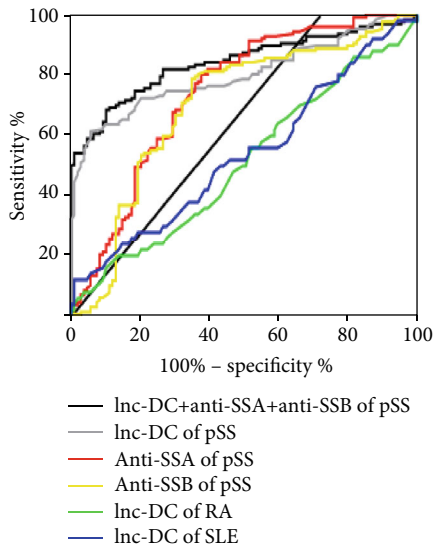

Figure 3: lnc-DC alone or combined with anti-SSA and anti-SSB for the discriminative ability of pSS patients from HC and other autoimmune disease.

determined whether there is a significant difference between the healthy controls and pSS patients. The pre- and posttest comparison was carried out using Bonferroni's test. The correlation between lnc-DC and clinical features was analysis by Spearman rank correlation coefficient test. Receiver operating characteristic curve (ROC) and area under curve (AUC) were used as the assessment indicators of sensitivity and specificity of pSS biomarkers for lnc-DC analysis. The data processing software used was the GraphPad Prism 7 software (GraphPad software, Inc., San Diego, CA). Mean ± standard deviation was used to describe the distribution of normal distribution quantitative data. Independent sample t-test was used to compare the differences between the two groups. One-way ANOVA was used to compare the differences between multiple groups. Median (quartile) was used to describe the distribution of nonnormal distribution quantitative data, Mann–Whitney U test was used to compare the differences between groups; frequency and composition ratio were used to describe the distribution of qualitative data, and chi-squared test or Fisher exact probability method was used to compare the differences between groups. All the tests were bilateral, and the difference was statistically significant ($P < 0.05$).

3. Results

3.1. The Level of lnc-DC Increased in pSS Patients as Compared with Healthy Controls and Other Autoimmune Diseases. The expressions of lnc-DC in 109 healthy controls (HC), 50 SLE, 50 RA, and 127 pSS patients were analyzed by qRT-PCR. As shown in Figure 1(a), the levels of lnc-DC were significantly elevated in pSS patients than those in HC, SLE, and RA patients ($P < 0.001$). Moreover, the levels of plasma lnc-DC in pSS patients with immune thrombocytopenia (ITP) increased dramatically than pSS patients without ITP ($P < 0.001$). A comparison of basic characteristics, the clinical manifestations, and laboratory findings of pSS patients with and without ITP is shown in Table 1.

3.2. The Plasma lnc-DC Level Is Positively Correlative with pSS Clinical Characteristics. To explore the relationship between the lnc-DC expression and the clinical characteristics of pSS patients, the results are listed in Table 2. As the results showed, the levels of anti-SSA, anti-SSB, ESR, and β_2-macroglobulin were higher in pSS patients compared with healthy controls. Moreover, the correlation analysis results showed that lnc-DC is positively correlative with anti-SSA (Figure 2(a)), anti-SSB (Figure 2(b)), ESR (Figure 2(c)), and β_2-macroglobulin (Figure 2(d)) expression but not related to the levels of RF, CRP, C3, and C4.

3.3. Identification of lnc-DC in Plasma as a Novel Biomarker for pSS. In the process of diagnosing pSS plasma biomarkers, the receiver operating characteristic (ROC) curve is used as a performance evaluation method for lnc-DC diagnosis. As shown in the data, an area under the curve (AUC) value for lnc-DC in pSS patients was 0.80. Notably, for lnc-DC combined with anti-SSA and anti-SSB, the AUC value was 0.84. Moreover, at the optimal cutoff value 1.06, the diagnostic sensitivity and specificity were 0.75 and 0.85, respectively. Meanwhile, we also generated ROC curves to analyze the diagnostic value of lnc-DC in SLE and RA to further confirm its specificity. And the AUC values were 0.54 and 0.51 for SLE and RA, respectively (Figure 3 and Table 3). All these results demonstrate that plasma lnc-DC can be used as a novel biomarker for the diagnosis of pSS in clinical.

3.4. The lnc-DC Levels in pSS Patients Decreased after Treatment. Dynamic changes reflecting the patients' condition could provide the clinical guidance for doctors. We therefore tentatively explored the efficacy monitoring capability of lnc-DC in patients receiving drug treatment. The level of plasma lnc-DC in 89 pSS patients, whose treatment with drugs after 6 months, decreased dramatically (Figure 4). The results indicated that dynamic changes of plasma lnc-DC in pSS patients can monitor the treatment efficacy.

4. Discussion

Primary Sjögren's syndrome (pSS) is an autoimmune disease with chronic organ-specific characteristics and is characterized by the production of auto-antibodies and the dysfunction of exocrine glands primarily including the lachrymal and salivary glands, which could lead to dry eyes and dry mouth [29, 30]. The incidence of pSS is occult, and the clinical situation varies greatly. Immune thrombocytopenia (ITP) is an immune-mediated disease. If the patient suffers from this disease, there will be abnormalities of platelets, or the production will be damaged, or the damage will be severe, resulting in varying degree of bleeding risk [9]. Although the current research on pSS patients has been explored for many years, the actual research also has many limitations because the lack of cognition of the specific clinical, prevalence, and immunological characteristics of ITP pSS patients during the initial study led to research and has a series of limitations.

Table 2: The results of clinical characteristics in HC, pSS, SLE, and RA patients.

Characteristic	HC	pSS patients	SLE patients	RA patients	F	P
Age	44.27 ± 8.53	48.59 ± 12.98*	47.25 ± 10.33	50.22 ± 14.75*	4.028	0.008
Ro (anti-SSA)	8.22 ± 0.66	13.82 ± 0.56*	7.01 ± 0.77*#	8.12 ± 0.98#&	1915.468	<0.01
La (anti-SSB)	6.78 ± 0.54	10.52 ± 0.44*	7.92 ± 1.33*#	6.39 ± 1.03*#&	607.159	<0.01
ESR (mm/hr)	7.75 ± 0.75	23.46 ± 2.43*	26.33 ± 6.17*#	45.34 ± 14.37*#&	437.691	<0.01
RF (IU/mL)	22.39 ± 14.77	140.29 ± 74.88*	135.45 ± 93.09*	196.77 ± 143.92*#&	69.471	<0.01
Immunoglobulin G (g/L)	9.51 ± 4.33	16.32 ± 8.32*	22.55 ± 9.26*#	13.85 ± 6.90*#&	40.896	<0.001
Immunoglobulin A (g/L)	2.57 ± 1.94	3.42 ± 1.28*	2.33 ± 1.73#	2.42 ± 1.57#	9.111	<0.001
Immunoglobulin E (IU/mL)	69.44 ± 52.15	76.32 ± 58.32	77.89 ± 56.37	70.42 ± 54.61	0.459	0.711
Immunoglobulin M (g/L)	1.47 ± 0.92	1.55 ± 0.93	3.92 ± 2.09*#	4.13 ± 2.41*#	70.399	<0.01
CRP (mg/L)	1.55 ± 0.96	4.02 ± 2.98*	4.55 ± 3.92*	3.19 ± 2.81*&	22.198	<0.01
Complement 3 (g/L)	0.79 ± 0.44	0.92 ± 0.62	1.15 ± 0.62*#	0.96 ± 0.53	4.956	0.002
Complement 4 (g/L)	0.20 ± 0.13	0.28 ± 0.17*	0.32 ± 0.19*	0.25 ± 0.14&	8.392	<0.001
β_2-microglobulin (mg/L)	1.12 ± 0.64	2.81 ± 1.09*	2.54 ± 1.08*	2.01 ± 1.37*#&	57.675	<0.01

ESR: erythrocyte sedimentation rate; RF: rheumatoid factor; CRP: C-reactive protein; $P < 0.05$ was considered statistically significant. One-way ANOVA was used for intergroup comparison, and lSD-T test was used for pairwise comparison as a whole.* vs. healthy controls $P < 0.05$ # vs. pSS patients $P < 0.05$ & vs. SLE patients $P < 0.05$.

Table 3: lnc-DC alone or lnc-DC combined with anti-SSA and anti-SSB for the discriminative ability of pSS patients from HC and other autoimmune disease such as SLE and RA.

Characteristic	AUC	SE	P value	95% CI	Sensitivity	Specificity
lnc-DC+antu-SSA+anti-SSB of pSS	0.84	0.03	<0.001	0.79~0.89	78.50	89.91
lnc-DC of pSS	0.80	0.03	<0.001	0.75~0.86	75.42	84.50
Anti-SSA of pSS	0.74	0.05	<0.001	0.68~0.81	72.31	62.39
Anti-SSB of pSS	0.70	0.05	<0.01	0.63~0.77	71.53	64.22
lnc-DC of RA	0.54	0.06	0.464	0.44~0.64	50.00	56.88
lnc-DC of SLE	0.51	0.06	0.836	0.41~0.61	64.09	40.37

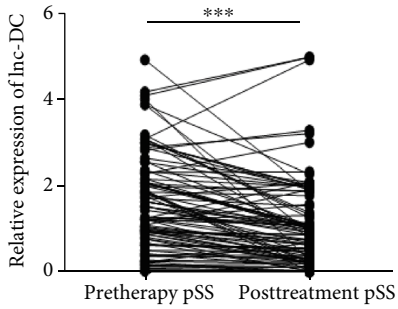

Figure 4: The expression of lnc-DC in plasma of 102 pSS patients before and after treatment. Compared with before treatment, 89 patients showed decreased expression of lnc-DC. ***$P < 0.001$, by paired sample t-test.

Usually, patients only start treatment when the condition is very obvious, which leads to the best treatment opportunity may be missed. In order to ensure a good treatment effect, diagnosis and treatment should be timely, and researchers should actively explore new biomarkers.

More and more evidence shows that noncoding RNA, especially microRNAs, plays an important role in the regulation of inflammatory signaling pathways [7, 8]. In recent years, lncRNAs, as a new regulator, are known by reports [31, 32]. Moreover, lncRNAs are widely involved in the gene expression and participate in immune disease [33, 34], and the miRNA-mRNA relationship needs further research, such as the mechanism of miRNA regulation in pSS progression, which might be affected by lnc-DC. However, the specific value application of lncRNAs in pSS is unclear, but the higher level of lnc-DC may participate in pSS without or with ITP.

The results of Wang et al. showed that through lnc-DC, the targets of signal transducer regulation and transcription activator 3 (STAT3) expression can be achieved, thereby modulating the differentiation of dendritic cell [19]. lnc-DC was also reported to mediate the STAT3 expression to regulate differentiation of Th17 cells and functions of T helper cells and B cells [35, 36]. Li et al. found that compared with healthy control, the level of lnc-DC was significantly lower in SLE patients [37]. Our research shows for the first time that the lnc-DC expression is significantly higher than that of plasma pSS patients. Compared with healthy controls, patients have other autoimmune diseases such as systemic lupus erythematosus and rheumatoid arthritis. In addition, we found that lnc-DC plasma levels positively correlated with

clinical manifestations, such as increasing the expression of anti-SSA, anti-SSB, ESR, and β_2-microglobulin. Recent studies have demonstrated that lncRNAs may act as effective and noninvasive biomarkers in gynecological diseases [38] and renal diseases [39]. However, it remains to be studied in pSS diagnosis of performance lncRNAs. Our research shows that the plasma lnc-DC has the potential to be the pSS-specific signature lncRNA and could function as a candidate biomarker for pSS. Meanwhile, the AUC of lnc-DC combined with anti-SSA and anti-SSB is much higher than other groups. And the risk score based on lnc-DC could discriminate pSS patients from SLE and RA. This diagnostic efficiency is relatively high that may be caused by the increased expression of DC leads to the specificity lnc-DC high, or lnc-DC regulates the STAT3 expression to mediate Th17 cells, and then, the increased Th17 cells can secrete a variety of cytokines, which leads to the occurrence and development of pSS patients.

However, several limitations in our study must be considered. First, our study is limited to the patients admitted in only one hospital in China, which may restrict the generalizability of the results. Second, the sample size was relatively small. Third, the causal relationship between lncRNAs and pSS revealed by our research is challenging. Thus, the role of lncRNAs in the pSS pathogenesis and development awaits further exploration, both in vivo and in vitro.

In conclusion, our results first demonstrated that plasma lnc-DC level could function as a novel biomarker specifically identifying pSS patients, which is of great importance in the diagnosis of pSS.

Data Availability

In this study, all the research data involved are presented in this article. All data generated or analyzed are included in this article.

Ethical Approval

The study was reviewed and approved by the Ethics Committee of Xuzhou Central Hospital, and the consent of the researchers and their families was obtained. The person in charge signed an informed consent.

Conflicts of Interest

The authors declare that they have no competing interests.

Authors' Contributions

CYH, CYQ, ZBB, SL, and NGP performed the study design. CYH, SL, CX, LJ, YDL, and WDP analyzed the data and wrote the manuscript. DC, SL, LJ CX, WDP, ZBB, and NGU collected and analyzed the data. All authors approved the final manuscript. The first author is Yanhong Chen.

Acknowledgments

The study took a huge heart, each of us into one, through meticulous observation and scientific analysis, concluded that the relevant mechanism of disease progression, and have a clear understanding of this; in this, we thank all the participants and the patients and families. Thanks to all at the same time for providing data on the health of patients. It has made an important contribution to the development of medical research. This work was supported by the science and technology project of XuZhou (KC18033).

References

[1] C. Efe, S. Wahlin, E. Ozaslan et al., "Autoimmune hepatitis/-primary biliary cirrhosis overlap syndrome and associated extrahepatic autoimmune diseases," *European journal of gastroenterology & hepatology.*, vol. 24, no. 5, pp. 531–534, 2012.

[2] Y. Sun, K. Haapanen, B. Li, W. Zhang, J. Van de Water, and M. E. Gershwin, "Women and primary biliary cirrhosis," *Clinical reviews in allergy & immunology.*, vol. 48, no. 2-3, pp. 285–300, 2015.

[3] L. Wang, M. E. Gershwin, and F. S. Wang, "Primary biliary cholangitis in China," *Current opinion in gastroenterology.*, vol. 32, no. 3, pp. 195–203, 2016.

[4] M. Podda, C. Selmi, A. Lleo, L. Moroni, and P. Invernizzi, "The limitations and hidden gems of the epidemiology of primary biliary cirrhosis," *Journal of autoimmunity.*, vol. 46, pp. 81–87, 2013.

[5] C. Selmi, P. S. C. Leung, D. H. Sherr et al., "Mechanisms of environmental influence on human autoimmunity: A national institute of environmental health sciences expert panel workshop," *Journal of Autoimmunity*, vol. 39, no. 4, pp. 272–284, 2012.

[6] G. F. Mells, A. Kaser, and T. H. Karlsen, "Novel insights into autoimmune liver diseases provided by genome-wide association studies," *Journal of autoimmunity.*, vol. 46, pp. 41–54, 2013.

[7] Y. Li and X. Shi, "MicroRNAs in the regulation of TLR and RIG-I pathways," *Cellular & molecular immunology.*, vol. 10, no. 1, pp. 65–71, 2013.

[8] R. M. O'Connell, D. S. Rao, and D. Baltimore, "microRNA regulation of inflammatory responses," *Annual review of immunology.*, vol. 30, no. 1, pp. 295–312, 2012.

[9] C. Neunert, W. Lim, M. Crowther, A. Cohen, L. Solberg, and M. A. Crowther, "The American Society of Hematology 2011 evidence-based practice guideline for immune thrombocytopenia," *Blood*, vol. 117, no. 16, pp. 4190–4207, 2011.

[10] M. Jallouli, M. Frigui, S. Marzouk et al., "Clinical implications and prognostic significance of thrombocytopenia in Tunisian patients with systemic lupus erythematosus," *Lupus*, vol. 21, no. 6, pp. 682–687, 2012.

[11] P. D. Ziakas, S. Giannouli, E. Zintzaras, A. G. Tzioufas, and M. Voulgarelis, "Lupus thrombocytopenia: clinical implications and prognostic significance," *Annals of the Rheumatic Diseases*, vol. 64, no. 9, pp. 1366–1369, 2005.

[12] P. Kapranov, J. Cheng, S. Dike et al., "RNA maps reveal new RNA classes and a possible function for pervasive transcription," *Science*, vol. 316, no. 5830, pp. 1484–1488, 2007.

[13] S. A. Patel and A. DeMichele, "Adding Adjuvant Systemic Treatment after Neoadjuvant Therapy in Breast Cancer: Review of the Data," *Current Oncology Reports*, vol. 19, no. 8, 2017.

[14] T. Hung, Y. Wang, M. F. Lin et al., "Extensive and coordinated transcription of noncoding RNAs within cell-cycle promoters," *Nature genetics.*, vol. 43, no. 7, pp. 621–629, 2011.

[15] K. C. Wang and H. Y. Chang, "Molecular mechanisms of long noncoding RNAs," *Molecular Cell*, vol. 43, no. 6, pp. 904–914, 2011.

[16] R. Spizzo, M. I. Almeida, A. Colombatti, and G. A. Calin, "Long non-coding RNAs and cancer: a new frontier of translational research?," *Oncogene*, vol. 31, no. 43, pp. 4577–4587, 2012.

[17] J. L. Knauss and T. Sun, "Regulatory mechanisms of long noncoding RNAs in vertebrate central nervous system development and function," *Neuroscience*, vol. 235, pp. 200–214, 2013.

[18] N. Schonrock, R. P. Harvey, and J. S. Mattick, "Long noncoding RNAs in cardiac development and pathophysiology," *Circulation research.*, vol. 111, no. 10, pp. 1349–1362, 2012.

[19] P. Mathiyalagan, S. T. Keating, X. J. Du, and A. El-Osta, "Interplay of chromatin modifications and non-coding RNAs in the heart," *Epigenetics*, vol. 9, no. 1, pp. 101–112, 2014.

[20] Y.-W. Hu, J.-Y. Zhao, S.-F. Li et al., "RP5-833A20.1/miR-382-5p/NFIA–Dependent Signal Transduction Pathway Contributes to the Regulation of Cholesterol Homeostasis and Inflammatory Reaction," *Arteriosclerosis, Thrombosis, and Vascular Biology*, vol. 35, no. 1, pp. 87–101, 2015.

[21] Y. Liu, J. F. Ferguson, C. Xue et al., "Tissue-specific RNA-Seq in human evoked inflammation identifies blood and adipose LincRNA signatures of cardiometabolic diseases," *Arteriosclerosis, thrombosis, and vascular biology.*, vol. 34, no. 4, pp. 902–912, 2014.

[22] P. Wang, Y. Xue, Y. Han et al., "The STAT3-binding long noncoding RNA lnc-DC controls human dendritic cell differentiation," *Science*, vol. 344, no. 6181, pp. 310–313, 2014.

[23] Y. Yang, Y. Cai, G. Wu et al., "Plasma long non-coding RNA, CoroMarker, a novel biomarker for diagnosis of coronary artery disease," *Clinical science.*, vol. 129, no. 8, pp. 675–685, 2015.

[24] R. Kumarswamy, C. Bauters, I. Volkmann et al., "Circulating long noncoding RNA, LIPCAR, predicts survival in patients with heart failure," *Circulation research.*, vol. 114, no. 10, pp. 1569–1575, 2014.

[25] J. Tang, R. Jiang, L. Deng, X. Zhang, K. Wang, and B. Sun, "Circulation long non-coding RNAs act as biomarkers for predicting tumorigenesis and metastasis in hepatocellular carcinoma," *Oncotarget*, vol. 6, no. 6, pp. 4505–4515, 2015.

[26] C. Vitali, S. Bombardieri, R. Jonsson et al., "Classification criteria for Sjogren's syndrome: a revised version of the European criteria proposed by the American-European consensus group," *Annals of the Rheumatic Diseases*, vol. 61, no. 6, pp. 554–558, 2002.

[27] R. Seror, P. Ravaud, S. J. Bowman et al., "EULAR Sjögren's syndrome disease activity index: development of a consensus systemic disease activity index for primary Sjögren's syndrome," *Annals of the Rheumatic Diseases*, vol. 69, no. 6, pp. 1103–1109, 2010.

[28] F. Rodeghiero, M. Michel, T. Gernsheimer et al., "Standardization of bleeding assessment in immune thrombocytopenia: report from the international working group," *Blood*, vol. 121, no. 14, pp. 2596–2606, 2013.

[29] R. I. Fox, "Sjögren's syndrome," *Lancet*, vol. 366, no. 9482, pp. 321–331, 2005.

[30] S. Gaidamakov, O. A. Maximova, H. Chon et al., "Targeted Deletion of the Gene Encoding the La Autoantigen (Sjogren's Syndrome Antigen B) in B Cells or the Frontal Brain Causes Extensive Tissue Loss," *Molecular and Cellular Biology*, vol. 34, no. 1, pp. 123–131, 2013.

[31] X. Yang, Y. Chen, J. Li et al., "Hypertonic saline maintains coagulofibrinolytic homeostasis following moderate to severe traumatic brain injury by regulating monocyte phenotype via expression of lncRNAs," *Molecular medicine reports.*, vol. 19, no. 2, pp. 1083–1091, 2019.

[32] R. Yarani, A. H. Mirza, S. Kaur, and F. Pociot, "The emerging role of lncRNAs in inflammatory bowel disease," *Experimental & Molecular Medicine*, vol. 50, no. 12, pp. 1–14, 2018.

[33] Y. Wu, F. Zhang, X. Li et al., "Systematic analysis of lncRNA expression profiles and atherosclerosis-associated lncRNA-mRNA network revealing functional lncRNAs in carotid atherosclerotic rabbit models," *Functional & Integrative Genomics*, vol. 20, no. 1, pp. 103–115, 2020.

[34] J. Fan, M. Cheng, X. Chi, X. Liu, and W. Yang, "A human long non-coding RNA LncATV promotes virus replication through restricting RIG-I-mediated innate immunity," *Frontiers in immunology.*, vol. 10, p. 1711, 2019.

[35] A. Goropevsek, M. Holcar, and T. Avcin, "The role of STAT signaling pathways in the pathogenesis of systemic lupus erythematosus," *Clinical reviews in allergy & immunology.*, vol. 52, no. 2, pp. 164–181, 2017.

[36] M. A. Kluger, S. Melderis, A. Nosko et al., "Treg17 cells are programmed by Stat3 to suppress Th17 responses in systemic lupus," *Kidney international.*, vol. 89, no. 1, pp. 158–166, 2016.

[37] J. Li, G. C. Wu, T. P. Zhang et al., "Association of long noncoding RNAs expression levels and their gene polymorphisms with systemic lupus erythematosus," *Scientific Reports*, vol. 7, no. 1, p. 15119, 2017.

[38] W.-T. Wang, Y.-M. Sun, W. Huang, B. He, Y.-N. Zhao, and Y.-Q. Chen, "Genome-wide Long Non-coding RNA Analysis Identified Circulating LncRNAs as Novel Non-invasive Diagnostic Biomarkers for Gynecological Disease," *Scientific Reports*, vol. 6, no. 1, 2016.

[39] J. M. Lorenzen, C. Schauerte, J. T. Kielstein et al., "Circulating long noncoding RNATapSaki is a predictor of mortality in critically ill patients with acute kidney injury," *Clinical chemistry.*, vol. 61, no. 1, pp. 191–201, 2015.

Hindawi
Journal of Immunology Research
Volume 2020, Article ID 7165230, 10 pages
https://doi.org/10.1155/2020/7165230

Research Article

HMGB1 Recruits TET2/AID/TDG to Induce DNA Demethylation in STAT3 Promoter in CD4$^+$ T Cells from aGVHD Patients

Xuejun Xu, Yan Chen, Enyi Liu, Bin Fu, Juan Hua, Xu Chen, and Yajing Xu

Department of Hematology, Xiangya Hospital, Central South University, Changsha, Hunan, China

Correspondence should be addressed to Yajing Xu; xyyajingxu@csu.edu.cn

Received 25 April 2020; Revised 14 August 2020; Accepted 31 August 2020; Published 24 September 2020

Academic Editor: Jie Tian

Copyright © 2020 Xuejun Xu et al. This is an open access article distributed under the Creative Commons Attribution License, which permits unrestricted use, distribution, and reproduction in any medium, provided the original work is properly cited.

STAT3 is highly expressed in aGVHD CD4$^+$ T cells and plays a critical role in inducing or worsening aGVHD. In our preceding studies, DNA hypomethylation in STAT3 promoter was shown to cause high expression of STAT3 in aGVHD CD4$^+$ T cells, and the process could be modulated by HMGB1, but the underlying mechanism remains unclear. TET2, AID, and TDG are indispensable in DNA demethylation; meanwhile, TET2 and AID also serve extremely important roles in immune response. So, we speculated these enzymes involved in the STAT3 promoter hypomethylation induced by HMGB1 in aGVHD CD4$^+$ T cells. In this study, we found that the binding levels of TET2/AID/TDG to STAT3 promoter were remarkably increased in CD4$^+$T cells from aGVHD patients and were significantly negatively correlated with the STAT3 promoter methylation level. Simultaneously, we revealed that HMGB1 could recruit TET2, AID, and TDG to form a complex in the STAT3 promoter region. Interference with the expression of TET2/AID/TDG inhibited the overexpression of STAT3 caused by HMGB1 downregulation of the STAT3 promoter DNA methylation. These data demonstrated a new molecular mechanism of how HMGB1 promoted the expression of STAT3 in CD4$^+$ T cells from aGVHD patients.

1. Introduction

Allogeneic hematopoietic stem cell transplantation (allo-HSCT) has been recognized as the exclusive treatment to cure hematopoietic malignancies, but acute graft-versus-host disease (aGVHD) is the primary limitation of the therapy [1–3]. Over the past decade, despite significant improvements in allo-HSCT, aGVHD remained the leading cause of transplant-related morbidity and mortality [4, 5].

Signal transducer and activator of transcription 3 (STAT3), an important signal transducer and activator of transcription, participates in regulating various biological processes [6]. Overexpressed STAT3 in aGVHD was found to be tightly linked to various disease progression [7, 8]. Our previous study showed the significantly increased expression of STAT3 was associated with DNA hypomethylation in STAT3 promoter in aGVHD CD4$^+$ T cells.

HMGB1, a group of nonhistone nucleoproteins, involves in mediating transcription and inflammatory processes [9, 10]. HMGB1 was found to drive DNA demethylation in CD4$^+$ T cells of systemic lupus erythematosus (SLE) patients [11]. DNA methylation is an epigenetic mechanism involved in regulating the gene expression [12]. The gene promoter hypermethylation could reduce gene expression, and conversely, demethylation of the promoter increased the gene expression [13, 14]. Our previous study revealed that HMGB1 was markedly overexpressed in CD4$^+$ T cells from aGVHD patients and was positively correlated with the STAT3 promoter DNA methylation level [7]. However, the exact mechanism by which HMGB1 decreases the DNA methylation level of STAT3 promoter remains unclear.

There are two pathways of DNA demethylation: passive and active [15]. During the cell division, DNA methyltransferases (DNMTs) are suppressed, which gradually lead to the decrease of the DNA methylation level [16]. This process is defined as passive DNA demethylation. Ten-eleven translocation (TET), Activation-induced cytidine deaminase (AID), and thymine-DNA glycosylase (TDG) are essential

Table 1: Clinic characteristics of patients.

	Total	Male	Median age	Diagnosis				Days to aGVHD onset median (range)
				ALL	AML	CML	MDS	
Non-aGVHD	23	13	33	7	10	4	2	
aGVHD	23	12	32	7	12	3	1	50 (21-87)

ALL: acute lymphoblastic leukemia; AML: acute myeloid leukemia; CML: chronic myeloid leukemia; MDS: myelodysplastic syndrome.

for active DNA demethylation in mammalian cells [17, 18]. 5-Methylcytosine (5-mC) can be turned into 5-hydroxymethylcytosine (5-hmC), 5-formylcytosine (5-fC), and 5-carboxylcytosine (5-caC) by TET proteins. Then, 5-hmC is catalyzed by AID into 5-hydroxymethyluracil (5hmU). Next, 5hmU is subsequently reduced to cytosine (C) by base excision repair (BER), which is induce by TDG. Moreover, 5-fC and 5-caC can be directly reduced to C by TDG. Through these two modes of action, the three enzymes initiate and maintain active DNA demethylation. So, we speculated that these enzymes stand a good chance of involving in the process that HMGB1 induced demethylation of STAT3 promoter in $CD4^+$ T cells from aGVHD patients.

In this study, we explored the specific process by which HMGB1 increases the expression of STAT3 in $CD4^+$ T cells from aGVHD patients and finally confirmed that HMGB1 could extensively recruit TET2, AID, and TDG to bind to STAT3 promoter, which in turn contributed to DNA demethylation of STAT3 promoter. Taken together, the result of this study uncovered the novel molecular mechanism of STAT3 demethylation induced by HMGB1 in aGVHD $CD4^+$ T cells.

2. Materials and Methods

2.1. Patients. A total of 46 patients who underwent allo-HSCT between 2017 and 2019, from HLA-identical sibling donors at the Central of Hematopoietic Stem Cell Transplantation of Xiangya Hospital, were included in this study. This study was approved by the human ethics committee of the Xiangya Hospital of Central South University, and written informed consent was obtained from all subjects. The clinical characteristics of these patients are shown in Table 1. The median time from transplantation onset to the start of aGVHD was 50 (21-87) days. The conditioning regimes were adopted as described in our previous study [7]. Assessment of aGVHD was conducted based on clinical symptoms in accordance with the accepted criteria [19]. The patients were divided into two groups according to whether or not they suffered from aGVHD. We simultaneously collected samples from patients at the onset of aGVHD ($n = 23$) and patients without aGVHD ($n = 23$). When patients were diagnosed with aGVHD, the blood samples were collected before treatment.

2.2. Culturing and Transfection of Cells. $CD4^+$ T cells were extracted from 40 ml venous peripheral blood using human CD4 beads (Miltenyi, Bergisch Gladbach, Germany) and cultured in human T cell culture medium (Lonza, Walkersville, MD, USA) supplemented with 10% fetal bovine serum (FBS) and 1% penicillin-streptomycin. $CD4^+$ T cells were transfected using the human T cell nucleofector kit and Amaxa nucleofector (Lonza, Walkersville, MD, USA). Briefly, $CD4^+$ T cells were collected and resuspended in 100 μl human T cell nucleofector solution, and then the cell suspension was mixed with plasmids. The mix was electrotransfected using the nucleofector program V-024 in the Amaxa nucleofector. The transfected cells were cultured in human T cell culture medium and harvested after 48 h. Jurkat cells were cultured in the RPMI 1640 media (Gibco, Rockville, MD, USA) containing 10% FBS and incubated at 37°C in 5% CO_2. The plasmids were transfected into Jurkat cells via electrotransfection as described above.

2.3. Western Blotting. The detailed procedure western blotting was performed as previously reported [7]. $CD4^+$ T cells were lysed in 1% NP40 lysis buffer [20 mM Tris/HCl (pH 7.2), 200 mM NaCl, 1% NP40] containing proteinase inhibitor (Thermo Pierce). Lysates were centrifuged at 12,000 g for 15 min at 4°C, and protein concentration was detected by the Bradford protein assay (Bio-Rad, CA, USA). Equal amounts of proteins were separated on SDS-PAGE gels and then transferred to PVDF membranes (Bio-Rad, CA, USA). Membranes were blocked with 5% nonfat milk in Tris-buffered saline containing 0.1% Tween-20 (TBST) buffer and immunoblotted with primary antibodies, including anti-HMGB1 (Abcam, MA, USA), anti-TDG (Abcam, MA, USA), anti-AID (Cell Signaling, BSN, USA), anti-TET2 (Abcam, MA, USA), anti-STAT3 (Cell Signaling, BSN, USA), and anti-GAPDH (Santa Cruz, CA, USA). Band intensity was quantified using Quantity One software (Bio-Rad, CA, USA).

2.4. ChIP-Real Time PCR. $CD4^+$ T cells were incubated in media with 1% formaldehyde for 20 min at room temperature, and then crosslinking was stopped with glycine (final concentration, 0.125 M) for 5 min. Cells were collected after washing twice, suspended in cold RIPA buffer [10 mM Tris-Cl (pH 8.0), 150 mM NaCl, 0.1% SDS, 0.1% DOC, 1% Triton X-100, 5 mM EDTA], and sonicated to shear the genomic DNA. Next, anti-TDG, anti-AID, and anti-TET2 antibodies were added, and then the mixture was incubated overnight at 4°C. Protein A agarose beads were added to collect the protein-DNA complexes. Samples were then washed and decrosslinked overnight at 65°C using sodium chloride (final concentration, 0.2 M). Finally, enriched DNA was recovered and amplified by real-time PCR. The ChIP-qPCR primers for STAT3 promoter are presented in Table 2.

Table 2: ChIP-qPCR primers for STAT3 promoter.

Segment position	Forward	Reverse	Product length
+71~+318	5′AGGAGCACCGAACTGTC-3′	5′-GCCCACTGACCAATGAG-3′	247
−226~−125	5′-GAGGGAACAAGCCCCAA-3′	5′-ACATCCCCAAGGTCCCA-3′	101
−2039–1754	5′-GGGTTGTGGAGAAAGGC-3′	5′-CATATTATCCGCTGATAG-3′	285

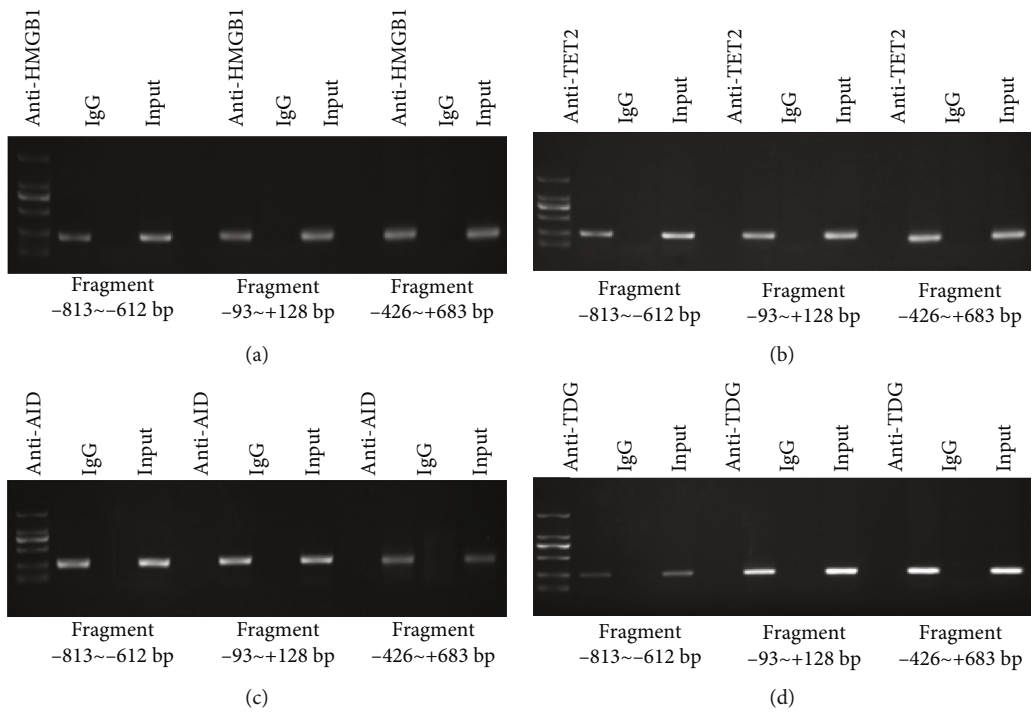

Figure 1: HMGB1, TET2, AID, and TDG were detected in STAT3 promoter. ChIP-PCR showed that HMGB1, (a) TET2, (b) AID, and (c) TDG bound to the STAT3 promoter region (-813 bp to +683 bp).

2.5. Coimmunoprecipitation (co-IP). Cell proteins were extracted by RIPA lysis buffer. Then, anti-HMGB1 antibody was added and incubated overnight at 4°C. Protein A/G agarose beads were added to samples and incubated for 2 hours at room temperature. Agarose beads were harvested by centrifugation at 3000 g for 2 min. Finally, the protein complex was eluted with loading buffer and analyzed by western blotting. Primary antibodies included anti-TET2, anti-AID, and anti-TDG.

2.6. Bisulfite Sequencing. Genomic DNA was extracted from $CD4^+$ T cells using the TIANamp genomic DNA kit (TIANGEN, Beijing, China). The EpiTect bisulfite kit (Qiagen, CA, USA) was utilized to convert bisulfite. Three CpG islands within the STAT3 promoter region were amplified by PCR. The PCR products were subcloned into a pGEM-T vector (Promega, WI, USA). Ten independent clones were sequenced for each amplified fragments. Primers used were as follows:

5′-GAATATTTTATGTATTTTA-3′ (forward 1) and 5′-ACAACAAAAAAAACATA-3′ (reverse 1); 5′-AGTTGTTTTTTTTATTGGT-3′ (forward 2) and 5′-CCCTACACCCCCTTCACC-3′ (reverse 2); 5′-GGGATTTTGGGGATGTTG-3′ (forward 3) and 5′-AAAAAACACAACTATCT-3′ (reverse 3).

2.7. Statistical Analysis. Variables were analyzed by Student's *t*-test (two groups) or single-factor analysis of variance (three groups). Correlations were analyzed using Pearson's correlation coefficient. All analyses were performed with SPSS 22.0 software. Statistical significance was set at $p < 0.05$.

3. Results and Discussion

3.1. HMGB1, TET2, AID, and TDG Bind to STAT3 Promoter. Our previous study showed that HMGB1 could induce DNA demethylation of STAT3 promoter to worsen aGVHD [7]. Hence, we hypothesized that some methylation-related enzymes played crucial roles in this process. We first explored whether HMGB1, TET2, AID, and TDG could bind to STAT3 promoter using a ChIP-PCR analysis in HMGB1/TET2/AID/TDG overexpressed Jurkat cells. Three pairs of primers that covered the STAT3 promoter −813 bp to +683 bp region were used. The results revealed that HMGB1, TET2, AID, and TDG could indeed bind to the STAT3 promoter −813 bp to +683 bp region (Figures 1(a)–1(c)).

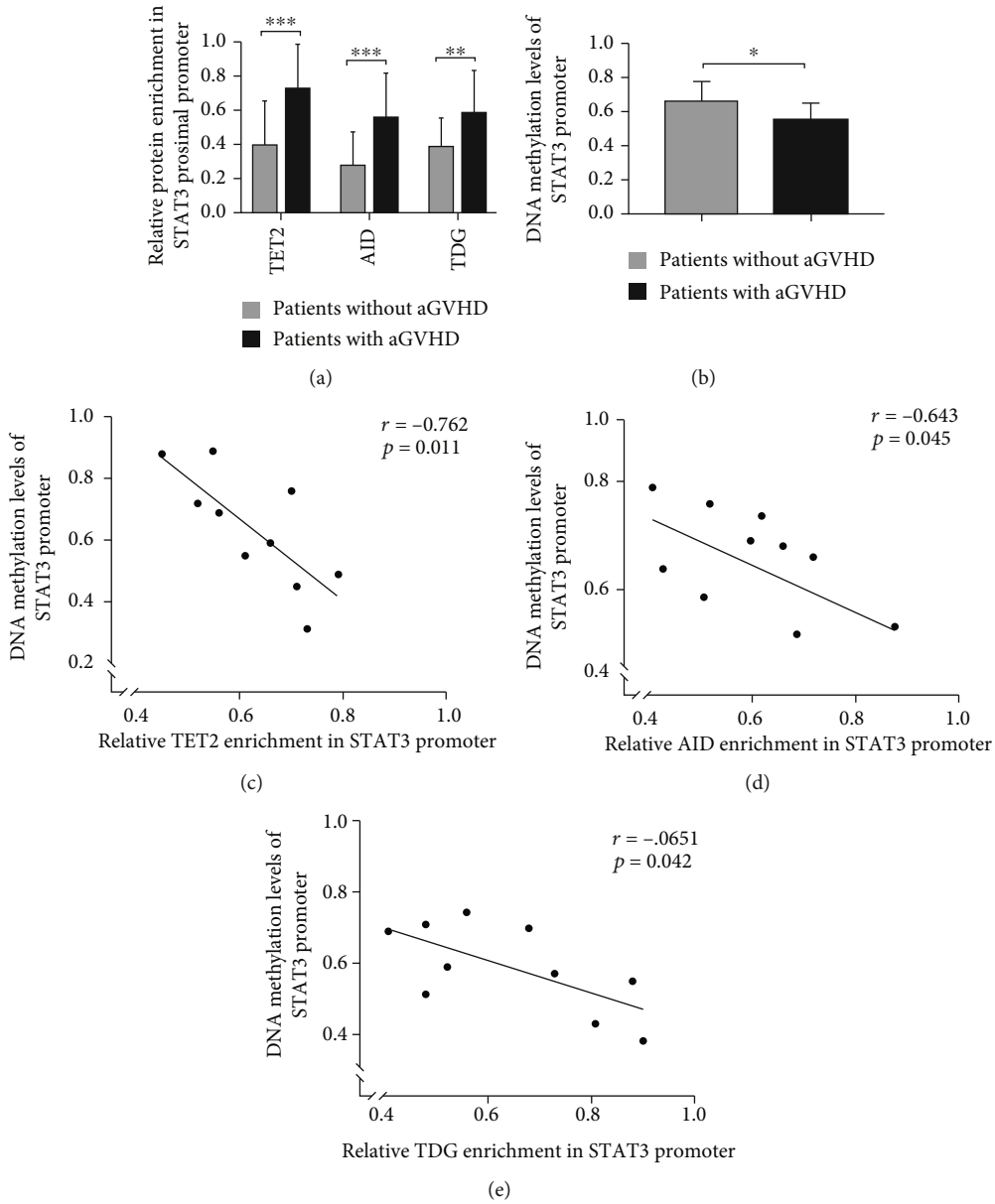

Figure 2: Binding level of TET2/AID/TDG in STAT3 promoter was extremely upregulated in aGVHD $CD4^+$ T cells. (a) ChIP-qPCR analysis of the binding level of TET2/AID/TDG in the STAT3 promoter region in $CD4^+$ T cells from patients with ($n = 23$) or without ($n = 23$) aGVHD. (b) DNA methylation level of STAT3 promoter in $CD4^+$ T cells from aGVHD patients ($n = 10$) or non-aGVHD patients ($n = 10$) (0 = unmethylated; 0.5 = 50%methylated). (c–e) Correlation between relative TET2, AID, and TDG enrichment and DNA methylation in STAT3 promoter in aGVHD-$CD4^+$ T cells ($r = -0.762$, $p = 0.011$; $r = -0.643$, $p = 0.045$; $r = -0.651$, $p = 0.042$; $n = 10$) (0 = unmethylated; 0.5 = 50%methylated); $^*p < 0.05$, $^{**}p < 0.01$, $^{***}p < 0.001$.

3.2. Binding Levels of TET2, AID, and TDG in STAT3 Promoter Were Obviously Enhanced in $CD4^+$ T Cells from aGVHD Patients. We investigated whether the binding levels of TET2/AID/TDG in STAT3 promoter were significantly upregulated in $CD4^+$ T cells of aGVHD patients. The binding levels of these proteins were measured by ChIP-qPCR in $CD4^+$ T cells from patients with or without aGVHD. Compared with patients without aGVHD, the binding levels were remarkably increased in $CD4^+$ T cells from aGVHD patients (Figure 2(a)). In addition, the DNA methylation of STAT3 promoter was detected in both groups. Figure 2(b) shows marked hypomethylation in STAT3 promoter in $CD4^+$ T cells from aGVHD patients as compared to non-GVHD $CD4^+$ T cells. As shown in Figures 2(c)–2(e), the relative TET2/AID/TDG enrichment in STAT3 promoter was inversely correlated with DNA methylation level of STAT3 promoter in aGVHD $CD4^+$ T cells. The core content of our study was to explore whether HMGB1 induced demethylation of STAT3 promoter by recruiting these DNA demethylases, and the three enzymes indeed participate in the process of DNA demethylation, and their functions are clear. In the other hand, certain studies have shown that TET, AID, and TDG could form complex to mediate the catalytic conversion of 5-methylcytosine to cytosine in the program of

DNA demethylation. Therefore, the three proteins were interfered or overexpressed simultaneously in our experiment. Firstly, interference plasmids were transfected into aGVHD $CD4^+$ T cells to repress the expression of TET2/AID/TDG (Figures 3(a)–3(c)). The binding levels of TET2/AID/TDG in STAT3 promoter were decreased after the TET2/AID/TDG interference in aGVHD $CD4^+$ T cells (Figure 3(d)). Moreover, the DNA methylation level of STAT3 promoter was increased in aGVHD $CD4^+$ T cells transfected with the TET2/AID/TDG interfering plasmid (Figure 3(e)). Next, the TET2/AID/TDG overexpression plasmids were transfected into non-aGVHD $CD4^+$ T cells (Figures 3(f)–3(g)). The binding levels were upregulated after the overexpression of TET2, AID, and TDG in $CD4^+$ T cells from non-aGVHD patients (Figure 3(h)). Simultaneously, the DNA methylation level of STAT3 promoter was significantly downregulated in non-GVHD $CD4^+$ T cells with the overexpression of TET2/AID/TDG (Figure 3(i)). Taken together, excessive accumulation of TET2/AID/TDG complexes was observed in the STAT3 promoter region in aGVHD $CD4^+$ T cells, which were strongly associated with DNA demethylation of STAT3 promoter.

3.3. HMGB1 Promoted TET2, AID, and TDG Binding to STAT3 Promoter. HMGB1 increased the expression of STAT3 by modulating DNA demethylation of STAT3 promoter in $CD4^+$ T cells, Hence, we investigated whether this process was correlated with TET2, AID, and TDG. Co-IP was performed in Jurkat cells to test whether HMGB1 form a complex with TET2, AID, and TDG. The results showed that HMGB1 coprecipitated with TET2, AID, and TDG (Figure 4(a)). Combine with Figure 1, we speculated that HMGB1 firstly bound to STAT3 promoter and then recruited TET2, AID, and TDG to form a complex in the promoter region to induce DNA demethylation. Next, we collected peripheral blood from patients with aGVHD or without aGVHD. pCDNA 3.1-HMGB1 was transfected into non-aGVHD $CD4^+$ T cells to increase the HMGB1 expression (Figures 4(b)–4(d)). In comparison to the negative control group, the binding levels of TET2/AID/TDG in STAT3 promoter were significantly increased in HMGB1-overexpressed non-aGVHD $CD4^+$ T cells (Figure 4(e)). Thereafter, HMGB1 was performed silenced in aGVHD $CD4^+$ T cells (Figures 4(f)–4(h)). Compared with control cells, the binding levels reduced greatly in HMGB1-deficient aGVHD $CD4^+$ T cells (Figure 4(i)). These data strongly demonstrated that HMGB1 could recruit TET2, AID, and TDG to bind to STAT3 promoter.

3.4. HMGB1 Regulated TET2/AID/TDG to Increase the STAT3 Expression through DNA Demethylation in STAT3 Promoter. We hypothesized that TET2/AID/TDG played important roles in increasing the STAT3 expression, and the process was regulated by HMGB1 in aGVHD. Normal $CD4^+$ T cells were divided into three groups based on different plasmid transfections (negative control plasmid; HMGB1 overexpression plasmid; HMGB1 overexpression plasmid and TET2/AID/TDG interference plasmid). The expression of the STAT3 and DNA methylation level of STAT3 promoter in $CD4^+$ T cells from diverse groups was measured by Western blot and bisulfite sequencing (Figures 5(a)–5(c)). Compared with the negative control group, the STAT3 expression was significantly increased in $CD4^+$ T cells transfected with HMGB1 overexpression plasmids. Strikingly, when the TET2/AID/TDG interference was superposed, the expression of STAT3 was also higher than that in the control group, while the expression sharply declined compared with the HMGB1-overexpressed group of $CD4^+$ T cells. Meanwhile, the DNA methylation level of STAT3 promoter was majorly decreased after the overexpression of HMGB1 in normal $CD4^+$ T cells. However, after the overexpression of HMGB1 and inhibition of TET2/AID/TDG in normal $CD4^+$ T cells, the methylation level was not obviously different from the control group. Compared with HMGB1-overexpressed $CD4^+$ T cells, the methylation level was increased in cells cotransfected with HMGB1 overexpression plasmids and TET2/AID/TDG interference plasmids. Taken together, these results demonstrated that HMGB1 could induce DNA demethylation of STAT3 promoter by recruiting TET2/AID/TDG. There may be other downstream molecules involved in the process by which HMGB1 facilitates the overexpression of STAT3 in aGVHD $CD4^+$ T cells.

4. Discussion

DNA methylation is a powerful epigenetic mechanism, and its function seems to vary based on the surrounding environment [20]. The regulation of gene transcription or chromatin structure induced by DNA methylation participates in various pathological processes, such as inflammation, and human diseases including immunological diseases [21, 22]. For example, DNA hypomethylation in STAT3 promoters contributed to rheumatoid arthritis by controlling the activation and differentiation of immune cells [23]. Therefore, it was important to explore the function of DNA methylation in aGVHD.

Demethylases as the vital driving forces involve in the process of active DNA demethylation [16]. The discovery of the TET family proteins marked the beginning of a completely new chapter to the history of DNA demethylation, and the TET proteins are the key molecules to start the program of DNA demethylation [24]. This family include three members: TET1, TET2, and TET3; thereinto, TET2 is mainly expressed in the hemopoietic system [24, 25]. Mediating the catalytic conversion of 5-mC to 5-hmC, 5-fC ,and 5-caC is the prominent function of TET proteins in the process of active DNA demethylation [26]. AID participates in adaptive immune response, which is predominantly found in mature B cells [27]. AID regulates the hematopoietic system by influencing the differentiation of bone marrow cells and red cells [28]. Besides, TET2 and AID could form a complex to induce DNA demethylation in biological processes [28]. TDG, the pivotal enzyme of BER, act as an important downstream molecule of TET and AID to regulate demethylation of CpG sites in DNA [29, 30]. From the above, TET and AID play important roles in the hemopoietic system and immune system, and they also engage in DNA demethylation with TDG.

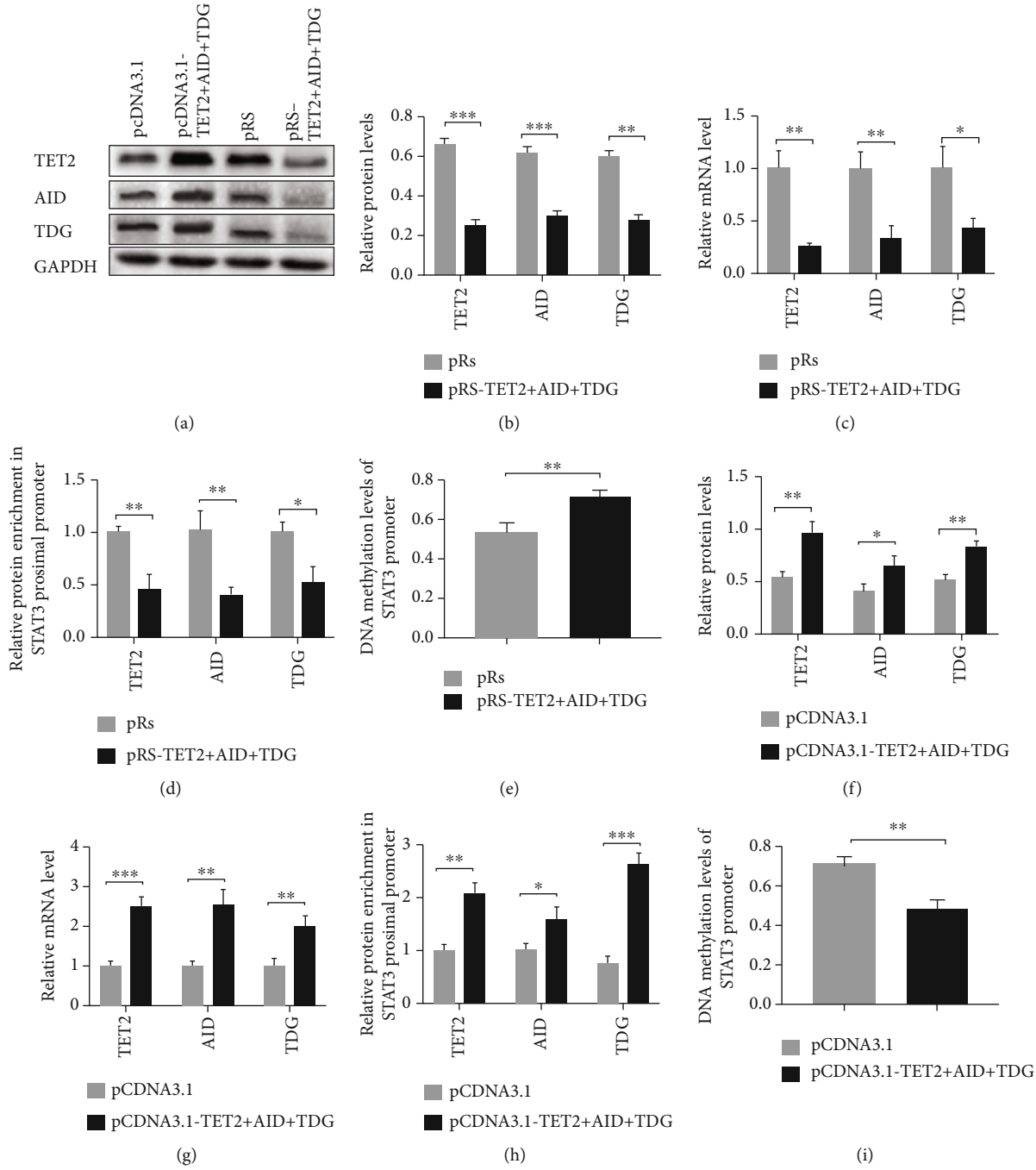

Figure 3: Interference with TET2/AID/TDG in aGVHD $CD4^+$ T cells could induce DNA hypermethylation of STAT3 promoter. (a) Representative Western blot results for TET2, AID, TDG, and GAPDH levels. (b), (c) Quantitative analysis of the (b) relative protein levels and (c) relative mRNA levels of TET2, AID, and TDG in aGVHD $CD4^+$ T cells transfected with TET2/AID/TDG interference plasmids or control plasmid. (d), (e) The binding levels of (d) TET2/AID/TDG in STAT3 promoter and (e) DNA methylation level of STAT3 promoter in TET2/AID/TDG-deficient aGVHD $CD4^+$ T cells or control aGVHD $CD4^+$ T cells. (f), (g) Quantitative analysis of the (f) relative protein levels and (g) relative mRNA levels of TET2, AID, and TDG in non-aGVHD $CD4^+$ T cells transfected with TET2/AID/TDG overexpression plasmids or control plasmids. (h), (i) (h) The binding levels and (i) DNA methylation level in TET2/AID/TDG overexpressed non-aGVHD $CD4^+$ T cells or control cells. Data represent the mean of three independent experiments (0 = unmethylated; 0.5 = 50%methylated); $^*p < 0.05$, $^{**}p < 0.01$, $^{***}p < 0.001$.

In addition, the enzymes are also relevant in the pathological processes. Increased 5-hmC, an important cause of overreactivity of $CD4^+$ T cells, was correlated with upregulated TET2 in SLE patients [31]. Besides, the overexpression of TET2 promoted follicular helper-like T cells to worsen SLE via increasing some regulatory factors (sialophorin, signal transducing activator of transcription 5b and B cell lymphoma 6), and the process was associated with DNA

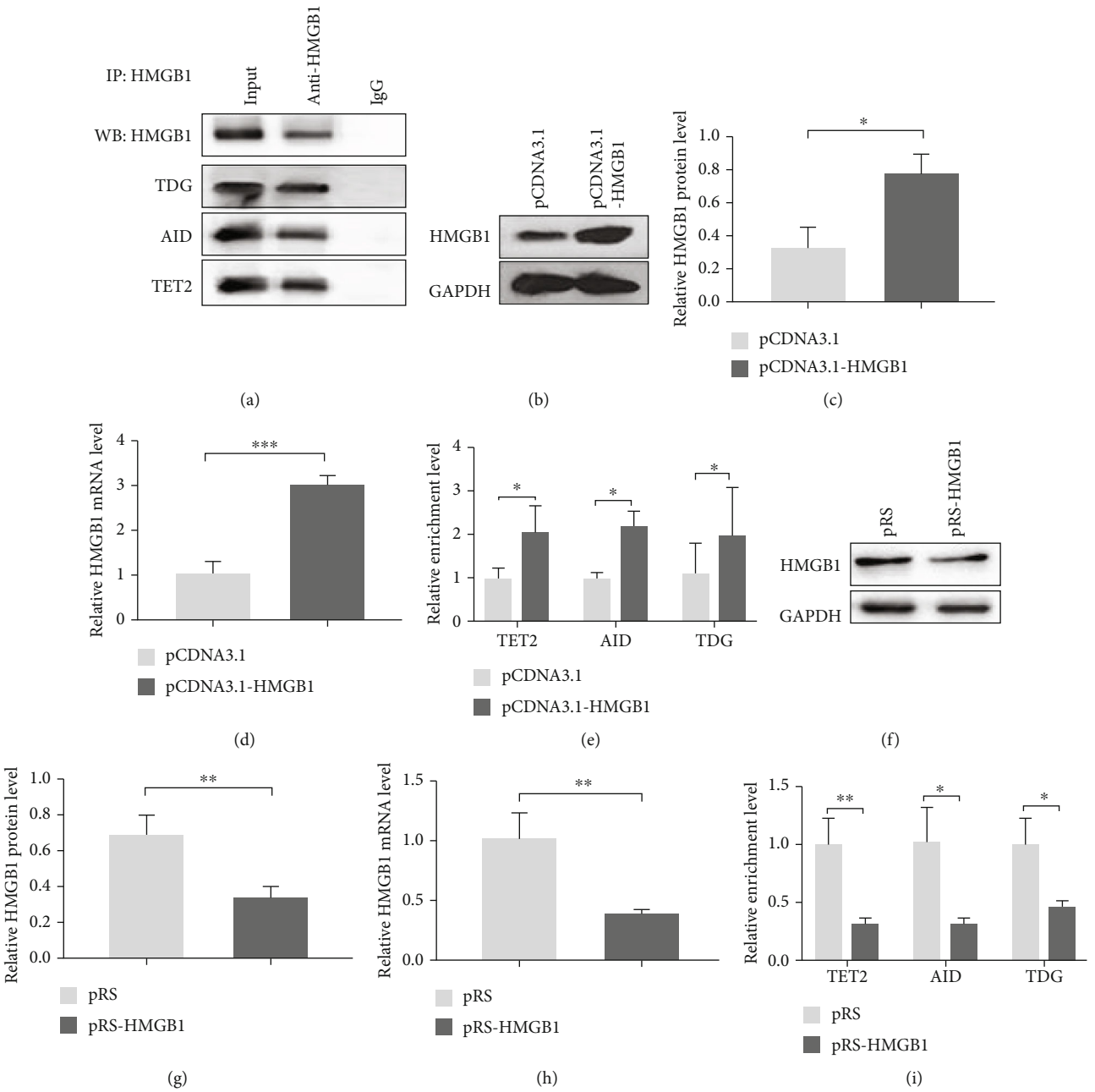

Figure 4: HMGB1 recruited TET2, AID, and TDG to bind to STAT3 promoter. (a) The combination of HMGB1 and TET2/AID/TDG was detected by Co-IP in Jurkat cells and analyzed by western blot analysis. (b–d) Representative western blotting results for (b) HMGB1, (c) relative HMGB1protein level, and (d) mRNA level in non-GVHD $CD4^+$ T cells transfected with the HMGB1 overexpression plasmid or negative control plasmid. (e) The binding levels of TET2/AID/TDG in STAT3 promoter in HMGB1-overexpressed non-aGVHD $CD4^+$ T cells and control cells. (f–i) After interference with HMGB1 in aGVHD $CD4^+$ T cells, representative western blotting results for (f) HMGB1, (g) relative HMGB1 protein level, (h) relative HMGB1 mRNA level, and (i) the binding levels were detected. Experiments were repeated three times. Data are presented as the mean ± SD of three independent experiments. $^*p < 0.05$, $^{**}p < 0.01$.

demethylation of these factors [32, 33]. The functions of AID in autoimmune diseases are well established. AID heterozygous MRL/lpr mice survived longer as compared to MRL/lpr mice, a significant model of SLE [34]. The excessive autoantibodies were correlated with the overexpression of AID in BXD2 mice, which are susceptible to autoimmune diseases [35]. Furthermore, the TET2/AID complex, which bound to the FA complementation group A (FANCA) promoter and induced its hypomethylation, facilitated oncogenic FANCA in diffuse large B cell lymphoma [36]. Our present study confirmed that TET2, AID, and TDG could form a complex, which was involved in DNA demethylation of STAT3 promoter in aGVHD-$CD4^+$ T cells.

HMGB1, derived from HMGB family, is ubiquitously expressed in whole adult tissues and plays a critical role in gene transcription [37, 38]. HMGB1 assists other molecules

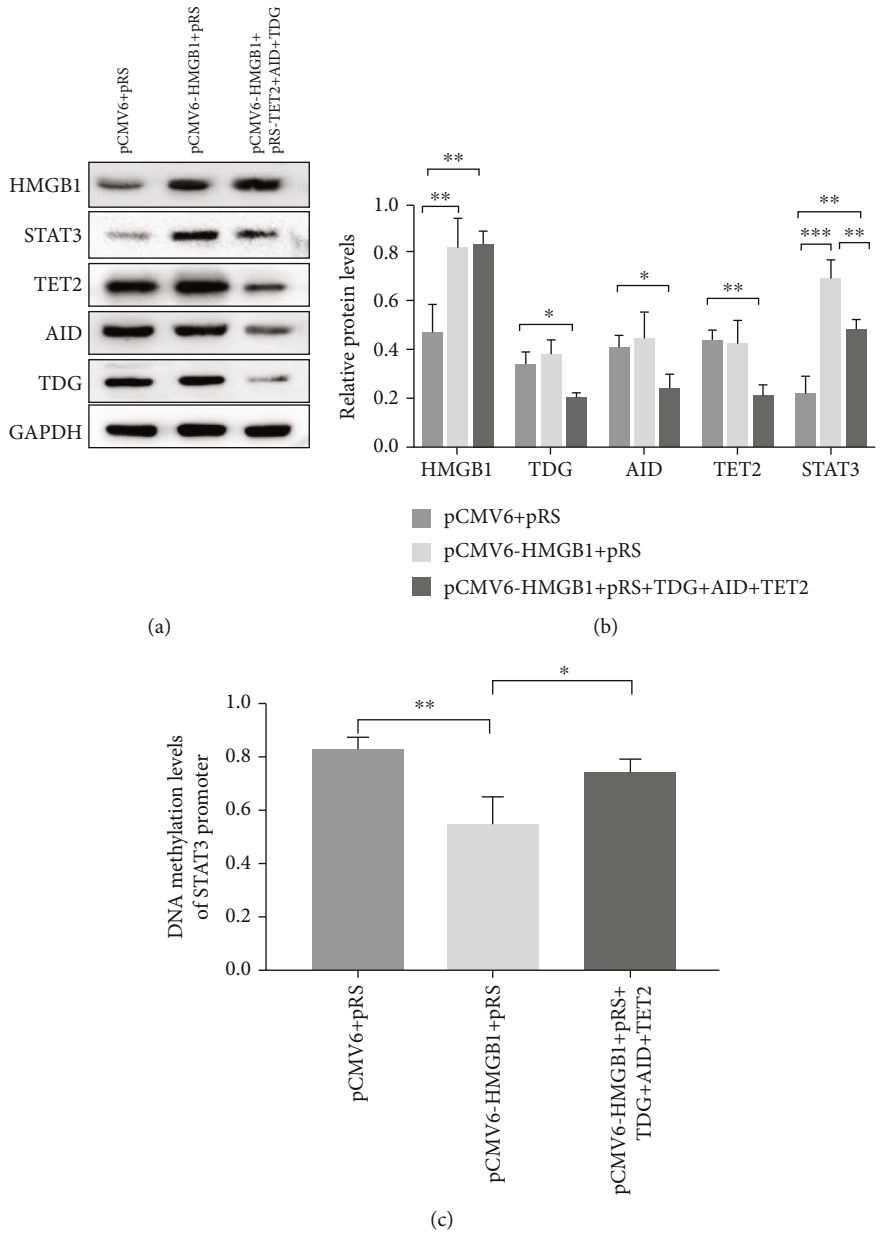

Figure 5: The overexpression of STAT3 induced by HMGB1 could be partially disrupted in $CD4^+$ T cells transfected with the TET2/AID/TDG interference plasmid. (a) Representative western blot results for HMGB1, TDG, AID, TET2, STAT3, and GAPDH levels. (b) Quantitative analysis of the relative protein levels of HMGB1, TDG, AID, TET2, and STAT3. (c) DNA methylation levels of STAT3 promoter in $CD4^+$ T cells transfected with different plasmids (control plasmids; HMGB1 overexpression plasmids; HMGB overexpression plasmids and TET2/AID/TDG interference plasmids); (0 = unmethylated, 1 = methylated). Data are presented as the mean ± SD of three independent experiments. $^*p < 0.05$, $^{**}p < 0.01$, $^{***}p < 0.001$.

such as organic cation/carnitine transporter1/2 and p53 to bind to target genes and facilitates DNA modification [39, 40]. HMGB1 could boost the Matn1 promoter activity via SRY-related high-mobility group box (SOX) trio in early chondrogenesis, and the binding efficiency of SOX trio in Matn1 promoter could be affected by HMGB1 [41]. Furthermore, HMGB1 formed complexes with proinflammatory factors to involve in inflammatory pathologies [42]. Reduction of HMGB1 could inhibit the expression of inflammatory cytokines [43]. Our results showed that HMGB1 increased the expression of STAT3 via recruiting TET2/AID/TDG to decrease DNA methylation level of STAT3 promoter. Moreover, there are other mechanisms underlying the overexpression of STAT3 induced by HMGB1 in $CD4^+$ T cells from aGVHD patients.

Moreover, the DNA methylation level continually undergoes a dynamic change. Cytosine is converted to 5-methylcytosine by DNA methyltransferases (DNMTs) using S-adenosyl-L-methionine to offer methyl to the C5 position of cytosine [44]. DNMTs play critical roles in the physiological and pathological processes. Varun et al. have shown that the methylation level of conserved noncoding sequence 2

(CNS2) played a decisive role to the Foxp3 expression, which was the critical factor to differentiation and maintenance function of Treg cells [45, 46]. The research exposed that TET2 and DNMTs were competitive and could not simultaneously bind to CNS2 [45]. When TET2 combined with CNS2, DNMTs could not make contact with CNS2, and the expression of Foxp3 or Treg cells will be at an advantage [45]. With the growth of the Treg cells, the disease severity will be gradually decreased in aGVHD patients. In addition, 5-Azac (5-azacytidine), the inhibitor of DNMTs, was utilized to prevent aGVHD in clinic and achieved good performance [47]. Inducing the demethylation of Foxp3 was an important function of 5-Azac in aGVHD [48]. From above studies, DNMTs will be inhibited in aGVHD patients with 5-Azac, and it may promote the combination between TET2 and CNS2. All the changes will increase Tregs to prevent aGVHD. On the contrary, our research revealed that massive TET2 aggravate progress of aGVHD by decreasing DNA methylation of STAT3 promoter. It is hint that the specific effect of demethylase or DNMTs in the disease process are dependent on their target gene. And to study the molecules, the upstream or downstream regulatory factors of the enzymes are of great practical significance. With the advent of the era of precision medicine, we have realized that more and more patients benefit from molecularly targeted drugs and personalized gene therapies. Therefore, exploring the precise effects of molecules in the pathological process may provide a new therapeutic target for disease prevention and treatment.

5. Conclusion

This study identified a mechanism of STAT3 over-expression in $CD4^+$ T cells from aGVHD patients. HMGB1 could recruit TET2, AID and TDG to facilitate expression of STAT3 via DNA hypomethylation of STAT3 promoter in aGVHD $CD4^+$ T cells. Suppression of TET2/AID/TDG expression through interference plasmids could partially decrease overexpression of STAT3 induced by HMGB1. These findings provide a theoretical basis to investigate new therapeutic targets for aGVHD prevention and treatment.

Data Availability

The data to support the findings of this study are available from the corresponding author upon request.

Conflicts of Interest

The authors declare no conflicts of interest regarding the publication of this paper.

Acknowledgments

Thanks to all of the subjects for their participation in the project. This work was supported by a grant from the National Natural Science Foundation of China (No. 81974002).

References

[1] Y. Chen, Y. Xu, G. Fu et al., "Allogeneic hematopoietic stem cell transplantation for patients with acute leukemia," *Chinese Journal of Cancer Research*, vol. 25, no. 4, pp. 389–396, 2013.

[2] B. R. Blazar, W. J. Murphy, and M. Abedi, "Advances in graft-versus-host disease biology and therapy," *Nature Reviews. Immunology*, vol. 12, no. 6, pp. 443–458, 2012.

[3] J. L. M. Ferrara, J. E. Levine, P. Reddy et al., "Graft-versus-host disease," *Lancet*, vol. 373, no. 9674, pp. 1550–1561, 2009.

[4] M. Murata, H. Nakasone, J. Kanda et al., "Clinical factors predicting the response of acute graft-versus-host disease to corticosteroid therapy: an analysis from the GVHD working group of the Japan Society for hematopoietic cell transplantation," *Biology of Blood and Marrow Transplantation*, vol. 19, no. 8, pp. 1183–1189, 2013.

[5] S. W. Choi, T. Braun, I. Henig et al., "Vorinostat plus tacrolimus/methotrexate to prevent GVHD after myeloablative conditioning, unrelated donor HCT," *Blood*, vol. 130, no. 15, pp. 1760–1767, 2017.

[6] Q.-R. Qi and Z.-M. Yang, "Regulation and function of signal transducer and activator of transcription 3," *World Journal of Biological Chemistry*, vol. 5, no. 2, pp. 231–239, 2014.

[7] Y. J. Xu, L. Li, Y. Chen et al., "Role of HMGB1 in regulation of STAT3 expression in CD4(+) T cells from patients with aGVHD after allogeneic hematopoietic stem cell transplantation," *Clinical Immunology*, vol. 161, no. 2, pp. 278–283, 2015.

[8] B. C. Betts, E. M. Sagatys, A. Veerapathran et al., "CD4+ T cell STAT3 phosphorylation precedes acute GVHD, and subsequent Th17 tissue invasion correlates with GVHD severity and therapeutic response," *Journal of Leukocyte Biology*, vol. 97, no. 4, pp. 807–819, 2015.

[9] L. Ulloa, F. M. Batliwalla, U. Andersson, P. K. Gregersen, and K. J. Tracey, "High mobility group box chromosomal protein 1 as a nuclear protein, cytokine, and potential therapeutic target in arthritis," *Arthritis and Rheumatism*, vol. 48, no. 4, pp. 876–881, 2003.

[10] S. Zheng, J. Yang, Y. Tang et al., "Effect of bone marrow mesenchymal stem cells transplantation on the serum and liver HMGB1 expression in rats with acute liver failure," *International Journal of Clinical and Experimental Pathology*, vol. 8, no. 12, pp. 15985–15992, 2015.

[11] Y. Li, C. Huang, M. Zhao et al., "A possible role of HMGB1 in DNA demethylation in CD4+ T cells from patients with systemic lupus erythematosus," *Clinical & Developmental Immunology*, vol. 2013, article 206298, 2013.

[12] O. Affinito, G. Scala, D. Palumbo et al., "Modeling DNA methylation by analyzing the individual configurations of single molecules," *Epigenetics*, vol. 11, no. 12, pp. 881–888, 2016.

[13] R. Zbieć-Piekarska, M. Spólnicka, T. Kupiec et al., "Development of a forensically useful age prediction method based on DNA methylation analysis," *Forensic Science International. Genetics*, vol. 17, pp. 173–179, 2015.

[14] N. Bhutani, D. M. Burns, and H. M. Blau, "DNA demethylation dynamics," *Cell*, vol. 146, no. 6, pp. 866–872, 2011.

[15] H. Wu and Y. Zhang, "Reversing DNA methylation: mechanisms, genomics, and biological functions," *Cell*, vol. 156, no. 1-2, pp. 45–68, 2014.

[16] K.-Y. Wang, C.-C. Chen, and C.-K. J. Shen, "Active DNA demethylation of the vertebrate genomes by DNA

methyltransferases: deaminase, dehydroxymethylase or demethylase?," *Epigenomics*, vol. 6, no. 3, pp. 353–363, 2014.

[17] A. Maiti and A. C. Drohat, "Thymine DNA glycosylase can rapidly excise 5-formylcytosine and 5-carboxylcytosine: potential implications for active demethylation of CpG sites," *Journal of Biological Chemistry*, vol. 286, no. 41, pp. 35334–35338, 2011.

[18] C. S. Nabel, H. Jia, Y. Ye et al., "AID/APOBEC deaminases disfavor modified cytosines implicated in DNA demethylation," *Nature Chemical Biology*, vol. 8, no. 9, pp. 751–758, 2012.

[19] D. Przepiorka, D. Weisdorf, P. Martin et al., "1994 consensus conference on acute GVHD grading," *Bone Marrow Transplantation*, vol. 15, no. 6, pp. 825–828, 1995.

[20] P. A. Jones, "Functions of DNA methylation: islands, start sites, gene bodies and beyond," *Nature Reviews. Genetics*, vol. 13, no. 7, pp. 484–492, 2012.

[21] T. Hamidi, A. K. Singh, and T. Chen, "Genetic alterations of DNA methylation machinery in human diseases," *Epigenomics*, vol. 7, no. 2, pp. 247–265, 2015.

[22] S. Horsburgh, P. Robson-Ansley, R. Adams, and C. Smith, "Exercise and inflammation-related epigenetic modifications: focus on DNA methylation," *Exercise Immunology Review*, vol. 21, pp. 26–41, 2015.

[23] K. Nakano, J. W. Whitaker, D. L. Boyle et al., "DNA methylome signature in rheumatoid arthritis," *Annals of the Rheumatic Diseases*, vol. 72, no. 1, pp. 110–117, 2013.

[24] M. Tahiliani, K. P. Koh, Y. Shen et al., "Conversion of 5-methylcytosine to 5-hydroxymethylcytosine in mammalian DNA by MLL partner TET1," *Science*, vol. 324, no. 5929, pp. 930–935, 2009.

[25] M. R. Branco, G. Ficz, and W. Reik, "Uncovering the role of 5-hydroxymethylcytosine in the epigenome," *Nature Reviews. Genetics*, vol. 13, no. 1, pp. 7–13, 2012.

[26] R. M. Kohli and Y. Zhang, "TET enzymes, TDG and the dynamics of DNA demethylation," *TDG and the dynamics of DNA demethylation, Nature*, vol. 502, no. 7472, pp. 472–479, 2013.

[27] M. Choudhary, A. Tamrakar, and A. K. Singh, "AID biology: a pathological and clinical perspective," *International Reviews of Immunology*, vol. 37, no. 1, pp. 37–56, 2018.

[28] H. Kunimoto, A. S. McKenney, C. Meydan et al., "Aid is a key regulator of myeloid/erythroid differentiation and DNA methylation in hematopoietic stem/progenitor cells," *Blood*, vol. 129, no. 13, pp. 1779–1790, 2017.

[29] T. Dodd, C. Yan, B. R. Kossmann, K. Martin, and I. Ivanov, "Uncovering universal rules governing the selectivity of the archetypal DNA glycosylase TDG," *Proceedings of the National Academy of Sciences*, vol. 115, no. 23, pp. 5974–5979, 2018.

[30] T. Lindahl, "Instability and decay of the primary structure of DNA," *Nature*, vol. 362, no. 6422, pp. 709–715, 1993.

[31] M. Zhao, J. Wang, W. Liao et al., "Increased 5-hydroxymethylcytosine in CD4(+) T cells in systemic lupus erythematosus," *Journal of Autoimmunity*, vol. 69, pp. 64–73, 2016.

[32] H. Wu, X. Huang, H. Qiu et al., "High salt promotes autoimmunity by TET2-induced DNA demethylation and driving the differentiation of Tfh cells," *Scientific Reports*, vol. 6, no. 1, p. 28065, 2016.

[33] X. Huang, H. Wu, H. Qiu et al., "The expression of Bcl-6 in circulating follicular helper-like T cells positively correlates with the disease activity in systemic lupus erythematosus," *Clinical Immunology*, vol. 173, pp. 161–170, 2016.

[34] C. Jiang, M. L. Zhao, and M. Diaz, "Activation-induced deaminase heterozygous MRL/lpr mice are delayed in the production of high-affinity pathogenic antibodies and in the development of lupus nephritis," *Immunology*, vol. 126, no. 1, pp. 102–113, 2009.

[35] H.-C. Hsu, P. Yang, J. Wang et al., "Interleukin 17-producing T helper cells and interleukin 17 orchestrate autoreactive germinal center development in autoimmune BXD2 mice," *Nature Immunology*, vol. 9, no. 2, pp. 166–175, 2008.

[36] J. Jiao, Y. Jin, M. Zheng et al., "AID and TET2 co-operation modulates FANCA expression by active demethylation in diffuse large B cell lymphoma," *Clinical and Experimental Immunology*, vol. 195, no. 2, pp. 190–201, 2019.

[37] D. S. Pisetsky, "The role of nuclear macromolecules in innate immunity," *Proceedings of the American Thoracic Society*, vol. 4, no. 3, pp. 258–262, 2007.

[38] M. Bustin and R. Reeves, "High-Mobility-Group Chromosomal Proteins: Architectural Components that Facilitate Chromatin Function," *Prog Nucleic Acid Res Mol Biol*, vol. 54, 1996.

[39] S. Zwilling, H. König, and T. Wirth, "High mobility group protein 2 functionally interacts with the POU domains of octamer transcription factors," *The EMBO Journal*, vol. 14, no. 6, pp. 1198–1208, 1995.

[40] L. Jayaraman, N. C. Moorthy, K. G. K. Murthy, J. L. Manley, M. Bustin, and C. Prives, "High mobility group protein-1 (HMG-1) is a unique activator of p53," *Genes & Development*, vol. 12, no. 4, pp. 462–472, 1998.

[41] T. Szénási, E. Kénesi, A. Nagy et al., "Hmgb1 can facilitate activation of the matrilin-1 gene promoter by Sox9 and L-Sox5/-Sox6 in early steps of chondrogenesis," *Biochimica et Biophysica Acta*, vol. 1829, no. 10, pp. 1075–1091, 2013.

[42] Y. N. Paudel, E. Angelopoulou, C. Piperi, V. R. M. T. Balasubramaniam, I. Othman, and M. F. Shaikh, "Enlightening the role of high mobility group box 1 (HMGB1) in inflammation: updates on receptor signalling," *European Journal of Pharmacology*, vol. 858, p. 172487, 2019.

[43] H. Mori, M. Murakami, T. Tsuda et al., "Reduced-HMGB1 suppresses poly(I:C)-induced inflammation in keratinocytes," *Journal of Dermatological Science*, vol. 90, no. 2, pp. 154–165, 2018.

[44] M. G. Goll and T. H. Bestor, "Eukaryotic cytosine METHYLTRANSFERASES," *Rev. Biochem*, vol. 74, no. 1, pp. 481–514, 2005.

[45] V. S. Nair, M. H. Song, M. Ko, and K. I. Oh, "DNA demethylation of the Foxp3 enhancer is maintained through modulation of ten-eleven- translocation and DNA methyltransferases," *Mol. Cells*, vol. 39, no. 12, pp. 888–897, 2016.

[46] S. Hori, T. Nomura, and S. Sakaguchi, "Control of regulatory T cell development by the transcription factor Foxp3," *Science*, vol. 299, no. 5609, pp. 1057–1061, 2003.

[47] X. Yang, F. Lay, H. Han, and P. A. Jones, "Targeting DNA methylation for epigenetic therapy," *Trends in Pharmacological Sciences*, vol. 31, no. 11, pp. 536–546, 2010.

[48] L. I. Sánchez-Abarca, S. Gutierrez-Cosio, C. Santamaría et al., "Immunomodulatory effect of 5-azacytidine (5-azaC): potential role in the transplantation setting," *Blood*, vol. 115, no. 1, pp. 107–121, 2010.

Hindawi
Journal of Immunology Research
Volume 2020, Article ID 2670527, 11 pages
https://doi.org/10.1155/2020/2670527

Research Article

sB7H3 in Children with Acute Appendicitis: Its Diagnostic Value and Association with Histological Findings

Xiaochen Du,[1,2] Yan Chen,[3] Jie Zhu,[4] Zhenjiang Bai,[1] Jun Hua,[1,2] Ying Li,[1] Haitao Lv,[5] and Guangbo Zhang[6]

[1]*Department of Emergency and Intensive Care Unit, Children's Hospital of Soochow University, Suzhou, Jiangsu Province 215025, China*
[2]*Department of Emergency, Children's Hospital of Wujiang District, Suzhou, Jiangsu Province 215200, China*
[3]*Department of General Surgery, The First Affiliated Hospital of Soochow University, Suzhou, Jiangsu Province 215006, China*
[4]*Department of Pediatric Surgery, Children's Hospital of Soochow University, Suzhou, Jiangsu Province 215025, China*
[5]*Department of Cardiology, Children's Hospital of Soochow University, Suzhou, Jiangsu Province 215025, China*
[6]*Institute of Clinical Immunology, The First Affiliated Hospital of Soochow University, Suzhou, Jiangsu Province 215006, China*

Correspondence should be addressed to Haitao Lv; haitaosz@163.com and Guangbo Zhang; zhanggbsuzhou@hotmail.com

Received 18 April 2020; Revised 19 June 2020; Accepted 27 July 2020; Published 1 September 2020

Guest Editor: Xinyi Tang

Copyright © 2020 Xiaochen Du et al. This is an open access article distributed under the Creative Commons Attribution License, which permits unrestricted use, distribution, and reproduction in any medium, provided the original work is properly cited.

Background. Several efforts have been made to find out a valuable marker to assist the diagnosis and differentiation of gangrenous/perforated appendicitis. We aimed to determine the diagnostic capacity of soluble B7H3 (sB7H3) in acute appendicitis (AA) and its accuracy as a predictor of the severity of appendicitis. *Methods*. 182 children were allocated into four groups as follows: control group (CG, 90), simple appendicitis (SA, 12), purulent appendicitis (PA, 49), and gangrenous appendicitis (GA, 31). Prior to appendectomy, blood was collected and sent for analysis of routine examination and cytokines (sB7H3 and TNF-α). We compared values of all measured parameters according to histological findings. Furthermore, we assigned AA patients into the nonperforated appendicitis group and the perforated appendicitis group. The diagnostic effects of significant markers were assessed by ROC curves. *Results*. Only the levels of CRP, FIB, and sB7H3 had a remarkable rising trend in AA-based groups, while differences in the levels of CRP and FIB between simple appendicitis and purulent appendicitis were not statistically significant. In addition, sB7H3 was found as the only marker in children with AA, which was markedly associated with the degree of histological findings of the appendix. Furthermore, sB7H3 had a high diagnostic value in predicting AA and complex appendicitis (PA+GA) in children. However, the diagnostic performance of sB7H3 for distinguishing PA from GA was not remarkable. Additionally, only the levels of CRP and sB7H3 were statistically different between the nonperforated appendicitis group and the perforated appendicitis group. The diagnostic performance of CRP and sB7H3 could not merely predict perforation of AA in children; however, the diagnostic performance was improved after combination. *Conclusions*. sB7H3 could be used as a valuable marker to predict the presence of AA and complex AA in children. However, the diagnostic value of sB7H3 to predict gangrenous/perforated appendicitis was not found to be remarkable. The combination of sB7H3 and CRP might improve the prediction of perforated appendicitis.

1. Introduction

Acute abdominal pain is one of the frequent chief complaints of children; acute appendicitis (AA) is the most common surgical emergency in the pediatric population [1]. It has been estimated that appendectomy was annually carried out on 72,000 children in the United States [2]. Compared with adults, performing a clinical diagnosis of appendicitis in children is often difficult due to their incomplete history and atypical symptoms.

Although controversy exists in the literature about the exact clinical classification, appendicitis can be classified as "simple" or "complicated." Complicated appendicitis is associated with a variety of potentially serious complications like

generalized peritonitis, abscess formation, and small bowel obstruction. Furthermore, a delayed diagnosis and surgery for AA are associated with increased perforation rate for both children and adults [3]. In addition, the perforation of the inflamed appendix may result in peritonitis or intra-abdominal abscess formation. Simultaneously, overdiagnosis may result in expensive interhospital transfers and unnecessary surgery.

White blood cell (WBC) count and C-reactive protein (CRP) are frequently used by surgeons in emergency departments to diagnose AA, especially in children, women at the age of fertility, and elderly patients when diagnosis is difficult. Studies on the diagnostic value of WBC and CRP for diagnosing appendicitis in children have reported contradictory results [4, 5]. It has been demonstrated that novel inflammatory biomarkers, such as calprotectin, lactoferrin, high-mobility group protein B1 (HMGB1), and hepcidin, appear to be promising for the diagnosis of suspected appendicitis [6, 7]. However, further exploration of these markers, as well as potential others, needs to be conducted [8].

Additionally, B7-H3, a new member of the B7 superfamily, acts as both a T cell costimulator and coinhibitor. The expression of B7-H3 protein can be induced by inflammatory cytokines, thereby playing a pivotal role in the regulation of T cell-mediated immune response [9]. Our previous studies have identified that circulating B7H3 levels in the cerebrospinal fluid (CSF) and plasma of children with bacterial meningitis are helpful markers to differentiate bacterial from aseptic meningitis, and circulating B7H3 level was demonstrated to be useful in evaluating the intensity of the infectious inflammatory process in the central nervous system of children [10]. Furthermore, we reported that patients diagnosed with sepsis, in contrast to healthy individuals, exhibited significant levels of raised plasma sB7H3 and that level correlated with the clinical outcome [11]. However, to date, no previous studies have assessed an association between sB7H3 level and AA.

Thus, the main aim of this prospective single-center study was to determine the diagnostic capacity of sB7H3 in pediatric patients with AA. Furthermore, the accuracy of sB7H3 as a predictor of the severity of appendicitis was assessed.

2. Materials and Methods

2.1. Study Population. A total of 92 children suspicious of having AA who were admitted to Children's Hospital of Soochow University (Suzhou, China) and underwent open or laparoscopic appendectomies between April 2015 and October 2015 were enrolled in the present study. Among them, 62 cases were male (Table 1). Included children aged at the range of 11 months and 14 years with continuous pain in the lower right abdomen and tenderness in the lower right abdomen who were highly suspicious of having AA. The diagnosis was conducted on the basis of pathological findings. Patients with symptoms who improved after conservative treatment, chronic appendicitis, and normal appendix were excluded.

In the present study, patients with AA were assigned to three groups based on the histological diagnosis: (a) simple appendicitis (SA) ($n = 12$), (b) purulent appendicitis (PA) ($n = 49$), and (c) gangrenous appendicitis (GA) ($n = 31$). The typical histology of AA at different stages was shown in Figure 1. Meanwhile, 90 nonemergency inguinal hernia patients, who were age and gender matched, without pain in the abdomen and respiratory symptom were taken as the control group (CG) into account during the same period. According to the operative notes, all patients with AA were allocated to the nonperforated appendicitis group ($n = 71$) and the perforated appendicitis group ($n = 21$).

2.2. Ethics and Consent. The present study was approved by the Ethics Committee of Children's Hospital of Soochow University (Suzhou, China), and the written informed consent was obtained from parents or guardians of the recruited children prior to their enrolment. All experiments and procedures were conducted in accordance with the Declaration of Helsinki.

2.3. Routine Examination Determinations. Prior to appendectomy, a peripheral blood was sampled at admission and sent for blood routine testing, in addition to analysis of liver function and fibrinogen (FIB) level. Additionally, 2 mL serum was collected and centrifuged. Plasma samples were harvested and stored at -80°C for further experiment of sB7H3 and tumor necrosis factor-α (TNF-α) levels.

2.4. Measurement of Plasma sB7H3 and TNF-α Levels. The level of TNF-α was measured by using an enzyme-linked immunosorbent assay (ELISA) kit (R&D Systems, Minneapolis, MN, USA). The sB7H3 analyses were determined by using enzyme-linked immunosorbent assay (ELISA) kits (Suzhou Xuguang Kexing Biological Technology Co. Ltd., Suzhou, China) as previously described [12].

2.5. Statistical Analysis. In the present study, statistical analysis was conducted by using SPSS 22.0 software (IBM, Armonk, NY, USA). Measured data were expressed as mean ± standard deviation (SD). Enumeration data were expressed as rate (%). Moreover, Student's t-test and Mann–Whitney U test were used for comparing normally distributed and nonnormally distributed data between the groups, respectively. For comparing more than two groups, one-way analysis of variance (ANOVA) was employed, in addition to the Kruskal-Wallis test if data were nonnormally distributed. A chi-square test was used for comparing the rates between the acute nonperforated appendicitis group and the perforated appendicitis group, and then, the multivariate logistic regression analysis was utilized for the statistically significant markers. The diagnostic efficiency of these markers was evaluated by receiver operating characteristic (ROC) curves, and the cutoff values and area under the ROC curve (AUROC) of these markers were determined. The statistical significance was set at a two-sided P value of 0.05.

Table 1: Demographic data and clinical characteristics of AA and control subjects.

Parameters	Control group ($N = 90$)	AA patients ($n = 92$)	AA-based groups ($N = 92$)			$H/F/\chi^2$	P
			SA ($N = 12$)	PA ($N = 49$)	GA ($N = 31$)		
Sex (M, %)	54 (60.00%)	62 (67.39%)	7 (58.33%)	36 (73.47%)	19 (61.29%)	2.871	0.412
Age (mean ± SD, years)	6.26 ± 2.48	$7.38 \pm 3.52^{\#\#\#}$	6.5 ± 1.78	7.80 ± 3.83	7.06 ± 3.50	4.830	0.185
Perforated appendicitis (N, %)	0 (0%)	21 (22.82%)$^{\#\#\#}$	0 (0%)	6 (12.24%)	15 (48.39%)	18.161	≤0.001
LOS (mean ± SD, days)	4.33 ± 0.91	$8.34 \pm 3.76^{\#\#\#}$	8.00 ± 2.09	7.65 ± 2.14	9.55 ± 5.63	122.480	≤0.001∗
Fever days (mean ± SD, days)	0	$2.23 \pm 1.86^{\#\#\#}$	1.17 ± 0.84	2.06 ± 1.78	2.90 ± 2.06	141.087	≤0.001∗
Thermal spike (mean ± SD, ˚C)	0	$38.69 \pm 0.67^{\#\#\#}$	38.42 ± 0.53	38.60 ± 0.64	38.90 ± 0.71	2.907	0.060
WBC (mean ± SD, 1000/μL)	9.38 ± 2.92	$16.72 \pm 5.51^{\#\#\#}$	15.04 ± 4.43	16.96 ± 5.30	17.00 ± 6.22	85.335	≤0.001∗
MCV (mean ± SD, fL)	78.99 ± 5.44	82.14 ± 4.83	82.08 ± 2.94	82.69 ± 4.42	81.29 ± 5.93	6.153	0.001∗
RDW (mean ± SD, %)	13.46 ± 1.66	14.10 ± 1.21	13.90 ± 0.84	14.12 ± 1.12	14.16 ± 1.48	3.053	0.030∗
MPV (mean ± SD, fL)	9.90 ± 0.80	$8.06 \pm 1.25^{\#\#}$	7.75 ± 1.09	8.14 ± 1.30	8.07 ± 1.25	79.596	≤0.001∗
PDW (mean ± SD, %)	10.92 ± 1.58	$13.06 \pm 2.99^{\#\#}$	12.51 ± 0.60	13.51 ± 3.20	12.57 ± 3.14	41.492	≤0.001∗
CRP (mean ± SD, mg/L)	0.42 ± 0.91	$61.21 \pm 52.18^{\#\#\#}$	28.92 ± 19.54	47.57 ± 43.87	95.27 ± 55.83	130.964	≤0.001∗
PLT (mean ± SD, 1000/μL)	320.1 ± 84.70	257.29 ± 78.63	260.75 ± 39.54	257.69 ± 86.67	255.32 ± 78.45	8.880	≤0.001∗
ALT (mean ± SD, U/L)	16.43 ± 6.41	15.37 ± 13.72	12.63 ± 3.44	14.77 ± 12.14	17.37 ± 17.37	0.818	0.486
AST (mean ± SD, U/L)	32.84 ± 10.45	32.52 ± 12.17	34.67 ± 8.39	32.03 ± 12.22	32.45 ± 13.51	0.184	0.907
ALP (mean ± SD, U/L)	262.81 ± 115.87	$205.20 \pm 55.31^{\#\#}$	199.34 ± 17.23	213.42 ± 55.60	194.48 ± 63.10	5.315	0.021∗
Tbil (mean ± SD, μmol/L)	7.07 ± 5.85	$12.98 \pm 9.29^{\#\#}$	10.33 ± 1.07	12.57 ± 7.91	14.66 ± 12.45	59.41	≤0.001∗
Ibil (mean ± SD, μmol/L)	4.94 ± 4.50	$8.64 \pm 7.40^{\#}$	6.92 ± 1.14	8.42 ± 6.60	9.67 ± 9.66	40.256	≤0.001∗
Dbil (mean ± SD, μmol/L)	2.13 ± 1.41	$4.31 \pm 2.57^{\#\#\#}$	3.41 ± 0.57	4.11 ± 2.00	5.00 ± 3.56	76.552	≤0.001∗
LDH (mean ± S D, U/L)	297.53 ± 99.64	284.81 ± 99.10	254.91 ± 21.28	283.61 ± 92.37	298.28 ± 124.20	3.787	0.285
FIB (mean ± SD, g/L)	2.50 ± 0.49	$3.61 \pm 1.08^{\#\#\#}$	3.21 ± 0.59	3.48 ± 0.86	3.99 ± 1.41	68.397	≤0.001∗
TNF-α (mean ± SD, pg/mL)	16.88 ± 5.18	$63.71 \pm 109.86^{\#\#\#}$	55.22 ± 33.73	56.13 ± 122.79	78.97 ± 108.19	28.930	≤0.001∗
sB7H3 (mean ± SD, ng/mL)	6.58 ± 2.38	$40.29 \pm 10.17^{\#\#\#}$	28.15 ± 4.50	40.02 ± 10.24	45.43 ± 7.24	143.057	≤0.001∗

AA: acute appendicitis; SA: simple appendicitis; PA: purulent appendicitis; GA: gangrenous appendicitis. Asterisks indicate that the reorganization data is nonnormal distribution, and the Kruskal Wallis test is used to analyze the differences between groups. The mean of other groups was compared by one-way ANOVA/Student's t-test for independent samples, and the rate was compared by the chi-square test. Statistically significant differences between AA patients and control group are shown in column 3 as $^{\#}P < 0.05$, $^{\#\#}P < 0.01$, and $^{\#\#\#}P < 0.001$. Statistically significant differences between four groups are shown in the last column. LOS: length of stay in hospital; WBC: white blood cell; MCV: mean corpuscular volume; RDW: red blood cell distribution width; MPV: mean platelet volume; PDW: platelet distribution width; CRP: C-reactive protein; PLT: platelet; ALT: alanine aminotransferase; AST: aspartate aminotransferase; ALP: alkaline phosphatase; Tbil: total bilirubin; Ibil: indirect bilirubin; Dbil: direct bilirubin; LDH: lactate dehydrogenase; FIB: fibrinogen; TNF-α: tumor necrosis factor-α.

3. Results

3.1. Demographic Data and Clinical Characteristics of Patients with AA. The demographic and clinical characteristics of patients with AA and CG are presented (Table 1). There was no difference in gender between the CG and the AA group ($P > 0.05$); the age of the AA group was slightly older than that of the CG ($P < 0.05$), but there was no significant difference in age between the CG and the AA-based group ($P > 0.05$). Perforated appendicitis and longer length of stay (LOS) in hospital in the AA group were significantly higher than those in the CG ($P < 0.05$), and there were differences between AA-based groups ($P < 0.05$). No fever in the CG was noted. But the number of fever days in the AA-based groups (SA, PA, and GA) showed an increasing trend ($P < 0.05$), and the difference in thermal spike was not statistically significant ($P > 0.05$).

The indexes in the AA group, including WBC, CRP, total bilirubin (Tbil), indirect bilirubin (Ibil), direct bilirubin (Dbil), FIB, TNF-α, and sB7H3, were significantly higher than those in the CG ($P < 0.05$), and there was a rising trend for these indexes among SA, PA, and GA in turn; however, the differences in CRP, FIB, and sB7H3 among the AA-based groups (SA, PA, and GA) were statistically

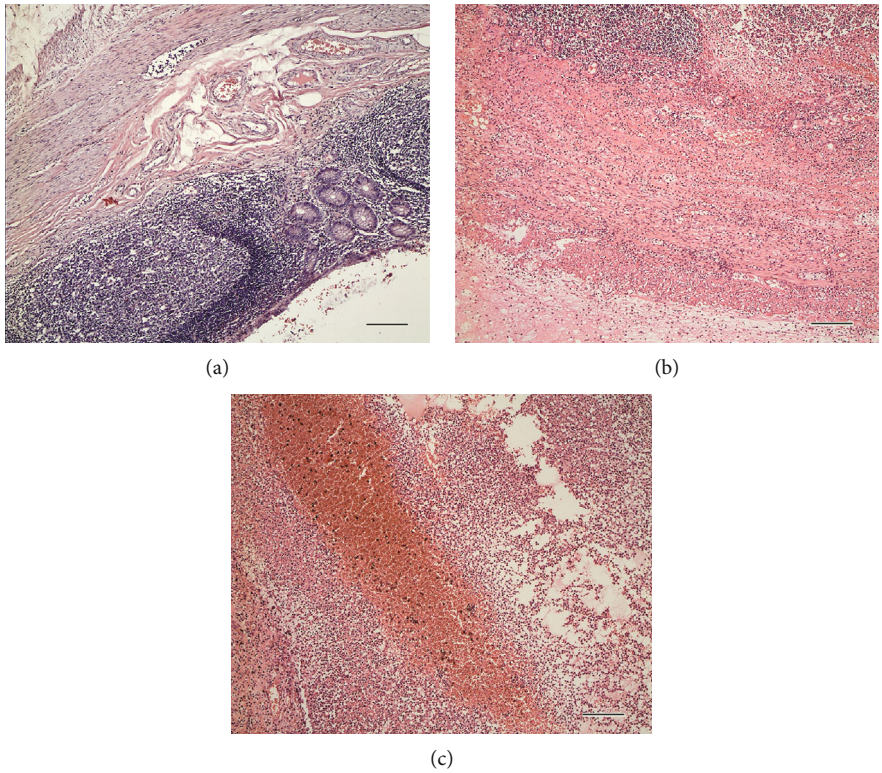

(a) (b) (c)

Figure 1: Typical histology of acute appendicitis at different stages (HE ×200). (a) Simple appendicitis: dilated and congested small blood vessels in the appendix wall, hyperplasia of mucosal lymphoid tissues, increased lymphoid follicles, enlarged germinal center, and obvious leukocyte adhesion in the local small mucosa of the mucosa. (b) Purulent appendicitis: dilated and congested small blood vessels in the appendix wall, neutrophil infiltration in each layer of tissue, fibrinous exudate, and necrosis in local mucosal layer tissue. (c) Gangrenous appendicitis: dilated and congested small blood vessels in the appendix wall, neutrophil infiltration in each layer of tissue, fibrinous exudate and necrosis, and hemorrhagic necrosis in whole layer of tissues. Internal scale bar = 50 μm.

significant ($P < 0.05$). In addition, the differences of CRP and FIB between the SA and PA groups were not statistically significant ($P > 0.05$) (Figure 2). Additionally, sB7H3 was found as the only marker in children with AA, which has remarkably associated with the degree of histological findings (Figure 1).

There were significant differences in mean corpuscular volume (MCV), red blood cell distribution width (RDW), mean platelet volume (MPV), platelet distribution width (PDW), platelet (PLT), and alkaline phosphatase (ALP) between the AA-based groups (SA, PA, and GA) and the CG, whereas the differences in alanine aminotransferase (ALT), aspartate aminotransferase (AST), and lactate dehydrogenase (LDH) were not statistically significant.

3.2. Analysis of Diagnostic Value of Markers for AA. The results of the receiver operating characteristic (ROC) curve analysis and evaluation of the above-mentioned parameters are expressed (Table 2). The markers with high accuracy ($0.9 < \text{AUROC} \leq 1$) for the diagnosis of AA were sB7H3 and CRP, respectively. The markers with moderate accuracy ($0.7 < \text{AUROC} \leq 0.9$) in the diagnosis of AA were WBC, Dbil, FIB, Tbil, PDW, Ibil, MCV, and RDW. The markers with low accuracy ($\text{AUROC} \leq 0.7$) in the diagnosis of AA were TNF-α (AUROC, 0.652), PLT (AUROC, 0.302), ALP (AUROC, 0.302), and MPV (AUROC, 0.119).

3.3. The Diagnostic Values of sB7H3 for Different Degrees of AA. The findings showed that sB7H3 had a high diagnostic accuracy for complex AA (PA+GA) (the cutoff value of sB7 H3 = 36.146 ng/mL, AUROC = 0.916). However, further results revealed that the diagnostic value of sB7H3 in distinguishing PA from GA in complex AA was not high (the cutoff value of sB7H3 = 34.950 ng/mL, AUROC = 0.748) (Figure 3).

The results of multivariate logistic regression analysis showed that only CRP ($t = -3.475$, $P = 0.002$) and sB7H3 ($t = -2.309$, $P = 0.023$) were statistically different between the nonperforated appendicitis group and the perforated appendicitis group. Further ROC curve analysis found that the AUROC values of CRP and sB7H3 were 0.734 (cutoff values of CRP = 67.005 mg/L, 0.714 SE, 0.747 SP) and 0.675 (cutoff values of sB7H3 = 48.033 ng/mL, 0.524 SE, 0.859 SP), respectively. However, the combination of a CRP level of 67.005 mg/L and a sB7H3 level of 48.033 ng/mL showed 57.1% SE and 84.5% SP, with AUROC of 0.735. The diagnostic performance of CRP and sB7H3 in children with AA was not remarkable, while the diagnostic performance was improved after combination (Table 3 and Figure4).

4. Discussion

Despite great familiarity with AA, this disease continues to pose a significant diagnostic challenge for clinicians. This is

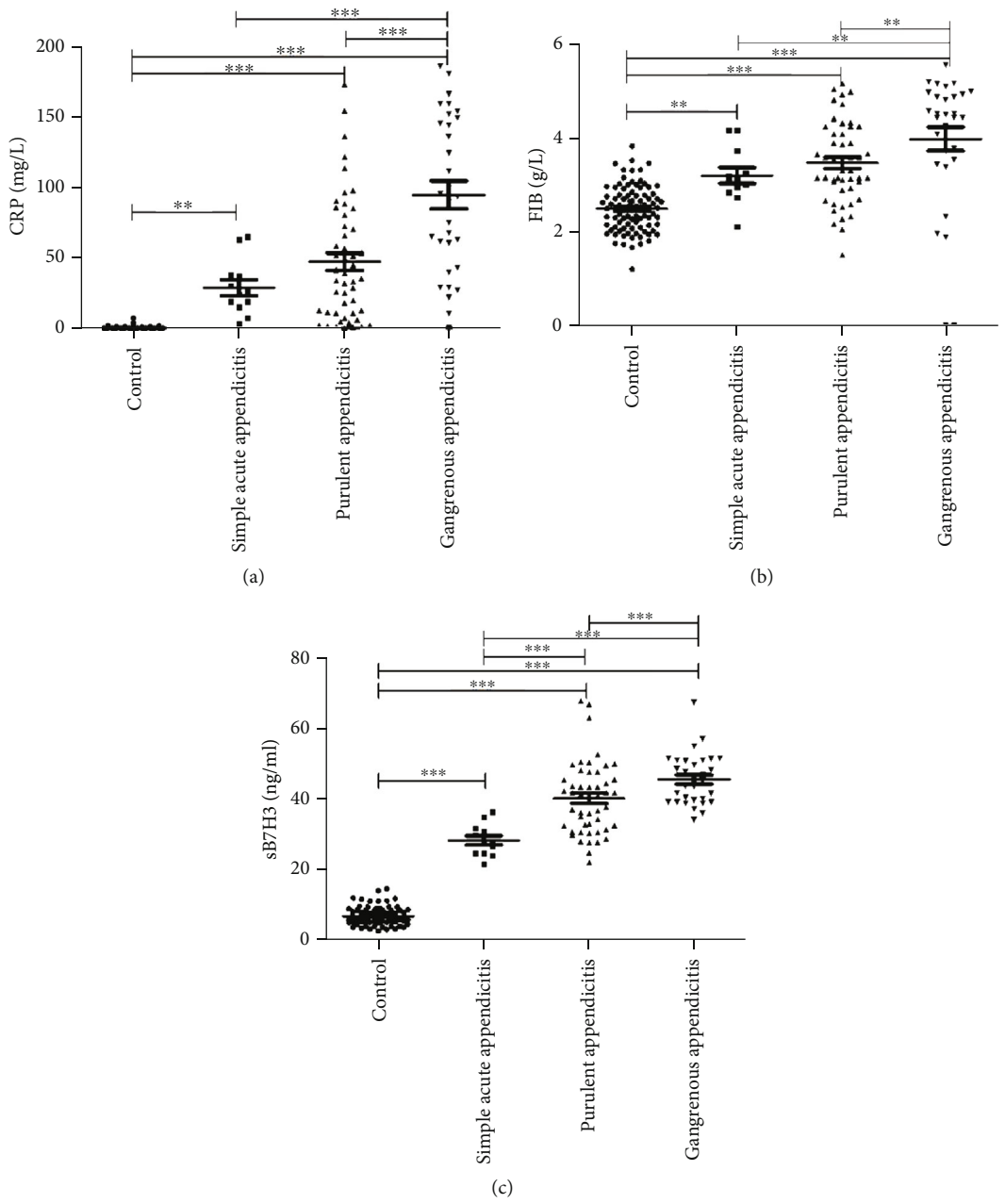

Figure 2: Distribution of CRP, FIB, and sB7H3 in the CG and the AA-based groups: (a) distribution of CRP, (b) distribution of FIB, and (c) distribution of sB7H3. Bars represent median values. Comparisons among the groups were performed using one-way analysis of variance with SNK t-test. Statistically significant differences between each patient group are shown as $*P < 0.05$, $**P < 0.01$, and $*** P < 0.001$. CG: control group; AA: acute appendicitis; CRP: C-reactive protein; FIB: fibrinogen; sB7H3: soluble B7H3.

partially confirmed in very young children whose history is not typical and whose examination results are also unreliable [13]. A delay in the diagnosis of AA could be attributed to nonspecific presentations, overlap of symptoms with a variety of common childhood illnesses, together with inability to express unreliable abdominal examination results in preschool children [14]. Biomarkers can improve the diagnostic performance of AA, especially in children, women at childbearing age, and elderly patients [15]. Traditional biomarkers, e.g., WBC, were found to have a moderate diagnostic performance, while being cost-effective in the diagnosis of AA. In contrast, novel biomarkers were found to be highly expensive, associating with complex compounds, while diagnostic performance can be improved [16].

Moreover, B7H3, also known as CD276, is an immune checkpoint molecule, belonging to the B7-CD28 family. This molecule is associated with costimulatory and coinhibitory functions in regulating T cell responses [17]. Expression of membrane CD276 (mB7H3) has been reported on dendritic cells, monocytes, activated T cells, and various carcinoma cells. The release of sB7H3 from cell surface is mediated by a matrix metalloproteinase and probably regulates

Table 2: The results of the receiver operating characteristic (ROC) curve analysis and evaluation of the above-mentioned parameters of blood markers for AA.

Parameters	Cutoff values	AUROC	Sensitivity (SE)	Specificity (SP)	PPV	NPV	+LR	-LR
sB7H3 (ng/mL)	17.850	1	1.000	1.000	1.000	1.000	—	0.000
CRP (mg/L)	1.905	0.983	0.935	0.967	0.966	0.935	0.280	0.001
WBC (1000/μL)	12.495	0.895	0.826	0.878	0.874	0.832	0.068	0.002
Dbil (μmol/L)	2.45	0.874	0.891	0.778	0.804	0.875	0.040	0.001
FIB (g/L)	3.11	0.845	0.728	0.911	0.893	0.766	0.082	0.003
Tbil (μmol/L)	8.315	0.831	0.761	0.789	0.787	0.763	0.036	0.003
PDW (%)	12.05	0.776	0.674	0.800	0.775	0.706	0.034	0.004
Ibil (μmol/L)	6.875	0.772	0.522	0.900	0.842	0.648	0.052	0.005
MCV (fL)	80.5	0.724	0.761	0.589	0.654	0.707	0.019	0.004
RDW (%)	12.85	0.711	0.902	0.456	0.629	0.820	0.017	0.002

The ROC curve is drawn by SPSS, and Youden's index is calculated by the corresponding coordinate value on the curve. The maximum value of Youden's index is the ideal cutoff value. AUROC: area under the curve; PPV: positive predictive value; NPV: negative predictive value; +LR: positive likelihood ratios; -LR: negative likelihood ratios; CRP: C-reactive protein; WBC: white blood cell; Dbil: direct bilirubin; FIB: fibrinogen; Tbil: total bilirubin; PDW: platelet distribution width; MCV: mean corpuscular volume; PDW: platelet distribution width; Ibil: indirect bilirubin; MCV: mean corpuscular volume; RDW: red blood cell distribution width.

B7H3R/B7H3 interactions in vivo [12]. Although no previous study has linked sB7H3 and appendicitis, there is a growing experience to use this marker for detecting other inflammatory conditions. For instance, sB7H3 levels could be significantly elevated in children with bacterial meningitis [10] and Mycoplasma pneumoniae pneumonia (MPP) [18]. Furthermore, Xu et al. [19] analyzed the sB7H3 levels in children with mild MPP and severe MPP and concluded that sB7H3 levels could be helpful for predicting the severity of MPP and investigating treatment efficacy.

In the present study, we included 92 AA patients and 90 inguinal hernia patients as CG to assess the role of sB7H3 levels for predicting the presence and degree of histological findings in children with AA. To our knowledge, this is the first study to evaluate the association between sB7H3 and AA. Although several blood markers can predict AA in children, our results showed that sB7H3 is the only marker, containing a significant correlation with the pathological degree of AA. Furthermore, we demonstrated that sB7H3 has a high diagnostic significance in predicting simple AA and complex AA (PA+GA) in children, and the corresponding values of AUROC were equal to 1.00 (cutoff value of sB 7H3 = 17.850 ng/mL) and 0.916 (cutoff value of sB7H3 = 36.146 ng/mL), respectively. However, the diagnostic performance of sB7H3 for distinguishing PA from GA was not found remarkable (cutoff value of sB7H3 = 34.950 ng/mL, AUROC = 0.746). In addition, our results also revealed that only CRP ($t = -3.475$, $P = 0.002$) and sB7H3 ($t = -2.309$, $P = 0.023$) were statistically different between the nonperforated appendicitis group and the perforated appendicitis group, with corresponding AUROC values of 0.734 (cutoff value of CRP = 67.005 mg/L) and 0.675 (cutoff value of sB7 H3 = 48.033 ng/mL), respectively. The diagnostic performance of CRP and sB7H3 was not significantly satisfactory to predict perforation of AA in children, while that performance was improved after combination. The AUROC value of 0.735 was achieved after combination of CRP with sB7H3 (57.1% SE and 84.5% SP). Thus, sB7H3 could be a beneficial marker for predicting the presence and severity of AA in children and might be involved in the pathogenesis of AA.

The exact pathogenesis of AA is multifactorial although it still remains elusive. It is irrefutable that obstruction of the lumen is usually present. In preschool children, this obstruction is typically due to lymphoid hyperplasia and less likely due to fecalith, as the appendix contains an excessive amount of lymphoid tissue in the submucosa [14]. Furthermore, the presence of a fecalith causes luminal obstruction, distention, and inflammation of the appendix wall, resulting in suppurative transmural inflammation, ischemia, infarction, and perforation of the appendix [20]. Numerous studies demonstrated that cytokines (e.g., interleukin-6 (IL-6)) [21] or acute phase proteins (e.g., CRP) could be used to predict the AA [1], control the severity of disease, and detect any complications [22]. Therefore, community-acquired intra-abdominal infection and inflammation play a significant role in the development of AA.

The findings of the present study demonstrated that the TNF-α level in the AA group was significantly higher than that in the CG, and there was a rising trend of TNF-α in the AA-based groups (SA, PA, and GA). Similar to our findings in appendicitis, a comparable result for TNF-α was found in a previously reported study [23]. The results of the current research revealed that bacteria, endotoxin, and other factors may cause an increase in the release of a number of cytokines (e.g., TNF-α) in AA. In addition, the results showed that sB7H3 and TNF-α both have a rising trend in the AA-based groups (SA, PA, and GA). Thus, the correlation between sB7H3 and TNF-α was investigated here. The findings disclosed positive correlations between plasma sB7H3 levels and TNF-α levels in patients with AA ($y = 1.3x + 9.85$, $R^2 = 0.087$, $P < 0.001$). However, no correlations were found between plasma sB7H3 levels and TNF-α levels in patients with SA ($P > 0.05$), PA ($P > 0.05$), and GA

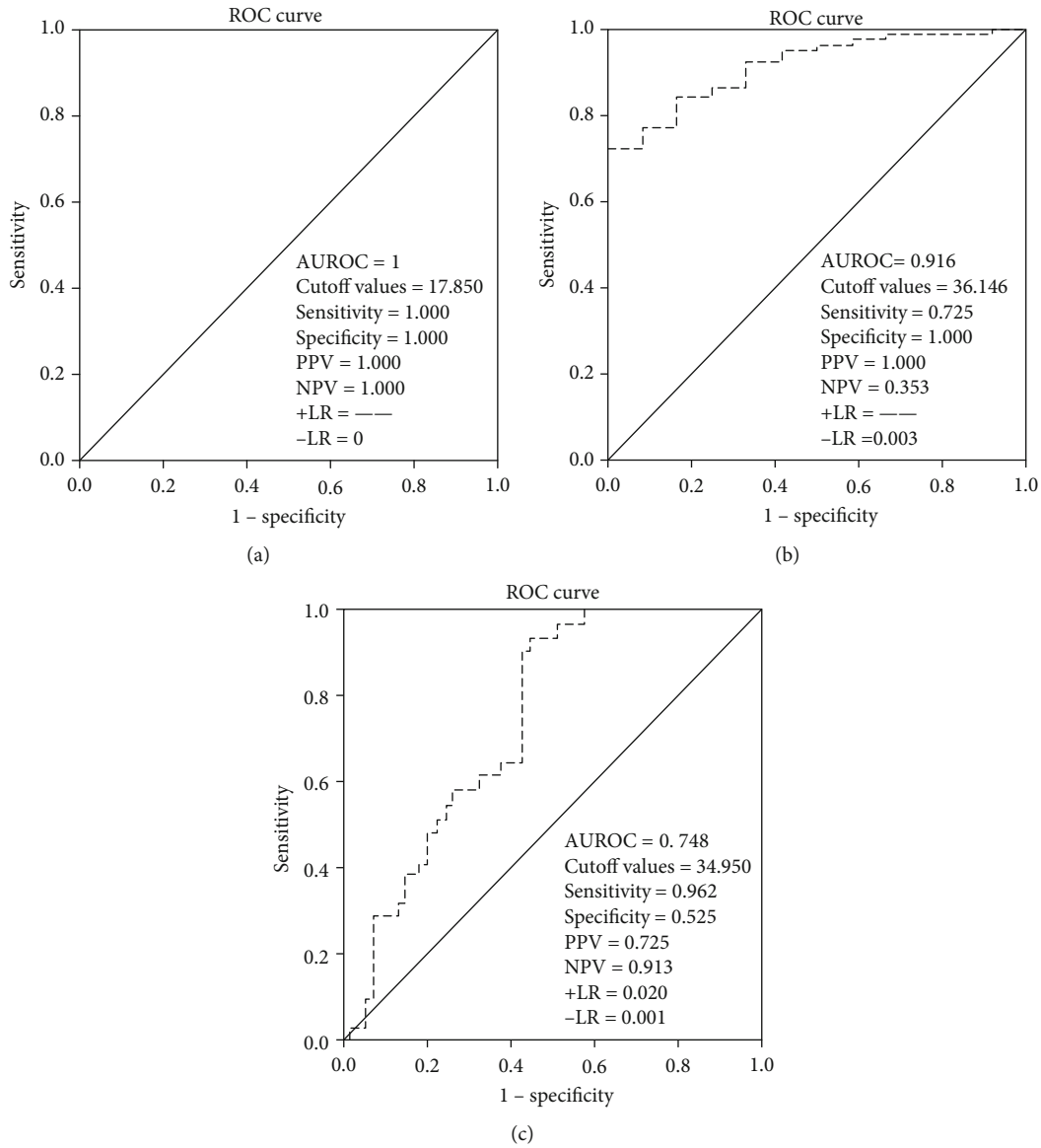

Figure 3: Different ROC curves and parameters for evaluation of sB7H3 for distinguishing different degrees of AA. The ROC curve is drawn by SPSS, and Youden's index is calculated by the corresponding coordinate value on the curve. The maximum value of Youden's index is the ideal cutoff value. (a) The ROC curve and parameters for evaluation of sB7H3 in the nonappendicitis group and the appendicitis group. (b) The ROC curve and parameters for evaluation of sB7H3 in the diagnosis of SA and complex AA (PA+GA). (c) The ROC curve and parameters for evaluation of sB7H3 for the diagnosis of PA and GA. AUROC: area under the curve; PPV: positive predictive value; NPV: negative predictive value; +LR: positive likelihood ratios; -LR: negative likelihood ratios.

($P > 0.05$). These data proved the existence of a relationship between sB7H3 with TNF-α. In our previous study, we observed that substantial amounts of sB7H3 were released from freshly isolated human monocytes upon stimulation with TNF-α compared with naive cells [11]. This evidence could explain the underlying mechanisms being responsible for the significantly elevated plasma sB7H3 levels observed in patients with AA.

The diagnostic accuracy of markers for the diagnosis of AA was found to be more accurate in the present study compared with previous studies, in which the AUROC values for WBC and CRP were 0.895 and 0.983, respectively (Table 2). A number of studies have taken nonspecific abdominal pain (NSAP) patients as CG into consideration. For instance, Oikonomopoulou et al. [24] selected 185 non-AA cases as CG. The CG included NSAP (151, 81.6%), followed by mesenteric lymphadenitis (16, 8.6%), ileitis (4, 2.2%), acute gastroenteritis (5, 2.7%), pneumonia (2, 1.1%), streptococcal pharyngitis (1, 0.5%), influenza type B virus (1, 0.5%), constipation (1, 0.5%), and intussusception (1, 0.5%). The AUROC values of leukocytes and CRP were 0.84 and 0.7, respectively. In another study, Kaiser et al. [7] recruited 25 NASP children who improved under conservative treatment and did not require surgical intervention and served as CG. The specific causes of NSAP were gastroenteritis (18, 72%), constipation (4, 16%), and abdominal cramps based on food intolerance

Table 3: Comparing patients' demographic data and clinical characteristics between the perforated appendicitis group and the nonperforated appendicitis group.

Parameters	Nonperforated appendicitis $N = 71$ (PA = 43, GA = 28)	Perforated appendicitis $N = 21$ (PA = 6, GA = 15)	$t/Z\chi^2$	P value
Sex (M, %)	46 (64.79%)	16 (76.19%)	0.959	0.328
Age (mean ± SD, years)	7.59 ± 3.54	6.67 ± 3.43	1.058	0.293
LOS (mean ± SD, days)	7.77 ± 2.11	10.24 ± 6.63	-1.679	0.108
Duration of fever (mean ± SD, days)	2.06 ± 1.74	2.81 ± 2.16	-1.647	0.103
Thermal spike (mean ± SD, ˚C)	38.63 ± 0.68	38.87 ± 0.63	-1.406	0.163
WBC (mean ± SD, 1000/μL)	16.89 ± 5.71	16.15 ± 4.87	-0.542	0.589
MCV (mean ± SD, fL)	82.13 ± 4.97	82.19 ± 4.46	-0.053	0.958
RDW (mean ± SD, %)	14.10 ± 1.09	14.11 ± 1.58	-0.008	0.993
MPV (mean ± SD, fL)	8.10 ± 1.31	7.96 ± 1.04	0.447	0.656
PDW (mean ± SD, %)	13.25 ± 2.76	12.44 ± 3.66	1.093	0.277
CRP (mean ± SD, mg/L)	49.80 ± 43.34	99.78 ± 61.54	-3.475	0.002∗
PLT (mean ± SD, 1000/μL)	255.65 ± 72.74	262.86 ± 97.85	-0.367	0.714
ALT (mean ± SD, U/L)	14.06 ± 10.70	19.79 ± 20.72	-1.219	0.214
AST (mean ± SD, U/L)	31.63 ± 12.04	35.52 ± 42.43	-1.290	0.200
ALP (mean ± SD, U/L)	207.91 ± 55.10	196.04 ± 56.37	0.863	0.391
Tbil (mean ± SD, μmol/L)	13.03 ± 9.66	12.84 ± 8.14	0.083	0.934
Ibil (mean ± SD, μmol/L)	8.82 ± 7.98	8.05 ± 5.05	0.414	0.680
Dbil (mean ± SD, μmol/L)	4.21 ± 2.26	4.69 ± 3.47	-0.749	0.456
LDH (mean ± SD, U/L)	274.47 ± 80.04	319.74 ± 143.54	-1.383	0.180
FIB (mean ± SD, g/L)	3.61 ± 0.90	3.63 ± 1.56	-0.037	0.971
TNF-α (mean ± SD, pg/mL)	58.85 ± 94.60	80.13 ± 152.39	-0.778	0.439
sB7H3 (mean ± SD, ng/mL)	38.99 ± 10.12	44.69 ± 9.29	-2.309	0.023∗

Asterisks (∗) indicate that the reorganization data is nonnormal distribution, and rank sum test is used to analyze the differences between groups. LOS: longer length of stay in hospital; WBC: white blood cell; MCV: mean corpuscular volume; RDW: red blood cell distribution width; MPV: mean platelet volume; PDW: platelet distribution width; CRP: C-reactive protein; PLT: platelet; ALT: alanine aminotransferase; AST: aspartate aminotransferase; ALP: alkaline phosphatase; Tbil: total bilirubin; Ibil: indirect bilirubin; Dbil: direct bilirubin; LDH: lactate dehydrogenase; FIB: fibrinogen; TNF-α: tumor necrosis factor-α.

(3, 12%). The AUROC values of leukocytes and CRP were 0.711 and 0.619, respectively. As a nonspecific response of the body, raised white blood cells and CRP levels are frequent in patients with acute and chronic gastroenteritis accompanied by vomiting, abdominal pain, dehydration, and other serious symptoms. This condition may be misdiagnosed as AA in several cases. Moreover, respiratory and urinary tract infections, as the causes of acute abdominal pain in children [25–27], may often accompany by elevated levels of leukocytes and CRP. However, these conditions do not occur in selective hernia surgery.

In addition, a number of studies on appendicitis have selected negative appendectomy patients as CG. However, Dubrovsky et al. [28] demonstrated that negative appendicitis is associated with greater morbidity, longer LOS, higher complication rate, and higher cost compared with nonperforated appendicitis. In addition, they identified a total of 156,660 nonincidental inpatient appendectomies from 2005 to 2011. They observed an overall decrease in the rate of both negative appendicitis (3.3% in 2005 to 1.8% in 2011, $P < 0.01$) and perforated appendicitis (27.1% in 2005 to 25.0% in 2011, $P < 0.01$). Similar results were noted in studies conducted by Chinese scholars. For instance, Jin et al. [29] expressed that the negative appendectomy rate was 1.53% (31/2015) in Chongqing (China). There were two patients with normal appendix according to the results of histology in that study. However, the negative appendectomy rate in a pediatric appendicitis study with a large sample size reached 10.75% (37/344) in Turkey [30] and 15.54% (186/1197) in three pediatric centers performed in Canada, Australia, and the UK [22]. Dubrovsky et al. [28] demonstrated higher proportion of gastrointestinal complications (obstruction or C. difficile infection) and respiratory complications (e.g., atelectasis or pneumonia) in negative appendicitis patients than in nonperforated appendicitis patients. Thus, patients with negative appendectomy rate may highly have higher levels of leukocytes and CRP than healthy individuals.

Therefore, compared with NSAP and negative appendectomy, we selected nonemergency inguinal hernia as CG, and the diagnostic efficiency of markers was relatively high. A recent study conducted by Sarsu et al. [6] also selected

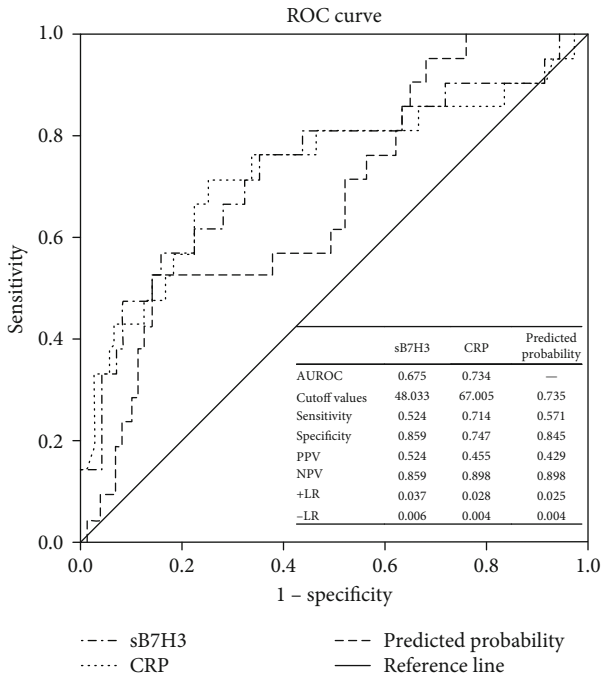

Figure 4: ROC curves and evaluation indexes of sB7H3 and CRP for the diagnosis of appendicitis with perforation. The ROC curve is drawn by SPSS, and Youden's index is calculated by the corresponding coordinate value on the curve. The maximum value of Youden's index is the ideal cutoff value. AUROC: area under the curve; PPV: positive predictive value; NPV: negative predictive value; +LR: positive likelihood ratios; -LR: negative likelihood ratios.

healthy controls and demonstrated that in diagnosis of complicated AA, AUROC for fecal lactoferrin, serum CPR, and serum HMGB-1 were determined as 1.00 and the cutoff level was determined as 25 μg/g feces, 670 ng/mL, and 30 ng/mL, respectively. In differential diagnosis of uncomplicated and complicated AA, the most accurate parameter was fecal lactoferrin with an AUROC of 0.977.

Studies on the role of hyperbilirubinemia in appendicitis were mainly concentrated on adult patients. In the present study, the bilirubin level in the AA group was significantly higher than that in the CG. Furthermore, our results demonstrated that the Dbil level had a higher SE and AUROC than the Tbil and Ibil levels for AA. These results were in agreement with Eren et al.'s achievements [31], in which hyperbilirubinemia, especially with elevated direct bilirubin levels, was elevated significantly in gangrenous/perforated appendicitis. However, there were no significant differences in Tbil, Dbil, and Ibil levels between the nonperforated appendicitis group and the perforated appendicitis group in the present study. This was found to be consistent with a meta-analysis conducted by Silva et al. [32], who demonstrated that the diagnostic value of hyperbilirubinemia cannot merely predict acute perforated appendicitis. Thus, hyperbilirubinemia may be a moderate marker to predict AA in children, while that cannot merely predict perforation.

In the present study, significantly higher values of PDW, MCV, and RDW were noted in children with AA. The AUROC values for PDW, MCV, and RDW were 0.776, 0.724, and 0.711, respectively. In addition, RDW had the highest SE of 0.902 and the lowest SP of 0.456. Furthermore, the results of the current research demonstrated that RDW values increased with progress of severity of appendicitis, while the difference was not statistically significant. There were no significant differences in PDW, MCV, RDW, and MPV between the nonperforated appendicitis group and the perforated appendicitis group. In agreement with the current research, another study [30] related to RDW on children who suspected of having appendicitis revealed that it might be precious for diagnosing AA in children, rather than utilizing for predicting perforation. In contrast to studies conducted on children, Boshnak et al. [33] reported that the PDW level in the positive appendectomy group was significantly higher than that in the negative appendectomy group. Significantly higher RDW level was only found in patients with AA who developed complications compared with those without complications. The diagnostic performance of RDW and PDW for diagnosing AA was not considerable; the AUROC values for PDW were determined as 0.696. Hence, increased levels of PDW and RDW combined with elevated WBC and neutrophil counts may be as advantageous for diagnosing cases suspected of having AA.

In the present study, the FIB level in patients with AA was significantly higher than that in the CG, and FIB level increased with progress of severity of appendicitis. However, there was no significant difference in the FIB level between SA and PA. Serum FIB level has been studied for diagnosing AA in a limited number of studies. Menteş et al. [34] investigated the diagnostic role of FIB in AA and found that the serum FIB level (accuracy, 68.16%) had a similar diagnostic value to WBC (accuracy, 72.14%). This result was comparable to that achieved in the present research. Our results showed that FIB and WBC both had moderate accuracy for diagnosing AA.

Perforated appendicitis is associated with short- and long-term complications, including peritonitis, sepsis, bowel intestinal obstruction, abscess formation, and fertility problems. Furthermore, the rate of perforated appendicitis is higher in children than in adults, especially in younger children (<5 years) [35, 36]. In the current study, the perforated rate of AA was 22.83% (21/92). Furthermore, there were significant differences in the levels of CRP and sB7H3 between the nonperforated appendicitis group and the perforated appendicitis group, in which the values of AUROC were 0.734 and 0.675, respectively. With combination of CRP and sB7H3, the value of AUROC in predicting perforated appendicitis was determined as 0.735. Although the younger age, the longer LOS, the longer duration of fever, and the higher levels of markers (RDW, NR, Dbil, FIB, and TNF-α) were found in the current research, the differences were not statistically significant. Buyukbese et al. [37] retrospectively studied 317 children who underwent appendectomy and found that the rate of complicated AA was 24.92% (79/317), and the CRP had the highest diagnostic value in predicting complicated appendicitis (AUROC, 0.887 L). Kim et al. [38] evaluated the predictive values of delta neutrophil index (DNI) and myeloperoxidase index (MPXI) in 105 children with AA and found that the complicated rate was

27.6% (29/105) and the CRP had the maximum value of AUROC (0.840) when cutoff was 40 mg/L. Being consistent with the present study, Kaiser et al. [7] also demonstrated that a combination of different inflammation markers may associate with higher AUROC value to predict complicated appendicitis.

As previously described, sB7H3 as a new biomarker has advantages in diagnostic efficiency over the old biomarkers (CRP, WBC, Dbil, etc.). However, the clinical application is inconvenient and more expensive now. If a commercial company intervenes later, the convenience and cost will definitely improve significantly.

The current study was limited by a relatively limited number of patients with AA, especially patients with SA. Nevertheless, the serum level of sB7H3 was only examined at the time of admission. Additionally, the time from the onset of symptoms to diagnosis of AA in children was not recorded. Therefore, further studies should be conducted on a larger sample size at different time points with inclusion of data of AA, in order to accurately assess the diagnostic value of sB7H3 for AA in children.

5. Conclusions

In summary, we noted significantly elevated sB7H3 level in children with AA, and sB7H3 levels remarkably associated with the degree of histological findings of the appendix. Hence, sB7H3 could be used as a precious marker to predict the presence of AA and complex AA in children. However, the diagnostic value of sB7H3 to predict gangrenous/perforated appendicitis was not notable. The combination of sB7H3 and CRP might improve the prediction of perforated appendicitis.

Data Availability

The data used to support the findings of this study are available from the corresponding author upon request.

Conflicts of Interest

The authors declare that they have no conflicts of interest.

Authors' Contributions

Xiaochen Du and Yan Chen contributed equally to this work.

Acknowledgments

This study was financially supported by the National Natural Science Foundation of China (Grant No. 81570455), Major Project of Natural Science Research of Jiangsu Provincial Department of Education (Grant No. 17KJA310004), and Suzhou Health Science and Technology Project (Gwzx201703).

References

[1] C. C. Glass and S. J. Rangel, "Overview and diagnosis of acute appendicitis in children," *Seminars in Pediatric Surgery*, vol. 25, no. 4, pp. 198–203, 2016.

[2] R. Benabbas, M. Hanna, J. Shah, and R. Sinert, "Diagnostic accuracy of history, physical examination, laboratory tests, and point-of-care ultrasound for pediatric acute appendicitis in the emergency department: a systematic review and meta-analysis," *Academic Emergency Medicine*, E. Alpern, Ed., vol. 24, no. 5, pp. 523–551, 2017.

[3] D. Papandria, S. D. Goldstein, D. Rhee et al., "Risk of perforation increases with delay in recognition and surgery for acute appendicitis," *Journal of Surgical research*, vol. 184, no. 2, pp. 723–729, 2013.

[4] E. Kim, G. Subhas, V. K. Mittal, and E. S. Golladay, "C-reactive protein estimation does not improve accuracy in the diagnosis of acute appendicitis in pediatric patients," *Intrenational Journal of Surgery*, vol. 7, no. 1, pp. 74–77, 2009.

[5] M. A. Beltrán, J. Almonacid, A. Vicencio, J. Gutiérrez, K. S. Cruces, and M. A. Cumsille, "Predictive value of white blood cell count and C-reactive protein in children with appendicitis," *Journal of Pediatric Surgery*, vol. 42, no. 7, pp. 1208–1214, 2007.

[6] S. B. Sarsu, A. B. Erbagci, H. Ulusal, S. C. Karakus, and Ö. G. Bulbul, "The place of calprotectin, lactoferrin, and high-mobility group box 1 protein on diagnosis of acute appendicitis with children," *Indian Journal of Surgery*, vol. 79, no. 2, pp. 131–136, 2017.

[7] M. Kaiser, M. Schroeckenfuchs, C. Castellani, G. Warncke, H. Till, and G. Singer, "The diagnostic value of hepcidin to predict the presence and severity of appendicitis in children," *Journal of Surgical Research*, vol. 222, pp. 102–107, 2018.

[8] D. J. Shogilev, N. Duus, S. R. Odom, and N. Shapiro, "Diagnosing appendicitis: evidence-based review of the diagnostic approach in 2014," *Western Journal of Emergency Medicine*, vol. 15, no. 7, pp. 859–871, 2014.

[9] A. I. Chapoval, J. Ni, J. S. Lau et al., "B7-H3: A costimulatory molecule for T cell activation and IFN-γ production," *Nature Immunology*, vol. 2, no. 3, pp. 269–274, 2001.

[10] X. Chen, G. Zhang, Y. li et al., "Circulating B7-H3 (CD276) elevations in cerebrospinal fluid and plasma of children with bacterial meningitis," *Journal of Molecular Neuroscience*, vol. 37, no. 1, pp. 86–94, 2009.

[11] G. Zhang, J. Wang, J. Kelly et al., "B7-H3 augments the inflammatory response and is associated with human sepsis," *The Journal of Immunology*, vol. 185, no. 6, pp. 3677–3684, 2010.

[12] G. Zhang, J. Hou, J. Shi, G. Yu, B. Lu, and X. Zhang, "Soluble CD276 (B7-H3) is released from monocytes, dendritic cells and activated T cells and is detectable in normal human serum," *Immunology*, vol. 123, no. 4, pp. 538–546, 2008.

[13] C. C. Luo, W. K. Chien, C. S. Huang et al., "Trends in diagnostic approaches for pediatric appendicitis: nationwide population-based study," *BMC Pediatrics*, vol. 17, no. 1, p. 188, 2017.

[14] H. H. Almaramhy, "Acute appendicitis in young children less than 5 years: review article," *Italian Journal of Pediatrics*, vol. 43, no. 1, p. 15, 2017.

[15] A. Bhangu, K. Søreide, S. Di Saverio, J. H. Assarsson, and F. T. Drake, "Acute appendicitis: modern understanding of pathogenesis, diagnosis, and management," *The Lancet*, vol. 386, no. 10000, pp. 1278–1287, 2015.

[16] A. Acharya, S. R. Markar, M. Ni, and G. B. Hanna, "Biomarkers of acute appendicitis: systematic review and cost-benefit trade-off analysis," *Surgical Endoscopy*, vol. 31, no. 3, pp. 1022–1031, 2017.

[17] M. Janakiram, U. A. Shah, W. F. Liu, A. Zhao, M. P. Schoenberg, and X. Zang, "The third group of the B7-CD28 immune checkpoint family: HHLA2, TMIGD2, B7x, and B7-H3," *Immunological Reviews*, vol. 276, no. 1, pp. 26–39, 2017.

[18] Z.-R. Chen, G.-B. Zhang, Y.-Q. Wang et al., "Soluble B7-H3 elevations in hospitalized children with *Mycoplasma pneumoniae* pneumonia," *Diagnostic Microbiology and Infectious Disease*, vol. 77, no. 4, pp. 362–366, 2013.

[19] Y. Xu, L. Yu, C. Hao et al., "Plasma soluble B7-H3 levels for severity evaluation in pediatric patients with *Mycoplasma pneumoniae* pneumonia," *International Immunopharmacology*, vol. 73, pp. 163–171, 2019.

[20] M. D. Stringer, "Acute appendicitis," *Journal of Paediatrics and Child Health*, vol. 53, no. 11, pp. 1071–1076, 2017.

[21] N. Hotic, E. Cickusic, D. Mesic, E. Husaric, A. Halilbasic, and E. Rahmanovic, "Leukocytes, C-reactive protein and interleukin-6 in acute appendicitis in children: diagnostic value and association with histological findings," *Acta Medica Saliniana*, vol. 39, no. 2, pp. 62–67, 2010.

[22] A. Zani, W. J. Teague, S. A. Clarke et al., "Can common serum biomarkers predict complicated appendicitis in children?," *Pediatric Surgery International*, vol. 33, no. 7, pp. 799–805, 2017.

[23] U. Sack, B. Biereder, T. Elouahidi, K. Bauer, T. Keller, and R.-B. Tröbs, "Diagnostic value of blood inflammatory markers for detection of acute appendicitis in children," *BMC Surgery*, vol. 6, no. 1, 2006.

[24] N. Oikonomopoulou, C. Míguez-Navarro, A. Rivas-García et al., "Assessment of proadrenomedullin as diagnostic or prognostic biomarker of acute appendicitis in children with acute abdominal pain," *American Journal of Emergency Medicine*, vol. 37, no. 7, pp. 1289–1294, 2019.

[25] C. E. Reust and A. Williams, "Acute abdominal pain in children," *American Family Physician*, vol. 93, no. 10, pp. 830–836, 2016.

[26] J. T. Kanegaye and J. R. Harley, "Pneumonia in unexpected locations: an occult cause of pediatric abdominal pain," *The Journal of Emergency Medicine*, vol. 13, no. 6, pp. 773–779, 1995.

[27] S. Vendargon, P. S. Wong, and K. K. Tan, "Pneumonia presenting as acute abdomen in children: a report of three cases," *Medical Journal of Malaysia*, vol. 55, no. 4, pp. 520–523, 2000.

[28] G. Dubrovsky, J. Rouch, N. Huynh, S. Friedlander, Y. Lu, and S. L. Lee, "Clinical and socioeconomic factors associated with negative pediatric appendicitis," *Journal of Surgical Research*, vol. 218, pp. 322–328, 2017.

[29] X. Jin, X. Li, D. Zhou et al., "The clinical study of early diagnosis of pediatric acute appendicitis—a 30-year experience," *Journal of Clinical Pediatric Surgery*, vol. 23, no. 4, pp. 259–262, 2013.

[30] G. Bozlu, H. Taskinlar, S. Unal, M. Alakaya, A. Nayci, and N. Kuyucu, "Diagnostic value of red blood cell distribution width in pediatric acute appendicitis," *Pediatrics International*, vol. 58, no. 3, pp. 202–205, 2016.

[31] T. Eren, E. Tombalak, I. A. Ozemir et al., "Hyperbilirubinemia as a predictive factor in acute appendicitis," *European Journal of Trauma and Emergency Surgery*, vol. 42, no. 4, pp. 471–476, 2016.

[32] F. R. Silva, M. I. da Rosa, B. R. Silva et al., "Hyperbilirubinaemia alone cannot distinguish a perforation in acute appendicitis," *ANZ Journal of Surgery*, vol. 86, no. 4, pp. 255–259, 2016.

[33] N. Boshnak, M. Boshnaq, and H. Elgohary, "Evaluation of platelet indices and red cell distribution width as new biomarkers for the diagnosis of acute appendicitis," *Journal of Investigative Surgery*, vol. 31, no. 2, pp. 121–129, 2017.

[34] O. Mentes, M. Eryilmaz, A. Harlak, E. Ozturk, and T. Tufan, "The value of serum fibrinogen level in the diagnosis of acute appendicitis," *Turkish Journal of Trauma and Emergency Surgery*, vol. 18, no. 5, pp. 384–388, 2012.

[35] V. A. B. van den Bogaard, S. M. Euser, T. van der Ploeg et al., "Diagnosing perforated appendicitis in pediatric patients: a new model," *Journal of Pediatric Surgery*, vol. 51, no. 3, pp. 444–448, 2016.

[36] K. Y. Kwan and A. L. Nager, "Diagnosing pediatric appendicitis: usefulness of laboratory markers," *American Journal of Emergency Medicine*, vol. 28, no. 9, pp. 1009–1015, 2010.

[37] S. Buyukbese Sarsu and F. Sarac, "Diagnostic value of white blood cell and C-reactive protein in pediatric appendicitis," *BioMed Research International*, vol. 2016, Article ID 6508619, 6 pages, 2016.

[38] O. H. Kim, Y. S. Cha, S. O. Hwang et al., "The use of delta neutrophil index and myeloperoxidase index for predicting acute complicated appendicitis in children," *PLoS One*, S. Esposito, Ed., vol. 11, no. 2, article e0148799, 2016.